THE EFFECT OF BTK INHIBITION ON PLATELET ACTIVATION BY GPVI AND CLEC-2

by

Phillip Lindsay Ross Nicolson

UNIVERSITY OF BIRMINGHAM

A thesis submitted to the University of Birmingham for the degree of DOCTOR OF PHILOSOPHY

Institute of Cardiovascular Sciences
College of Medical and Dental Sciences
University of Birmingham
October 2018

Abstract

Background

The novel Btk inhibitor ibrutinib has recently been introduced into the clinic for treatment of lymphoproliferative disorders (LPDs) where it is unexpectedly associated with major bleeding. It has been shown to block GPVI and CLEC-2-mediated platelet function with the former correlating with bleeding. This contrasts with patients who are deficient in GPVI or Btk who experience minor/no bleeding respectively. Mice that lack CLEC-2 also have no bleeding diathesis but are protected from thromboinflammation.

Aims

This study aims to investigate the discrepancy between the bleeding seen with ibrutinib and those that lack Btk. It also aims to examine whether ibrutinib can block CLEC-2 signalling in mouse and human venous thrombosis.

Results

Ibrutinib blocks GPVI signalling due to off-target effects which occur because of the high clinical doses that are used. It blocks CLEC-2 signalling at ~50-fold lower concentrations and reduces venous thrombosis rates in patients taking it for LPD.

Conclusions

Lowering the dose of ibrutinib or developing a more specific Btk inhibitor would ameliorate the major bleeding that is seen with ibrutinib. Btk inhibitors are suitable for further study as inhibitors of CLEC-2 signalling in human venous thrombosis.

Publications arising from this thesis

Manuscripts

- **Nicolson PLR**, Hughes CE, Watson S, Nock SH, Hardy AT, Watson CN, Montague SJ, Malcor JD, Thomas MR, Tomlinson MG, Pratt G, Watson SP. Inhibition Of Btk By Btk-Specific Concentrations Of Ibrutinib And Acalabrutinib Delays But Does Not Block Platelet Aggregation To GPVI. Haematologica. 2018;103(12):2097-2108 DOI: 10.3324/haematol.2018.193391

Book Chapter

- Haining EJ, **Nicolson PLR**, Onselaer MB, Poulter NS, Thomas MR, Rayes J and Watson SP. (2019). 'GPVI and CLEC-2' in Michelson AD *(ed.) Platelets, 4th edition*. Elsevier/Academic Press, pp 213-226.

Dedication

I would like to dedicate this thesis to my wife Pippa and my children William and Emily without whom I would not have achieved the spiritual, physical and psychological nourishment necessary to sustain me throughout this degree.

Acknowledgements

This work was supported by the University of Birmingham Institute of Cardiovascular Sciences and the Institute of Translational Medicine as well as the British Heart Foundation through the clinical research training fellowship (FS/17/20/32738). I would particularly like to acknowledge Lorraine Harper for enabling me to get on the first rung of the ladder to start this work.

First and foremost for help in almost every aspect of laboratory work I want to thank the incredible Stef Watson without whom numerous experiments would have failed due to lack of expertise and reagents. Practical help with other aspects of laboratory work was received from Craig Hughes and Alex Hardy for the aggregation and biochemical assays; from Alex Bye and Jon Gibbins for the Ca^{2+} mobilisation assay; from Vicky Simms and Steve Thomas for the flow adhesion assays; from Abs Khan, Natalie Poulter, Jeremy Pike and Dee Kavanagh for the spreading and super-resolution microscopy assays and Lizzie Haining, Julie Rayes and Alex Brill as well as all the staff at the Biomedical Services Unit for the animal work. Social and gastronomic support in the lab was obtained through close collaboration with Abs Khan, Natalie Poulter, Chris Smith and Pushpa Patel.

For help with collection and provision of patient blood I would like to thank Mark Crowther, Nick Pemberton, Salim Shafeek, Kate Arthur, Gaynor Pemberton, Lesley Candlin and Rebekah Hart at Worcestershire Royal Hospital, Shankara Paneesha, Aarnoud Huissoon, Hayley Clifford, Alison Hardy and Melanie Kelly

at Birmingham Heartlands Hospital and Guy Pratt, Tina McSkeane, Gillian Marshall and Michelle Harry at the Queen Elizabeth Hospital. For help with collection of human blood and tissue and collaboration on the same I would also like to thank Rachel Brown from the Queen Elizabeth Hospital, Jane Steele and Gareth Bicknell from the Human Biomaterials Resource Centre and John Welsh and Mark Kahn from the University of Pennsylvania in Philadelphia. I would also like to thank Andrew Wilkinson and Robert Neely from the School of Chemistry at the University of Birmingham for their help with the chemical analysis of ibrutinib and acalabrutinib. For working so diligently under my supervision and providing work to go towards the conclusions of this thesis (even if not directly examinable) I want to thank Josh Hinds. In particular for help with statistical analysis for fellowship applications and work included in this thesis I would like to thank Peter Nightingale from the Queen Elizabeth Hospital for so willingly giving up his time for me. I would also like to thank Gill Lowe, Guy Pratt, Gayle Halford and Mike Tomlinson for helping me learn to cope with Steve Watson. The gratitude for this also extends to every other member of the Birmingham Platelet Group.

Outside the lab I would like to thank my parents and parents-in-law for their ongoing support with childcare to enable conference travel and unsociable working hours. I would also like to thank my good friends Ian Butler and Parag Gajendragadkar for forcing me out on my bike to the Clent hills and Italian Dolomites respectively. I would like to thank Iain Johnston, Alessandro Di Maio, Matt MacKenzie and Abs Khan for similarly dragging me out to music rehearsal

studios in Digbeth. I would also like to thank Dave Grohl, Nate Mendel, Taylor Hawkins and Chris Shiflett as well as Shawn Crahan, Craig Jones, Mick Thomson, Corey Taylor, Sid Wilson, Chris Fehn, Jim Root, Alessandro Venturella, Jay Weinberg, Joey Jordison, Paul Gray and Donnie Steele for fuelling the thesis writing process.

Finally I would like to thank my supervisors, Steve Watson and Guy Pratt, for their unfailing support before and throughout this work. For many practical, financial and psychological reasons, without Steve, none of what follows would have been possible.

I also want to thank him for bringing me down a peg or two at the times when my confidence outweighed my abilities; “Pip, in science, you never prove anything”.

Table of Contents

List of Figures

List of Tables

Abbreviations

AC	Adenylyl cyclase
ACD	Acid citrate dextrose
ADAM	A disintegrin and metalloproteinase domain-containing protein
ADP	Adenosine diphosphate
AE	Adverse event
AEBSF	4-(2-aminoethyl)benzenesulfonyl fluoride hydrochloride
AF	Atrial fibrillation
AF488	Alexa Fluor 488
AF647	Alexa Fluor 647
ALL	Acute lymphoblastic leukaemia
AM	Acetoxymethyl
ANOVA	Analysis of variance
ATP	Adenosine triphosphate
AV	Arteriovenous
BAT	Bleeding Assessment Tool
BSA	Bovine serum albumin
Btk	Bruton's tyrosine kinase
cAMP	cyclic adenosine monophosphate
CD	Cluster differentiation
CDF	Cancer drugs fund
cGMP	cyclic guanosine monophosphate
cGVHD	Chronic graft-vs-host-disease
CLEC-2	C-type lectin-like receptor 2
CLL	Chronic lymphocytic leukaemia
CML	Chronic Myeloid Leukaemia
COX-1	Cyclooxygenase 1
CRP	Collagen related peptide
Csk	C-src tyrosine kinase
CTCAE	Common terminology criteria for adverse events
CTEPH	Chronic thromboembolic pulmonary hypertension
CVA	Cerebrovascular accident
Cys	Cysteine
DAG	1,2-diacylglycerol
DALY	Disability-adjusted life year
$DiOC_6$	3,3′-dihexyloxacarbocyanine iodide
DMSO	Dimethyl sulfoxide
DOAC	Direct oral anticoagulant
dSTORM	Direct stochastic optical reconstruction microscopy
DVT	Deep vein thrombosis
ECL	Enhanced chemiluminescence
ECM	Extracellular matrix
EDTA	Ethylenediaminetetraacetic acid
EGFR	Epidermal growth factor receptor

FCR	Fludarabine, Cyclophosphamide, Rituximab
FITC	Fluorescein isothiocyanate
FL	Follicular lymphoma
Gln	Glutamine
GPCR	G-protein-coupled receptor
GPIb	Glycoprotein Ib
GPIIb/IIIa	Glycoprotein IIb/IIIa
GPV	Glycoprotein V
GPVI	Glycoprotein VI
GPIX	Glycoprotein IX
HBRC	Human Biomaterial Resource Centre
HEPES	4-(2-hydroxyethyl)-1-piperazineethanesulfonic acid
HRP	Horseradish peroxidase
IHD	Ischaemic heart disease
INR	International normalised ratio
IP	Intraperitoneal
IP_3	Inositol 1,4,5-trisphosphate
ISTH	International Society on Thrombosis and Haemostasis
ITAM	Immunoreceptor tyrosine-based activation motif
ITIM	Immunoreceptor tyrosine-based inhibitory motif
ITP	Immune thrombocytopenia
IV	Intravenous
IVC	Inferior vena cava
JAK	Janus kinase
KD	Kinase dead
LAT	Linker for activation of T-cells
LEC	Lymphatic endothelial cell
LH	Lithium heparin
LMWH	Low molecular weight heparin
LPD	Lymphoproliferative disorder
LTA	Light transmission aggregometry
mAb	Monoclonal antibody
MAPK	Mitogen-activated protein kinase
MCL	Mantle cell lymphoma
MI	Myocardial infarction
MZL	Marginal zone lymphoma
NFAT	Nuclear factor of activated T-cells
NICE	National Institute for Health and Clinical Excellence
NK	Natural killer
NO	Nitric oxide
OD	Optical density
OS	Overall survival
pAb	Polyclonal antibody
PAGE	Polyacrylamide gel electrophoresis
PAR	Protease-activated receptor
PBS	Phosphate buffered saline
PCC	Prothrombin complex concentrate
PDE	Phosphodiesterase

PE	Pulmonary embolism
PE	Phycoerythrin
PEG	Polyethylene glycol
PFA	Platelet function analyser
PF4	Platelet factor 4
PFS	Progression-free survival
PGI_2	Prostaglandin I2 (also known as prostacyclin)
PH	Plekstrin homology
PI3K	Phosphoinositide 3-kinase
PIP_2	Phosphatidylinositol 4,5-bisphosphate
PIP_3	Phosphatidylinositol 3,4,5-trisphosphate
PIP5K	Phosphatidylinositol-4-phosphate 5-kinase
PKC	Protein kinase C
PKG	Protein kinase G
PLC	Phospholipase C
PM	Post mortem
PPP	Platelet poor plasma
PRP	Platelet rich plasma
PTS	Post-thrombotic syndrome
pY	Phosphotyrosine
RA	Rheumatoid arthritis
Rcptr	Receptor
RCT	Randomised controlled trial
RhoA	Ras homolog gene family, member A
SAE	Serious adverse event
SDS	Sodium dodecyl sulfate
SEM	Standard error of the mean
SFK	Src family kinase
SH	Src homology
SLL	Small lymphocytic lymphoma
SLP76	SH2 domain containing leukocyte protein of 76kDa
STAT	Signal transducer and activator of transcription proteins
Syk	Spleen tyrosine kinase
TIRF	Total internal reflection fluorescence
TH	Tec homology
TKI	Tyrosine kinase inhibitor
TP	Thromboxane-prostanoid
TPO	Thrombopoetin
TxA_2	Thromboxane A_2
UFH	Unfractionated heparin
VKA	Vitamin K antagonist
VTE	Venous thromboembolism
VWF	Von Willebrand's factor
WCC	White cell count
WM	Waldenström's macroglobulinaemia
WT	Wild type
XID	X-linked immunodeficiency
XLA	X-linked agammaglobulinaemia

Y	Tyrosine

Word count: 44,316

CHAPTER 1: GENERAL INTRODUCTION

1.1 Introduction to platelets

Platelets are small, anucleate, cell fragments that circulate in the blood with a normal level in humans of 150 - 450 x10^9/l. They are involved in formation of a haemostatic plug to prevent excessive bleeding in response to vessel wall injury. They are also involved in preventing leakage from the vasculature at sites of inflammation (so called inflammatory haemostasis). Bleeding can occur if the platelet count is low, with its severity depending on the degree and cause of thrombocytopenia, and the need for a "second hit" e.g. an inflammatory insult.

Platelets are only found in mammals. Their counterpart in other vertebrates is the nucleated thrombocyte. It is likely that they evolved from the haemocytes of marine invertebrates which have dual functions as cells that phagocytose pathogens and also aggregate together to prevent leakage of blood/haemolymph (Levin 2013; Martin et al. 2007).

1.1.1 Platelet production

Platelets are produced by bone marrow cells called megakaryocytes. These are large multinucleate cells with an average of 16 times the normal number of

chromosomes. They form thin projections of cytoplasm containing cell membrane called pro-platelets. Pro-platelets extend through sinusoidal epithelial cells to reach directly into the blood vessels which permeate throughout the bone marrow (Kaushansky 2005). Platelets are made directly from the megakaryocyte cytoplasm with surrounding cell membrane which forms buds and separates from these pro-platelet projections. Each megakaryocyte produces about 2000-3000 platelets and 10^{11} are produced every day (Harker et al. 2000).

Platelet production is mainly regulated by the production and consumption of thrombopoetin (TPO). TPO is produced in the liver at a constant rate. In the normal physiological setting, most of this TPO binds to TPO receptors on platelets, whereupon it is internalised and degraded. This leaves any remaining TPO to act on the TPO receptor on megakaryocytes where, via the JAK-STAT pathway, it acts as to increase both the maturation and number of megakaryocytes leading to further platelet production (Kuter 2013). If the platelet count drops, then less TPO is bound up by the TPO receptors on platelets and more is available to stimulate megakaryocytes. The converse also applies if the platelet number increases.

Once released by the megakaryocyte, each platelet circulates for up to 10 days before being taken up by the reticuloendothelial system in the spleen and liver (Josefsson et al. 2013).

1.1.2 Platelet structure

As previously stated, platelets are small and anucleate; measuring only 2-3 μm

in diameter. They are discoid in shape and are highly granular. This granularity results from a mixture of three main types of organelles; α-granules, dense granules and lysosomes. Platelets have an internal open canalicular system. At the surface of the platelet this serves to increase the surface area of the platelet membrane and act as a conduit for granule release. The dense tubular system is involved in storage and internal release of Ca^{2+}.

In addition, platelets have an actin cytoskeleton and microtubule system. Actin polymerisation occurs on platelet activation and causes a radical shape change from discoid to flat with multiple projections. This dramatically increases its surface area, increasing the structural stability of any developing thrombus (Hartwig 2013).

1.1.3 Platelet function

1.1.3.1 The role of platelets in haemostasis and thrombosis

Haemostasis is defined as the prevention of bleeding through formation of a clot at the site of vessel injury whereas thrombosis is the pathological formation of such a clot. There are two main types of haemostasis; classical haemostasis and inflammatory haemostasis (sometimes known as vascular integrity), these are described in more detail below. There are also two main types of thrombosis; arterial and venous. The former involves platelets and the latter has been thought historically to not rely on platelet activation but there is increasing evidence to the contrary (see later).

The importance of platelets in classical haemostasis is outlined by the severe

bleeding that occurs after injury in patients who are thrombocytopenic or those that have platelet function disorders such as Bernard Soulier Syndrome or Glanzmann's Thrombasthaenia which are due to mutations in GPIb and integrin αIIbβ3, respectively. Their role in inflammatory haemostasis is seen in thrombocytopenic patients and animals who experience petechiae, bruising and endothelial thinning during inflammation or sepsis.

Thrombosis is one of the leading causes of morbidity and mortality in the world. This is the case in high as well as low or middle-income countries. Arterial thrombosis, incorporating ischaemic heart disease (IHD) and stroke (cerebrovascular accident; CVA), is responsible for 25% of deaths worldwide. Venous thromboembolism (VTE), which incorporates deep vein thrombosis (DVT) and pulmonary embolism (PE) is a major source of morbidity and has a not-insignificant mortality. The world-wide incidence of VTE and PE has not been reported (Temgoua et al. 2017). But the annual incidence of VTE in western Europe is 100-700/100,000 with PE contributing 60/100,000 (Belohlavek et al. 2013). PE has untreated and treated mortality rates of 30% and 8% respectively. VTE that results in hospitalisation is the leading cause of loss of disability adjusted life years (DALYs) in middle and low-income countries and the second highest cause of DALY loss in high income countries (Raskob et al. 2014). This is because 30% of patients who suffer from a deep vein thrombosis (DVT) will go on to develop post-thrombotic syndrome (PTS) (Belohlavek et al. 2013) and 4% of patients who develop a PE will go on to develop chronic thromboembolic pulmonary hypertension (CTEPH). Patients suffering from PTS have a chronically swollen and painful leg, sometimes with

associated skin ulceration. CTEPH is a chronic condition which is also associated with long term morbidity and mortality from right ventricular dysfunction (McNeil & Dunning 2007; Keeling et al. 2011).

1.1.3.2 Functions of platelets outside haemostasis

As well as what is considered to be their main function of prevention of bleeding at times of vascular injury platelets are integral to a number of other critical processes such as blood-lymphatic separation and inflammation. They also contribute to other non-thrombotic pathologies such as cancer progression.

Blood-lymphatic separation occurs during embryonic development. During this process, platelets are activated by ligation of their C-type lectin receptor CLEC-2 by podoplanin on lymphatic endothelial cells (LECs). Mice without CLEC-2 die *in utero* and post-mortem examination reveals extensively blood filled lymphatic vessels (S. P. Watson et al. 2010).

As might be expected from the dual function of haemostasis and immunity of the haemocytes in some marine invertebrates, platelets have not completely lost their role in innate immunity in mammals despite their evolution to specialised haemostatic cells. Platelets can recognise pathogens and form a clot surrounding them to help prevent their local and systemic spread (Brühl et al. 2012). This process is called immunothrombosis.

Much recent research has established that, through expression of platelet agonists, cancer cells are able to manipulate platelets to help them with the processes of tissue invasion, lymphatic and haematogenous spread as well as promoting growth in secondary sites. Some of these processes may involve

platelet CLEC-2 activation leading to cancer cells being coated with platelets (Astarita et al. 2012) and facilitating their survival in the circulation by making them resistant to shear stress and attack from Natural Killer (NK) cells (Leblanc & Peyruchaud 2016). Indeed, inhibition of CLEC-2's interaction with podoplanin has been shown to suppress cancer metastasis *in vitro* (Chang et al. 2015) although there are a wealth of other ways in which platelets could enable cancer metastasis.

1.1.4 Major platelet receptors and ligands

In order to perform their various functions, platelets need to be activated. This occurs in three main steps:

i) Agonists bind to their receptors on the platelet surface and early platelet activation signalling occurs. The various different signalling events of the different pathways downstream of each individual receptor converge on a common pathway.
ii) This common pathway causes "inside-out" activation of integrin αIIbβ3 (otherwise known as GPIIb/IIIa) and granule secretion. Granule secretion results in multiple positive feedback loops.
iii) Subsequent "outside-in" activation of integrin αIIbβ3 by its ligands also acts as positive feedback.

The two main types of receptors on the surface of platelets that facilitate this early platelet activation are G protein-coupled receptors (GPCRs) and those linked to an immunoreceptor-tyrosine-based-activation-motif (ITAM). These, as

well as the platelet adhesion receptors, are discussed below.

1.1.4.1 GPCRs

GPCRs are 7 transmembrane domain proteins that transmit their signals principally through membrane bound heterotrimeric G proteins, but also through arrestins and G-protein coupled receptor kinases. The major ligands that activate platelets via GPCRs are adenosine diphosphate (ADP), thromboxane A_2 (TxA_2) and thrombin. These bind to $P2Y_1$ / $P2Y_{12}$ for ADP, the thromboxane-prostanoid receptors TPα and TPβ for TxA_2 and the protease-activated receptors PAR1 and PAR4 for thrombin. Some GPCRs are regulated by rapid internalisation after activation.

With the exception of thrombin and the protease-activated receptors (PARs), all of the GPCR ligands and receptors interact in the conventional way with ligand binding causing a conformational change of the receptor. The relevant coupled subunits for each receptor and their downstream signalling cascade is summarised in Figure 1.1. As a protease, thrombin cleaves the amino terminus of the PAR. The new N-terminus acts as a tethered ligand, binds to the receptor and activates it (K. J. Clemetson & J. M. Clemetson 2013).

The importance of each of these receptors and their ligands is reflected in the phenotypes of those who lack the receptor and also their therapeutic use as drug targets. Patients who lack $P2Y_{12}$ have a bleeding disorder and drugs which inhibit $P2Y_{12}$ such as clopidogrel and ticagrelor are used clinically as a treatment for arterial thrombosis (Dorsam & Kunapuli 2004). Mice lacking TP are protected from atherosclerosis and aspirin is used widely in clinical practice

to inhibit TxA_2 production and thus treat numerous diseases resulting from atheroma formation (Smyth 2010). Direct thrombin inhibitors are used in the treatment of VTE and have a side effect of bleeding. Mice lacking PAR4 have impaired haemostasis and are protected against thrombosis (Hamilton et al. 2004). Drugs targeting PARs have been developed but have mostly failed to show sufficient efficacy in clinical trials when compared to aspirin for treatment of arterial thrombosis (Tricoci et al. 2012).

1.1.4.2 ITAM receptors

An ITAM is a conserved sequence of amino acids comprising two YxxL motifs separated by 6-12 amino acid residues and is denoted Yxx(L/I)x6-12Yxx(L/I). They are found in the intracellular region of receptors on many haematopoetic cells. In platelets they are found on FcγRIIA, the FcRγ chain which is linked non-covalently to Glycoprotein VI (GPVI) and also in a truncated form (a so called hemITAM) on CLEC-2 (Boulaftali et al. 2014). Upon ligand binding in platelets, the receptors dimerise or cluster and the tyrosine residues in the ITAM are phosphorylated by Src family kinases (SFKs). This enables binding of spleen tyrosine kinase (Syk) to the ITAM and subsequent activation of a signalling cascade involving many adapter proteins, tyrosine kinases and enzymes such as linker for activation of T-cells (LAT), Bruton's tyrosine kinase (Btk) and phospholipase Cγ2 (PLCγ2). The ultimate effector of this signalling cascade is internal mobilisation of Ca^{2+}. The signalling of GPCRs and ITAM receptors is summarised in Figure 1.1.

GPVI is the main platelet receptor for collagen. It is a type 1 transmembrane

receptor that is part of the immunoglobulin superfamily and is only expressed on megakaryocytes and platelets (Jandrot-Perrus et al. 2000). It associates non-covalently with FcRɣ chain (S. P. Watson et al. 2010). There are approximately 3-4000 copies of GPVI per human platelet (Burkhart et al. 2012) making it the most prevalent ITAM linked receptor on platelets.

After initial activation, platelet adhesion to collagen is also supported by integrin α2β1. Activation of GPVI leads to shedding through the metalloproteinases ADAM10 and ADAM17. Patients lacking GPVI have a mild bleeding disorder. In addition to its well established role as the main collagen receptor it has also recently been identified as a receptor for fibrin and fibrinogen but the biological importance of this interaction is, as yet, unclear (Alshehri et al. 2015; Mammadova-Bach et al. 2015; Mangin et al. 2018).

CLEC-2 is a C-type lectin-like type II transmembrane receptor. It has several exogenous ligands such as the snake venom rhodocytin and the polysaccharide fucoidan but podoplanin is the only known endogenous ligand. Under normal conditions podoplanin is not present in the vasculature and comes into contact with CLEC-2 during development or when there is damage or leakage in the vessel wall. Rather than two YxxL motifs it only contains a single YxxL which is downstream of a tri-acidic amino acid region (DEDG) (S. P. Watson et al. 2010). CLEC-2, therefore, exists as a homodimer so that two phosphorylated hemITAMs can still bind to the tandem Src Homology (SH)2 domains of Syk and activate downstream signalling. It is expressed in high numbers on megakaryocytes and platelets; 3700 copies per platelet in human platelets (Burkhart et al. 2012) and 40,000 in mouse platelets (Zeiler et al. 2014). The

reason for the markedly greater in expression in mouse platelets is not known. In mouse models it appears to play a minimal or no role in haemostasis but, as shall be explored later, it is essential in the pathogenesis of venous thrombosis. There is no known human condition where patients are deficient in CLEC-2.

FcγRIIA is a low affinity receptor for the Fc region of IgG. It plays a role in linking platelets to immunity as well as a pathological role in heparin-induced thrombocytopenia (Arman et al. 2014).

1.1.4.3 Adhesion receptors

GPIb-IX-V is a platelet surface receptor complex consisting of GPIbα, two GPIbβ subunits, GPIX and a loosely associated GPV subunit (R. Li & Emsley 2013). Its primary function, for which no signalling is required, is to bind to von Willebrand's factor (VWF) at high shear. The presence of the receptor is very important for haemostasis as evidenced by patients who lack it (Bernard Soulier Syndrome) who have a lifelong, often severe, bleeding disorder. No drugs against GPIb have yet been licensed.

Integrin αIIbβ3 is a platelet receptor for fibrinogen and fibrin and several other extracellular matrix (ECM) proteins including VWF that, along with other integrins, is normally kept in a low affinity state. As shown in Figure 1.1, when activated by "inside-out" signalling from other receptors it undergoes conformational change to a high affinity conformation. Binding of the activated form to monomeric ligands does not induce signalling but results in adhesion. Multimeric ligands, by contrast, bind and activate "outside-in" intracellular signalling. The latter enables stable platelet adhesion and spreading,

aggregation, thrombus formation, clot retraction and further degranulation. This receptor is also of crucial importance to maintain haemostasis. Patients with Glanzmann's thrombasthaenia lack this receptor and have a lifelong severe bleeding disorder. Drugs targeting this receptor such as abciximab and eptifibatide are used for treatment of myocardial infarction (MI) but their use is restricted to the hospital because of the risk of excessive bleeding.

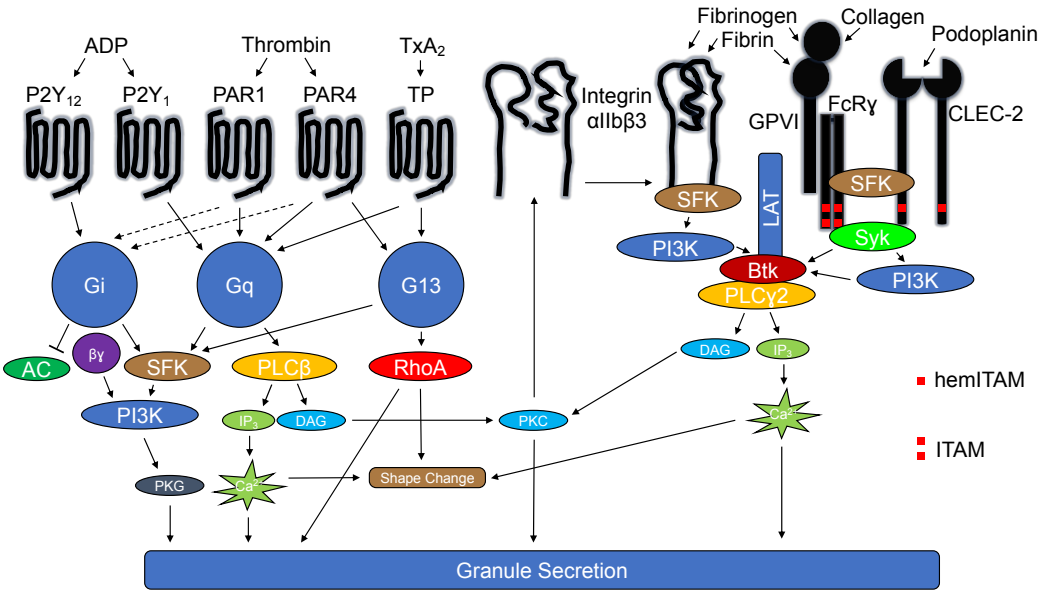

Figure 1.1: Schematic of platelet GPCR and ITAM receptor signalling. Platelets can be activated by many ligands via different GPCR and ITAM receptors. All pathways converge in Ca^{2+} release and PKC activation resulting in shape change and granule secretion. βγ: Beta-gamma subunits of all heterotrimeric G-proteins. PI3K: phosphoinositide 3-kinase. AC: adenylate cyclase. RhoA: Ras homolog gene family, member A. IP_3: inositol trisphosphate. DAG: 1,2-diacylglycerol. PKC: protein kinase C. PKG: protein kinase G. Adapted from Li *et al.* 2010)

1.2 Haemostasis

1.2.1 Classical Haemostasis

In the classical descriptions of haemostasis, the process is separated into primary and secondary haemostasis with primary haemostasis involving the formation of the initial platelet plug and secondary haemostasis being the activation and addition of coagulation cascade proteins (also known as clotting factors) to strengthen it. In reality, the two processes occur simultaneously, but the division is useful for descriptive purposes.

Primary haemostasis: Within the vasculature platelets are marginalised to the outer aspects of the blood vessels by the red blood cells. During normal conditions platelets are kept in an inactive state through numerous mechanisms such as the endothelial release of nitric oxide (NO) and prostacyclin (PGI_2). But when there is a breach in the blood vessel lining platelets are activated. Vascular injury exposes the subendothelial collagen to the flowing blood. Free VWF in the blood is captured by the collagen. This is then able to bind to platelets under the high shear rates present in the arteries and arterioles by binding to the GPIb-V-IX receptor complex on the platelet surface. The fast on/off interaction between VWF and GPIb causes platelets to roll at low speeds over the area of damage (Andrews & Berndt 2013). This is called rolling adhesion. The reduced speed of platelets then enables collagen to bind directly to GPVI on the platelet surface (Z. Li et al. 2010). This activates GPVI and results in Ca^{2+} mobilisation within the platelet. This causes platelet shape change, granule release and activation of surface integrins. Inside-out activation of integrin α2β1 and αIIbβ3 results in much more stable binding of platelets to collagen and other platelets/fibrin/VWF respectively. The degranulation of platelets releases numerous proteins and small molecules which promote

platelet further platelet recruitment, activation and thrombus growth.

Secondary Haemostasis: Tissue Factor released from damaged endothelium as well as negatively charged phospholipids inserted into the platelet surface membrane during degranulation activate clotting factors and provide a scaffold for assembly of these clotting factors into complexes. Via a tightly regulated sequence of activation steps and feedback loops the clotting factors converge on and activate Factor X and thrombin which ultimately cleaves fibrinogen into fibrin and it is cross-linked fibrin that provides the major source of structural support for the clot.

GPVI, therefore, is critical for initial platelet activation on contact with collagen. The recent discovery that it is also a ligand for fibrin could indicate an additional role in thrombus growth and stability (Bender et al. 2017). This important role is also evidenced by patients with congenital or acquired GPVI deficiency who have been described in the literature, all of whom have mild bleeding symptoms (Arthur et al. 2007; Onselaer et al. 2017).

Consistent with only having a single endogenous ligand which is not present in the vasculature under normal conditions, CLEC-2 does not appear to play any significant role in haemostasis. Studies examining the role of CLEC-2 in maintaining haemostasis either show no effect of CLEC-2 deficiency / inhibition or merely a minor contribution (Hughes et al. 2010; Suzuki-Inoue et al. 2010; May et al. 2009; Bender et al. 2013).

1.2.2 Inflammatory haemostasis

Vascular integrity is the prevention of leakage of blood from vessels during

circumstances other than vascular injury. The leakage occurs through sites of breach in the vessel wall caused by immune cell transmigration. This process increases markedly during inflammation. This gives rise to the term inflammatory haemostasis. It has shown to occur in mice in multiple studies (Boulaftali et al. 2018) and also occurs in humans where it is recognised that platelet transfusion thresholds need to be higher in thrombocytopenic patients with concomitant inflammation (Estcourt et al. 2016). This form of haemostasis occurs independently of most major platelet receptors including integrin αIIbβ3. It does, however, depend heavily on GPVI and, to a lesser extent, CLEC-2 activation.

1.3 Platelets in thrombosis and thromboinflammation

1.3.1 Arterial thrombosis

Arterial thrombosis occurs in areas where there is diseased vessel wall (plaque). The plaque ruptures, exposing its contents to the flowing blood. Platelets then adhere and activate rapidly. These thrombi have a high platelet content and are white in colour. Because of the well known role of platelets in the pathophysiology of arterial thrombosis there are numerous strategies used to inhibit platelets to treat this disease. Inhibition of production of TxA_2 is performed with aspirin. $P2Y_{12}$ is blocked with clopidogrel, prasugrel or ticagrelor. Phosphodiesterase (PDE) induced breakdown of cyclic adenosine

monophosphate (cAMP) is inhibited with dipyridamole. Integrin αIIbβ3 activation is blocked with eptifibatide, abciximab or tirofiban. All of these carry the common side effect of causing both major and minor bleeding. There are also numerous other antiplatelet agents in development such as GPVI inhibitors as well as PAR inhibitors. It is hoped that these will be able to treat arterial thrombosis without giving rise to major bleeding.

1.3.2 Venous thrombosis

Venous clots typically form as a DVT behind the venous valves of the iliac, femoral, popliteal and calf veins with the latter being the most common (Yoshimura et al. 2012). These clots cause painful swelling of the affected area due to localised inflammation and pressure build up within the vessel. There is also often tenderness and erythema of the overlying skin.

They are classically thought to occur in areas where there is disturbance to blood flow, blood contents or the vessel wall (known as Virchow's triad). If unstable thrombus from the clot is dislodged it travels through the venous system and the right side of the heart and can settle in the pulmonary vasculature. If this occurs in a small vessel then it may merely cause some pulmonary ischaemia resulting in a small amount of chest pain and dyspnoea. If it lodges in a large vessel, however, then a large part of the lung can lose its blood supply and become infarcted. Furthermore, if the embolised thrombus lodges at the bifurcation of the pulmonary artery (a so-called saddle embolus) then this can result in sudden death because all blood flow in the body travels through this single point.

Traditionally VTE is treated with medications that inhibit proteins in the coagulation cascade. Historically treatment of a venous thrombosis was done with oral vitamin K antagonists (VKAs) such as warfarin for somewhere between 6 weeks and lifelong depending on the circumstances of the clot (Keeling et al. 2011).

Because they do not directly inhibit the action of the clotting factors, but rather prevent their production, they have a slow onset of action, often of several days. If more acute manipulation of the patient's coagulation system is required (e.g. if a patient on a VKA needed to undergo surgery) then they would be admitted to hospital and infused intravenously with the short acting anticoagulant unfractionated heparin (UFH). This can be stopped and the patient's coagulation activity will return to normal rapidly to enable surgery to take place (Keeling et al. 2016).

In the 1990s derivatives of UFH have been developed in the form of low molecular weight heparins (LMWHs). These can be dosed subcutaneously, have a rapid onset and have a more predictable therapeutic activity when compared to UFH as well as a longer half-life. They are used in acute venous thrombosis to rapidly anticoagulate patients whilst VKA levels are up-titrated and in patients who are unable to tolerate the frequent blood monitoring required for VKA treatment (Keeling et al. 2011). In some settings they have been shown to have superior efficacy to VKAs such as VTE associated with cancer (H. G. Watson et al. 2015). They are also used in lower, prophylactic, doses in patients deemed to be at high risk for VTE. These are typically those in hospital undergoing surgery, with significantly reduced mobility, with cancer or

other inflammatory conditions (Schulman et al. 2017).

Even more recently oral drugs which directly inhibit coagulation cascade proteins have been introduced into clinical use. These are termed Direct-acting Oral Anticoagulants (DOACs). For some instances of venous thrombosis treatment and prophylaxis they have replaced the older medications as standard of care due to superior efficacy and/or an improved side effect profile (Keeling et al. 2011; National Institute for Health and Care Excellence 2018c). It is important to note, however, that all of these agents have a side effect of bleeding. 3% of patients on warfarin will experience a major or fatal bleeding event each year and this compares with a rate of about 1.5-2% for patients on DOACs (Crowther & Warkentin 2008). If a patient on medication experiences major bleeding this is significant life event for them. Not only does a major bleed itself carry with it a significant risk of death of 8-11% (Chai-Adisaksopha et al. 2015), but it also results in a subsequent cessation of the causative drug and an increased rate of post bleed thrombosis. It carries a significant cost to the healthcare service in terms of the expense of any admission for bleeding as well as a chronic cost associated with any long term physical disability that results from it (particularly with intracerebral haemorrhage). It also causes a lot of psychological harm to patients (Hutter & Kreitschmann-Andermahr 2014; Fumagalli et al. 2014). The bleeding rates are such that, despite the improved safety of the DOACs over VKAs, anticoagulants are still contraindicated in some patients with a history or high risk of bleeding. Presently these patients have no adequate treatment strategy.

Platelets have not historically been thought to be involved in the

pathophysiology of VTE. The age-old dichotomy states that venous thrombi are made up of red cells and fibrin and are platelet poor, whereas arterial thrombi are platelet rich. But antiplatelet agents are, in fact, used for VTE prophylaxis in some patient groups. They protect against VTE but have a lower bleeding risk than anticoagulants (Castellucci et al. 2013). There are an increasing number of studies showing a benefit when using antiplatelet agents as part of the management strategy for treating patients with VTE. Aspirin has been shown to reduce VTE recurrence if used as a long term maintenance therapy after anticoagulation treatment had been discontinued (Becattini et al. 2012; Brighton et al. 2012). Indeed, in order to look for specific VTE scenarios where antiplatelets might be as efficacious as anticoagulants; a Cochrane review is being performed to compare them as treatment for VTE (Flumignan et al. 2016).

1.3.3 Immunothrombosis and thromboinflammation

Immunothrombosis is the process by which platelets contribute to the function of the innate immune system by forming thrombi in vessels which catch / wall off bacteria. Thromboinflammation is the pathological formation of venous thrombi in response to inflammatory stimuli. They are terms that are unfamiliar to most clinicians. But despite this it is well known that inflammation is associated with increased rates of VTE. They have been shown to occur in numerous animal models.

Immunothrombosis most frequently occurs in the microvasculature, particularly the hepatic and splenic sinusoids (Engelmann & Massberg 2012). Here, neutrophils, monocytes, fibrin and platelets recognise pathogens and form a

small clot surrounding them which helps to prevent their local and systemic spread (Brühl et al. 2012; Engelmann & Massberg 2012). These clots in the microvasculature do not cause disturbance of blood flow because of the large volume of collateral flow that goes on the liver and spleen. It is, however, when this process occurs in larger veins or the non-hepatosplenic microvasculature that it can initiate over-activation of platelets and the coagulation cascade and ultimately cause pathological thromboinflammation (Wakefield et al. 2008). There are no human diseases where thromboinflammation is known definitively to occur. It is, however, suspected to play a role in the development of disseminated intravascular coagulation (DIC), arterial atherothrombosis and venous thrombosis (Engelmann & Massberg 2012). It is not yet known whether it plays a role in all types of VTE or merely some distinct subtypes that are yet to be identified (Engelmann & Massberg 2012). It is compelling, however, that VTE rates are increased in patients who have inflammatory disease. Indeed, the incidence of VTE in patients with inflammatory bowel disease is 3-fold higher than in the general population (Papa et al. 2014). It is also possible that all DVT has a hitherto undiscovered inflammatory component.

1.3.4 ITAM receptors as new targets in thrombosis and thromboinflammation

Given that ITAM receptors play an important role in inflammatory haemostasis, it may not come as a surprise to learn that they are also important in thromboinflammation. In a mouse model of hepatic vein thrombosis induced by *S typhimurium* there is up-regulation of the CLEC-2 ligand podoplanin in the

liver. In particular this occurs at the site of vascular breach and it is here that platelets interact with podoplanin expressed on inflammatory macrophages and this triggers the inflammation-driven occlusive thrombosis. Indeed, the venous thrombosis is markedly reduced in the absence of platelet CLEC-2 or in the absence of macrophages (Hitchcock et al. 2015). Furthermore, in a mouse model of DVT induced by inferior vena cava (IVC) stenosis podoplanin is upregulated in the IVC wall. Platelets penetrate the damaged vessel wall and are activated by podoplanin which leads to further platelet recruitment and thrombus growth. The thrombus size is dramatically reduced in the absence of platelet CLEC-2 and in the presence of an anti-podoplanin antibody (Payne et al. 2017).

Together these data show that up-regulation of podoplanin in the vessel wall interacts with platelet CLEC-2 and triggers venous thrombosis in the setting of thromboinflammation in mice. This may represent a novel anti-thrombotic target but studies showing podoplanin up-regulation in the vasculature in human venous thrombosis are lacking.

1.4 Bruton's tyrosine kinase (Btk) and its inhibitors

1.4.1 Btk

Btk is a member of the Tec family of cytosolic tyrosine kinases and mediates phosphorylation and activation of PLCɣ2 downstream of many receptors in haematopoetic cells. It was initially identified in 1993 as the non-functional protein in the immunodeficiency syndrome X-linked agammaglobulinaemia (XLA) which was first described by Colonel Ogden Bruton in 1952 (Tsukada et al. 1993; Vetrie et al. 1993). Its predominant role is in B-cells where it acts downstream of the B-cell receptor (BCR) to promote differentiation and maturation (Akinleye et al. 2013). It is expressed in myeloid and erythroid progenitors at lower levels (Weers et al. 1993). It is also present in platelets where it is phosphorylated downstream of the ITAM receptors GPVI, FcɣRIIA (Quek et al. 1998; Oda et al. 2000) and CLEC-2 (Manne et al. 2015) and the adhesion receptors GPIb-IX-V and integrin αIIbβ3 (Suzuki-Inoue et al. 2004; Atkinson et al. 2003).

1.4.1.1 Structure

Btk is one of the five members of the Tec family of kinases which also includes Tec, Itk, Bmx and Txk (also known as Rlk). All except Txk share the same structure with a Plekstrin Homology (PH) domain, adjacent Tec Homology (TH) domain, Src Homology (SH) 3 and SH2 domains as well as a kinase domain at

the C-terminus of the protein (Kawakami et al. 1999). The Tec kinases are one of the largest family of cytoplasmic tyrosine kinases alongside SFKs (Akinleye et al. 2013).

The structure of Btk is shown in Figure 1.2. The N-terminal PH domain is critical for trafficking of Btk to the inner aspect of the cell membrane because it mediates its interaction with phosphatidylinositol 3,4,5-trisphosphate (PIP_3) (Varnai et al. 1999). The TH domain is adjacent (Vihinen et al. 1994). Its N-terminal end contains the zinc finger Btk motif and the proline rich region at its C-terminal end which serves a point of interaction with other proteins such as Protein Kinase C β (PKCβ) (Kang et al. 2001). Initial activation occurs by phosphorylation at tyrosine (Y) 551. This is situated in the activation loop in the kinase domain (Wahl et al. 1997). The adenosine triphosphate (ATP) binding site, catalytic apparatus and allosteric inhibitory segments are located in this domain as well (Oppermann et al. 2009). Full activation requires autophosphorylation at Y223 in the SH3 domain (Wahl et al. 1997). It is not clear, however, whether this is a result of dimerisation and phosphorylation by another Btk molecule or true self phosphorylation (Mohamed et al. 1999). Y223 is in a YxxM motif that is common to all the Tec family kinases except Tec and its phosphorylation means that it becomes a docking site for SH2 domains on other kinases and adapters such as phosphoinositide 3-kinase (PI3K). Like other kinases and adapters, the SH2 domain is important for interactions with other proteins such as LAT (Mohamed et al. 1999).

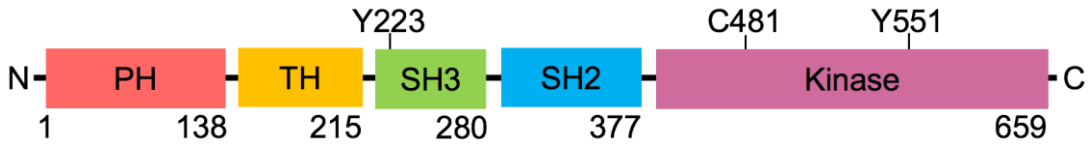

Figure 1.2: The Structure of Btk.
The non-receptor tyrosine kinase Btk has 659 amino acids. It consists of PH, TH, SH3, SH2 and kinase domains. The latter incorporates the transphosphorylation site Y551 and ATP binding loop which contains C481.

1.4.1.2 Signalling and interactions with other kinases and adapters

In resting conditions, Btk is cytosolic, unphosphorylated and catalytically inactive. Btk activation is a complex process which is summarised in Figure 1.3. The first step is translocation to the lipid rafts of the plasma membrane (Varnai et al. 1999). This occurs when PI3K generates PIP_3 from membrane bound phosphatidylinositol 4,5-bisphosphate (PIP_2). Btk can then bind to PIP_3 on the inner surface of the plasma membrane via its PH domain. During this translocation process the PH/TH domain associates with phosphatidylinositol-4-phosphate 5-kinase (PIP5K) and brings this to the plasma membrane as well (Salto et al. 2003).This makes more PIP_2 which allows PI3K to produce more PIP_3 and enables further Btk recruitment (Salto et al. 2003). Tec can also associate with PIP5K and bring it to the plasma membrane (Salto et al. 2003).

In platelets, LAT and SH2 domain containing leukocyte protein of 76 kDa (SLP76) are phosphorylated by Syk and this enables them to associate with the SH2 domain on Btk. Btk is phosphorylated at Y551 by the SFK Lyn and also by Syk (Yang & Desiderio 1997). Along with LAT and SLP76, Btk forms a signalling complex with Syk itself and other kinases and adapters called the LAT signalosome (Boulaftali et al. 2014; Zhou et al. 2013; Judd et al. 2002). Btk

then undergoes autophosphorylation at Y223 and becomes catalytically active (Park et al. 1996).

Phosphorylated tyrosine residues in the LAT signalosome form docking sites for the SH2 domain of PLCɣ2 (Watanabe et al. 2001). PLCɣ2 is then phosphorylated and activated by Btk and Syk (Rodriguez et al. 2001). Following this it produces inositol 1,4,5-trisphosphate (IP_3) and 1,2-diacylglycerol (DAG) leading to the activation of many downstream effectors including internal Ca^{2+} mobilisation. PLCɣ2 has four phosphorylation sites, two in the SH2-SH3 linker (Y753 and Y759) and two in the C-terminal region (Y1197 and Y1217). The degree to which each of these phosphorylation sites contributes to PLCɣ2 activation and indeed which tyrosine residues are phosphorylated by Syk and which by Btk is contentious. A summary of the findings of the available literature on phosphorylation of PLCɣ2 by Btk and Syk is shown in Table 1.1.

One of the principal mechanisms of regulation of Btk activation is through phosphorylation of Serine (S) 180 in the TH domain by PKCβ. This causes Btk to move back to the cytoplasmic compartment from the membrane, thus preventing it from activating PLCɣ2 (Kang et al. 2001).

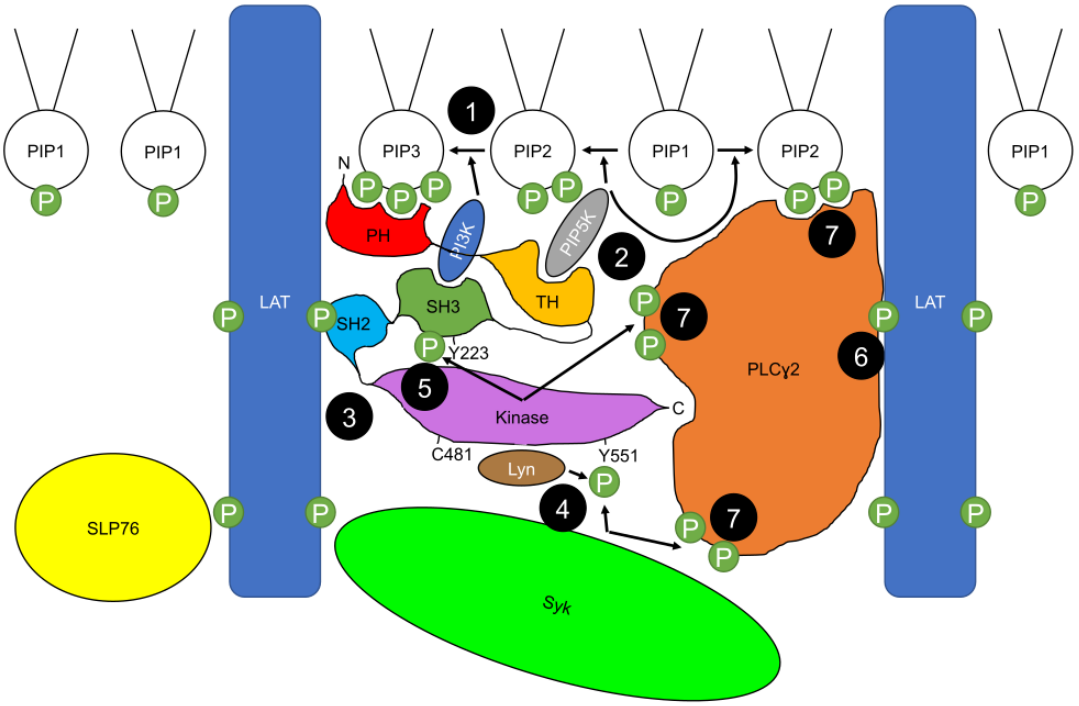

Figure 1.3: Mechanism of Btk activation and its subsequent activation of PLCɣ2. (1) PI3K catalyses PIP_2 to PIP_3. The PH domain of Btk binds to PIP_3 enabling Btk translocation from cytosol to lipid rafts of the plasma membrane (Varnai et al. 1999). The SH3 domain of Btk associates with PI3K (2) PH/TH domain associates with PIP5K and brings it to the membrane with Btk. This produces more PIP_2 substrate for PI3K which is then able to recruit more Btk. (3) Btk associates with phosphorylated LAT, SLP76 and Syk via its SH2 domain and forms the LAT signalosome (4) Btk is phosphorylated at Y551 by the SFK Lyn and also by Syk. (5) Btk autophosphorylates at Y223 and becomes catalytically active. (6) SH2 domain of PLCɣ2 binds to phosphorylated LAT. (7) PLCɣ2 is activated by a mixture of Syk and Btk mediated phosphorylation and through a phosphorylation independent interaction with Btk, likely to be PIP5K induced production of PIP_2.

Author	Cell type	Receptor	Agonist	pY753 + pY759 (SH2-SH3 linker region)			pY1197 + pY1217 (C-terminal region)			Notes
				Phosphorylated?	Required for activation?	TK responsible for pY	Phosphorylated?	Required for activation?	TK responsible for pY	
Watanabe *et al*. 2001	DT40	BCR	Anti-IgM	Yes	Partially	Mainly Btk. Syk partially.	Yes	Yes	Btk	
Humphries *et al*. 2004	Human and mouse B cells	BCR	Pervanadate	Yes	Partially	Mainly Btk	Yes	Partially	Not Btk	
Kim *et al*. 2004	Ramos / Mouse B cells	BCR	Anti-IgM	Yes	Yes	-	No	No	-	Basal pY753 present
Kim *et al*. 2004	Jurkat	CD3	OKT-3 mAb	Yes	-	-	No	-	-	Basal pY753 present
Kim *et al*. 2004	Platelets	GPVI	Convulxin	Yes	-	-	No	-	-	No basal pY753
Kim *et al*. 2004	Fibroblasts	PDGFR	PDGF	No	-	-	No	-	-	

Table 1.1: Existing studies and their findings regarding Btk and Syk mediated PLCɣ2 phosphorylation.
There have been multiple studies investigating the kinases responsible for PLCɣ2 phosphorylation at specific tyrosine residues and how these phosphorylation events relate to PLCɣ2 kinase activity. Their results are summarised here. PDGF = Platelet Derived Growth Factor. PDGFR = PDGF Receptor.

1.4.1.3 Role of Btk in B cells

XLA is an X-linked immunodeficiency syndrome caused by a congenital dysfunction or lack of Btk. It results in a complete lack of mature B-cells due to a block in B-cell development at the Pro-B to Pre-B-cell transition and a resultant susceptibility to bacterial infections which can be life threatening. Historically most affected individuals with this condition would die from one of these infections in childhood or adolescence. After introduction of prophylactic treatment with intravenous pooled immunoglobulin, however, life expectancy is fairly normal.

The Btk gene is located on the X chromosome. There are many different mutations that result in XLA. Patients with PH domain mutations and those which result in a heavily truncated protein get a “classical” XLA manifestation with no mature B cells (Vihinen et al. 1995; Vihinen et al. 1997). Mutations in the kinase domain that result in the expression of a normal protein with no autophosphorylation activity cause a less severe phenotype (Gaspar et al. 1998) although it is not often possible to predict the severity of the immunodeficiency from the particular mutation that the patient has (Holinski-Feder et al. 1998). All of the mutations are held in a registry for mutations associated with XLA called BTKbase (Vihinen 1995).

X-linked Immunodeficiency (XID) is a murine immunodeficiency syndrome caused by a specific point mutation in the PH domain of the Btk gene that prevents the resultant protein’s association with PIP_3 (Rawlings et al. 1993). There is also a knockout mouse with a complete homozygous deficiency of Btk (Btk-/-). Both of these mice have reduced populations of B cells but the

phenotype is less severe than for humans (Kerner et al. 1995; W. N. Khan et al. 1995). This difference in phenotype is attributed to a much higher amount of Tec in murine B cells than in human B cells. Double knock out mice lacking both Btk and Tec have a complete lack of mature B-cells resembling human XLA (Ellmeier et al. 2000).

Its role in the development of B-cell lymphoproliferative disorders (LPDs) has been extensively studied. Inappropriate activation of Btk-dependent pathways have been implicated in maintaining a malignant phenotype in a wide variety of cancers. Survival and progression of LPDs is promoted by dysregulated Btk activity (Vassilev et al. 1998; Kuppers 2005; Buggy & Elias 2012). Indeed it seems that constitutive Btk activation enhances the development of leukaemia in mouse models and is a necessary step in the series of events leading to development of chronic lymphocytic leukaemia (CLL) in patients (Kil et al. 2013). There are also other cancers with gain of function mutations in Btk such as chronic myeloid leukaemia (CML), colorectal cancer and acute lymphoblastic leukaemia (ALL) (Akinleye et al. 2013).

Because of the prevalence of upregulated Btk in LPDs several pharmaceutical and bio-technology companies have targeted Btk in these disorders. In the last 4-5 years, Btk inhibitors have entered clinical practice for the treatment of LPDs such as CLL, small cell lymphoma (SLL) and mantle cell lymphoma (MCL) (Byrd et al. 2013) (see Section 1.4.2).

1.4.1.4 Role of Btk in platelet ITAM signalling

There is only a small amount of literature on the role of Btk in platelets. Most of the understanding of the function and signalling has been gained from studies in B-cells with assumptions made that it performs a similar role in platelets. Platelets from patients with XLA have normal thrombin responses but partial inhibition of GPVI-mediated platelet function which can be overcome at higher concentrations of agonist (Quek et al. 1998). No patients with XLA are reported to have any symptoms or signs of excessive bleeding, be that spontaneous or as a result of trauma.

Biochemical studies have shown that Btk is phosphorylated downstream of GPVI, FcγRIIA, CLEC-2, integrin αIIbβ3 and GPIb-IX-V (Oda et al. 2000; Suzuki-Inoue et al. 2004; Manne et al. 2015; Atkinson et al. 2003). It has also been shown to be phosphorylated in response to thrombin-mediated platelet activation in one study (Quek et al. 1998) but not in another (Oda et al. 2000). Tec has also been shown to be phosphorylated downstream of GPVI, integrin αIIbβ3 and GPIb-IX-V (Suzuki-Inoue et al. 2004; Atkinson et al. 2003).

Of note, however are the subtle differences in the role of Btk in the different signalling cascades. GPVI stimulation results in Syk autophosphorylation, Btk phosphorylation at Y551 and Y223 and PLCγ2 phosphorylation at Y753 and Y759 (with other PLCγ2 phosphorylation sites not studied) (Suzuki-Inoue et al. 2004). CLEC-2 stimulation results in Syk and Btk autophosphorylation as well as PLCγ2 phosphorylation at Y759 but treatment with the Btk inhibitor ibrutinib, even at very low concentrations (10 nM), unexpectedly causes loss of Syk as well as Btk and PLCγ2 phosphorylation. This has led to the proposal that Btk lies upstream of Syk in CLEC-2 signalling (Manne et al. 2015) (see Figure 1.4)

whereas it is clear it lies downstream of Syk in GPVI signalling (Atkinson et al. 2003) (see Figure. 1.1).

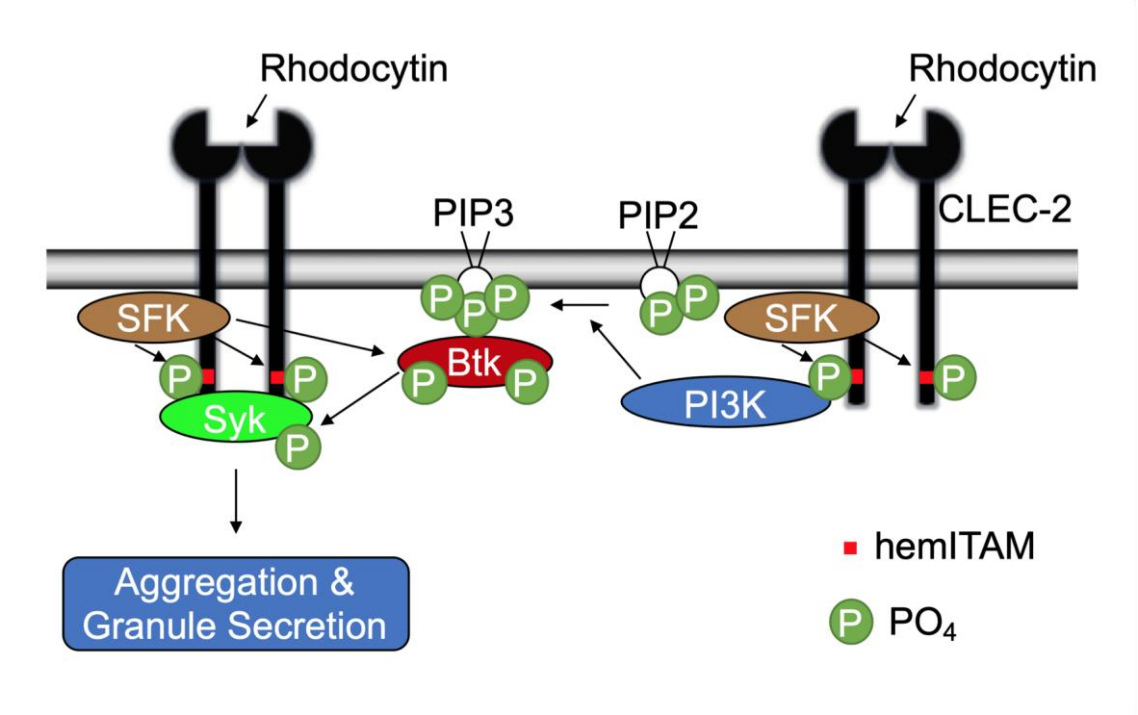

Figure 1.4: Model for Btk regulating Syk activation downstream of CLEC-2. After CLEC-2 ligation SFKs phosphorylate the HemITAM which binds Syk and activates PI3K. PI3K then generates PIP_3 which binds Btk and recruits it to the plasma membrane. Btk then, once phosphorylated by SFKs, phosphorylates and activates Syk. Adapted from Manne *et al* (Manne et al. 2015).

Studies in mice again highlight the extra signalling redundancy provided by Tec in mouse platelets as Btk-/- mice have almost normal aggregation in response to GPVI ligation whereas Btk and Tec double knockout mice have completely impaired functional and biochemical responses (Atkinson et al. 2003). Spreading on fibrinogen is unaffected, even in the double knockout mice, showing that Btk and Tec do not play a functional role in integrin αIIbβ3 outside-in signalling even though they are phosphorylated downstream of integrin activation (Atkinson et al. 2003).

1.4.2 Btk inhibitors

Btk inhibitors are a novel class of oral tyrosine kinase inhibitor that have only recently been introduced into clinical practice for treatment of B-cell LPDs. Early trial data showed an unexpected side effect of major haemorrhage and this was attributed in early reports to inhibition of platelet activation by GPVI. This is obviously at odds with the existing literature on Btk and bleeding where patients with XLA do not suffer from any bleeding but this has yet to be explored further. Btk inhibitors were first developed in 2009 (Honigberg et al. 2010) but were not licensed until 2014 in the US and 2017 in the UK (Liang et al. 2018; National Institute for Health and Care Excellence 2018a). They are broadly separated into two types; those that bind covalently to Cys481 in the ATP binding site in the kinase domain and thus prevent kinase activity and those that reversibly associate to the SH3 domain when Btk is in its inactive conformation and prevent change to the active conformation (Liang et al. 2018). The irreversible inhibitors share a core structural element but are linked to different side chains but the same is not said of the reversible inhibitors (Liang et al. 2018).

Of the many Btk inhibitors in development, three, so far, have been approved in the US. These are ibrutinib and acalabrutinib, which are currently only used for the treatment of haematological malignancies and PRN-1008 which is licensed for the treatment of the autoimmune skin condition pemphigus vulgaris (Liang et al. 2018). The only one licensed in the UK is ibrutinib.

Ibrutinib (PCI-32765, imbruvica) is an irreversible Btk inhibitor and was the first Btk inhibitor to be developed. It has an IC_{50} for Btk of 0.5-1.5 nM *in vitro* and for the other relevant kinases in platelets (C-src terminal kinase (Csk), Tec, Fyn, Src, and Lyn) it has an IC_{50} of 2.3, 10, 96, 171 and 200 nM respectively

(Honigberg et al. 2010; Barf et al. 2017). It does not inhibit Syk directly.

In the US it is approved for use in the treatment of relapsed CLL, MCL, Waldenström's macroglobulinaemia (WM) and marginal zone lymphoma (MZL) and has very recently been licensed for the treatment of chronic graft-vs-host-disease (cGVHD) after allogeneic stem cell transplant. In the UK it only has approval from NICE for use in relapsed or del17p / TP53 mutated CLL and also in MCL in patients who have relapsed or are unsuitable for chemo-immunotherapy (National Institute for Health and Care Excellence 2018a; National Institute for Health and Care Excellence 2018b). It can also be used for treating relapsed WM if Cancer Drugs Fund (CDF) funding is approved (National Institute for Health and Care Excellence 2017). For treatment of CLL/SLL, WM and cGVHD it is used at a dose of 420 mg once daily (roughly equivalent to 6 mg/kg) and for MCL and MZL 560 mg (~8 mg/kg) once daily is used.

It is much more tolerable than conventional chemotherapy agents. But it still has some significant side effects. These are atrial fibrillation (AF), bleeding and diarrhoea. The former is mediated by effects on the Btk regulated PI3K/Akt pathway or possibly off-target effects on other tyrosine kinases (Wiczer et al. 2017; McMullen et al. 2014). The latter two are reported to be due to off-target effects of the drug downstream of platelet GPVI and on the epidermal growth factor receptor (EGFR) in the gastrointestinal mucosa respectively (Wu et al. 2016; Byrd et al. 2016). Because of these side effects the use of ibrutinib in autoimmune conditions has not been approved. Reversible inhibitors may have a more tolerable side effect profile but none of these have come to market yet (Liang et al. 2018).

Acalabrutinib (ACP-196, calquence) is structurally related to ibrutinib and is also an irreversible inhibitor. Compared to ibrutinib it has a lower potency for inhibiting Btk (it has an IC_{50} for Btk that is 5-fold higher (5 nM)) but it has a higher selectivity over other tyrosine kinases. Its IC_{50} for Tec is 126 nM and it has been shown that it does not inhibit Fyn, Lyn and Src (Barf et al. 2017). For this reason it is claimed that it has a more tolerable side effect profile. In the only reported phase II clinical trial it did not cause atrial fibrillation or major bleeding (Byrd et al. 2016), but it does still caused some unpleasant gastrointestinal side effects (Liang et al. 2018).

It was granted FDA approval for treatment of relapsed MCL in 2017 but is yet to be approved in the UK or Europe and so its use is limited to clinical trials outside the USA. It is used at a single dose of 100 mg (~1.5 mg/kg) twice daily. Because of the improved side effect profile it is being trialled in autoimmune conditions such as rheumatoid arthritis (RA) as well as in some solid organ cancers and various other haematological malignancies.

PRN-1008 is a reversible covalent Btk inhibitor (Langrish et al. 2017). It has an IC_{50} for Btk of 1.3 nM *in vitro* (Liang et al. 2018). It has undergone phase II trials in immune thrombocytopenia (ITP) and the autoimmune skin condition Pemphigus vulgaris. It has been granted orphan drug status for the treatment of the latter (Principia Biopharma 2017). Other drugs reportedly showing promise for the treatment of LPDs and/or autoimmune diseases include CC-292 (Spebrutinib), ONO/GS-4059 (Tirabrutinib) and BGB-3111 (Zanubrutinib) (Liang et al. 2018). All of these bind covalently to Cys481.

1.5 Aims of the Thesis

It is clear from the above information that further prophylaxis/treatments for VTE / thromboinflammation that do not cause bleeding are required and that inhibition of platelet CLEC-2 is a hitherto unexplored drug target with a critical role in both of these conditions, as shown in mice, but apparent lack of involvement in classical haemostasis. Btk inhibitors may be an ideal class of drug to use for this purpose because they are oral, they have been shown to potently inhibit CLEC-2 signalling at very low concentrations and most are irreversible and thus would inhibit Btk for the lifetime of the platelet in an analogous way to aspirin.

Several questions need to be answered, however, before this hypothesis can be taken forward to clinical trials. Firstly, the current explanation that ibrutinib causes bleeding through inhibition of GPVI needs further exploration as, although GPVI inhibition is associated with bleeding, absence of Btk in patients with XLA is not (most likely because of the presence of Tec). The bleeding is therefore likely to be due to an off-target effect of the drug. Secondly, if Btk blockade is to be used as a means of blocking CLEC-2 then understanding Btk's role downstream of CLEC-2 activation is crucial. The controversial model of Btk lying upstream of Syk in this setting as proposed by Manne *et al.* needs further investigation. Finally, despite CLEC-2 clearly being critical for mouse thrombosis, this same role has not been shown in humans. Evidence supporting this role of CLEC-2 in human thrombosis is essential.

The aims of this thesis therefore are to:

i) Determine whether the bleeding seen with ibrutinib is due to off-target effects downstream of GPVI rather than being mediated through inhibition of

Btk.

ii) Explore the role that Btk plays downstream of CLEC-2.

iii) Investigate the role of Btk in VTE in mice and humans.

CHAPTER 2: MATERIALS AND METHODS

2.1 Materials

2.1.1 Antibodies and reagents

The α-phosphotyrosine (4G10) monoclonal antibody (mAb) was from Millipore (Abingdon, UK). The HRP-conjugated Goat α-rat IgG (SC 2032) and α-Syk pAb (SC-1077) were from Santa Cruz Biotechnology (Dallas, USA). The α-Btk pAb (SAB3500372) was from Sigma-Aldrich (Poole, UK). The α-LAT pAb (06-807) was from Merck Millipore (Burlingon, MA). Phosphospecific pAbs against Syk pY525/6, PLCɣ2 pY759 and pY1217 were from Cell Signalling Technology (Hitchin, UK), against LAT pY200, SLP76 pY145, PLCɣ2 pY753 and pY1197, Btk pY223 and pY551 were from Abcam (Cambridge, UK) and against Src pY418 was from Life Technologies (Carlsbad, CA). The α-Tec pAbs (BL17 and BL19) were a gift from Michael G Tomlinson (Birmingham, UK) and have been described previously (Tomlinson et al. 1999). The anti-human podoplanin mAb (NZ-1) was from eBioscience (Waltham, MA). The mouse α-human CLEC-2 antibody AYP1 was made in house and has been previously described (Gitz et al. 2014). (Ibrutinib (PCI-32765) and acalabrutinib (ACP-196) were from Selleckchem (Munich, Germany). Eptifibatide was from GSK (Brentford, UK). The FITC-conjugated rat α-mouse CD41 mAb was from BD Biosciences (San Jose, CA). Alexa Fluor 488-conjugated Phalloidin, the PE-conjugated rat α-mouse mAb against CD41 and FITC-conjugated IgG1 and IgG2b negative

control mAbs as well as the AF 647 conjugated goat α-mouse secondary pAb were from ThermoFisher (Waltham, MA). The FITC-conjugated rat α-mouse P-selectin mAb and PE-conjugated rat α-mouse integrin αIIbβ3 mAb were from Emfret Analytics (Eibelstadt, Germany). The FITC-conjugated rat α-mouse, HRP-conjugated α-mouse and α-rabbit secondary pAbs and Hyperfilm enhanced chemiluminescence (ECL) autoradiography film were from Amersham Biosciences (GE Healthcare, Bucks, UK). Glucose, pH 7 and pH 10 buffer solutions, Bolt running buffer, Bolt antioxidant, ECL reagent and the Ca^{2+} sensitive reporter precursor dye Fura-2-AM were from ThermoFisher (Waltham, MA). Heparin was from LEO Laboratories Ltd (Hurley, UK). Collagen related peptide (CRP) was from Richard Farndale (Cambridge, UK). Collagen was made from equine tendon and sourced from Takeda (Linz, Austria). Rhodocytin was provided as a gift from Johannes A Eble (Münster, Germany). PAR1 peptide was from Severn Biotech (Kidderminster, UK). PAR4 peptide was from Alta Biosciences (Birmingham, UK) Podoplanin-Fc was made in house in HEK 293T-cells and has been previously described (Navarro-Núñez et al. 2015). Non-fatty acid free Bovine Serum Albumin (BSA) was from First Link (UK) ltd (Birmingham, UK). ChronoLume® and ATP standard were from ChronoLog Corporation (Havertown, PA). Methanol and ethanol were from VWR Chemicals (Lutterworth, UK). Transblot Turbo western blotting buffer and the Rat IgG2b negative control pAb (SDS 10303) were from Bio-Rad (Kidlington, UK). Histo-Clear (d-limonene) was from National Diagnostics (Atlanta, GA). ImmPACT DAB peroxide reagent was from Vector Labs (Burlingame, CA). Uti-Lyse erythrocyte lysing reagent was from Dako North America Inc (Carpinteria, CA). All other reagents were purchased from Sigma-Aldrich (Poole, UK).

2.1.2 Chemical analysis of inhibitors

Purity assessment of individual batches of ibrutinib and acalabrutinib was performed by High Performance Liquid Chromatography and Liquid Chromatography Mass Spectrometry. Individual batches of inhibitor were compared to each other using lumiaggregometry to CRP in washed platelets as a bioassay. Concentration calculations for each batch of inhibitor were adjusted to reflect their differences in potency in this bioassay when compared to the measured chemical concentration.

2.2 Blood collection and preparation

2.2.1 Blood collection

Blood was taken from consenting patients or healthy, drug-free volunteers, into 4% sodium citrate. Blood from patients with CLL, who were not taking concomitant antiplatelet medication, was taken at 2-3 hours after the ingestion of Btk inhibitor on the final day of a treatment cycle. If patients were not being treated with Btk inhibitors but instead were receiving standard chemotherapy with Fludarabine, Cyclophosphamide and Rituximab (FCR) then citrated blood was taken immediately before any pre-medication was given prior to the first day of a chemotherapy cycle.

Mice were culled by CO_2 asphyxiation following isofluorane anaesthesia. 900 µl of whole blood was removed from the IVC using a 25 gauge needle with a 1 ml syringe containing 100 µl of heparin (100 units/ml) or 100 µl Acid Citrate

Dextrose (ACD) depending on whether platelets were to be prepared as platelet rich plasma (PRP) or washed platelets respectively. The anticoagulated blood was then immediately combined with 200 µl of heparin (10 units/ml) or 200 µl modified Tyrode's-HEPES buffer for PRP or washed platelets respectively.
For analysis of platelet activation in whole blood by flow cytometry mice were bled via saphenous vein puncture with a 26 gauge needle followed by collection of 30 µl of blood into a Sarstedt Microvette 300 lithium heparin (LH) capillary tube (Sarstedt AG & Co. KG, Nümbrecht, Germany) that was pre-coated with heparin. No more than 200 µl of blood was taken by this method from a single mouse over the course of an experiment.

2.2.2 Human platelet preparation

For preparation of PRP, whole blood was centrifuged at 200 g for 20 minutes at room temperature. The supernatant PRP was removed and the remaining red cells were centrifuged at 1,000 g for 10 minutes to yield a supernatant of platelet poor plasma (PPP) to act as a blank.

For preparation of washed platelets 10% volume of ACD was added to the whole blood before centrifugation at 200 g for 20 minutes at room temperature. Washed platelets were obtained by centrifugation of the supernatant PRP at 1,000 g for 10 minutes in the presence of 0.2 µg/ml PGI_2. The supernatant was discarded and the platelet pellet resuspended in 24 ml modified-Tyrode's-HEPES buffer (134 mM NaCl, 0.34 mM Na_2HPO_4, 2.9 mM KCl, 12 mM $NaHCO_3$, 20 mM HEPES, 5 mM glucose, 1 mM $MgCl_2$; pH 7.3) and 3 ml ACD, re-centrifuged at 1,000 g for a further 10 minutes in the presence of 0.2 µg / ml

PGI_2 and resuspended in modified-Tyrode's-HEPES buffer to a concentration of 4×10^8/ml for aggregation and biochemistry unless otherwise stated. Platelets were rested for 30 minutes prior to use in any experiments.

For preparation of ADP-sensitive washed platelets 10% volume of ACD was added to the whole blood before centrifugation at 100 g for 20 minutes at room temperature. PRP supernatant was removed and re-centrifuged at 300 g for 20 minutes. The resultant platelet pellet was then resuspended in modified-Tyrode's-HEPES buffer to $4x10^8$/ml.

2.2.3 Mouse platelet preparation

For preparation of murine PRP, whole blood anticoagulated with heparin was centrifuged at 2,000 rpm for 5 minutes using a MicroCentaur bench top centrifuge (Sanyo Electric Co. Ltd, Osaka, Japan). The PRP and a third of the rest of the blood was then centrifuged at 200 g for 6 minutes in a swinging bucket centrifuge to pellet erythrocytes. The PRP was removed and transferred to another 1.5 ml tube. 200 µl of modified-Tyrode's-HEPES buffer was added to the remaining erythrocytes and re-centrifuged at 200 g in the swinging bucked centrifuge for another 6 minutes. The PRP from this spin was collected and pooled with existing the PRP. If needed, the remaining erythrocytes were centrifuged at 1,000 g for 10 minutes to create a supernatant of PPP to use as a blank tube for light transmission aggregometry (LTA). Platelet concentration in PRP was measured but not adjusted.

For preparation of murine washed platelets the same process as for PRP was followed except whole blood anticoagulated with ACD was used and, following pooling of PRP, the total volume of PRP was brought up to 1 ml using modified-

Tyrode's-HEPES buffer. 1 µl of PGI_2 (1 mg/ml) was added before platelets were pelleted by centrifugation at 1,000 g for 6 minutes. Supernatant was then aspirated and the platelet pellet was resuspended in 400 µl modified-Tyrode's-HEPES buffer. Platelets were then made up to $4x10^8$/ml unless otherwise stated. At this point, platelets were rested for 30 minutes before performing an experiment.

2.2.4 Full blood counts

For analysis of total white cell and platelet counts in whole blood, blood was taken into 3.2-4% citrate or ethylenediaminetetraacetic acid (EDTA) at 1.8 mg/ml and analysed using a UniCel DxH 800 Haematology Analyser(Beckman Coulter, Brea, CA) or a Sysmex XN-1000 Haematology Analyser (Sysmex, Kobe, Japan).

2.3 Platelet function testing

2.3.1 Light transmission aggregometry (LTA)

300 µl of washed platelets or PRP was added to glass vials and warmed to 37°C in a Model 700 aggregometer (ChonoLog, Havertown, PA) for 5 minutes prior to stimulation. 3 µl of 100X agonist was added under stirring conditions (1200 rpm) followed by measurement of aggregation for 3-5 minutes. If inhibitors were being used, they were incubated for 5 minutes in stirring conditions after the platelets had been warmed unless otherwise stated. The blank vial was either filled with 300 µl of PPP or modified-Tyrode's-HEPES buffer depending on whether the experiment was being performed on PRP or

washed platelets respectively. Inhibitors used were ibrutinib (17 nM - 70 μM), acalabrutinib (50 nM - 200 μM) or vehicle (dimethyl sulfoxide, DMSO). Results are displayed as final % aggregation.

2.3.2 Dense granule release

During LTA, 5 μL ChronoLume® (a commercial reagent containing a D-luciferin-luciferase mixture) was added 1 minute prior to insertion of glass vials into the measurement chamber of the aggregometer. Light production by luciferase was measured by the Model 700 aggregometer. Calibration was performed by adding 5 μl of 2 μM (i.e. 2 nmol) ATP standard at the end of the experiment.

2.3.3 Measurement of $[Ca^{2+}]_i$

Platelets were loaded with the Ca^{2+} sensitive dye Fura-2-AM by incubation of PRP with 2 μM Fura-2-AM for 1 hour at 30°C. Platelets were then washed by centrifugation at 300 g for 20 min and resuspended in modified-Tyrode's-HEPES buffer. Fura-2-loaded platelets were incubated with inhibitors or vehicle for 5 minutes at 37°C prior to addition of agonists. Fluorescence measurements with excitation at 340 and 380 nm and emission at 510 nm were recorded over a period of 5 minutes using a NOVOstar plate reader (BMG Labtech GmbH, Ortenberg, Germany) for experiments with ibrutinib or a FlexStation (Molecular Devices LLC, San Jose, CA) for experiments with acalabrutinib. $[Ca^{2+}]_i$ was calculated using the ratio of the 340 and 380 nm excitation signals according to the method of Grynkiewicz et al (Grynkiewicz et al. 2001).

2.3.4 Flow cytometry

5 µl of heparinised whole blood was diluted to 45 µl using phosphate buffered saline (PBS) in the presence or absence of fluorophore conjugated antibody before being stimulated with 5 µl of 10X agonist. This was then incubated with the stated antibodies for 30 minutes at room temperature in the dark. Following this, erythrocytes were lysed using 50 µl of Uti-Lyse erythrocyte lysing reagent A (Dako North America Inc. Carpinteria, CA) for 10 minutes and fixed using 500 µl of Uti-Lyse erythrocyte lysing reagent B (Dako North America Inc. Carpinteria, CA) for 10 minutes. Samples were then analysed using an Accuri C6 Flow Cytometer (BD Biosciences, San Jose, CA).

2.3.5 Platelet adhesion under flow

Micro-capillaries on Cellix Vena8 Fluoro+ Biochips (Cellix Limited, Dublin, Ireland) were pre-incubated with 100 µl of 50 µg/ml collagen or 100 µg/ml podoplanin-Fc overnight at 4°C. Excess unbound agonist was then removed and capillaries were flushed with 5 mg/ml fatty acid free heat-denatured BSA and left to block for 1 hour at room temperature. Micro-capillaries were then flushed with PBS and kept for up to 24 hours before being used for flow adhesion assays.

For experiments investigating the effect of *in vitro* addition of inhibitor; 200 µl washed platelets at $10x10^8$/ml were incubated with inhibitor/vehicle for 5 minutes. Platelets were added back to non-ACD treated autologous red blood cells (250 µl) and PPP (50 µl) to a final concentration of $4x10^8$/ml. Blood was incubated with 4 µM of the lipid dye 3,3'-dihexyloxocarbocyanine iodide ($DiOC_6$) for 5 minutes immediately prior to flow to aid visualisation. Micro-capillaries

were flushed through with modified-Tyrode's-HEPES buffer for 3 minutes and then blood for 3-5 minutes at the stated shear rates followed by modified-Tyrode's-HEPES buffer for a further 3 minutes. Micro-capillaries were subsequently fixed with 10% neutral buffered formalin solution and platelet adhesion was viewed using a Zeiss Axio Observer 7 microscope (Carl Zeiss AG, Oberkocken, Germany) at 20X magnification using fluorescence intensity emitted at 520 nm. Platelet surface coverage on flow adhesion micro-capillary images were measured using ImageJ 1.5 (National Institutes of Health, USA). For the *in vitro* experiments analysing flow over podoplanin-Fc, and also experiments using *ex vivo* inhibitors and blood from patients with XLA, adhesion of platelets was performed under direct vision during flow with images taken every second using the same microscope and objective. For these experiments where adhesion was visualised in real-time platelet surface coverage and cluster size was analysed using the KNIME 3.4 analytics platform (KNIME.com AG, Konstanz, Germany) with Ilastik 1.1.2 machine learning software (University of Heidelberg, Germany) used to automatically and reproducibly identify platelets.

2.3.6 Platelet spreading

Glass coverslips were coated with 10 µg/ml collagen or podoplanin-Fc at 4°C overnight before excess agonist was aspirated and coverslips were blocked with 5mg/ml fatty acid free heat-denatured BSA for 1 hour at room temperature. Coverslips were then washed using PBS. 300 µl washed platelets at $2x10^7$/ml was added onto the coverslip and left to spread for 45 minutes at 37°C before non-adherent platelets were removed by aspiration and remaining platelets

were fixed using 10% neutral buffered formalin solution for 10 minutes. Coverslips were then washed three times using PBS to remove the fixative. For *in vitro* experiments platelets were either pre-treated with inhibitor or vehicle or had these added 30 minutes after spreading had started. Platelets were probed using Alexa Fluor 488-conjugated phalloidin before imaging using a Zeiss Axio Observer 7 microscope (Carl Zeiss AG, Oberkocken, Germany) at 63X magnification using fluorescence intensity emitted at 520 nm. Information on average spread platelet size and number of adherent platelets was analysed using the KNIME 3.4 analytics platform (KNIME.com AG, Konstanz, Germany) with Ilastik 1.1.2 machine learning software (University of Heidelberg, Germany) used to automatically and reproducibly identify platelets.

2.3.7 Platelet receptor clustering

50 µl washed platelets at $2x10^7$/ml were added to Glass bottomed dishes (MatTek Corporation, Ashland, MA) coated with 10 µg/ml collagen or podoplanin-Fc at 4°C and left to spread for 45 minutes at 37°C before removal of non-adherent platelets and subsequent fixation using 10% neutral buffered formalin. For *in vitro* experiments platelets were either pre-treated with inhibitor or vehicle or had these added 30 minutes after spreading had started. Platelets were probed using the mouse anti-CLEC-2 antibody AYP1 and a goat anti-mouse secondary antibody conjugated to Alexa Fluor 647 as well as Alexa Fluor 488-conjugated phalloidin. Super-resolution imaging was performed in switching buffer using an Eclipse Ti-E N-STORM microscope (Nikon Corporation, Tokyo, Japan) in (Direct Stochastic Optical Reconstruction Microscopy (dSTORM) mode as described by Poulter *et al* (Poulter et al. 2017). Images were reconstructed using the ThunderSTORM plugin in ImageJ 1.5 as described by Khan *et al* (A. O. Khan et al. 2017). Cluster analysis was then performed on the reconstructed images using persistence based clustering as has been recently described by Pike *et al* (Pike et al. 2018).The clustering was examined using the open-source software KNIME 3.4 (KNIME.com AG, Konstanz, Germany) and the R package 'RMSLM'. The local neighbourhood radius was set to 20nm, and the persistence threshold to 10 detections. Cluster area was calculated by placing a circle of radius 30 nm over every detection in a cluster and calculating the union of these circles. This was estimated using a grid with pixel size 5 nm and image based dilation. Clusters with less than 20 detection were discarded.

2.4 Biochemical and histological analysis

2.4.1 Protein phosphorylation

Washed platelets were pre-treated with 9 μM eptifibatide to block integrin αIIbβ3 activation. Agonists were added while stirring at 1200 rpm in an aggregometer at 37°C for 180 seconds unless stated otherwise. Stimulations were performed in the presence of ibrutinib (17 nM - 7 μM), acalabrutinib (50 nM – 200 μM) or vehicle (DMSO). For whole cell lysate experiments; activation was terminated with 5X SDS reducing sample buffer. For immunoprecipitation; $8x10^8$/ml platelets were used and reactions were terminated by addition of 2X ice-cold Nonidet P-40 lysis buffer containing the protease inhibitors sodium orthovanadate (5 mM), leupeptin (10 μg/ml), AEBSF (200 μg/ml), aprotinin (10 μg/ml) and pepstatin (1 μg/ml). Platelet lysates were pre-cleared, and detergent-insoluble debris was discarded. An aliquot was dissolved with SDS sample buffer for detection of total tyrosine phosphorylation. Lysates were incubated with either the indicated antibodies and protein A- or protein G-Sepharose. Lysates were separated by SDS-PAGE, electro-transferred, and Western blotted. Western blots were probed with the stated antibodies and imaged using ECL autoradiography film. For analysis of levels of phosphorylation, Western blot films were scanned and band intensity measured using ImageJ 1.5 (National Institutes of Health, USA) with values normalised to basal levels.

2.4.2 Immunohistochemistry

Paraffin embedded histological sections were de waxed and dehydrated with d-

limonene and ethanol respectively. Antigen retrieval was performed with citrate buffer. Endogenous peroxide was blocked with 3% hydrogen peroxide. Slides were probed with stated antibodies and imaged using a Zeiss Axio Scan Z1 slide scanner (Carl Zeiss AG, Oberkocken, Germany).

2.5 Animal experimentation and the IVC stenosis model

All mouse experiments were performed using wild type (WT) mice on a C57/Bl6 genetic background which were sourced from Charles River Laboratories Inc. (Wilmington, MA). For *ex vivo* platelet function assays and *in vivo* thrombosis assays 8 week old C57/Bl6 WT male mice were dosed by intraperitoneal (IP) injection with 35 mg/kg ibrutinib or vehicle (5% DMSO, 30% Polyethylene glycols (PEG) 300, 5% Tween 20, 60% deionised water) once daily for the stated number of days. Blood was taken at the stated times and platelet function analysis was performed as described above.

The IVC stenosis model was performed by Alex Brill as described by Payne *et al*. (Payne et al. 2017). In brief, mice were anaesthetised using isofluorane and then a laparotomy was performed. Side branches of the IVC were identified and tied off before the IVC itself was stenosed with a ligature, using a 30-gauge spacer to maintain a small degree of vessel patency. The incision was then closed and mice were allowed to recover from surgery. Buprenorphine was used pre- and post-operatively for analgesia. Mice were then culled 48 hours after the surgery and the IVC was examined for the presence, size and weight of thrombus.

2.6 Approvals and ethics

Ethical approval for collecting blood from patients with CLL and healthy volunteers was granted by the National Research Ethics Service (10/H1206/58) and Birmingham University Internal Ethical Review (ERN_11-0175) respectively. Work on patients with XLA and venous thrombosis tissue had ethical approval via the University of Birmingham Human Biomaterial Resource Centre (HBRC); Project 16-251 Amendment 1. Mouse work was conducted under the Home Office project licence P0E98D513 for *in vitro* and *ex vivo* analysis of platelet function and biochemistry and PPL 40/3745 for the *in vivo* thrombosis assay.

2.7 Statistical analysis

All data are presented as mean ± standard error of the mean (SEM) with statistical significance taken as $p < 0.05$ unless otherwise stated. Dose response curves were plotted and IC_{50} values were calculated using GraphPad Prism 7 (GraphPad Software Inc. La Jolla, Ca). Correlation of aggregation and tyrosine phosphorylation was assessed using Pearson's correlation coefficient. Statistical analysis was performed using one or two-way ANOVA with corrections for multiple comparisons as stated. Statistical analysis of the IC_{50} values was performed using Welch's t-test. Statistical analysis of the results of randomised controlled trials (RCTs) using ibrutinib and dasatinib were performed using a Cox regression analysis with a stratified cohort approach (as described by Giganti *et al.* (Giganti et al. 2015)) in the open source statistical package R 3.5.1. All other statistical analyses were performed using GraphPad Prism 7 (GraphPad Software Inc. La Jolla, Ca).

CHAPTER 3: THE EFFECT OF BTK INHIBITION ON PLATELET GPVI FUNCTION

3.1 Introduction

As alluded to previously there is a discrepancy in the literature when the information on the role GPVI plays in haemostasis is put together with what is known about the role of Btk downstream of GPVI and the observations of the haemostatic effects of Btk inhibitors. More specifically; GPVI deficient patients have a mild bleeding phenotype, patients with Btk mutations (XLA) have impaired GPVI-mediated platelet function but do not bleed and patients treated with Btk inhibitors (ibrutinib) have an increased rate of both mild and life-threatening bleeding and this is reported to be due to blockade of GPVI-mediated platelet function.

What follows is a discussion of the evidence underlying the role of Btk in GPVI signalling as elucidated from the use of Btk deficient patients and mice, the bleeding phenotype experienced by GPVI deficient patients and also of the anti-haemostatic and anti-platelet effects of the Btk inhibitor ibrutinib.

3.1.1 The effect of Btk deficiency on platelet GPVI function

Downstream of GPVI Btk activates PLCγ2 with resultant production of the second messengers IP_3 and DAG. It has been shown in other cell types that it

does this by phosphorylating some or all of PLCγ2's four tyrosine residues in the SH3-SH2 linker and C-terminal regions.

Consistent with this; patients with XLA and Btk knockout mice have blocked GPVI-mediated functional platelet responses but these can be overcome when high concentrations of agonist are used (Quek et al. 1998; Atkinson et al. 2003). Likewise overall PLCγ2 phosphorylation is significantly reduced but not lost entirely (Quek et al. 1998). The explanation for this incomplete blockade is that the other Tec family kinase in platelets, Tec, can substitute for Btk in its absence but because it is present in ~10-fold lower amounts than Btk (Burkhart et al. 2012; Zeiler et al. 2014), the lack of Btk still manifests in a defect at modest concentrations of agonist. It is also possible that the residual phosphorylation of PLCγ2 is mediated by Syk instead of/as well as Tec.

3.1.2 The bleeding phenotype of GPVI deficient patients

Patients with congenital or acquired defects in GPVI or its downstream signalling are rare, but a total of 17 patients have been described (Sugiyama et al. 1987; Moroi et al. 1989; Ryo et al. 1991; Arai et al. 1994; Tsuji et al. 1997; Takahashi & Moroi 2001; Boylan et al. 2004; Nurden et al. 2004; Bellucci et al. 2004; Kojima et al. 2006; Dunkley et al. 2007; Hermans et al. 2009; Dumont et al. 2009; Matus et al. 2013). The common symptoms, signs and investigation findings they all share are typical mild "platelet-type" bleeding (including ecchymoses, petechiae, menorrhagia and prolonged post-injury/surgical bleeding as well as bleeding peripartum), normal "coagulation screens", prolonged bleeding times and reduced aggregation responses on LTA to collagen, CRP or convulxin.

It has been stated in previous reviews on this topic that the fact that the patients described had additional complications, such as thrombocytopenia, made it unclear as to whether the bleeding was due partially or completely to the defect in collagen response (S. P. Watson et al. 2010). Whilst this is true of 8 of the patients described (three had moderate/severe thrombocytopenia associated with immune thrombocytopenia, ITP) (Sugiyama et al. 1987; Takahashi & Moroi 2001; Kojima et al. 2006), one had unexplained mild thrombocytopenia (Boylan et al. 2004), three had concurrent haematological malignancies but normal or low-normal platelet counts (Bellucci et al. 2004; Dunkley et al. 2007), and one had concurrent grey platelet syndrome (Nurden et al. 2004)), there are 9 patients who have no other complicating factors (i.e. they had normal platelet counts and no other medical conditions). All of these 9 patients had a suspected or proven congenital deficiency in GPVI or its downstream signalling and suffered from mild lifelong bleeding symptoms as described above (Ryo et al. 1991; Arai et al. 1994; Tsuji et al. 1997; Hermans et al. 2009; Dumont et al. 2009; Matus et al. 2013). Of particular note is that in the patients with ITP, the mild bleeding symptoms persisted in all of them after normalisation of their platelet count and in one of the patients with haematological malignancy, the bleeding symptoms had persisted since childhood, a long time before her lymphoma diagnosis at age 60.

It is certainly important to state, however, that case reports of mild bleeding in 17 patients still represents quite a paucity of information and it may well be that positive reporting bias is playing a role here; i.e. there could be many more GPVI deficient people in the population who have not been diagnosed because they lack any bleeding symptoms. It is also important to compare the relatively

mild symptoms of the small number of patients described here with the much more severe bleeding and the wealth of information surrounding deficiencies in other platelet receptors such as GPIb and integrin αIIbβ3.

3.1.3 The anti-haemostatic effects of ibrutinib

During the first trials of ibrutinib in MCL and CLL safety concerns were raised about its effect on bleeding (Byrd et al. 2013; Wang et al. 2015). Of the 196 patients studied 5% suffered from severe bleeding events such as subdural haematomas and haemorrhages following invasive procedures. Minor bleeding events occurred in ~16% of patients. Further information was published claiming concomitant anticoagulants or other underlying reasons for each of the patients suffering a major haemorrhage (Jones et al. 2017; Jones et al. 2014) and, as such, a recommendation was made that ibrutinib should not be co-administered with VKAs (Byrd et al. 2014; Janssen 2015; Burger et al. 2016; Chanan-Khan et al. 2016) and to withhold ibrutinib for 3-7 days before and after invasive procedures (Treon et al. 2015; Janssen 2015).

Further information was given showing “clotting screen” data from 25 patients. Platelet counts, Factor VIII levels, VWF antigen and activity levels were normal. Platelet Function Analyser (PFA) testing, however showed that 22 had prolonged closure times when tested with the epinephrine cartridges prior to starting treatment and a further 19 patients developed a transient defect during ibrutinib treatment. ADP closure times were normal (Lipsky et al. 2015).

Results from a subsequent trial where the use of warfarin was contraindicated was also published showing that the major bleeding rate had reduced to 1% (Jones et al. 2017; Jones et al. 2014). Further studies, however, have shown

ongoing minor bleeding rates of 28% in patients not on concomitant anticoagulant or antiplatelet treatment (Wang et al. 2015) and a systematic review that included RCTs showed a statistically significant 3-fold higher rate of bleeding of any grade in ibrutinib treated patients (Yun et al. 2017). Although it has been argued that, because bleeding events occur mostly in the first 6 months of treatment, the LPD itself, as well as the ibrutinib, may be contributing to the bleeding side effect (Jones et al. 2017).

3.1.4 The anti-platelet effects of ibrutinib

The first study looking at the effect of ibrutinib on platelet function showed reduced collagen-induced whole blood multiplate aggregation in 22 MCL/CLL patients whose blood had been treated *in vitro* with ibrutinib. It argued that, because Btk was involved downstream of many platelet receptors, ibrutinib may cause bleeding of its own accord and the bleeding seen in the trials should not just be dismissed as caused by VKAs (Rushworth et al. 2013).

Further studies then followed which showed that ibrutinib had no effect, in PRP *ex vivo*, on ADP mediated platelet responses but that it inhibited GPVI-mediated platelet aggregation at low and high concentrations of agonist and adhesion to fixed VWF at arterial shear. Importantly mild bleeding in these patients correlated with the degree of inhibition of platelet aggregation to high concentrations of GPVI agonist and adhesion to VWF (Kamel et al. 2015; Levade et al. 2014).

In vitro work included in one of these publications showed that ibrutinib at pharmacologically achieved concentrations inhibits GPVI-mediated platelet function in washed platelets and PRP and that this does also blocks Btk pY223

and downstream PLCɣ2 phosphorylation. Surprisingly they also showed that the same concentration inhibits whole cell tyrosine phosphorylation and Src phosphorylation at Y418 (Levade et al. 2014). In further *in vitro* work they showed that pharmacologically achieved concentrations of ibrutinib inhibit firm but not rolling adhesion to VWF and interpreted this as blocking inside-out signalling downstream of GPIb-IX-V (Levade et al. 2014).

Another group looked at the effect of *in vitro* ibrutinib on GPVI function with immobilised ligands as well as looking at its effects on integrin αIIbβ3 outside-in signalling. Using a fixed and supra-therapeutic concentration of ibrutinib that reduced Src pY418 (1 μM) they showed inhibited spreading and abrogated Ca^{2+} mobilisation on CRP, collagen and fibrinogen and reduced adhesion to CRP and fibrinogen but not collagen. Under arterial shear conditions they showed that 1 μM ibrutinib treatment had no effect on overall platelet surface coverage but that aggregate size started to tail off after 3 minutes of flow over collagen (presumably also reflecting an inhibition of inside-out signalling). Clot retraction in whole blood was also impaired by 1 μM ibrutinib (Bye et al. 2015).

In similar studies, but with two structurally related Btk inhibitors rather than ibrutinib itself, another group showed that, at concentrations where both inhibitors blocked Btk pY223 but one of the inhibitors also inhibited Src pY418, CRP induced P-selectin expression was blocked by both inhibitors but CRP, fibrinogen and collagen induced platelet spreading was only blocked by the inhibitor that blocked Src pY418. They also showed that both inhibitors reduced the surface coverage of platelets binding to collagen under arterial shear (Rigg et al. 2016). Interestingly dosing of these inhibitors to primates caused loss of *ex vivo* platelet aggregation to low concentration CRP but did not cause any

prolongation of their bleeding times (Rigg et al. 2016).

As well as studies looking at platelet function in classical haemostasis, another group looked at how the maintenance of inflammatory haemostasis was affected by ibrutinib. Unlike the studies discussed above, they used mouse platelets to perform their assays. They found that, while pharmacologically relevant concentrations of *in vitro* ibrutinib blocked aggregation to low concentrations of collagen, very high concentrations of ibrutinib (5 μM) were required to inhibit aggregation responses to high concentrations of collagen and in flow cytometry assays using activated integrin αIIbβ3, rather than P-selectin expression, as a marker of activation. They also found that this high concentration of ibrutinib was ineffective at blocking platelet aggregation when PRP was studied rather than washed platelets. Interestingly, in two models of inflammation induced vascular damage they found that, while thrombocytopenic mice had skin and alveolar haemorrhage in response to skin inflammation and lung injury respectively, even *in vitro* ibrutinib treated platelets could prevent haemorrhage when transfused into the mice. Though what they found when they re-tested the aggregation responses of the platelets at the end of the assay was that a small amount of platelet response had returned despite complete inhibition being demonstrated at the beginning of the experiment (Lee et al. 2017). Consistent with the lack of bleeding time results in the ibrutinib-analogue dosed Baboons used by Rigg *et al*. Lee *et al*. also found that when mice were treated with intraperitoneal (IP) ibrutinib at 6.25-12.5 mg/kg, this had no effect on saphenous vein thrombus formation or haemorrhage in response to laser injury or complete transection of the vein unless the mice also had an additional genetic knock-out of the $P2Y_{12}$ receptor (Lee et al. 2017).

In the studies outlined above there are a number of unexplained findings and also some discrepant results:

i) In the experiments by Levade *et al.* the same concentration of ibrutinib (0.5 μM) blocks aggregation in response to GPVI ligation in washed platelets and in PRP despite the drug being 97% plasma protein bound (Honigberg et al. 2010). Moreover, in dose response studies, they show that the minimum ibrutinib concentration that blocks Btk pY223 is 0.5 μM but that at this same concentration whole cell tyrosine phosphorylation is also lost, implying an upstream and downstream blockade as well as the on-target effect on Btk (Levade et al. 2014). They also show that adhesion to VWF under flow is inhibited by ibrutinib at 0.5 μM. They interpret this result as showing a blockade of Btk in GPIb mediated inside-out activation of integrin αIIbβ3. They do not reflect on the possibility of an off-target effect nor do they consider the results of Suzuki-Inoue *et al.* who show that this process is independent of PLCɣ2 phosphorylation, and therefore presumably also independent of Btk (Suzuki-Inoue et al. 2004).

ii) In the studies done by Bye *et al.* they use a single concentration of ibrutinib (1 μM) that they themselves show has some off-target effects on Src pY418. They use this concentration regardless of whether they are treating platelets or whole blood. They do not seem to consider that the dosing requirements may change if plasma proteins, which bind ibrutinib heavily, are introduced into the assay. This may be why, in contrast to the results of Rigg *et al*, they fail to show any change in surface coverage

in their flow adhesion assays (Bye et al. 2015). An alternative explanation is offered by the results of an identical assay performed by Busygina *et al*. where both *in vitro* and *ex vivo* ibrutinib is used. They show that adhesion in this assay is critically dependent on integrin α2β1 and on GP1b (neither of which require signalling for adhesion). Like Rigg *et al*, they make no comment on overall aggregate sizes however (Busygina et al. 2018).

iii) The results of the assays involving fibrinogen are interesting. Studies by Atkinson *et al.* in Tec kinase deficient mice have previously shown that neither Btk nor Tec are required for integrin αIIbβ3 outside-in signalling (Atkinson et al. 2003). This contrasts with the results obtained by Bye *et al.* and Rigg *et al.* where platelet spreading on fibrinogen is inhibited (Rigg et al. 2016). Perhaps the explanation for these discrepant results is, again, off-target effects of ibrutinib, particularly when it is seen that the ibrutinib analogue that has no effect on Src pY418 does not block fibrinogen binding but the ibrutinib analogue that inhibits Src pY418 does (Rigg et al. 2016).

Because of the known redundancy that exists between Tec kinases, it has been suggested that off-target inhibition of Tec as well as Btk by ibrutinib is responsible for many of the findings seen above (Shatzel et al. 2015). Indeed this is the rationale behind the development of acalabrutinib, which is much more Btk-specific (Byrd et al. 2016). Despite this, early reports from the trials using acalabrutinib still have low grade bleeding of up to 18%, not at all dissimilar to rates reported with ibrutinib (Shatzel et al. 2015). In addition, if the

effects on platelets were mediated through Tec inhibition, then these effects should be irreversible. The results from the studies in mice where some recovery in platelet function was seen would, therefore, argue against this (Lee et al. 2017).

So while it is clear from these studies that ibrutinib, at currently used clinical doses, does inhibit multiple aspects of platelet function and that these correlate with the increase in bleeding seen with its use, it is not clear at all which effects are mediated through the inhibition of Btk and which are caused by off-target effects. It is not clear, even, which other tyrosine kinases might be responsible for the off-target effects. What follows aims to answer these questions.

3.2 Results

3.2.1 Ibrutinib dose-dependently inhibits GPVI-mediated platelet function

3.2.1.1 Ibrutinib inhibits GPVI-mediated platelet aggregation in PRP

Given the >10-fold differences in concentrations of ibrutinib that inhibit GPVI-mediated platelet aggregation in PRP between different studies (Levade et al. 2014; Lee et al. 2017) LTA was performed by adding ibrutinib *in vitro* to healthy donor PRP. Ibrutinib caused a dose-dependent inhibition of aggregation (see Figure 3.1A) with complete blockade of aggregation at 70 μM and an IC_{50} of 25 μM (see Table 3.2). This is considerably higher than the inhibitory concentration used by Levade *et al*. (Levade et al. 2014) but the delay in aggregation seen at 7 μM is similar to the results of Lee *et al* (Lee et al. 2017).

3.2.1.2 Ibrutinib inhibits GPVI-mediated platelet aggregation in washed platelets

Because some studies showed that the concentrations of ibrutinib required to block GPVI-mediated platelet aggregation in washed platelets were the same as in PRP (Levade et al. 2014), and some studies showed a >10-fold difference in concentration (Lee et al. 2017) LTA was extended to include the addition of ibrutinib to washed platelets. Washed platelets were isolated from citrated blood of healthy donor volunteers and incubated with ibrutinib for

5 minutes as for the PRP experiments. As in PRP, ibrutinib inhibited GPVI-mediated platelet aggregation in washed platelets in a dose-dependent manner (see Figure 3.1B). But in contrast to PRP, the dose response curve was left-shifted approximately 20-fold with complete blockade at 1.7 μM and an IC_{50} at 1.2 μM (see Table 3.2). It was noted that at very low concentrations of ibrutinib (70 nM) there was a delay in aggregation but with maximal aggregation still reached.

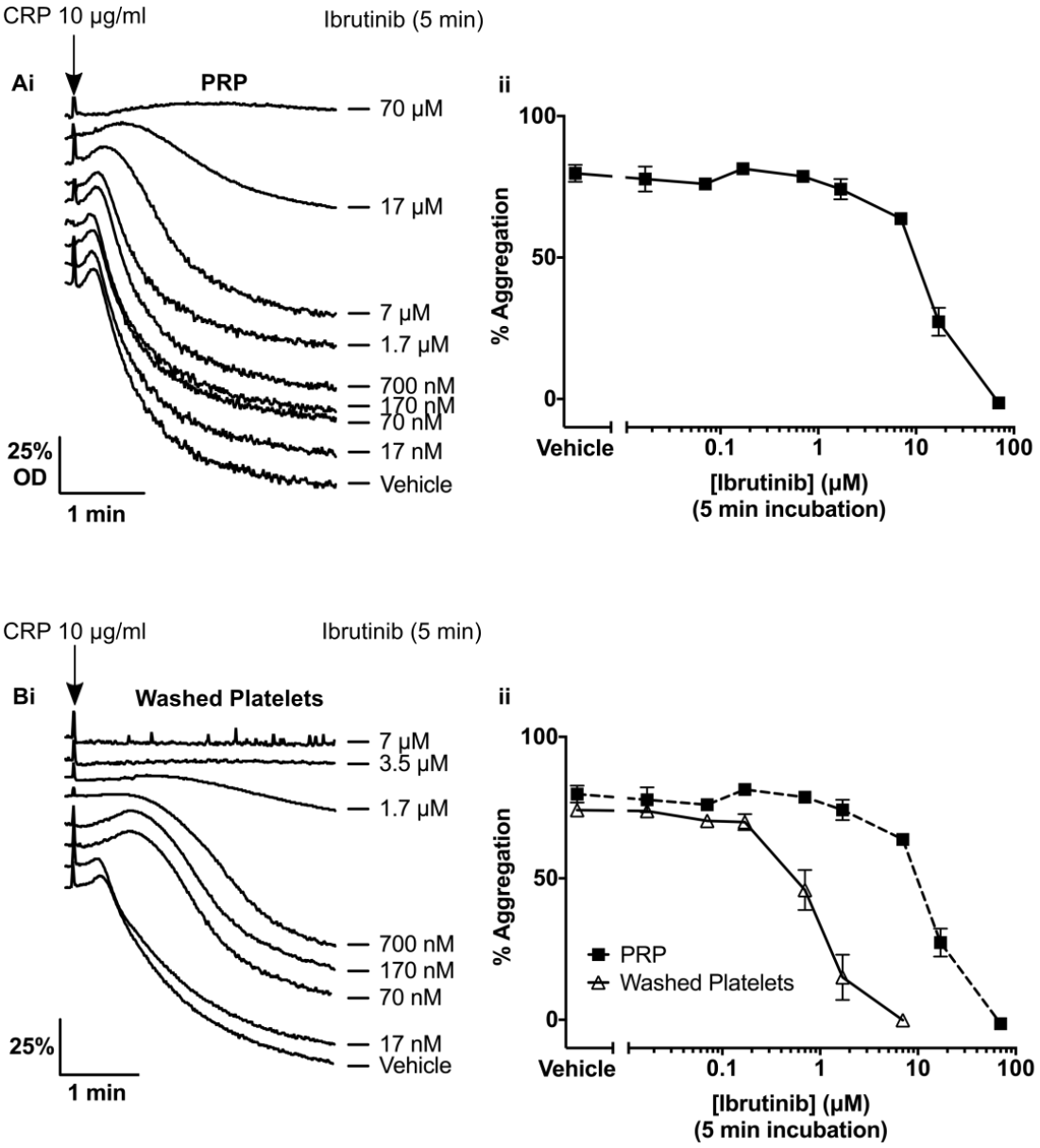

Figure 3.1: Ibrutinib dose-dependently inhibits GPVI-mediated platelet aggregation in PRP and washed platelets.
PRP (A) or washed platelets at $4x10^8$/ml (B) isolated from healthy donors was stimulated with CRP 10 µg/ml for 3 minutes after incubation with ibrutinib or vehicle at the stated concentrations for 5 minutes. Representative traces of LTA with (Ai) PRP and (Bi) washed platelets of three and six identical experiments respectively. Dose response curves for (Aii) PRP and (Bii) washed platelets (n=3 and n=6 respectively). The curve from Aii is shown as a dotted line in Bii to enable easy comparison. Results are shown as mean ± SEM.

The washed platelet dose response curve was slightly right-shifted when compared to the results of previous studies with similar experimental conditions (Levade et al. 2014; Bye et al. 2015). One possible explanation was the use of different agonists in these studies, so the same experiment was performed using the physiological agonist (collagen) instead of CRP. The results were similar regardless of the agonist used (see Figure 3.2A).

3.2.1.3 Inhibition of GPVI-mediated platelet aggregation by ibrutinib is not affected by the presence BSA

Another possible reason for the discrepancy between these results and those of Levade et al (Levade et al. 2014) and Bye et al (Bye et al. 2015) was the possibility that ibrutinib was becoming adsorbed to the sides of the aggregometer tube with less drug available for binding to the platelets. In order to investigate if this was happening, 0.3% BSA was added to the washed platelets and the same GPVI-mediated LTA in the presence of ibrutinib was performed. The results showed a small, but not statistically significant, reduction in aggregation in those aggregations performed with BSA in the vehicle and ibrutinib treated platelets (see Figure 3.2B).

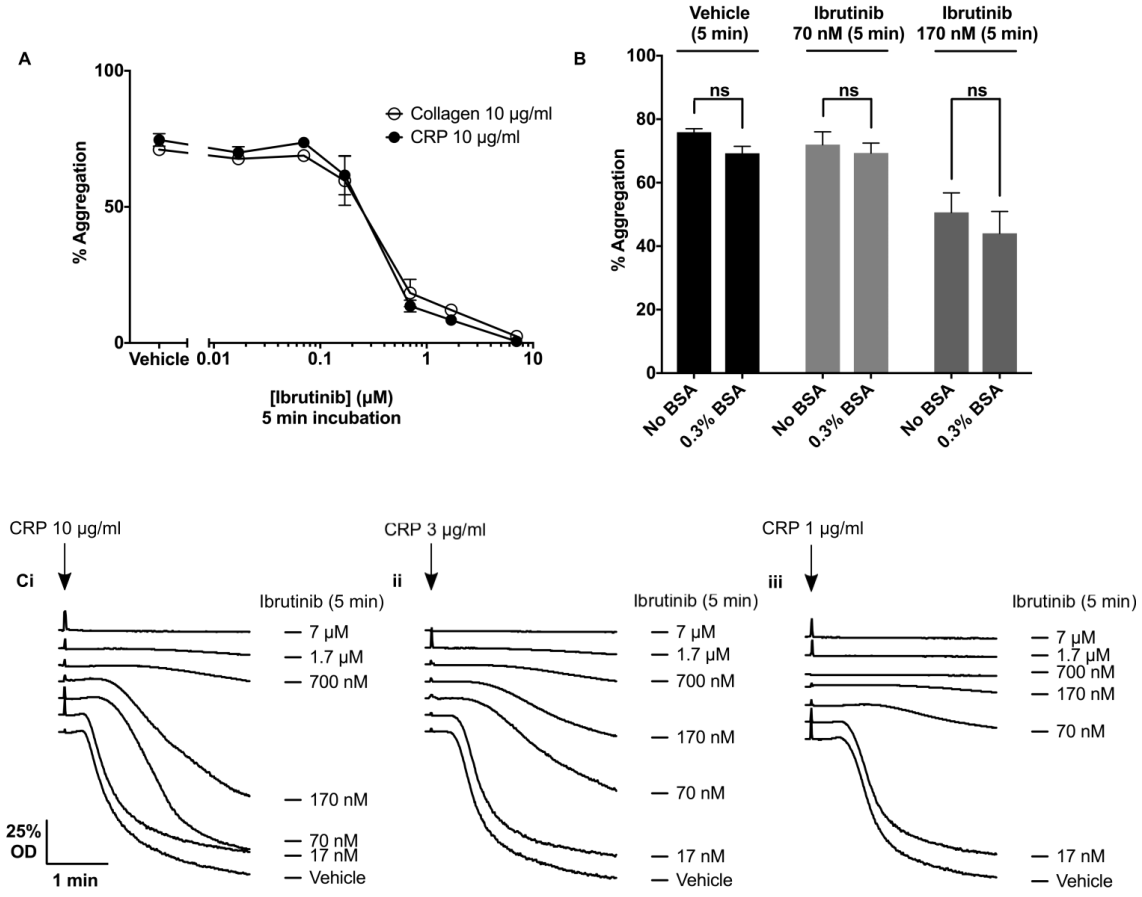

Figure 3.2: Ibrutinib dose-dependently inhibits aggregation stimulated by collagen or CRP, this is not enhanced by the presence of BSA but is made more potent by lowering the agonist concentration.
Healthy donor washed platelets at 4 x 10^8/ml were incubated with ibrutinib or vehicle for 5 minutes. (A) Dose response curve for ibrutinib inhibited aggregation when stimulated with CRP 10 µg/ml or collagen 10 µg/ml for 3 minutes (n=3). (B) The ibrutinib or vehicle was also incubated in the presence or absence of 0.3% BSA (Fatty acid free, boiled). They were then stimulated with CRP 10 µg/ml for 3 minutes (n=6). (C) Separately, without 0.3% BSA, the washed platelets were also stimulated with CRP at (i) 10 µg/ml (ii) 3 µg/ml or (iii) 1 µg/ml (n=1). All mean results shown ± SEM. Statistical analysis was with one way ANOVA. ns = non-significant.

3.2.1.4 The sensitivity to blockade by ibrutinib of GPVI-mediated platelet aggregation is dependent on concentration of agonist used

As well as different agonists, different concentrations of agonist might contribute to the slight right shift of the dose response curve when compared to previous studies. In fact, in the Levade *et al*. study there were a range of different agonist

concentrations used for each assay without comment on how these might have affected the results (Levade et al. 2014).

An experiment was performed, therefore, to include lower concentrations of CRP and this showed that GPVI-mediated platelet activation was more sensitive to inhibition by ibrutinib at lower concentrations of agonist (see Figure 3.2C). Of note, the concentration of ibrutinib (70 nM) at which delay to aggregation is seen with high concentrations of CRP (10 µg/ml) results in almost complete blockade of aggregation at low concentrations (1 µg/ml). Because there is no consensus on what is a physiologically relevant concentration of CRP and because the previous studies that showed a correlation between inhibition of GPVI-mediated platelet function and bleeding used high concentrations of agonist, further experiments proceeded using CRP 10 µg/ml as the agonist. Washed platelets were used for all further *in vitro* experiments because of the high degree of drug protein binding in PRP. BSA was not added to these platelets because of the lack of effect seen in Figure 3.2.

3.2.1.5 Ibrutinib inhibits GPVI-mediated platelet granule release

Platelet granule secretion plays a key role in platelet activation and so the effect of ibrutinib on GPVI-mediated granule secretion was also studied. Chronolume® treated washed platelets were stimulated with CRP in the presence or absence of ibrutinib in the same conditions as for LTA. As with LTA, ibrutinib dose-dependently inhibited platelet granule release (see Figure 3.3A) but the dose response curve was left-shifted when compared to the aggregation curve with an IC_{50} of 250 nM (see Table 3.2) and 700 nM causing

complete blockade.

3.2.1.6 Ibrutinib inhibits GPVI-mediated Ca^{2+} mobilisation

Ca^{2+} mobilisation is another crucial step in platelet activation. Thus experiments measuring Ca^{2+} mobilisation using exactly the same conditions as for LTA were attempted but these failed. If platelets were prepared with gentler spin steps, however (see Chapter 2), then it was possible to measure Ca^{2+} mobilisation in a 96 well plate using the Ca^{2+} sensitive dye Fura-2 AM.

This showed that ibrutinib also dose-dependently inhibited GPVI-mediated platelet Ca^{2+} mobilisation with a similar IC_{50} to that for aggregation (see Figure 3.3B and Table 3.2).

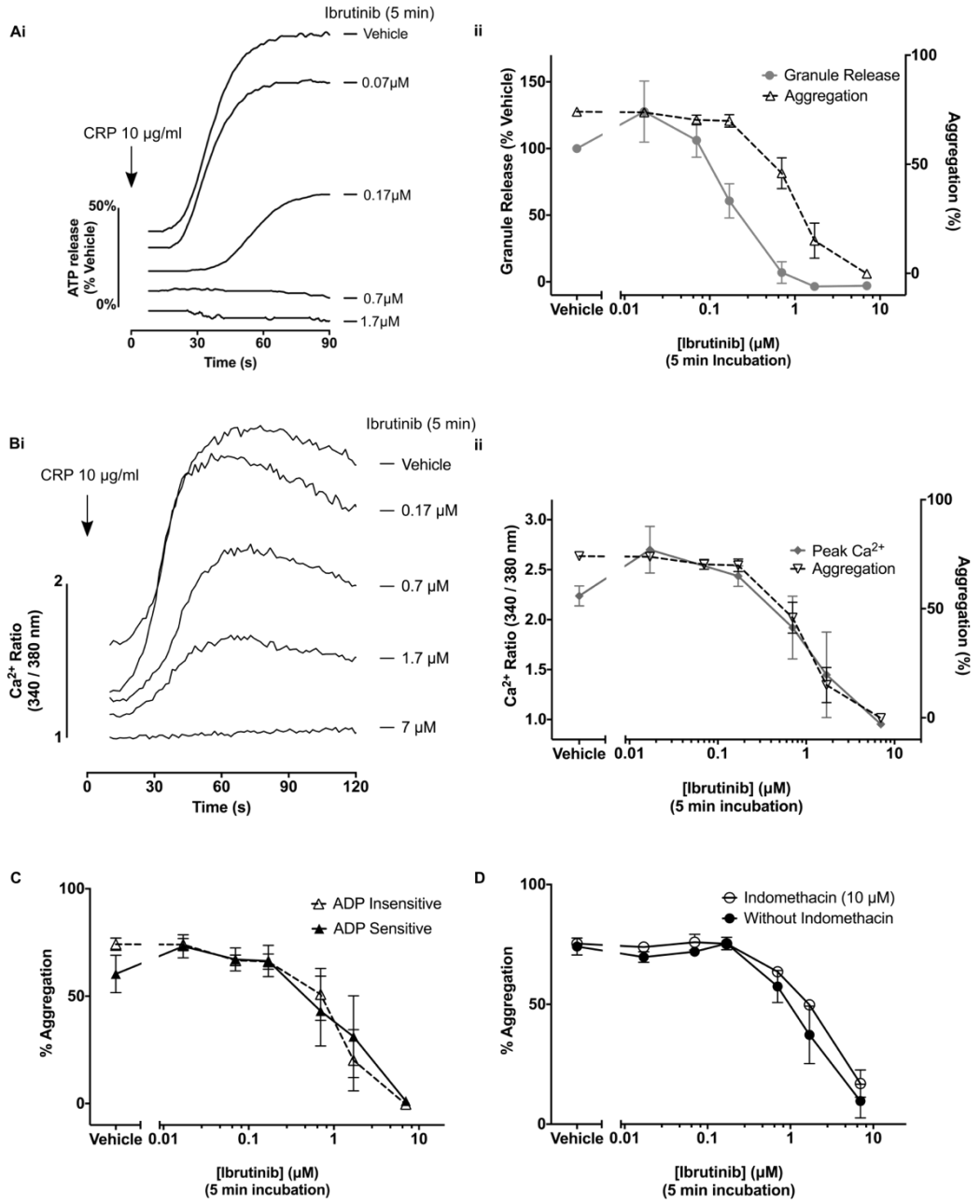

Figure 3.3: Ibrutinib dose-dependently inhibits GPVI-mediated granule release and Ca^{2+} mobilisation.
Healthy donor washed platelets at $4x10^8$/ml were treated with (A) Chronolume®, (B) the Ca^{2+} sensitive dye Fura-2 AM (C) nothing or (D) indomethacin (10 μM) then incubated with ibrutinib or vehicle for 5 minutes before being stimulated with CRP (10 μg/ml). Platelets from (B) and (C) were prepared using the ADP-sensitive method. (Ai) Representative ATP secretion trace from 3 identical experiments. (Aii) Dose response curve for granule release (n=3). (Bi) Representative luminescence trace from three identical experiments. (Bii) Dose response curve for Ca^{2+} mobilisation (n=3). (C) Dose response curve for aggregation for platelets prepared by ADP-sensitive or insensitive methods (n=3). (D) Dose response curve for aggregation for normally prepared platelets in the presence or absence of indomethacin (n=3). For A-C the dose response curve for LTA with ibrutinib treated normally prepared platelets is shown to enable comparison. All mean data is shown ± SEM.

3.2.1.7 ADP-sensitive human platelets display the same sensitivity to ibrutinib at inhibiting GPVI-mediated platelet aggregation as ADP-insensitive platelets

The method of platelet preparation used for the Ca^{2+} mobilisation experiments means that the platelets are able to be stimulated by ADP. It has previously been shown that traditional washed platelet preparation down-regulates the $P2Y_1$ receptor and this is what renders them insensitive to stimulation with ADP (Koessler et al. 2016).

Because of the different method of platelet preparation for the LTA and Ca^{2+} mobilisation assays. It needed to be established if this was introducing variability into the data. Therefore LTA using washed platelets prepared by the traditional and also the ADP-sensitive methods in the presence or absence of ibrutinib was performed using CRP 10 µg/ml as an agonist. This showed there was no difference in the sensitivity of GPVI-mediated platelet aggregation to ibrutinib regardless of which preparation method was used (see Figure 3.3C).

3.2.1.8 GPVI-mediated platelet aggregation in wild type mouse platelets has the same sensitivity to blockade by ibrutinib as human healthy donor platelets

Because of the discrepancy seen between the human platelet results of Levade et al and those of Lee et al. for mouse platelets, LTA using washed mouse platelets was performed in exactly the same conditions as for human platelets. Results in Figure 3.4 show that, like human platelets, ibrutinib also dose-

dependently inhibits mouse GPVI-mediated platelet function with a similar IC_{50} (see Table 3.2).

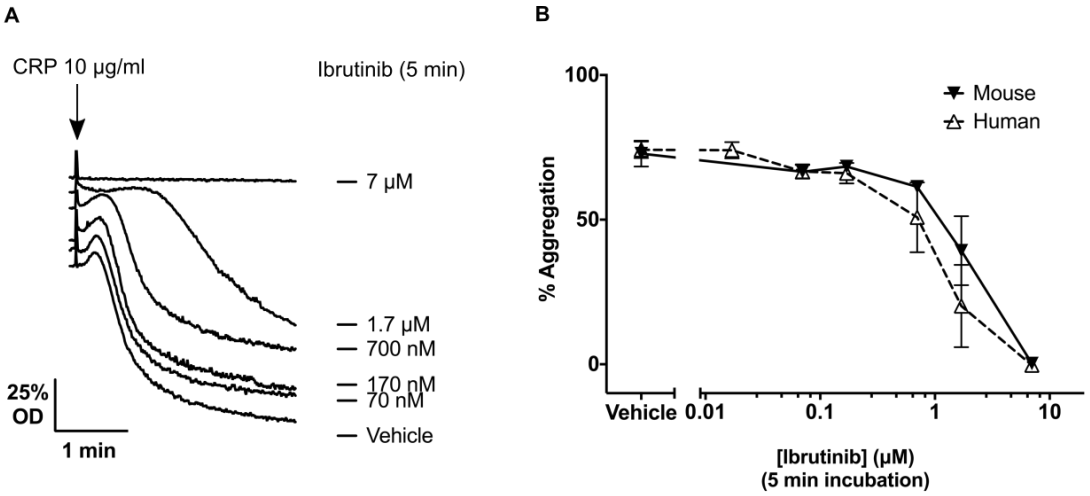

Figure 3.4: Ibrutinib dose-dependently inhibits GPVI-mediated mouse platelet aggregation with the same potency as for human platelets.
WT mouse washed platelets at $4x10^8$/ml were incubated with ibrutinib or vehicle for 5 minutes prior to being stimulated with CRP 10 µg/ml for 3 minutes. (A) Trace representative of 3 identical experiments. (B) Dose response curve for mouse aggregation (n=3). Curve for human platelet aggregation is shown as a dotted line for comparison. Results shown are mean ± SEM.

3.2.2 The inhibition of GPVI-mediated platelet function is reversible

The blockade of GPVI-mediated platelet function by ibrutinib has been postulated to be due to inhibition of Btk along with inhibition of the related non-receptor tyrosine kinase Tec (Byrd et al. 2016). If this was the case then the inhibition of GPVI-mediated platelet function by ibrutinib would be irreversible as Tec shares a conserved Cysteine in its ATP binding loop, equivalent to the Cys481 of Btk, which ibrutinib binds to irreversibly. (Brown et al. 2004) One existing study hints that inhibition of GPVI-mediated platelet function might not

be irreversible (Lee et al. 2017). Another suggests it is irreversible on the basis of mixing studies (Levade et al. 2014). Irreversible inhibition is characterised by being time-dependent and not able to be reversed despite washing out of excess drug.

3.2.2.1 Complete blockade of GPVI-mediated platelet aggregation is not time-dependent

To investigate whether the inhibition of GPVI-mediated platelet function by ibrutinib was time-dependent, platelets were incubated with ibrutinib or vehicle for increasing periods of time before stimulating with CRP. High concentrations of ibrutinib were able to inhibit GPVI-mediated platelet function after only a very short incubation (30 seconds) (see Figure 3.5Ai). The prolonged lag time seen with low concentrations of ibrutinib (70 nM) was only present after 5 minutes of incubation and the extent of the delay increased with lengthening incubation time but the overall aggregation percentage did not decrease with time (see Figure 3.5Aii-iv). This is consistent with the full blockade of aggregation, seen with high concentrations of ibrutinib, being due to a reversible action, but the delay, seen with low concentrations, being secondary to an irreversible action.

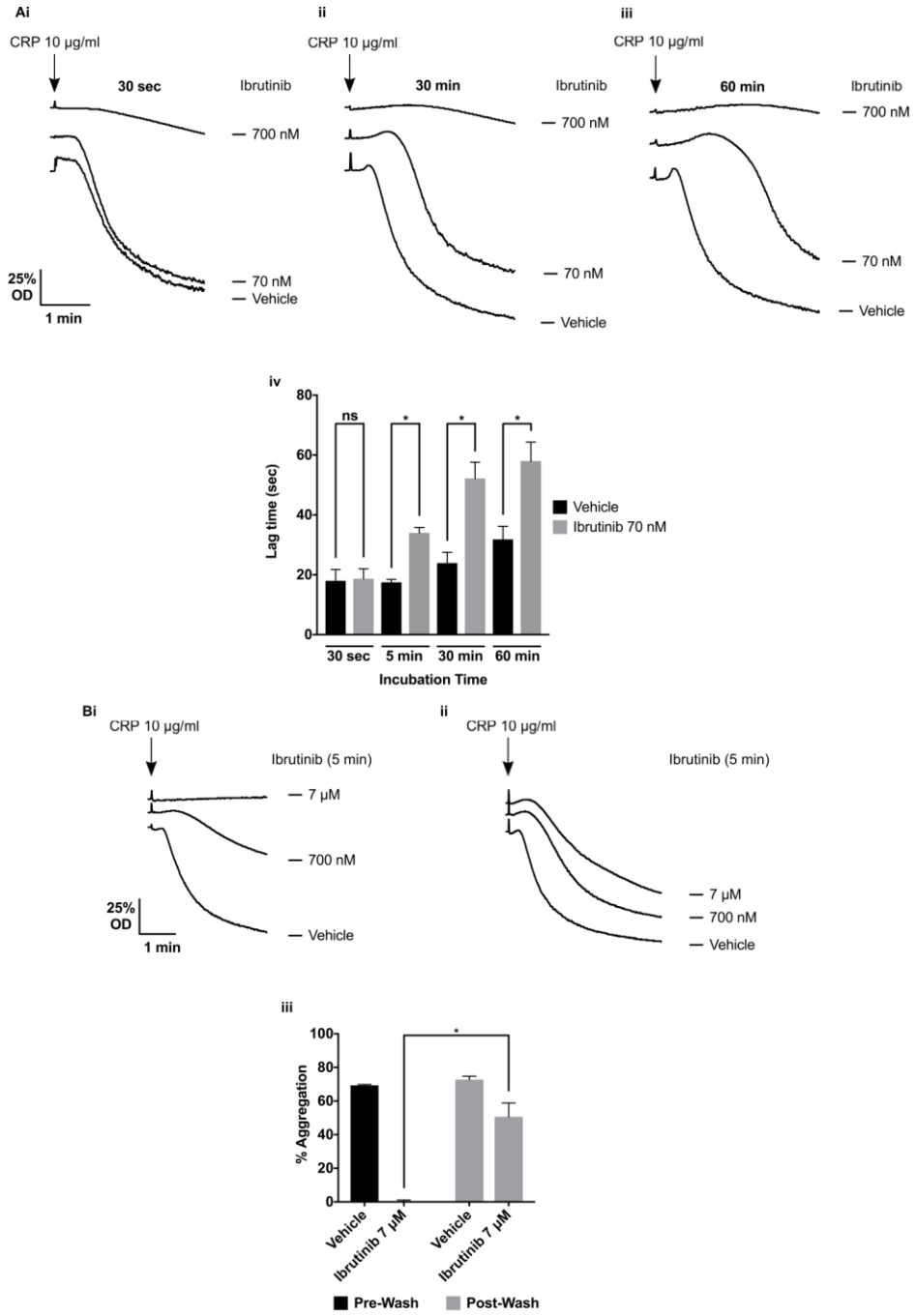

Figure 3.5: Complete blockade of GPVI-mediated platelet aggregation by ibrutinib is reversible and not time-dependent.
Human healthy donor washed platelets at $4x10^8$/ml were incubated with ibrutinib or vehicle for 30 seconds - 60 minutes before being stimulated with CRP 10 µg/ml. (Ai-iii) Representative aggregation traces from one of the three identical experiments. (iv) Mean data showing the effect of ibrutinib incubation time on the lag time between addition of agonist and beginning of aggregation (n=3). (Bi) Platelets were also incubated with ibrutinib or vehicle for 5 minutes before being stimulated with CRP 10 µg/ml. (ii) Alongside, washed platelets treated identically with either ibrutinib or vehicle were washed twice in modified-Tyrode's-HEPES buffer and resuspended back to $4x10^8$/ml. Platelets were then stimulated with CRP 10 µg/ml. (iii) Mean data (n=3). All results shown are mean ± SEM and were analysed with one-way ANOVA.* $P<0.05$, ns = non-significant.

3.2.2.2 Complete blockade of GPVI-mediated platelet aggregation is reversible

To directly test the reversibility of ibrutinib's effects on GPVI function; washed platelets were incubated with high concentrations of ibrutinib for 5 minutes before stimulation with CRP to ensure that full blockade had been achieved (see Figure 3.5Bi). Platelets incubated for 5 minutes with this same concentration of ibrutinib were then washed twice in modified Tyrode's-HEPES buffer in order to wash off the excess drug and then they too were stimulated with CRP. Strikingly, and in disagreement to results by Levade *et al.* which suggested that Btk inhibition was sufficient to block GPVI-mediated activation, the platelets where the excess ibrutinib had been washed out were able to aggregate fully to CRP (see Figure 3.5Bii-iii). The slight delay that had been noted in other aggregation experiments persisted, however, and was not able to be washed out.

3.2.3 Ibrutinib dose-dependently inhibits phosphorylation events downstream of the GPVI receptor

In order to investigate the effects of ibrutinib on the phosphorylation events downstream of the platelet GPVI receptor, and to see how changes in individual phosphorylation events influence the functional response of platelets to stimulation of the GPVI-receptor, platelet lysates were prepared. Ideally, these would be prepared using conditions that were identical to those used for the functional studies.

3.2.3.1 Pattern of inhibition of GPVI-mediated tyrosine phosphorylation is not affected by presence or absence of the integrin αIIbβ3 inhibitor eptifibatide

Normal practice for preparing platelet lysates with which to make western blots is to add reducing sample buffer under stirring but non-aggregating conditions by using the integrin αIIbβ3 inhibitor eptifibatide at a concentration of 9 μM. This is considered necessary to ensure there is no interference from signalling downstream of integrin αIIbβ3 which might alter the phosphorylation events downstream of GPVI.

To study whether or not the relevant signalling events changed in the absence of eptifibatide lysates were made in exactly the same conditions as for aggregations in the presence or absence of 9 μM eptifibatide. Results showed that pan-phosphorylation events were enhanced in the presence of eptifibatide

(see Figure 3.6A). This was particularly the case for proteins with a molecular weight > 100 kDa or those < 55 kDa. In order to study individual phosphorylation events phosphospecific antibodies were used and showed that it was possible to detect ibrutinib's inhibition of Btk pY223 in both conditions but downstream phosphorylation of the large molecular weight protein PLCɣ2 at Y1217 was much easier to detect in the presence of eptifibatide (see Figure 3.6A). Because it was crucial that the assay was sensitive enough to detect blockade of PLCɣ2 phosphorylation, further experiments were performed in the presence of 9 μM eptifibatide.

3.2.3.2 Level of phosphorylation post stimulation of the GPVI receptor is time-dependent

The next step taken to optimise conditions for making platelet lysates was to determine the optimum time point after stimulation to lyse the platelets. Therefore, as 70 nM ibrutinib was sufficient to block Btk pY223, platelets were incubated with either 70 nM ibrutinib or vehicle for 5 minutes prior to stimulation with CRP 10μg/ml and then reducing sample buffer was added at 20, 45, 90 and 180 seconds. The resultant lysates were then probed with the pan-phosphotyrosine antibody 4G10 as well as phosphospecific antibodies for pY residues upstream and downstream of Btk pY223.

For all samples peak phosphorylation levels were seen at 180 seconds with some, such as LAT pY200, being achieved more quickly than this (see Figure 3.6B). No loss of intensity following peak phosphorylation was seen at any point. As for aggregation experiments, these results led to the decision to use the time point of 180 seconds following stimulation with CRP to lyse platelets for

all future experiments.

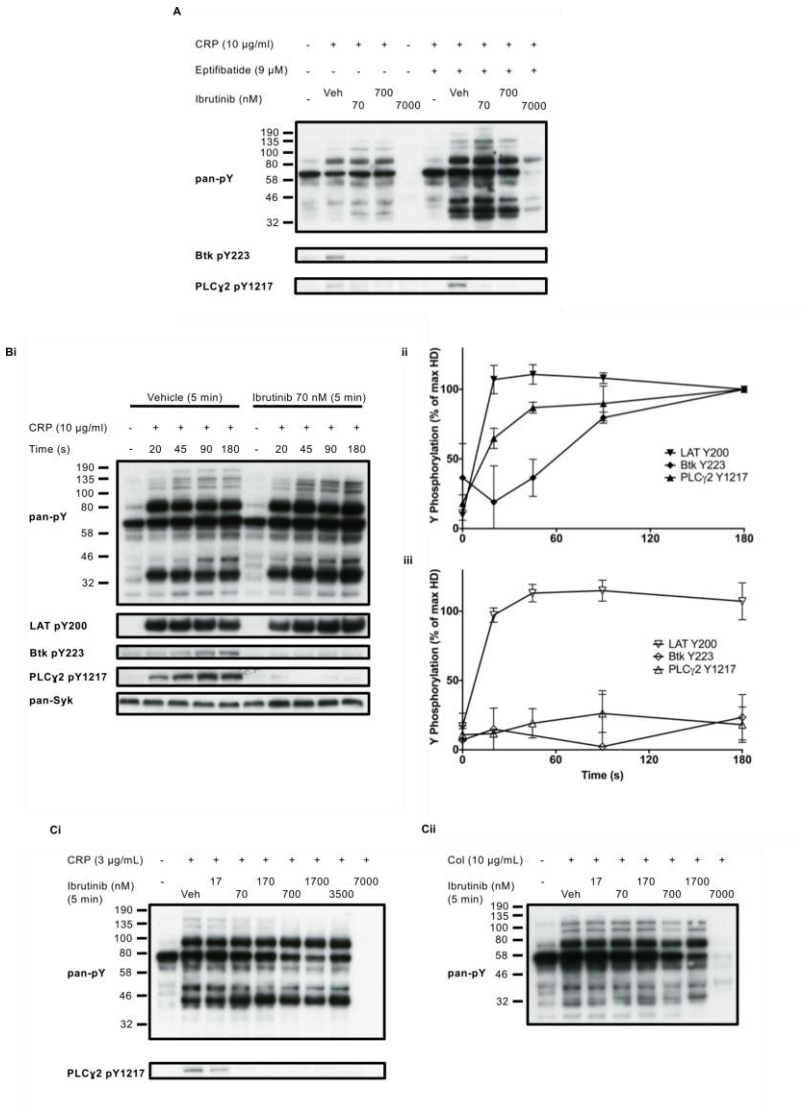

Figure 3.6: The level of phosphorylation of tyrosine residues on kinases and adapter proteins downstream of the GPVI receptor rises after stimulation and does not decrease up to 180 seconds. The pattern of inhibition of this phosphorylation by ibrutinib is not affected by treatment with eptifibatide or agonist concentration.

Healthy donor washed human platelets at $4x10^8$/ml were incubated with ibrutinib or vehicle for 5 minutes prior to stimulation. Platelets were then lysed with 5X reducing sample buffer after addition of agonist. Whole cell lysates were then separated by SDS-PAGE and Western blots were probed for whole cell phosphorylation or kinase phosphorylation with the stated antibodies downstream of the platelet GPVI receptor. (A) Representative blot of platelets incubated with ibrutinib or vehicle in the presence or absence of eptifibatide 9 µM and lysed 3 minutes after addition of CRP 10 µg/ml. Result shown is from two similar experiments. (B) Platelets incubated with ibrutinib or vehicle in the presence of eptifibatide 9 µM, stimulated with CRP 10 µg/ml and then lysed at the stated times. (i) Representative blot of three identical experiments. (ii, iii) Mean phosphorylation levels ± SEM for the vehicle and ibrutinib treated platelets were calculated by comparing band intensity to that of the 180 second stimulated vehicle control band (n=3). (C) Platelets were stimulated with (i) CRP 3 µg/ml or (ii) collagen 10 µg/ml 5 minutes before lysis. Blots are representative of a single experiment with CRP and three identical experiments with collagen.

3.2.3.3 Pattern of inhibition of GPVI-mediated tyrosine phosphorylation is not affected by the GPVI agonist used or its concentration

Biochemical studies are traditionally done with high concentrations of agonists in order to maximise the level of protein phosphorylation. Hitherto, all tests to optimise conditions for biochemical studies had been done using 10 µg/ml CRP as the agonist. Given that lowering the concentration of agonist increased the sensitivity of the platelets to inhibition by ibrutinib it was necessary to investigate whether lowering of the agonist concentration changed the concentration at which Btk pY223 was inhibited. Platelets were incubated with ibrutinib or vehicle and lysed 180 seconds after stimulation with 3 µg/ml CRP and probed with the pan-phosphotyrosine antibody 4G10 as well as the phosphospecific antibodies for Btk pY223 and PLCɣ2 pY1217. This showed that the pattern of inhibition of overall tyrosine phosphorylation as well as PLCɣ2 pY1217 was similar to that for platelets stimulated with 10 µg/ml CRP (see Figure 3.6Ci). Probing for Btk pY223 failed in this assay.

It has been shown above that ibrutinib's dose-dependent inhibition of GPVI-mediated platelet aggregation is unchanged whether collagen or CRP is used as the agonist. It was important to establish whether this interchangeability extended to biochemical studies. Thus platelets lysed 180 seconds after stimulation with collagen 10 µg/ml in the presence or absence of ibrutinib were probed with 4G10. The pattern of inhibition of whole cell phosphorylation was identical to that of platelets stimulated with CRP 10µg/ml (see Figure 3.6Cii). For this reason, and to maintain consistency between different assays, further biochemical studies were limited to stimulation with 10 µg/ml CRP as for

functional studies.

3.2.3.4 Ibrutinib inhibits autophosphorylation of Btk Y223 and downstream PLCγ2 phosphorylation at a lower IC_{50} than it inhibits aggregation. Inhibition of Src pY418 occurs at a higher IC_{50}.

It has been shown above that CRP induces robust whole cell tyrosine phosphorylation in platelets and that this is dose-dependently inhibited by ibrutinib. A detailed analysis of the dose response to ibrutinib on a wide range of proteins downstream of the GPVI receptor was investigated using phosphospecific antibodies.

Autophosphorylation of Btk at Y223 and downstream phosphorylation of PLCγ2 at Y753, Y759, Y1197 and Y1217 was reduced to basal levels by a low concentration of ibrutinib (70 nM) (see Figure 3.7Ai-ii). In contrast, phosphorylation of Btk on Y551, which is mediated by Src family kinases (Wahl et al. 1997), and proteins that lie upstream of Btk, namely Src Y418, Syk Y525/6, SLP76 Y145 and LAT Y200, was not altered (see Figure 3.7Ai,iii-iv). Inhibition of phosphorylation of Src on its activation site, Y418, was observed at a tenfold higher concentration of ibrutinib and shown to correlate with inhibition of aggregation (Pearson's correlation coefficient 0.959) (see Figure 3.7Ai,iv). Inhibition of whole cell phosphorylation and phosphorylation of Syk Y525/6, SLP76 Y145, Btk Y551 and LAT Y200 was seen at 7 μM ibrutinib which is tenfold higher than the maximal concentration in patients (see Figure 3.7Ai,iii-iv). Where analysable the IC_{50} values for each phosphorylation event are included in Table 3.2. Despite having a single good quality blot for inclusion in

the images seen in Figure 3.7Ai, the PLCγ2 pY1197 antibody generally gave very poor blots that could not be quantified and so its further use was abandoned.

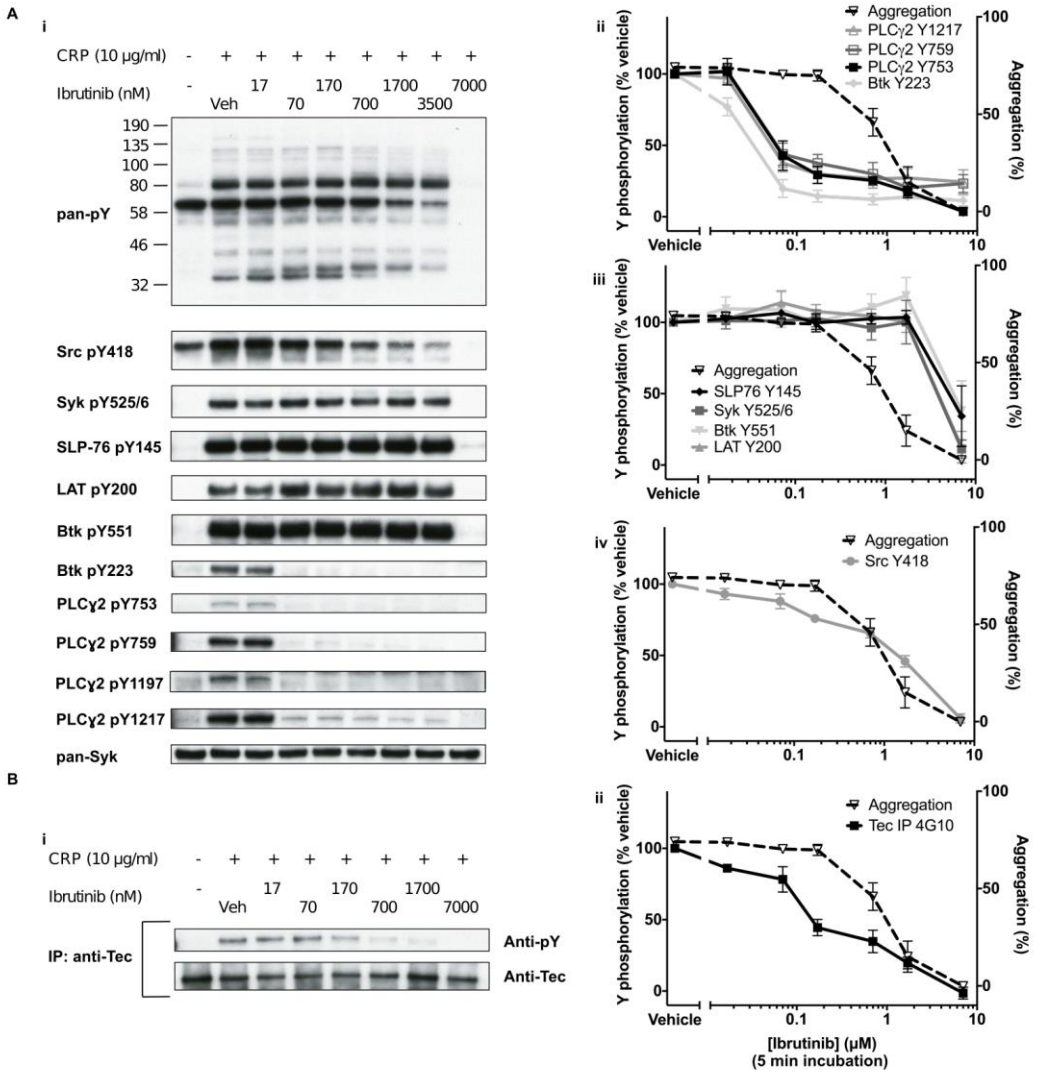

Figure 3.7: Ibrutinib inhibits Btk pY223 and downstream PLCγ2 phosphorylation at a lower concentrations than that which inhibits aggregation.
(A) Eptifibatide (9 µM) treated washed human platelets at 4×10^8/ml were incubated with ibrutinib or vehicle for 5 minutes followed by stimulation with CRP 10 µg/ml for 3 minutes. Samples were lysed with 5X SDS reducing sample buffer after 3 minutes. Whole cell lysates were then separated by SDS-PAGE and underwent Western blot with the stated antibodies for whole cell phosphorylation, kinases and proteins downstream of GPVI. (i) Blots are representative of four identical experiments. (ii-iv) Percentage tyrosine phosphorylation as compared to vehicle platelets was measured and is represented as the means ± SEM (n=4). The dose response curve for inhibition of washed platelet aggregation is shown as a dotted line to enable comparison. (B) Eptifibatide (9 µM) treated washed human platelets at 8×10^8/ml were stimulated with CRP 10 µg/ml after incubation with ibrutinib or vehicle for 5 minutes. After 3 minutes platelets were lysed with 2X ice cold lysis sample buffer. Lysates were pre-cleared and Tec was immunoprecipitated before addition of SDS reducing sample buffer and separation by SDS-PAGE and underwent Western blot with the anti-pY antibody 4G10. Membranes were stripped and then re-probed with the pan-Tec antibody. (i) Blots are representative of three identical experiments. (ii) The percentage of tyrosine phosphorylation as compared to vehicle treated platelets was measured and is represented as the means ± SEM (n=3).

3.2.3.5 Ibrutinib inhibits Tec phosphorylation at a higher concentration than for Btk pY223 but lower than that which inhibits aggregation

Tec is the only other Tec family kinase expressed in platelets (Burkhart et al. 2012). Ibrutinib is known to irreversibly inhibit Tec with an IC50 about 150 fold higher than that with which it inhibits Btk. (Honigberg et al. 2010). Due to the absence of phosphospecific antibodies for Tec, the effect of ibrutinib on Tec phosphorylation was investigated following immunoprecipitation and re-probing with the antiphosphotyrosine mAb 4G10. The effect of ibrutinib on Tec phosphorylation was biphasic with partial blockade at 170 nM and full blockade observed at 7 μM (see Figure 3.7B) consistent with there being two phosphorylation sites on Tec analogous to those on Btk. The IC_{50} of ibrutinib for Tec was unable to be calculated because of the biphasic nature of the dose response curve.

3.2.3.6 Blockade of GPVI-mediated platelet aggregation by ibrutinib is not affected by indomethacin

Given that it is generally accepted that PLCγ2 activation is required for Ca^{2+} mobilisation and subsequent activation of platelets, it was surprising that GPVI-mediated platelet aggregation and Ca^{2+} mobilisation were able to occur in the absence of any detectable PLCγ2 phosphorylation. This could be due to PLCγ2 activation occurring in the absence of phosphorylation, or it could be that the other major PLC isoform in platelets, PLCβ, is responsible for the Ca^{2+} mobilisation. The major route of PLCβ stimulation following GPVI activation is

via TP receptor stimulation with TxA_2. Production of TxA_2 can be blocked by indomethacin.

To test whether PLCβ was responsible for the Ca^{2+} mobilisation, platelets were stimulated by CRP 10 µg/ml in the presence or absence of indomethacin 10 µM for 3 minutes after being incubated with ibrutinib or vehicle for 5 minutes. There was no difference in the sensitivity of platelets to ibrutinib whether or not indomethacin was present (see Figure 3.3). This implies that PLCβ mediated Ca^{2+} mobilisation does not account for the difference seen between Ca^{2+} mobilisation and PLCγ2 phosphorylation when platelets are inhibited with low concentrations of ibrutinib.

3.2.3.7 Ibrutinib's inhibition of Btk Y223 autophosphorylation and downstream PLCγ2 phosphorylation is irreversible but upstream inhibition of Src Y418 is reversible.

To further investigate whether blockade of GPVI-mediated platelet activation by ibrutinib is secondary to its inhibition of Btk or an off-target effect the washout experiment described for the LTA experiments was repeated but with lysis of platelets at 3 minutes following stimulation with CRP 10 µg/ml.

The results showed that, consistent with ibrutinib's known irreversible binding to Btk, the effect of ibrutinib on Btk pY223 and downstream PLCγ2 phosphorylation was irreversible (see Figure 3.8). They also reveal that, like aggregation, ibrutinib's inhibition of Src pY418 was fully reversible along with variable and less consistent effects on other phosphorylation events such as LAT pY200 and Syk pY525/6 (see Figure 3.8).

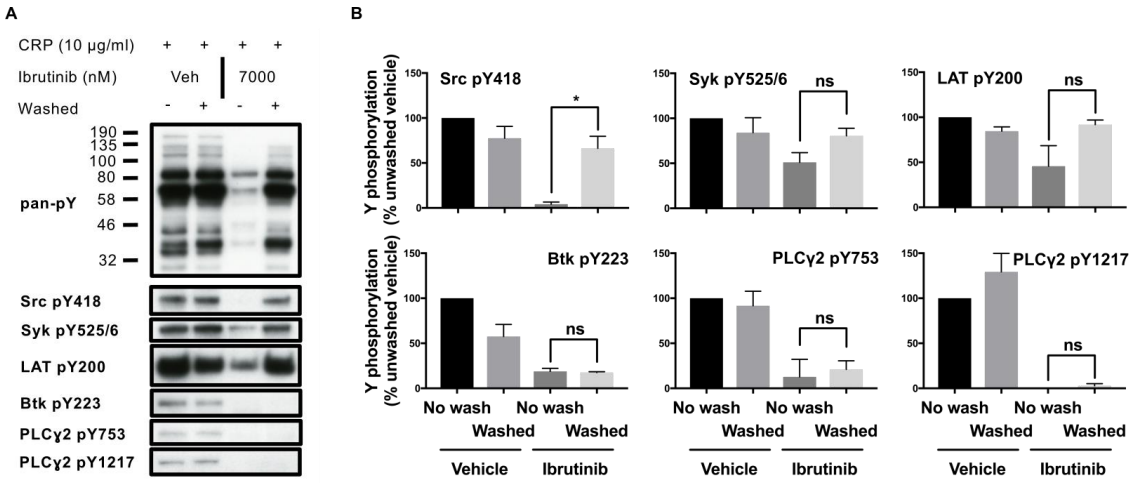

Figure 3.8: Phosphorylation of Btk at Y223 and PLCγ2 at Y753 and Y1217 is irreversible whereas Src pY418 is reversible.
Eptifibatide (9 µM) treated human healthy donor washed platelets at 4x10^8/ml were incubated with ibrutinib or vehicle for 5 minutes. They were then stimulated with CRP 10 µg/ml for 3 minutes prior to addition of 5X SDS reducing sample buffer. Alongside, platelets treated with ibrutinib or vehicle in the same way were washed twice in modified-Tyrode's-HEPES buffer before being stimulated with CRP 10 µg/ml. After 3 minutes these platelets too were lysed with 5X SDS reducing sample buffer. Whole cell lysates were then separated by SDS-PAGE and Western blot with the stated antibodies for whole cell phosphorylation, kinases and proteins downstream of GPVI. (A) Blots are representative of three identical experiments. (B) Percentage tyrosine phosphorylation as compared to non-washed vehicle platelets was measured and is represented as the means ± SEM (n=3). Results were analysed statistically using a paired two-tailed t-test* P<0.05, ns = non-significant.

3.2.3.8 Ibrutinib's inhibition of tyrosine phosphorylation downstream of mouse GPVI mimics human GPVI.

The inhibitory effect of ibrutinib on tyrosine phosphorylation downstream of the platelet GPVI receptor in mice was also studied using exactly the same conditions as used for the experiments on human platelets. Representative blots of whole cell phosphorylation and specific phosphorylation events as well as quantification data is shown in Figure 3.9. Like the results in human platelets, ibrutinib inhibited Btk pY223 and downstream PLCγ2 phosphorylation at lower concentrations than it inhibited aggregation, but these concentrations were not

quite as low as for human platelets (see Table 3.2). It also inhibited Src pY418 with an IC_{50} of 350 nM (but with very wide confidence intervals). Also like in human platelets, ibrutinib only inhibited whole cell phosphorylation and upstream phosphorylation at high concentrations (7 µM).

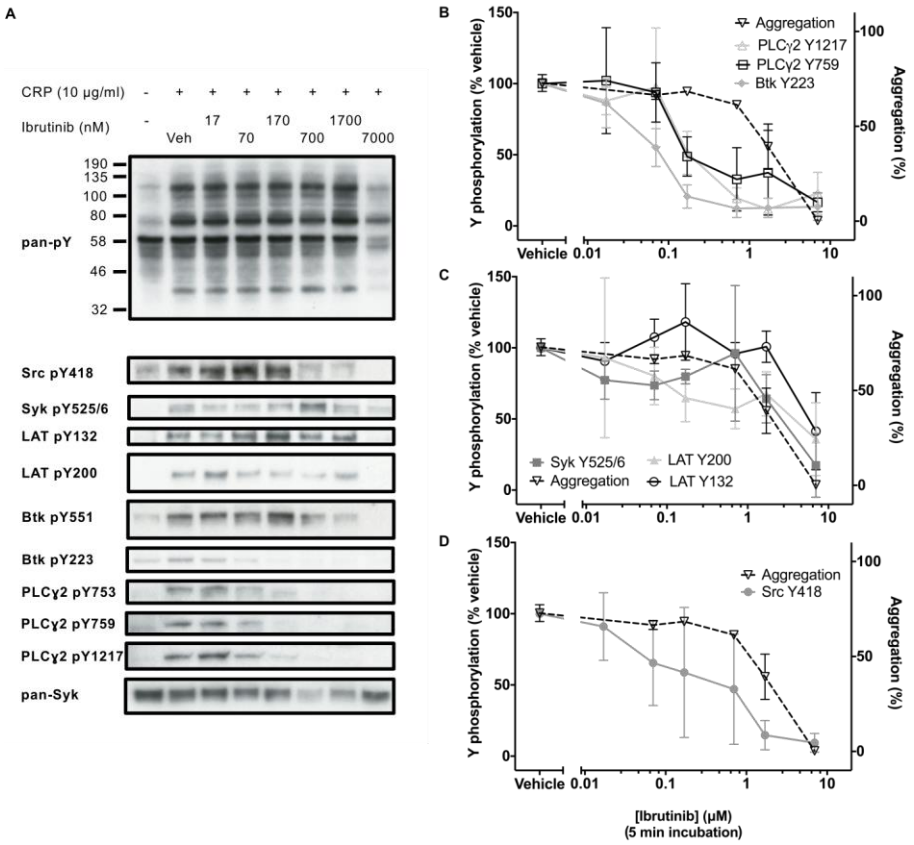

Figure 3.9: Ibrutinib dose-dependently inhibits GPVI-mediated Btk and downstream PLCγ2 phosphorylation in WT mouse platelets at lower concentrations than it inhibits aggregation in washed platelets.
Eptifibatide (9 µM) treated WT mouse platelets at $4x10^8$/ml were incubated with ibrutinib or vehicle for 5 minutes prior to stimulation with CRP 10 µg/ml. After stimulation for 3 minutes, platelets were lysed with 5X SDS reducing sample buffer. Whole cell lysates were then separated by SDS-PAGE and Western blot with the stated antibodies for whole cell phosphorylation, kinases and proteins downstream of GPVI. (A) Blots are representative of four similar experiments. Percentage tyrosine phosphorylation as compared to vehicle treated platelets was measured and is represented as the means ± SEM (n=3) for proteins downstream (B) and upstream (C) of Btk autophosphorylation as well as for Src pY418 (D). The dose response curve for inhibition of LTA is included as a dotted line to enable comparison.

3.2.4 Btk-specific concentrations of ibrutinib only have a very small

effect on spreading of platelets on immobilised collagen

Another important measure of platelet function is their ability to spread on a fixed ligand. The effect of ibrutinib on platelet spreading on immobilised collagen was assessed using washed platelets isolated from healthy donors. These were allowed to spread on collagen coated coverslips for 45 minutes prior to fixation, antibody staining and imaging. Platelets were treated with ibrutinib 170 nM or vehicle either for 5 minutes prior to spreading or for 15 minutes, after spreading had been ongoing for 30 minutes (see Figure 3.10). Confirmation of the expected effect on aggregation was confirmed prior to commencing the spreading experiment (not shown).

There was a statistically significant, but very small, reduction of platelet spreading area when ibrutinib was added to the platelets before spreading took place. There was also a statistically significant, but even smaller, increase in platelet spread area when ibrutinib was added after spreading had commenced (see Figure 3.10B).

There was no effect of adding ibrutinib on number of adherent platelets regardless of when the ibrutinib was added (see Figure 3.10C).

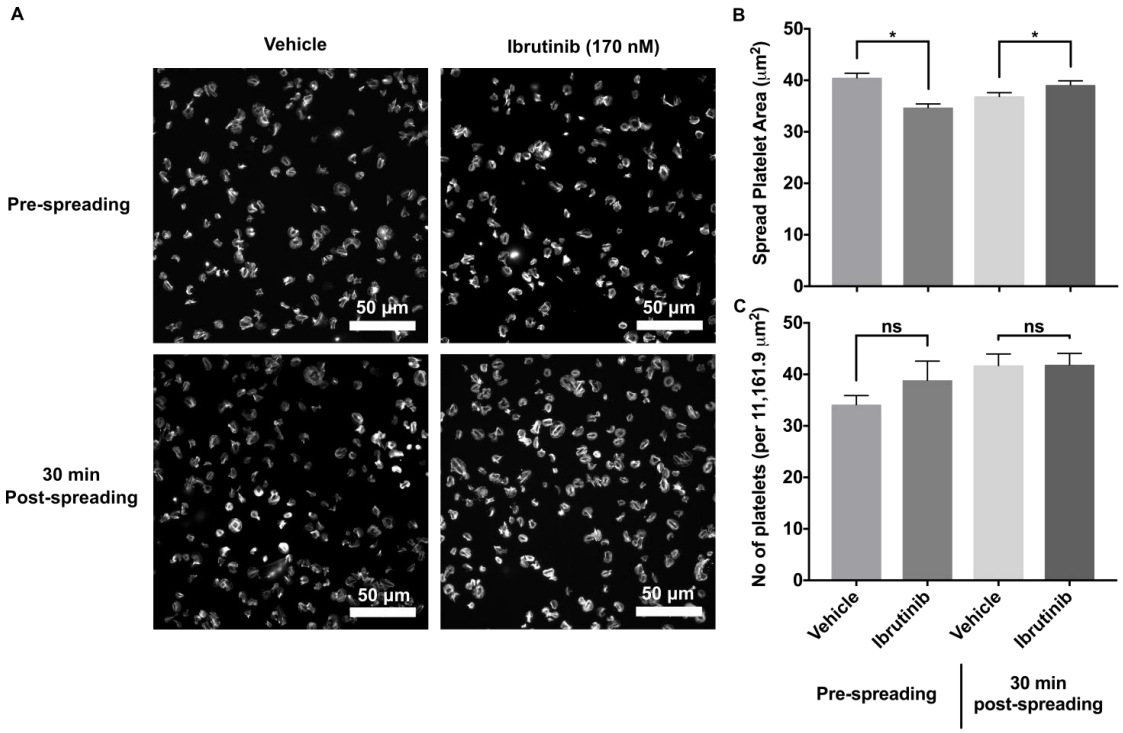

Figure 3.10: Btk-specific concentrations of ibrutinib only have a very small effect on spreading of platelets on immobilised collagen.
Human healthy donor washed platelets at $2x10^7$/ml were incubated with ibrutinib (170 nM) or vehicle for 5 minutes before spreading on collagen coated coverslips at 37°C for 45 minutes. Simultaneously, untreated platelets were spread on collagen coated coverslips at 37°C for 30 minutes before ibrutinib (170 nM) or vehicle was added and incubated for 15 minutes at 37°C. Coverslips were then washed to remove non-adherent platelets before fixation with formalin and staining with Phalloidin-488. (A) Representative images of three identical experiments. Ilastik machine learning software was used to automatically and reproducibly identify platelets. Data on platelet number and surface area was measured using the KNIME analytics platform. (B) Mean data ± SEM (n=3). Statistical analysis performed using two-tailed Welch's t-test. (C) Mean data ± SEM (n=3). Statistical analysis performed using a one-way ANOVA with Tukey's correction for multiple comparisons.

3.2.5 Acalabrutinib dose-dependently inhibits GPVI-mediated platelet function and tyrosine phosphorylation

In order to further corroborate which effects of ibrutinib are mediated by its effects on Btk and which by off-target effects the second generation, more Btk-specific, inhibitor acalabrutinib was used. Similar assays to those with ibrutinib

were performed.

3.2.5.1 Acalabrutinib dose-dependently inhibits GPVI-mediated platelet aggregation

Like ibrutinib, acalabrutinib added to washed platelets prior to stimulation with CRP 10 µg/ml also inhibited GPVI-mediated platelet aggregation in a dose-dependent manner. This is shown in Figure 3.11A-B. This was similar to the effect of ibrutinib but it occurred at higher concentrations. The IC_{50} for acalabrutinib's inhibition of aggregation was ~20-fold higher than that for ibrutinib (see Table 3.2). Also like the results seen with ibrutinib, there was a delay in aggregation at 2 uM acalabrutinib (not quantified).

3.2.5.2 Acalabrutinib dose-dependently inhibits GPVI-mediated granule release

The effects of acalabrutinib on platelet function were extended to look at granule secretion. As for aggregation and like that seen with ibrutinib, acalabrutinib inhibited GPVI-induced granule secretion in a dose-dependent manner but with the dose response curve slightly left-shifted (see Figure 3.11C-D and Table 3.2).

3.2.5.3 Acalabrutinib dose-dependently inhibits GPVI-mediated Ca^{2+} mobilisation

Acalabrutinib's effects on platelet function were further extended to look at Ca^{2+} mobilisation. Again, as for aggregation and granule secretion, acalabrutinib inhibited GPVI-induced Ca^{2+} mobilisation in a dose-dependent manner over a similar concentration range with a similar IC_{50} to that for inhibition of granule release (ie slightly left-shifted when compared with aggregation) (see Figure 3.11E-F and Table 3.2).

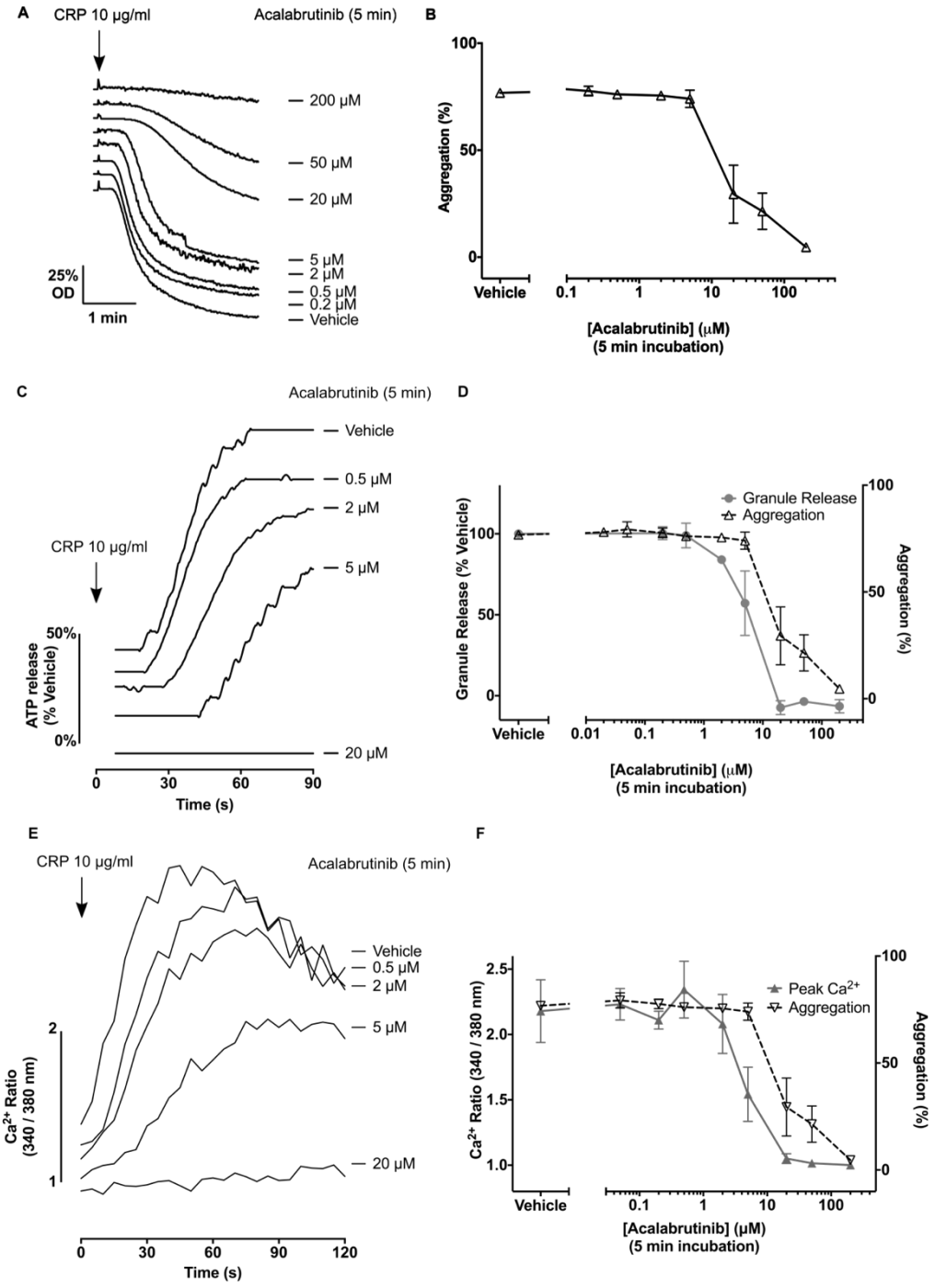

Figure 3.11: Acalabrutinib inhibits GPVI-mediated platelet function in a dose-dependent manner.
Human healthy donor washed platelets at $4x10^8$/ml were incubated with acalabrutinib or vehicle for 5 minutes before stimulation with 10 µg/ml CRP. (A) LTA trace representative of six identical experiments and (B) dose response curve (n=6) is shown as mean ± SEM. (C) Representative trace and (D) dose response curve for granule release from 3 identical experiments. The equivalent curve for LTA is shown as a dotted line to allow comparison. Results shown are mean ± SEM. (E) Representative trace from three identical experiments and (F) dose response curve (n=3) for Ca^{2+} mobilisation. Results shown are mean ± SEM.

3.2.5.4 Acalabrutinib inhibits Btk Y223 and downstream PLCɣ2 phosphorylation with a lower IC_{50} than its inhibition of aggregation but leaves upstream phosphorylation unaffected

As for ibrutinib, functional experiments with acalabrutinib were expanded by looking further into the biochemical signalling pathway using Western blot with the same phosphospecific antibodies. This showed similar overall inhibition of pan-phosphotyrosine levels, Btk Y223 and downstream phosphorylation of PLCɣ2 (see Figure 3.12Ai-ii). It also showed a similar lack of inhibition of phosphorylation upstream of Btk Y223 (see Figure 3.12Aiii). Notably however, unlike inhibition with ibrutinib, Src pY418 was unaffected by even very large concentrations of acalabrutinib (see Figure 3.12Aiv). Like ibrutinib, acalabrutinib inhibited Tec phosphorylation in a biphasic dose-dependent manner (see Figure 3.12B) over a lower concentration range than that which inhibited aggregation. The IC_{50} for the inhibition of Tec phosphorylation could not be calculated because of the biphasic nature of the curve.

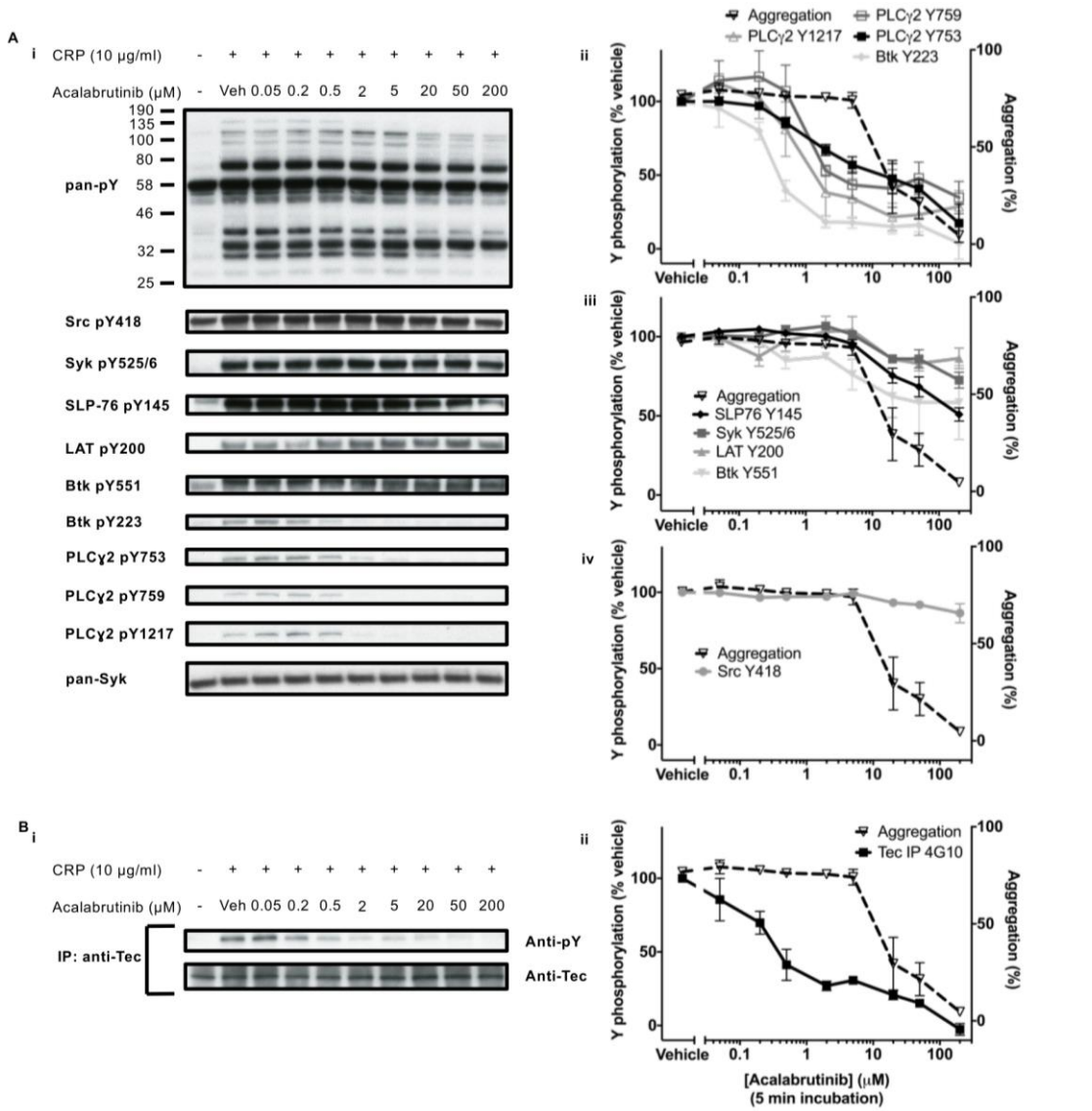

Figure 3.12: Acalabrutinib inhibits Btk pY223 and downstream PLCγ2 phosphorylation at a lower concentration than that which inhibits aggregation.
(A) Eptifibatide (9 µM) treated washed human platelets at 4×10^8/ml were incubated with acalabrutinib or vehicle for 5 minutes followed by stimulation with CRP 10 µg/ml for 3 minutes. Samples were lysed with 5X SDS reducing sample buffer after 3 minutes. Whole cell lysates were then separated by SDS-PAGE and underwent Western blot with the stated antibodies for whole cell phosphorylation, kinases and proteins downstream of GPVI. (i) Blots are representative of three identical experiments. (ii-iv) Percentage tyrosine phosphorylation as compared to vehicle platelets was measured and is represented as the means ± SEM (n=3). The dose response curve for inhibition of washed platelet aggregation is shown as a dotted line to enable comparison. (B) Eptifibatide (9 µM) treated washed human platelets at 8×10^8/ml were stimulated with CRP 10 µg/ml after incubation with acalabrutinib or vehicle for 5 minutes. After 3 minutes platelets were lysed with 2X ice cold lysis sample buffer. Lysates were pre-cleared and Tec was immunoprecipitated before addition of SDS reducing sample buffer and separation by SDS-PAGE and underwent Western blot with the anti-pY antibody 4G10. Membranes were stripped and then re-probed with the pan-Tec antibody. (i) Blots are representative of three identical experiments. (ii) The percentage of tyrosine phosphorylation as compared to vehicle treated platelets was measured and is represented as the means ± SEM (n=3).

3.2.6 Btk-specific concentrations of ibrutinib have no effect on adhesion or aggregation to collagen in whole blood under flow conditions at arterial shear

Btk-specific concentrations of ibrutinib fail to inhibit GPVI-mediated platelet aggregation, granule release and Ca^{2+} mobilisation stimulated with high concentrations of CRP but can block at low concentrations of CRP. The significance of this observation was investigated by using the more physiological flow adhesion assay in whole blood. To circumvent the issue of ibrutinib's high level of plasma protein binding and so achieve a known degree of Btk inhibition washed platelets were isolated from citrated healthy donor whole blood and incubated with 70 nM ibrutinib for 5 minutes before being reconstituted with autologous platelet poor plasma and red cells to a final platelet concentration of 400 $x10^9$/l. To confirm Btk inhibition, the expected effect of delayed platelet aggregation to CRP was verified before reconstitution (see Figure 3.13A). The reconstituted blood was then flowed through a collagen coated glass capillary at arterial shear rates for 3 minutes before being fixed, after which 5 images were taken, equally spaced along the capillary. Platelet coverage was unchanged when compared to vehicle treated controls (see Figure 3.13B-C).

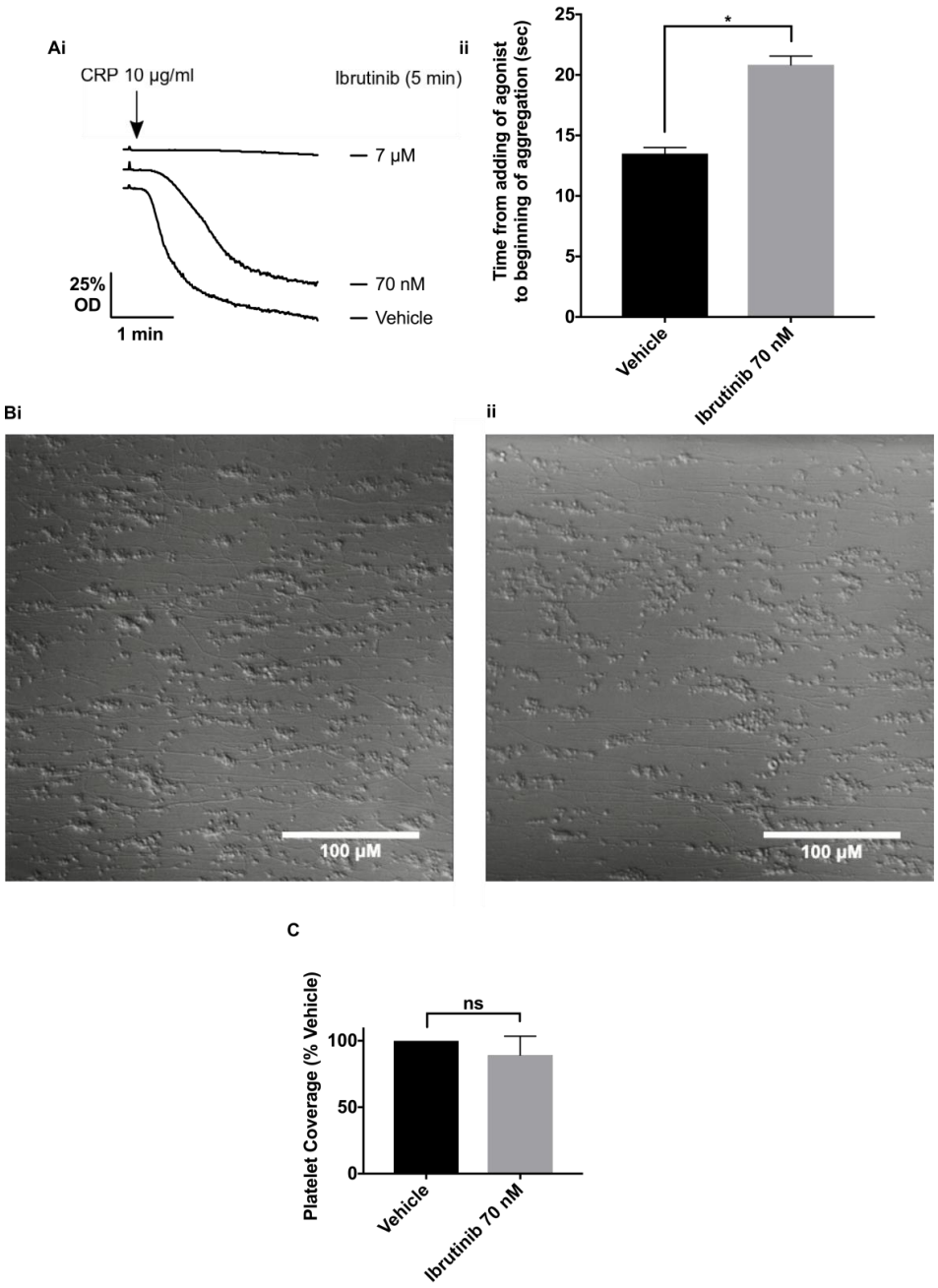

Figure 3.13: *In vitro* low concentration ibrutinib has no effect on adhesion to collagen under flow.
Human healthy donor washed platelets at $10x10^8$/ml were incubated with ibrutinib or vehicle for 5 minutes. (A) A 300 µl aliquot of these platelets was stimulated with CRP 10 µg/ml to measure LTA. (i) Representative trace of three identical experiments and (ii) results shown as mean ± SEM (n=3). The remainder of the platelets were reconstituted with autologous red cells and PPP to a final platelet concentration of $400x10^9$/l and incubated with $DiOC_6$ dye for 5 minutes before being flowed over collagen at 1000 s^{-1} for 3 minutes. Flow capillaries were then flushed with modified-Tyrode's-HEPES buffer and fixed with formalin before being imaged in DIC and Fluorescent channels on a Zeiss Axio inverted microscope at 20X magnification. Representative images are shown in (B). ImageJ was used to analyse platelet surface coverage. Results are shown in (C) as mean ± SEM (n=3). Statistical analyses by paired t-tests. *P<0.05, ns = non significant.

3.2.7 Platelets taken ex vivo from patients on Btk inhibitors

3.2.7.1 Platelets taken from untreated patients with CLL have partially inhibited GPVI-mediated platelet aggregation

In order to study the effects of Btk inhibitors *ex vivo* it was necessary to use patients with B-cell lymphoproliferative disorders as these were the only patients prescribed these drugs. There have been reports that patients with CLL with high white cell counts have reduced whole blood platelet aggregation in response to stimulation with ADP because of excess activity of leukocyte ecto-nucleotidase (Glenn et al. 2009). It was important to establish if a similar reduction occurs in response to GPVI ligation.

Initial studies were done, therefore, on untreated patients with CLL as well as those same patients after treatment with a single cycle of a “standard” chemotherapy regimen containing the purine analogue fludarabine, the alkylating agent cyclophosphamide and the anti-CD20 antibody rituximab (FCR). These showed that, in untreated patients with CLL, there was a non-statistically significant trend to reduced platelet aggregation in PRP to all concentrations of CRP, the thrombin receptor agonist PAR1-peptide and ADP and a significant reduction in platelet aggregation in response to medium and high concentrations of collagen (see Figure 3.14A). There was no significant increase in platelet count following the chemotherapy to explain the improved aggregation but the white cell count (WCC) did decrease, although this was not statistically significant because of the large variation in WCCs in CLL patients prior to starting treatment (see Figure 3.14Biii). These results confirmed that it

was necessary to include pre-treatment platelet function testing when proceeding to analysis of GPVI-mediated platelet function of patients on Btk inhibitors.

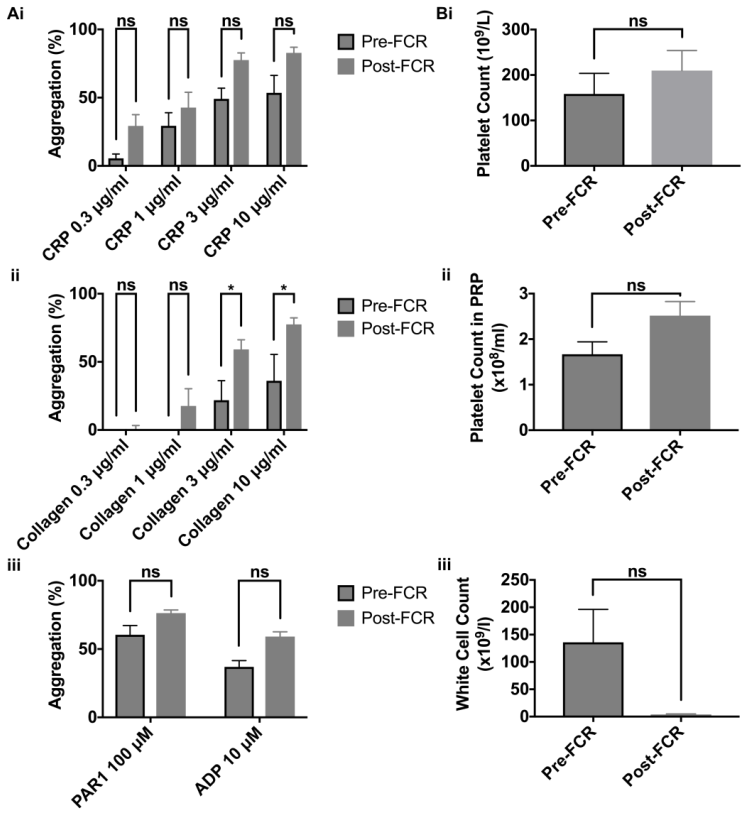

Figure 3.14: Patients with CLL who have received chemotherapy have increased platelet aggregation responses to collagen but aggregation in response to CRP, PAR1 peptide and ADP are unchanged.
PRP was isolated from the blood of four patients with CLL immediately prior to treatment with FCR chemotherapy and then again from the same patients immediately prior to their second cycle of chemotherapy. (A) Optical density of PRP was measured over 3 minutes following stimulation with (i) CRP 0.3 - 10 µg/ml, (ii) collagen 0.3 - 10 µg/ml, (iii) PAR1 peptide 100 µM and ADP 10 µM. Results shown are mean ± SEM of four identical experiments. Statistical analysis was performed with a 2-way ANOVA with Sidak's multiple comparison test. (B) White cell and platelet counts in whole blood as well as platelet counts in the isolated PRP were measured and are shown as mean ± SEM with statistical analysis performed using a two tailed paired t-test (n=4). *P<0.05, ns = non-significant.

3.2.7.2 Platelets from patients on ibrutinib show reduced platelet aggregation in response to GPVI activation

Studies were extended to include patients before and after taking ibrutinib 420 mg once daily as a single agent or in combination with rituximab 375 mg/m^2 once monthly. Because of the relative difficulty in identifying and acquiring blood pre-treatment, not all patients on treatment were able to have platelet function analysis pre-treatment as well as post-treatment.

Results showed a significant reduction in GPVI-mediated platelet aggregation to low (CRP), medium and high (CRP and collagen) concentrations of agonist in the patients taking ibrutinib (see Figure 3.15Ai-ii). There was no difference, however, in the response to stimulation by GPCR agonists PAR1 peptide or ADP (see Figure 3.15Aiii). There was no difference in the whole blood or PRP platelet count between treatment groups (see Figure 3.15Bi-ii) and, similar to the results on chemotherapy treated patients, there was no difference in the whole blood WCC (see Figure 3.15Biii). Although, again, this probably merely reflects the highly variable nature of pre-treatment white cell counts in patients with CLL generally.

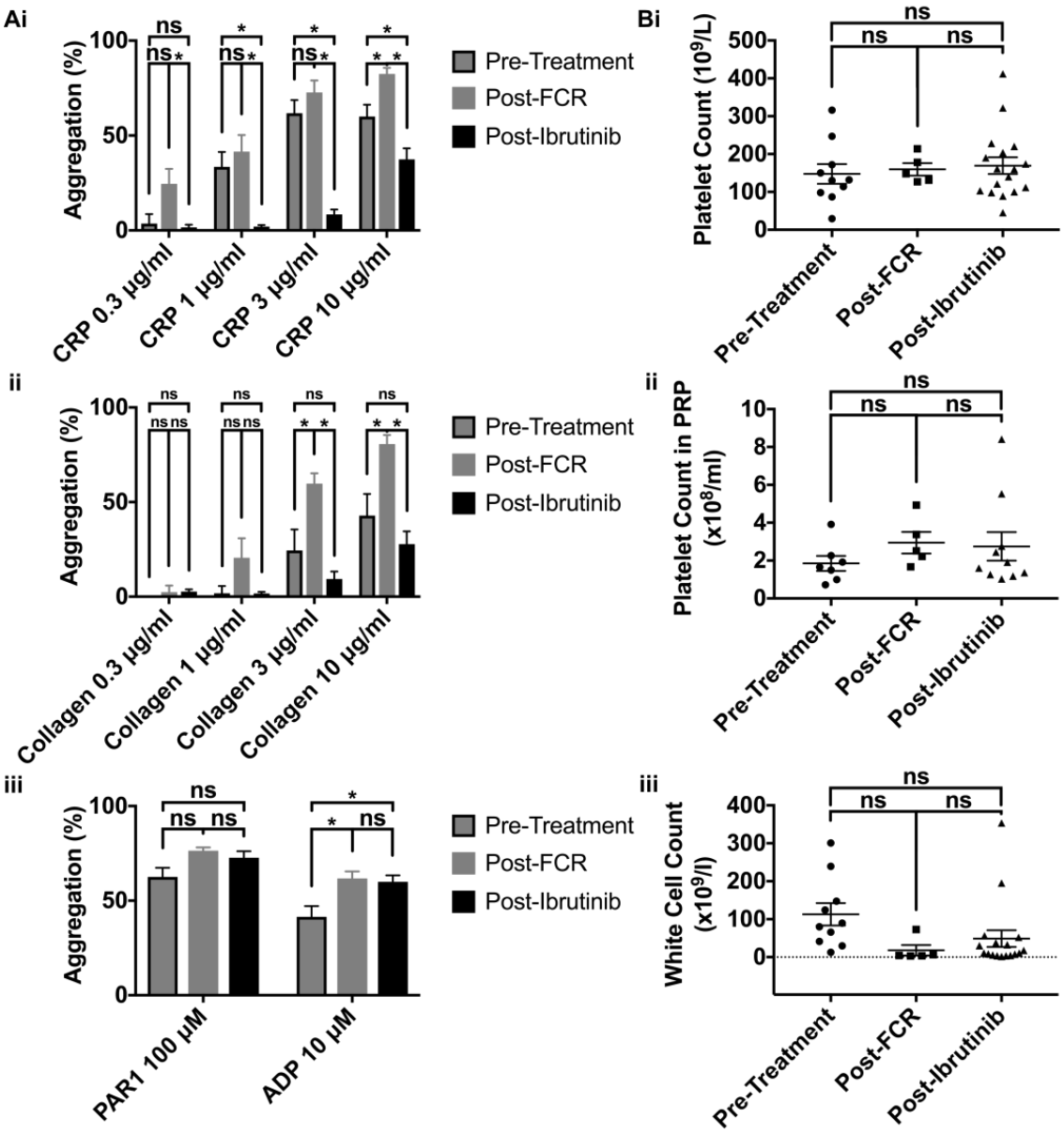

Figure 3.15: Ibrutinib inhibits GPVI-mediated platelet function *ex vivo*.
PRP was isolated from the blood of patients with CLL immediately prior to and following treatment with FCR or ibrutinib based chemotherapy regimens. (A) Optical density of PRP was measured over 3 minutes following stimulation with (i) CRP 0.3 - 10 µg/ml, (ii) collagen 0.3 - 10 µg/ml, (iii) PAR1 peptide 100 µM and ADP 10 µM. Results shown are mean ± SEM (Pre-treatment n=9, Post-FCR n=5, Post-ibrutinib n=12). Statistical analysis was performed with a 2-way ANOVA with Tukey's multiple comparison test. (B) White cell and platelet counts in whole blood as well as platelet counts in the isolated PRP were measured and are shown as mean ± SEM with statistical analysis performed using a 1-way ANOVA with Tukey's multiple comparison test. *P<0.05, ns = non-significant.

3.2.7.3 Platelets taken from patients on acalabrutinib have delayed but normal magnitude of GPVI-mediated platelet aggregation

To match the *in vitro* studies, experiments were extended to include patients with CLL taking the second generation Btk inhibitor acalabrutinib at 100mg twice daily. At the time of performing this work this drug was only available to patients through being involved in clinical trials and hence there were not many patients available for analysis. This meant that only three patients taking acalabrutinib were able to be sampled.

Patients taking acalabrutinib had a reduced magnitude of platelet aggregation in response to low and medium concentrations of GPVI agonists collagen and CRP but normal responses to high concentrations when compared to ibrutinib treated patients (see Figure 3.16Bi-ii). Like the *in vitro* platelets treated with acalabrutinib or low concentration ibrutinib however, this aggregation to high concentration agonist was delayed (see Figure 3.16A). There was no difference in the platelet aggregation response to GPCR agonists PAR1 peptide and ADP (see Figure 3.16Biii). There was no difference in the whole blood platelet count or WCC or the PRP platelet count in acalabrutinib and ibrutinib treated patients (see Figure 3.16C).

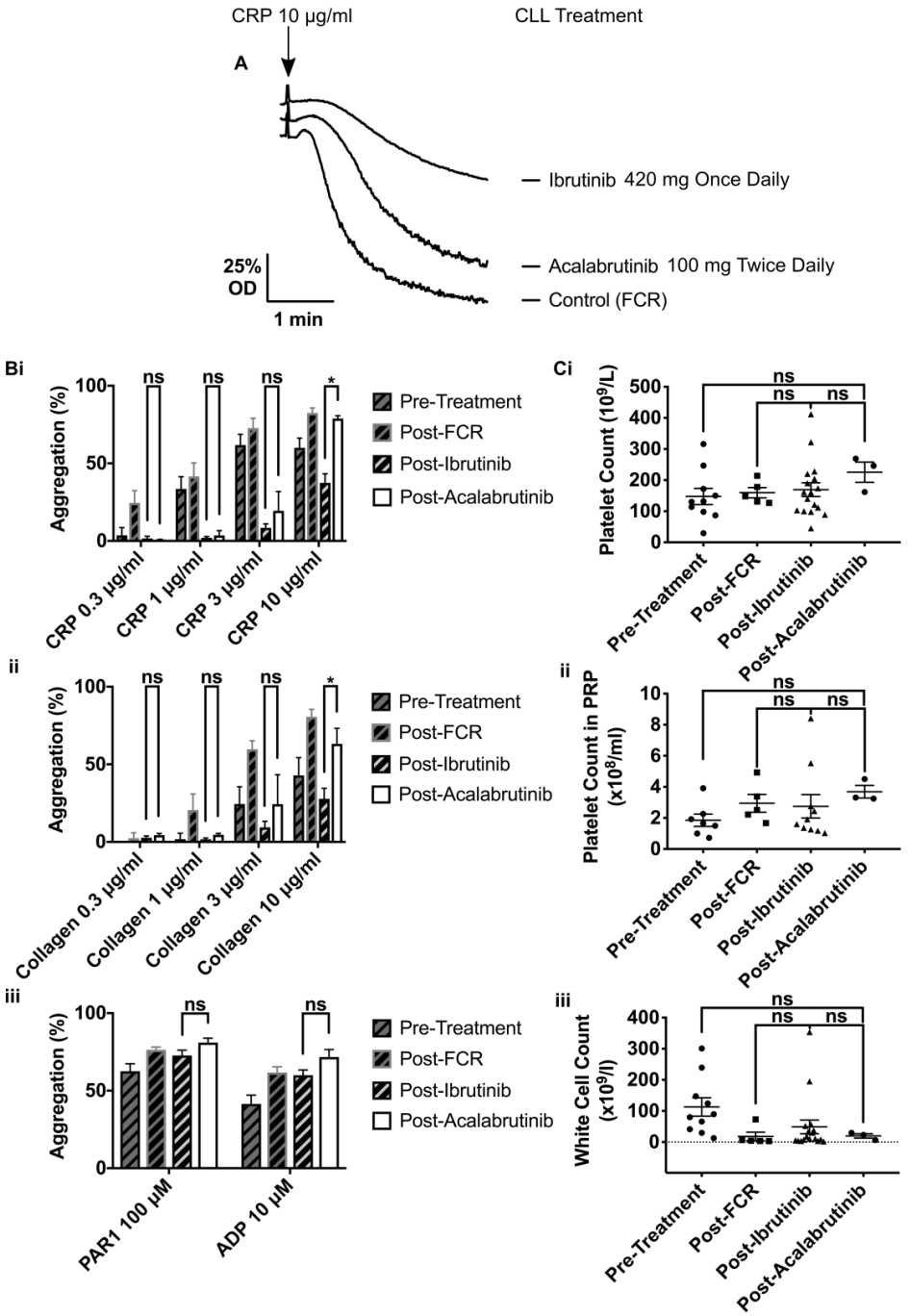

Figure 3.16: Acalabrutinib does not inhibit GPVI-mediated platelet function *ex vivo*.

PRP was isolated from the blood of three patients with CLL following treatment with acalabrutinib 100 mg twice daily. Data from Figure 3.15 is included to enable comparison. Optical density of PRP was measured over 3 minutes following stimulation with CRP 10 µg/ml (A) Representative LTA traces of PRP. (B) Mean optical densities ± SEM (n=3) following 3 minutes of stimulation with (i) CRP 0.3 - 10 µg/ml, (ii) collagen 0.3 - 10 µg/ml, (iii) PAR1 peptide 100 µM and ADP 10 µM. Statistical analysis was performed with a 2-way ANOVA with Tukey's multiple comparison test. (C) White cell and platelet counts in whole blood as well as platelet counts in the isolated PRP were measured and are shown as mean ± SEM with statistical analysis performed using a 1-way ANOVA with Tukey's multiple comparison test. *P<0.05, ns = non-significant.

3.2.7.4 Platelets taken from patients on ibrutinib and acalabrutinib have inhibited Btk Y223 and downstream PLCγ2 phosphorylation

Ex vivo experiments were extended to include studies looking at the phosphorylation events downstream of the GPVI receptor. Because of the limited volumes of blood available from these patients with leukaemia, phosphorylation studies had to be limited and did not include examination of Syk pY525/6 or SLP76 pY145. Like the *in vitro* results, whole cell tyrosine phosphorylation was generally intact but closer inspection revealed a missing band at ~ 145 kDa in both ibrutinib and acalabrutinib treated patients (see Figure 3.17A). Further analysis using phosphospecific antibodies showed that Btk Y223 and downstream PLCγ2 phosphorylation at Y753, Y759 and Y1217 was reduced in the Btk inhibitor treated patients but upstream phosphorylation at Btk Y551 and LAT Y200 was unaffected. Interestingly, and unlike the *in vitro* studies, there was no inhibition of Src pY418 in any patients treated with Btk inhibitors (see Figure 3.17A-B).

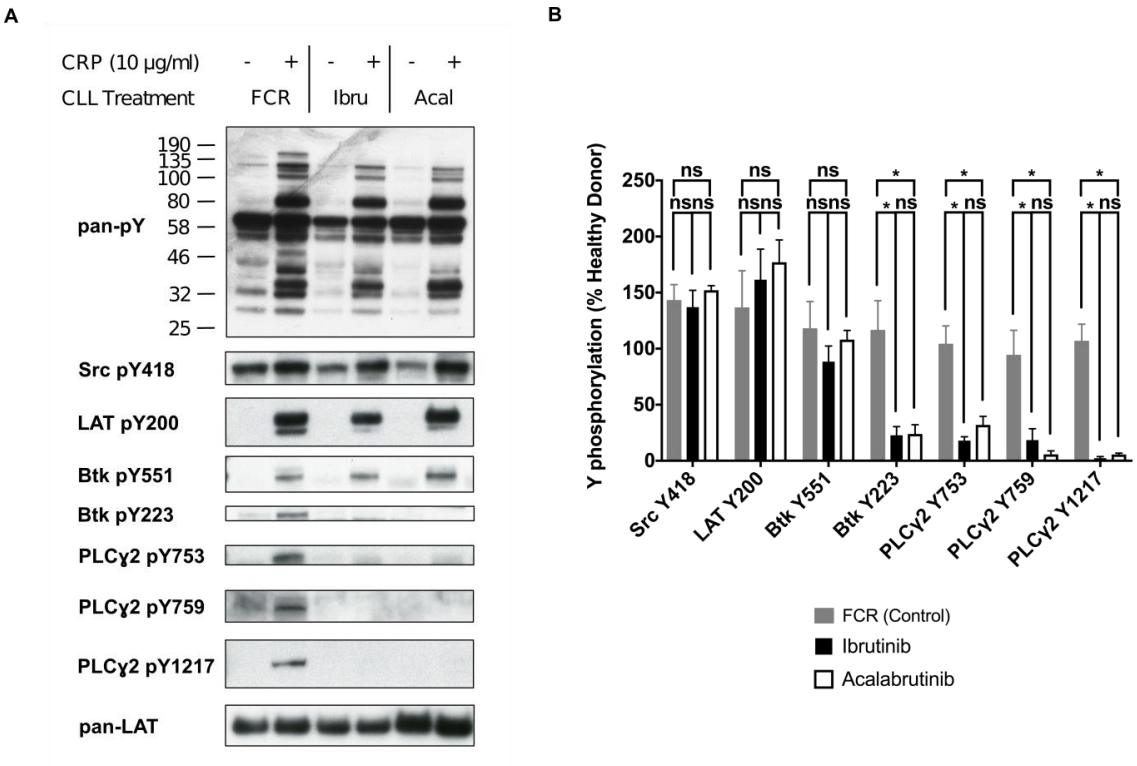

Figure 3.17: Patients treated with Btk inhibitors have reduced Btk Y223 and downstream PLCγ2 phosphorylation.
Eptifibatide (9 µM) treated washed human platelets at 4×10^8/ml from patients with CLL treated with FCR, ibrutinib or acalabrutinib were stimulated with CRP 10 µg/ml. Samples were lysed with 5X SDS reducing sample buffer after 3 minutes. Whole cell lysates were then separated by SDS-PAGE and underwent Western blot with the stated antibodies for whole cell phosphorylation, kinases and proteins downstream of GPVI. (A) Blots are representative of similar blots from twelve patients; four treated with FCR, five with ibrutinib and three with acalabrutinib. (B) Percentage tyrosine phosphorylation as compared to healthy donor platelets was measured and is represented as the means ± SEM (FCR n=4, ibrutinib n=5, acalabrutinib n=3). Statistical analysis was performed with a two way ANOVA with Tukey's multiple comparison test.

3.2.7.5 Platelets taken from patients on Btk inhibitors spread normally on collagen

The effect of Btk inhibition in platelet spreading on immobilised collagen was also assessed by washed platelets isolated from healthy donors and those taking ibrutinib 420 mg once daily and 100 mg acalabrutinib twice daily and allowing them to spread on collagen coated coverslips for 45 minutes prior to

fixation, antibody staining and imaging. No pre-treatment or FCR treated patients were used for this study because of a lack of availability at the time of performing the spreading experiments.

The results shown in Figure 3.18 indicate that Btk inhibition has very little effect, with the only statistically significant finding being that the spread platelet area of patients taking ibrutinib was more than those taking acalabrutinib or the healthy donors. The change is minor and its physiological significance is uncertain.

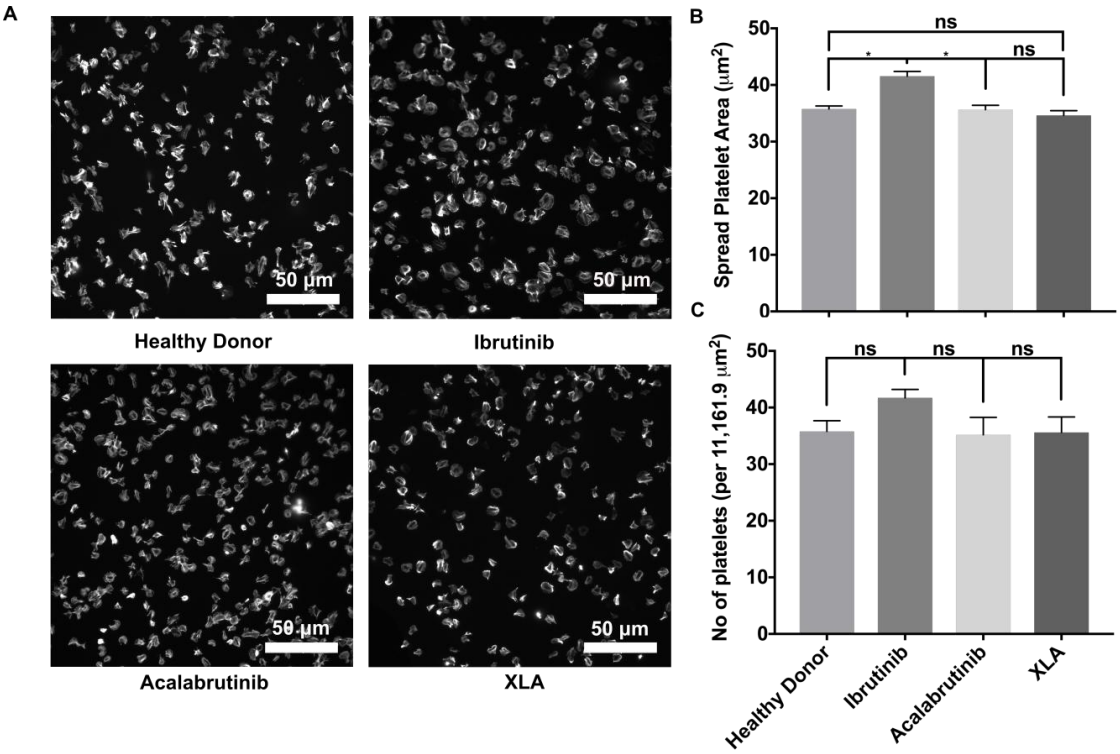

Figure 3.18: Patients on Btk inhibitors or those with XLA have minimally changed platelet adhesion and spreading when bound to immobilised collagen.
Washed platelets at $2x10^7$/ml from healthy human donors, patients taking ibrutinib or acalabrutinib and those with XLA were incubated on collagen coated coverslips at 37°C for 45 minutes. Coverslips were then washed to remove non-adherent platelets before fixation with formalin and staining with Phalloidin-488. (A) Representative images. Ilastik machine learning software was used to automatically and reproducibly identify platelets and data on platelet number and surface area was measured using the KNIME analytics platform. (B) and (C) Data shown as Mean ± SEM for healthy donors (n=5), ibrutinib (n=4), acalabrutinib (n=2) and XLA patients (n=2). Statistical analysis performed using a one-way ANOVA with Tukey's correction for multiple comparisons.

3.2.7.6 Platelets taken from patients on Btk inhibitors have normal adhesion to collagen under flow conditions at arterial shear

The effect of pharmacological Btk inhibition with ibrutinib and acalabrutinib was tested in a more physiological *ex vivo* flow adhesion assay. Whole blood from healthy donors and patients treated with ibrutinib or acalabrutinib was flowed over immobilised collagen at arterial shear. Rather than merely measuring the percentage surface coverage with platelets after three minutes of flow, the experimental method was further optimised to include fluorescence microscopy during flow. This enabled the study of change in surface coverage and aggregate size over time. Analysis methods were also developed so that they were automated and thus more reproducible. This enabled the measurement of mean aggregate size as well as total area covered. At the time of performing this assay, there were no patients taking FCR or pre-treatment Btk inhibitor patients available for inclusion.

Interestingly, as shown in Figure 3.19A, C and E, there was no difference in the platelet coverage or aggregate size over time when using blood from ibrutinib treated patients when compared to healthy controls. The same appears to be true for patients treated with acalabrutinib (Figure 3.19 Bi, D and F) but, because only two acalabrutinib patients were available for this assay, statistical analysis is inappropriate.

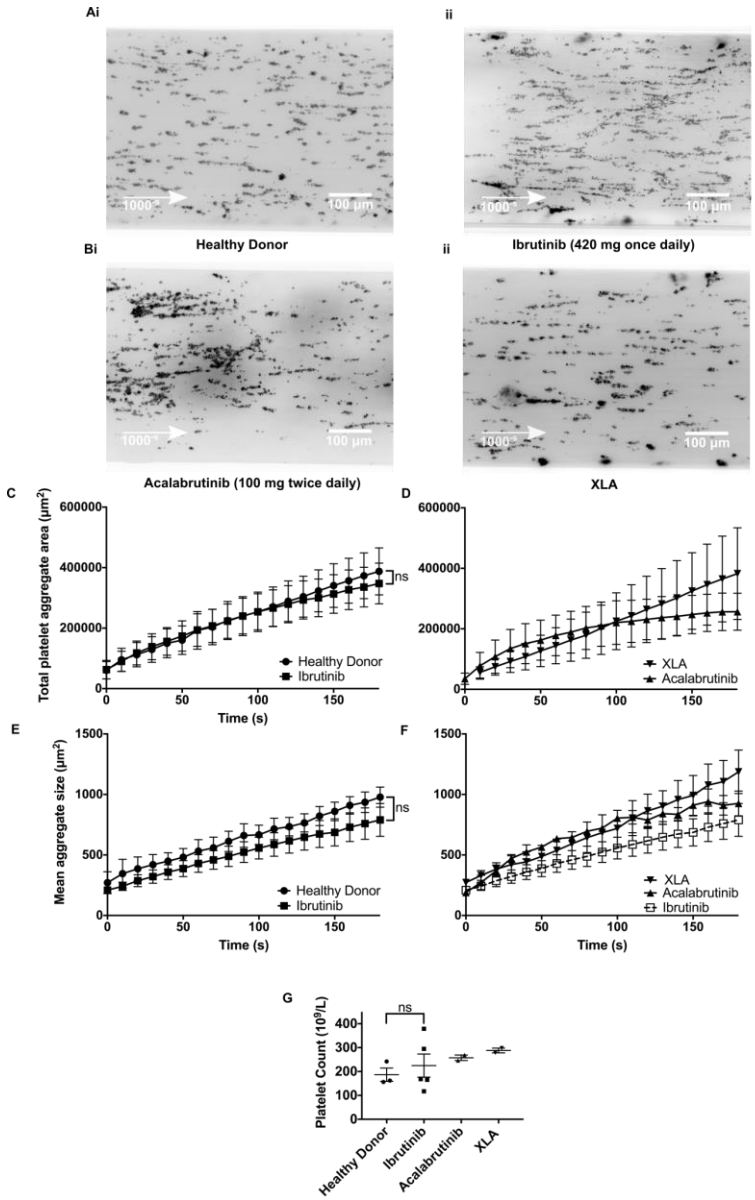

Figure 3.19: *Ex vivo* Btk inhibition has no effect on adhesion to collagen under conditions of arterial flow.

Whole blood from healthy donors, patients treated with ibrutinib or acalabrutinib or those with XLA was incubated with $DiOC_6$ dye for 5 minutes before being flowed across a capillary coated with collagen 100 µg/ml at 1000 s^{-1} for 3 minutes. Images were taken every second using fluorescent channels on a Zeiss Axio inverted microscope at 20X magnification. (A) Representative images from (i) healthy donors, patients treated with (ii) ibrutinib 420 mg once daily, (iii) acalabrutinib 100 mg twice daily or (iv) patients with XLA. Ilastik 1.1.2 machine learning software was used to automatically and reproducibly identify platelets. Data on platelet surface area coverage and cluster size was measured using the KNIME 3.4 analytics platform. Mean data ± SEM showing increase in total platelet aggregate area over time of (C) healthy donors (n=4) and ibrutinib treated patients (n=5) and (D) acalabrutinib treated patients (n=2) and those with XLA (n=2). Mean data ± SEM showing increase in mean aggregate size over time of (E) healthy donors and ibrutinib treated patients and (F) acalabrutinib treated patients and those with XLA, the results from ibrutinib treated patients is included for comparison. (G) Platelet counts from donors and patients. Statistical analysis was performed with two-way ANOVA (C and E) or one-way ANOVA (G). ns=non significant.

3.2.8 Platelets taken ex vivo from patients with XLA

Given there are differences seen in the GPVI-mediated platelet responses between the healthy donor platelets and patients treated with ibrutinib and acalabrutinib a useful way of establishing whether these effects were due to the specific actions on Btk or off-target effects was to acquire platelets from patients with XLA.

3.2.8.1 Sampled XLA patients do not express Btk

There are multiple different mutations in patients with XLA that result in the same phenotype of lacking mature B-cells. Some mutations result in complete loss of protein expression whereas some produce a non-functioning protein. Six patients with XLA were recruited and had their platelets studied. These patients were all unrelated. Information on their individual mutations was already available from the west midlands regional genetics laboratory (see Table 3.1). All except one of the of the patients had previously described mutations and the single patient with a previously non-described mutation (patient 5) was predicted to to abolish the 5' donor splice site of exon 12. Some mutations, despite only changing the protein structure subtly, still result in absence of Btk because of problems in protein trafficking from the rough endoplasmic reticulum to the cytosol. In order to test this lysed platelets were probed with an antibody to the N-terminus of the Btk protein and this failed to detect Btk in any of the

sampled patients thus confirming lack of Btk expression (see Figure 3.20A).

Patient	Mutation	Predicted effect
1	c.1750+1G>A	5' donor splice site of exon 17 abolished (K. W. Chan et al. 2006)
2	c.700C>T	Stop codon at Gln234 (Tani et al. 2002)
3	c.710del	Frameshift with premature termination (Jo et al. 2001)
4	c.1820C>A	Mutation likely to affect the kinase domain (Bradley et al. 1994)
5	c.974+1G>A	5' donor splice site of exon 12 abolished
6	g.57977–58025_68800–68848dup	Duplication of exons 6-18 resulting in frameshift with premature termination (Endo et al. 2011)

Table 3.1: Btk mutations and their predicted effects.
DNA sequencing of the Btk gene was performed by the West Midlands Regional Genetics Service and this information on the genetic mutations present in the sampled patients with XLA was provided by Dr Aarnoud Huissoon from Birmingham Heartlands Hospital.

3.2.8.2 Platelets from patients with XLA have delayed GPVI-mediated platelet aggregation but a normal amplitude of response when compared with healthy donors

In order to look at the functional effects of the absence of Btk, PRP was isolated from the patients with XLA and then stimulated with GPVI agonists and GPCR agonists with optical density measured over the course of 3 minutes. As expected, the results showed that there was low level / no aggregation at low concentrations of GPVI agonist but normal aggregation percentages with high concentrations of CRP and collagen when compared to healthy donor washed platelets (see Figure 3.20B). Like for the patients taking acalabrutinib and the *in vitro* experiments where healthy donor washed platelets were treated with acalabrutinib or low concentration ibrutinib there was delayed GPVI-mediated aggregation in the platelets from patients with XLA treated with high concentration GPVI agonists (see Figure 3.20Cii-iii). There was no statistically significant difference in platelet count between the patients with XLA and

healthy donors (but there was a trend to a higher platelet count in the patients with XLA) (see Figure 3.20Ci). This is probably accounted for by the higher haematocrit and consequential lower PRP volume with higher platelet concentration in the patients with XLA as they were all male whereas the healthy donors included males and females. There is no evidence in the literature that patients with XLA have higher platelet counts.

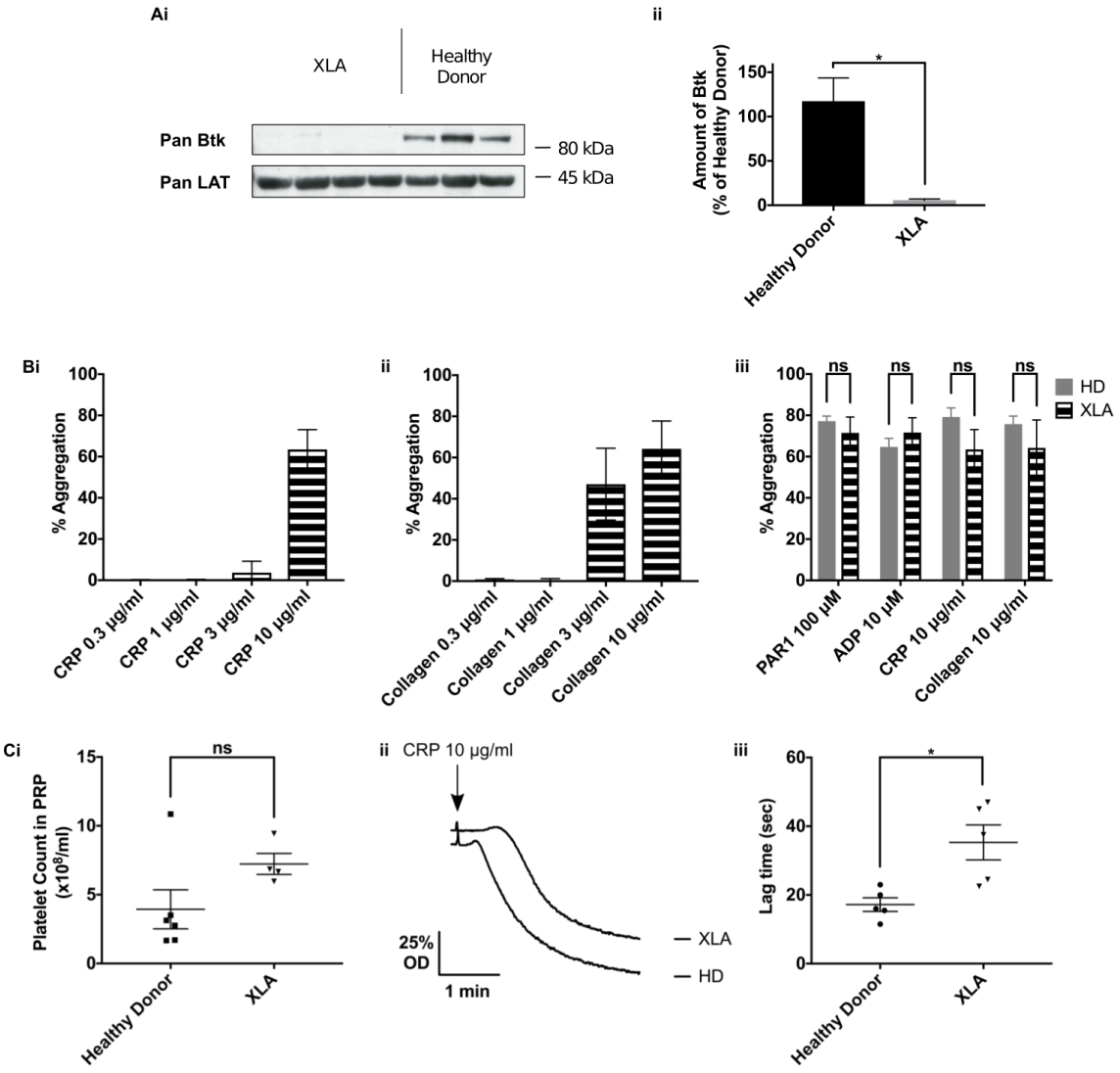

Figure 3.20: Patients with XLA lack Btk expression and have normal but delayed aggregation in response to high concentrations of GPVI agonist.
(A) Eptifibatide (9 µM) treated unstimulated platelets at $4x10^8$/ml from 6 patients with XLA and 3 healthy donors were lysed with 5X SDS reducing sample buffer. Whole cell lysates were then separated by SDS-PAGE and underwent Western blot with the anti-Btk antibody SAB3500372. (i) Representative blot, (ii) quantification of band intensity compared to mean healthy donor. Results shown are mean ± SEM. Statistical analysis by unpaired t-test. *P<0.05, ns = non-significant. (B) PRP from patients with XLA was stimulated with increasing concentrations of (i) CRP and (ii) collagen and optical density was measured for 3 minutes. (iii) Aggregation responses after stimulation with PAR1 peptide 100 µM, ADP 10 µM, CRP 10 µg/ml and collagen 10 µg/ml were compared to those from healthy donors. Results shown are mean ± SEM for four patients with XLA and six healthy donors. Statistical analysis was performed using a two way ANOVA with Sidak's correction for multiple comparisons. (C) (i) Platelet counts in PRP from the same patients/donors were measured and are shown as mean ± SEM. (ii) Representative trace and (iii) mean data ± SEM of aggregation from patients with XLA or donors stimulated with CRP 10 µg/ml (n=5). Statistical analysis was performed with a two tailed unpaired t-test. *P>0.05, ns = non-significant.

3.2.8.3 Platelets from patients with XLA are more sensitive to inhibition by ibrutinib

Given the difference in results between platelets ibrutinib treated patients and those with XLA when stimulated with GPVI agonists the next step was to see if addition of ibrutinib to platelets from XLA patients had any additional effect. Surprisingly, even at low concentrations that were previously shown to inhibit Btk pY223 (70 nM) without any other off-target effect, ibrutinib completely inhibited GPVI-mediated platelet aggregation to high concentrations of CRP (10 µg/ml) (see Figure 3.21A). This occurred at a similar IC_{50} (86 nM) to that at which ibrutinib inhibited Btk pY223 in healthy donor platelets (see Table 3.2).

3.2.8.4 Platelets from patients with XLA have normal PLCɣ2 phosphorylation and ibrutinib inhibits this at concentrations previously thought to be Btk-specific

In order to investigate this difference between healthy donors and patients with XLA further, phosphorylation events downstream of the GPVI receptor in the patients with XLA were studied. These confirmed lack of Btk pY223 but, consistent with previous publications that examined total PLCɣ2 phosphorylation, they showed that PLCɣ2 phosphorylation in patients with XLA looked preserved (albeit with slightly lower intensities) at tyrosines in the SH2-SH3 linker and the C-terminal region (see Figure 3.21B-C). Indeed, in contrast to the results seen with healthy donor washed platelets, the dose response curve for inhibition of aggregation and PLCɣ2 phosphorylation by ibrutinib overlie each other and have similar IC_{50}s (see Figure 3.21C).

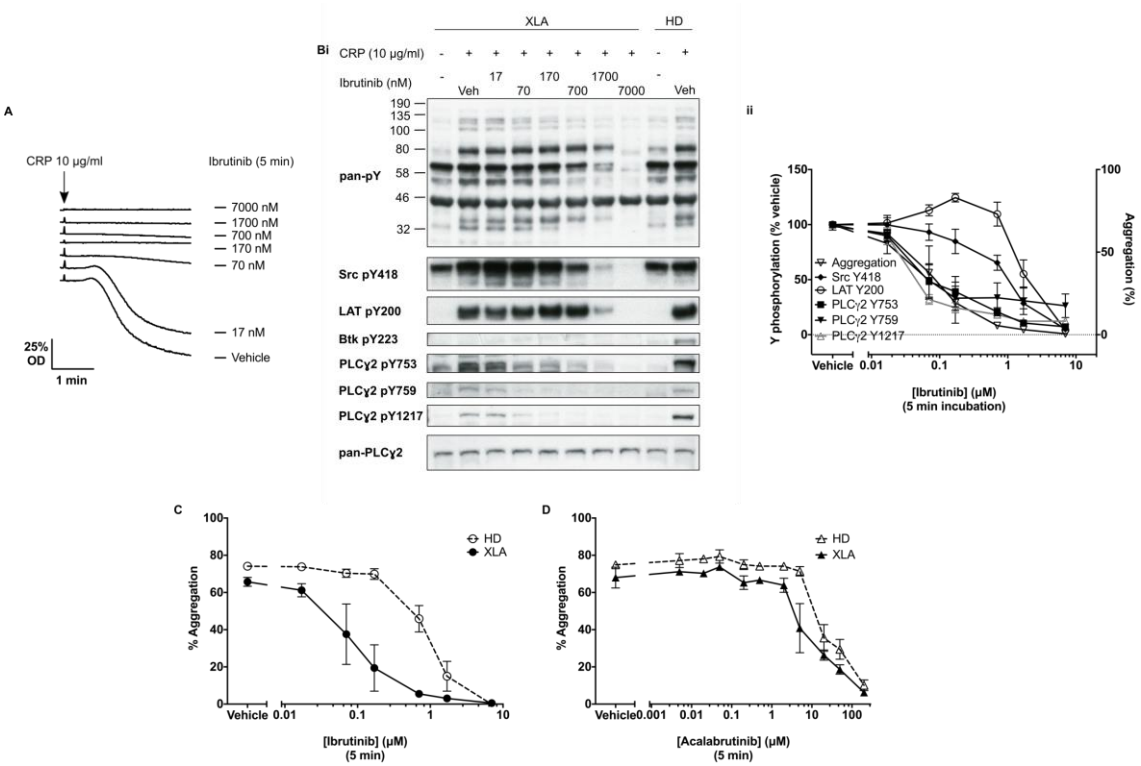

Figure 3.21: Platelets from patients with XLA are more sensitive to inhibition of GPVI-mediated platelet aggregation by ibrutinib than healthy donor platelets. Washed platelets from patients with XLA at $4x10^8$/ml incubated with ibrutinib or vehicle for 5 minutes before being stimulated with CRP 10 µg/ml. Optical density was measured for a further 3 minutes. (A) Representative trace. The same platelets were treated in the same way but in the presence of eptifibatide (9 µM) before being lysed with 5X SDS reducing sample buffer after 3 minutes. Whole cell lysates were then separated by SDS-PAGE and underwent Western blot with the stated antibodies for whole cell phosphorylation, and kinases downstream of GPVI. (B) (i) Blots are representative of similar blots from four patients. (ii) Percentage tyrosine phosphorylation as compared to vehicle treated platelets as well as aggregation percentage was measured and is represented as the means ± SEM (n=4). (C - D). Dose response curves of platelets from patients with XLA treated with ibrutinib/acalabrutinib or vehicle. Equivalent dose response curves from healthy donor experiments are included as dotted lines for comparison.

3.2.8.5 Platelets from patients with XLA have a normal sensitivity to blockade with acalabrutinib

Because of the difference in the sensitivity to ibrutinib of platelets from healthy donors and platelets from patients with XLA further studies were done with acalabrutinib. Acalabrutinib was added *in vitro* to platelets taken from patients

with XLA.

In stark contrast to the results when ibrutinib was used, the sensitivity of platelets from patients with XLA to the inhibitory effects of acalabrutinib was similar as for platelets from healthy donors (see Figure 3.21D and Table 3.2).

3.2.8.6 Platelets from patients with XLA have normal spreading on collagen

Platelet spreading experiments using blood from patients with XLA was also performed. As shown in Figure 3.18, platelets from patients with XLA have normal spreading and adhesion characteristics on immobilised collagen. The results from patients with XLA are identical to those from healthy donors.

3.2.8.7 Platelets taken from patients with XLA have normal adhesion to collagen under flow conditions at arterial shear

For a more physiological assessment of the effect of Btk inhibition on platelet function *ex vivo*, blood from patients with XLA was flowed over collagen at arterial shear. Blood from only two patients was sourced and so statistical analysis is inappropriate but, consistent with the results for *in vitro* Btk inhibition with low concentration ibrutinib, there appears to be no difference in overall platelet coverage or aggregate size between healthy donors and patients with XLA (Figure 3.19:Bii, D and F).

Ibrutinib containing figures	Name of Curve	IC_{50} (μM)	95% C.I. (μM)
3.1	HD PRP Aggregation	25.14	16.79— 39.48
3.1	HD Aggregation	1.19	0.730 — 1.950
3.3	HD Secretion	0.25	0.121— 0.548
3.3	HD Ca^{2+} Mobilisation	1.88	0.445— 22.18
3.4	WT Mouse Aggregation	2.804	1.503— 5.663
3.7	HD Btk pY223	0.023	0.14 — 0.036
3.7	HD PLCγ2 pY1217	0.035	0.19 — 0.065
3.7	HD PLCγ2 pY759	0.048	0.26 — 0.088
3.7	HD PLCγ2 pY753	0.055	0.29 — 0.105
3.7	HD Syk pY525/6	-	-
3.7	HD LAT pY200	-	-
3.7	HD SLP76 pY145	-	-
3.7	HD Btk pY551	-	-
3.7	HD Src pY418	2.1	1.240— 3.700
3.3	HD Aggregation w/o indomethacin	2.489	1.340— 50.16
3.3	HD Aggregation with indomethacin	4.56	3.312— 6.447
3.9	WT Mouse Btk pY223	0.053	0.024 — 0.111
3.9	WT Mouse PLCγ2 pY1217	0.177	0.43 — 0.747
3.9	WT Mouse PLCγ2 pY759	0.164	0.27 — 1.663
3.9	WT Mouse PLCγ2 pY753	-	-
3.9	WT Mouse Syk pY525/6	-	-
3.9	WT Mouse LAT pY200	-	-
3.9	WT Mouse Btk pY551	-	-
3.9	WT Mouse Src pY418	0.349	0.20 — 7.109
3.21	XLA Aggregation	0.086	0.37 — 0.212
3.21	XLA Src pY418	1.24	0.667— 2.311
3.21	XLA LAT pY200	-	-
3.21	XLA PLCγ2 pY753	0.069	0.35 — 0.208
3.21	XLA PLCγ2 pY759	0.033	0.10 — 0.104
3.21	XLA PLCγ2 pY1217	0.035	0.014 — 0.087
Acalabrutinib containing figures			
3.11	HD Aggregation	21.25	12.27— 37.11
3.11	HD Secretion	6.37	3.706— 11.02
3.11	HD Ca^{2+} Mobilisation	5.317	2.843— 10.15
3.12	HD Btk pY223	0.308	0.177— 0.549
3.12	HD PLCγ2 pY1217	0.88	0.393— 2.070
3.12	HD PLCγ2 pY759	1.211	0.479— 3.244
3.12	HD PLCγ2 pY753	2.75	1.200— 6.590
3.12	HD Syk pY525/6	-	-
3.12	HD LAT pY200	-	-
3.12	HD SLP76 pY145	-	-
3.12	HD Btk pY551	-	-
3.12	HD Src pY418	-	-
3.21	XLA Aggregation	8.918	4.425 — 18.86

Table 3.2: IC_{50} values for all dose response curves for experiments involving stimulation with CRP and inhibition with ibrutinib and acalabrutinib
Dose-response curves from all figures in Chapter 3 are summarised in this table. Confidence intervals are provided to better enable comparison between curves.

3.3 Discussion

The headline results of this line of enquiry into the effect of Btk inhibitors on GPVI-mediated platelet function are:

i) PLCγ2 and subsequent platelet activation can still occur in the absence of PLCγ2 phosphorylation as long as Btk is present. Analogous to what has been shown in B-cells, this also shows a non-kinase dependent, adapter role of Btk.

ii) The inhibitory effect of Btk inhibitors on GPVI-mediated platelet function is mediated through non-Tec family kinase off-target effects but the exact identify of this off-target effect is unknown.

3.3.1 Btk Adapter role and its phosphorylation of PLCγ2

These results show clearly that Ca^{2+} mobilisation and platelet activation can occur at ibrutinib and acalabrutinib concentrations where PLCγ2 phosphorylation is lost. This is apparent on the whole cell phosphorylation blots in Figure 3.7Ai and Figure 3.12Ai where there is loss of phosphorylation at a band of ~140 kDa at 70 nM ibrutinib and 2 μM acalabrutinib respectively. This is also seen in the blots using phosphospecific antibodies. It is definitively shown at pY753 and pY759. It would probably also be the case for pY1197 but for the poor performance of this particular antibody in all but one of the experiments. Loss of phosphorylation at Y1217 is seen in almost all experiments at these low concentrations of Btk inhibitor but there is a trace of ongoing low level phosphorylation at this site at higher concentrations of Btk inhibitor in some experiments (see Figure 3.7Aii). It could be that the semi-quantitative method of

measuring the relative phosphorylation intensities was not sensitive enough to pick up this low level phosphorylation consistently or the apparent low level phosphorylation that is occasionally seen could merely represent a slight overexposure of the western blot membrane or low-level basal activation. The results of the XLA patient studies also support an adapter function for Btk in addition to its kinase role. They show definitively that, in the absence of Btk, PLCɣ2 phosphorylation at pY753 and pY1217 is required for platelet activation. Further work showing the adapter role was performed by collaborators and published recently (Nicolson et al. 2018). Here, Btk deficient DT40 cells (which also do not contain Tec) were transfected with GPVI and the FcRɣ chain along with WT or kinase dead (KD) Btk. Both forms of Btk were sufficient to restore Ca^{2+} mobilisation as measured by the nuclear factor of activated T-cells (NFAT) assay.

These experiments do not give any mechanistic insight into how Btk can act as an adapter but there is pre-existing evidence of this being the case for Btk in B-cells. KD Btk has been shown to reconstitute BCR signalling in Btk deficient DT40 cells (Tomlinson et al. 2001). The same has been shown in A20 B cells (Salto et al. 2003) This latter, and another, study showed that the process is probably mediated through Btk's association with PIP5K and its production of PIP_2, which acts as a substrate for PLCɣ2 to produce IP_3 and DAG even when it is not activated through phosphorylation (Sekiya et al. 1999; Salto et al. 2003). These studies also give some more information in platelets about which tyrosines on PLCɣ2 are phosphorylated by Btk and which by Syk or other Tec family kinases. From the work with ibrutinib and acalabrutinib in human healthy donor or WT mouse platelets it appears that Btk is required for phosphorylation

of tyrosines in both the SH2-SH3 linker as well as in the C-terminal region. The work with XLA patients, however, clearly shows that these can be phosphorylated in the absence of Btk. In this instance it is likely that Tec (and not Syk) is responsible for the residual phosphorylation. This hypothesis is supported by the reversibility of high concentration ibrutinib's inhibition of Syk activation but irreversibility of the PLCγ2 phosphorylation seen in Figure 3.8 and also by Figure 3.12 where Syk activation is unaffected by high concentration acalabrutinib, but PLCγ2 phosphorylation at all sites is lost.

3.3.2 Off-target effects

These results show definitively that both ibrutinib and acalabrutinib block GPVI-mediated platelet function through non-Tec family kinase off-target effects and, in the case of ibrutinib, this occurs at pharmacologically achieved concentrations. Btk inhibition alone is insufficient to inhibit any assay used to assess platelet function downstream of GPVI except in aggregation when very low concentrations of agonist are used (1 μg/ml CRP). This is consistent with the already published studies involving XLA patients (Quek et al. 1998) and Btk deficient mice (Atkinson et al. 2003) and it explains why major bleeding is seen with ibrutinib but not with acalabrutinib (Shatzel et al. 2015).

Some differences between these results and some previous studies need further explanation and elaboration however. Levade *et al.* found that the concentration of ibrutinib required to inhibit GPVI-mediated Btk pY223 in a flow cytometry assay (0.5 μM) was the same as the concentration that inhibited platelet aggregation. In the same series of experiments, however, using western blotting they also show loss of whole cell phosphorylation at this same

concentration (Levade et al. 2014) whereas the concentration required to block whole cell phosphorylation in the results above (Figure 3.7) is >10 fold higher than that required to block Btk pY223. This probably reflects the different assays used to assess Btk pY223. The only thing to add here is that the results seen using XLA patient platelets (Figure 3.21) show definitively that Btk is not required for GPVI-mediated platelet activation. Taken together, these results imply that the conclusions of Levade *et al*; that ibrutinib blocks GPVI-mediated platelet activation via its effects on Btk, are incorrect. Rigg *et al*, however, also show that one of their ibrutinib analogues blocks GPVI-mediated platelet activation at concentrations that do not inhibit Src pY418. The explanation for this is probably that they used a different assay to measure platelet activation (P-selectin expression as measured by flow cytometry). Experiments performed in Chapter 5 below also show that P-selectin expression is lost at lower levels of ibrutinib than those that inhibit aggregation downstream of GPVI (see Figure 5.1).

The concentration of agonist in *in vitro* studies of platelet function that represents a “physiological concentration” is a controversial topic. The closest *in vitro* assay to physiological conditions is the flow adhesion assay. It is likely that high agonist concentrations are closest to *in vivo* activation levels however, particularly given the difference in bleeding symptoms seen between GPVI deficient patients and those with XLA. In support of this, the flow adhesion assays showed no effect with Btk-specific concentrations of ibrutinib *in vitro* or with blood *ex vivo* from patients with XLA. There was a trend towards a difference in adhesion to collagen between the patients with CLL treated with ibrutinib and those with XLA (see Figure 3.19). Indeed, in a more recent study

Bye *et al*. reported thrombus instability on collagen in a flow adhesion assay in blood from patients treated with ibrutinib. This is consistent with the findings that Btk kinase function is not required for platelet adhesion to collagen under flow, but that off-target effects of ibrutinib occurring with higher concentrations mediate this inhibition (Bye et al. 2017). The reason for the studies performed here not detecting this thrombus instability in ibrutinib treated patients probably lies in the design of the assay. The studies from other groups that detected a thrombus instability in ibrutinib treated patients or blood treated *in vitro* with high concentrations of ibrutinib/ibrutinib analogue either used higher shear rates than used in these experiments (2200 s^{-1} vs 1000 s^{-1}) and/or studied adhesion over a longer time period (5-10 mins vs 3 mins) (Rigg et al. 2016; Bye et al. 2015; Bye et al. 2017). The lack of effect on adhesion to collagen under flow could, however, be explained by the results of Busygina *et al*. They found the assay was dependent on GPIb and integrin α2β1 mediated adhesion rather than GPVI (Busygina et al. 2018).

The experiments above show that this off-target effect of Btk inhibitors is not mediated through inhibition of Tec. Tec phosphorylation is seen to be lost in a biphasic way when platelets are inhibited with ibrutinib or acalabrutinib (Figure 3.7Bii and 3.12Bii) and that this occurs at lower concentrations than those that cause blockade of GPVI-mediated platelet function. The other piece of evidence in support of a non-Tec kinase off-target effect is striking in both its clarity and simplicity; the blockade of GPVI-mediated platelet aggregation by ibrutinib is reversible but the corresponding inhibition of GPVI-mediated PLCγ2 phosphorylation is irreversible (Figure 3.5 and Figure 3.8). The only irreversible part of the platelet aggregation curve is the delay seen at concentrations which

just inhibit Btk pY223.

The identity of the kinase targeted by this off-target action of the Btk inhibitors is not known. SFKs would seem a strong possibility because the inhibition of Src pY418 strongly correlates with loss of aggregation and, like aggregation, this inhibition of phosphorylation is reversible (The antibody raised against Src pY418 detects phosphorylation of the active site of Src, Lyn and Fyn). In support of this, Src pY418 inhibition is seen at the 1 μM ibrutinib (and ibrutinib analogue) concentration used by Bye *et al*. and Rigg *et al*. in their experiments where they see loss of platelet adhesion to collagen under flow (Bye et al. 2015; Rigg et al. 2016). What goes against this, however, is that ibrutinib treated patients have normal Src pY418 and that acalabrutinib does not inhibit Src pY418 but, like ibrutinib, still inhibits GPVI-mediated platelet aggregation at ~50-fold higher concentrations than those which inhibit Btk pY223 (Table 3.2). It is possible, however that the ibrutinib treated patients did have inhibition of Src pY418 but that this effect was washed out during the process of isolating washed platelets. The same explanation could apply for why there was no effect seen in the spreading assays performed on the platelets isolataed from Btk inhibitor treated patients. Other tyrosine kinases, present in platelets, that have been shown to be inhibited by ibrutinib (with no data published on acalabrutinib) include Csk. This would seem an unlikely kinase for causing blockade of aggregation when inhibited, however, as it is a negative regulator of SFK phosphorylation.

These results show that, despite acalabrutinib's more favourable selectivity to Btk over other Src, Syk and Tec kinases in *in vitro* kinase assays, the window between Btk inhibition and blockade of GPVI-induced aggregation *in vitro* is

similar to that of ibrutinib. Despite this, acalabrutinib, but not ibrutinib, fails to block GPVI-mediated platelet activation *ex vivo*. It is likely that this is because of the differential dosing and pharmacodynamics of the two Btk inhibitors. Acalabrutinib is used at a dose of 1.5 mg/kg twice daily (Byrd et al. 2016; Barf et al. 2017) and ibrutinib at a single daily dose of 6 mg/kg in CLL or 8 mg/kg in MCL. Pharmacokinetic studies have shown that ibrutinib achieves Btk occupancy of >95% at doses of 2.5 mg/kg but that doses of 6 mg/kg are required to maintain this over 24 hours (Advani et al. 2012). Acalabrutinib at 1.5 mg/kg twice daily also achieves full Btk occupancy over 24 hours (Byrd et al. 2016). The peak unbound plasma concentration of ibrutinib in patients is 0.5 μM (Levade et al. 2014) and that of acalabrutinib 1.3 μM (Byrd et al. 2016). The half-life of ibrutinib is 4-8 hours (Advani et al. 2012). The half-life of acalabrutinib is 1 hour (Byrd et al. 2016). Despite the peak concentration of acalabrutinib being approximately 2-fold higher than the concentration of ibrutinib, the 5-fold lower potency of acalabrutinib as an inhibitor of Btk (Barf et al. 2017) means that, in potency terms, it is dosed at a lower level consistent with the lack of inhibition of GPVI. This implies that ibrutinib could be used at a lower concentration to achieve Btk blockade. Indeed, there is retrospective clinical evidence that doses less than 6 mg/kg are as effective as 6 mg/kg at treating CLL (Banerjee et al. 2016) and a prospective clinical trial using doses as low as 2.5 mg/kg has just been reported showing adequate Btk inhibition (Bose et al. 2016; Chen et al. 2018).

During the writing of this thesis, Bye *et al.* reported complete blockade of platelet aggregation to high concentrations of collagen in patients receiving ibrutinib or acalabrutinib (Bye et al. 2017), in contrast to the findings of the

above experiments. Bye *et al.* used the Optimul 96 well microtitre assay to measure aggregation rather than the widely used light transmission aggregometry (LTA). It has been shown that Optimul is a more sensitive assay than LTA (Lordkipanidzé et al. 2014; M. Chan et al. 2018). It is probable that the delay in onset of aggregation observed using LTA by concentrations of ibrutinib or acalabrutinib that just block Btk manifest as complete blockade in the Optimul assay.

The results of this work explain the lack of major bleeding side effects experienced by patients taking acalabrutinib relative to ibrutinib and suggest that the major bleeding side effect of ibrutinib can potentially be abolished by reducing the dose. Further, this study also shows that the bleeding caused by ibrutinib is not due to an irreversible action. This predicts that the GPVI blockade wears off over a period of 24 hours as the drug is cleared (Advani et al. 2012). Logically therefore, in the event of a major bleed, there may be no need to use expensive and potentially harmful platelet transfusions to correct the signalling deficit. Each clinical scenario should be judged on its own merits, however, and individual clinician discretion is crucial.

In conclusion; the present study shows that inhibition of Btk kinase activity causes only partial inhibition of GPVI signalling in platelets and provides evidence that Btk supports GPVI signalling by functioning as an adapter protein as well as a kinase. The excessive bleeding induced by ibrutinib relative to acalabrutinib is likely to reflect a non-Tec family kinase off-target inhibitory effect of ibrutinib, possibly on SFKs.

CHAPTER 4: THE EFFECT OF BTK INHIBITION ON PLATELET CLEC-2 FUNCTION

4.1 Introduction

In the late 1990's and early 2000's when platelet studies using XLA patients and Btk/Tec knockout mice were being performed, platelet CLEC-2 had not been identified and thus platelets from these sources have not yet been used to study Btk's role in CLEC-2 mediated platelet function. It is only since the introduction of the Btk inhibitors that ibrutinib has been used as a tool to try and elucidate the function of Btk downstream of platelet CLEC-2. Even so, there is very little existing literature on this topic. In fact there are only two papers, one by Manne *et al*. and one by Lee *et al* (Manne et al. 2015; Lee et al. 2017). The latter only having a single relevant experiment. What follows will describe the findings of these studies as far as is relevant to Btk and CLEC-2 and highlight what is still unknown.

4.1.1 The current understanding of the role of Btk in CLEC-2 mediated platelet function

In the study by Manne *et al*. it is shown that ibrutinib completely blocks CLEC-2 mediated aggregation in human and mouse platelets at very low concentrations (10 nM). They also demonstrate the same thing for granule secretion in human

platelets (Manne et al. 2015). These concentrations are much lower than those required to block any aspect of GPVI-mediated platelet function in any published study. This contrasts directly with results from Lee *et al*. where 500-fold higher concentrations of ibrutinib (5 μM) were required to block CLEC-2 mediated mouse platelet aggregation (Lee et al. 2017). The nature of the agonist or its concentration could perhaps explain this difference; Manne *et al*. used very low concentrations of rhodocytin for their mouse studies (10 nM) and a wide range for their human studies (30 - 300 nM) whereas Lee *et al.* used a single concentration of podoplanin-Fc (2 μg/ml) for their experiments.
In contrast to their results with ibrutinib, Manne *et al*. show that XID mouse platelets (i.e. those lacking the PH-domain of Btk) still have some residual aggregation in response to CLEC-2 ligation with low concentrations of agonist. Even more interestingly, they show that addition of 5 nM ibrutinib completely blocks this response (Manne et al. 2015). However, they do not explicitly state that this shows an off-target effect of ibrutinib, even at this very low concentration.

CLEC-2 mediated signalling events in ibrutinib treated platelets have only been studied by Manne *et al*. They show in human and mouse platelets that low concentration ibrutinib is sufficient, downstream of CLEC-2, not only to block Btk Y223 and downstream PLCɣ2 phosphorylation (as is the case for GPVI-mediated signalling events) but also to inhibit “upstream” signalling events such as Syk autophosphorylation such as is only seen at very high concentrations of ibrutinib downstream of GPVI. From this they deduce that Btk lies upstream of Syk when activated by CLEC-2 ligation (see Figure 1.4).

A potential confounder for these results, not considered in their manuscript by Manne *et al*. is CLEC-2's reliance on secondary mediator feedback for full activation to occur. It was shown by Pollitt *et al*. that CLEC-2 signalling, unlike GPVI, is critically dependent on secondary mediator feedback via ADP and TxA_2 (Pollitt et al. 2010). The platelet preparation method used by Manne *et al*. down-regulates the $P2Y_1$ receptor, thus removing part of this secondary feedback.

Further evidence of ibrutinib's off-target effects against Tec can be deduced from the *in vivo* experiments performed by Manne *et al*. using Btk and Tec knockout mice. They show that Btk/Tec double knockout mouse embryos, but not mice deficient only in Btk or Tec, have evidence of blood lymphatic mixing analogous to that seen in CLEC-2 deficient mice (Manne et al. 2015). Therefore function of both Btk and Tec has to be blocked before platelet function downstream of CLEC-2 is affected.

4.1.2 What this study adds

Given that CLEC-2 is a potentially attractive drug target for thrombosis because of its critical role in venous thrombosis but lack of contribution to haemostasis, and the Manne *et al.* paper shows that very low concentrations of ibrutinib are required to inhibit CLEC-2 it seems plausible that Btk inhibition may be a way of selectively targeting platelet CLEC-2 function therapeutically.

The aim of this set of experiments therefore is to clarify the difference seen between the results of the Lee *et al*. and Manne *et al*. studies as regards ibrutinib dosing and to explore the underlying mechanism behind ibrutinib's apparent low concentration inhibition of CLEC-2 signalling. They will focus on

how this differs from its effects on GPVI function which mediate bleeding, with particular attention paid to the novel model of signalling events downstream of CLEC-2 as described by Manne *et al*. In doing so the feasibility of Btk inhibition as a surrogate way of blocking platelet CLEC-2 function will be evaluated for taking forward to more translational studies.

4.2 Results

4.2.1 Btk inhibition blocks CLEC-2 mediated platelet function

4.2.1.1 Ibrutinib inhibits CLEC-2 mediated platelet aggregation in PRP

GPVI and CLEC-2 share many similar features within their signalling cascades. Initial studies were performed to see if the concentration-response for inhibition of CLEC-2 function by ibrutinib was similar to that against GPVI.

The agonist concentration that most closely matches the level of physiological CLEC-2 stimulus is not known. But because of the possibility that these experiments might comprise part of the justification for a new anti-thrombotic indication for Btk inhibitors and in order to match the experiments that had been performed looking at GPVI, maximal concentrations of CLEC-2 agonist were used. Unlike for the experiments investigating GPVI signalling, no agonist dose finding studies were performed. The concentration of 300 nM rhodocytin was chosen for all in vitro CLEC-2 assays as this is known to be a maximal

concentration *in vitro* (Parguina et al. 2012).

Firstly, ibrutinib was added to healthy human donor PRP prior to performing LTA. The inhibitory effects are shown in Figure 4.1Ai and B and the IC_{50} of this and each subsequent dose response curve in this chapter are shown in Table 4.1. Blockade of aggregation was achieved at 7 μM. This is a high concentration but of note it is 10-fold lower than the concentration required to block aggregation in PRP stimulated with CRP 10 μg/ml.

4.2.1.2 Ibrutinib inhibits CLEC-2 mediated platelet aggregation in washed platelets

Similar experiments were performed in washed platelets. Results are shown in Figure 4.1Aii and B with IC_{50} values shown in Table 4.1. As for the results for GPVI stimulated platelets, removal of plasma proteins resulted in ~100-fold increase in potency with complete inhibition at 70 nM. Strikingly however, and different to the results with GPVI stimulation, complete inhibition of CLEC-2 mediated aggregation was seen at 10-fold lower concentrations of ibrutinib than are required to block GPVI-mediated aggregation. This is in line with the results of Manne *et al* (Manne et al. 2015). The IC_{50} for this assay was similar to that for blockade of Btk pY223 in GPVI stimulated platelets; namely 23 nM.

4.2.1.3 Ibrutinib inhibits CLEC-2 mediated platelet granule release

Functional studies were extended to include the measurement of ATP release from CLEC-2 stimulated platelets. As for LTA, platelets were inhibited with increasing concentrations of ibrutinib. These experiments were performed by a

medical student (Josh Hinds) undergoing an intercalated BMedSci degree who was under working under supervision as part of this project. The results, shown in Figure 4.1Aiii and B and Table 4.1, show that ibrutinib inhibits CLEC-2 mediated granule release at similar concentrations to those that inhibit aggregation.

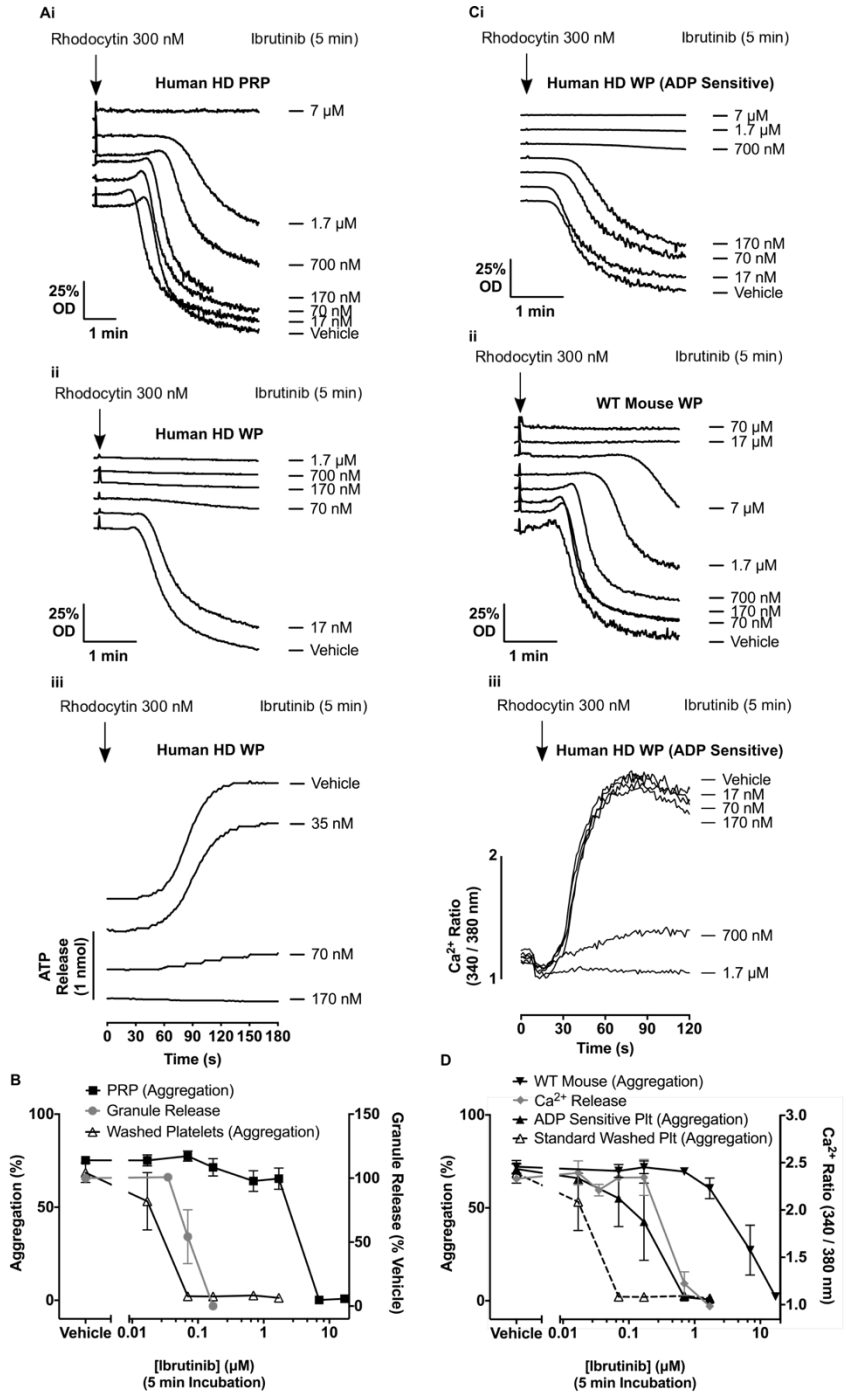

Figure 4.1: Ibrutinib dose-dependently inhibits CLEC-2 mediated platelet

aggregation, granule release and Ca^{2+} mobilisation.

(A) (i) PRP and (ii, iii) washed platelets at $4x10^8$/ml isolated from healthy donors were stimulated with rhodocytin 300 nM after incubation with ibrutinib or vehicle at the stated concentrations for 5 minutes. LTA and granule release measurements were then undertaken for 5 and 3 minutes respectively. Representative traces of three identical aggregation (i, ii) and granule secretion experiments (iii). (B) Dose response curves (n=3) for Ai-iii. (C) Human ADP-sensitive (i, iii) and WT mouse (ii) washed platelets at $4x10^8$/ml were incubated with vehicle or ibrutinib for 5 minutes prior to stimulation with rhodocytin 300 nM for 3 minutes. Representative trace of (i, ii) LTA and (iii) Ca^{2+} mobilisation from 3 identical experiments. (D) Dose response curves (n=3) for Ci-iii. All results are shown as mean ± SEM.

4.2.1.4 Ibrutinib inhibits CLEC-2 mediated Ca^{2+} mobilisation and platelet aggregation in ADP-sensitive platelets with a lower potency than it inhibits aggregation in standard platelets

Further functional studies were performed using ibrutinib to inhibit CLEC-2 mediated Ca^{2+} mobilisation. As previously mentioned, the method of platelet preparation for the Ca^{2+} mobilisation assay differs from the standard method as it needs lower centrifugation speeds and does not require the addition PGI_2. This protocol produces platelets which are ADP sensitive as opposed to standard methodology which down-regulates the $P2Y_1$ receptor and renders platelets ADP insensitive (Koessler et al. 2016). Experiments attempting to use platelets prepared using standard methods in the Ca^{2+} mobilisation assay were unsuccessful.

The results, shown in Figure 4.1Ciii and D and Table 4.1 show that ibrutinib is less potent at inhibiting Ca^{2+} mobilisation under these conditions than it is at inhibiting CLEC-2 mediated aggregation in washed platelets produced by standard methods. To see if the reason for this discrepancy was because of the different method of platelet preparation ibrutinib was also used to inhibit platelet aggregation as measured by LTA. The results of this experiment (Figure 4.1Ci

and D and Table 4.1) show ibrutinib has a similar potency for inhibition of CLEC-2 mediated platelet aggregation as for Ca^{2+} mobilisation in ADP-sensitive platelets.

4.2.1.5 WT mouse platelets are less sensitive to blockade of CLEC-2 mediated platelet aggregation by ibrutinib than human platelets, regardless of preparation method

The function of CLEC-2 on mouse platelets is better understood than in human platelets and so, because future experiments were planned to use pharmacological Btk inhibition in *in vivo* mouse thrombosis assays, it was necessary to test whether ibrutinib blocked CLEC-2 function in mouse platelets as in human platelets.

Ibrutinib was added to WT mouse washed platelets *in vitro* in exactly the same conditions as for human washed platelets. Results are shown in Figure 4.1Cii and D and Table 4.1. Surprisingly, the concentration of ibrutinib required to inhibit CLEC-2 mediated mouse platelet aggregation was over 500-fold higher than for human platelets. Consistent with the studies of Lee *et al.* this concentration was modestly higher than that required to inhibit GPVI-mediated mouse platelet aggregation (Lee et al. 2017).

4.2.1.6 Platelets taken from patients on ibrutinib and acalabrutinib have inhibited CLEC-2 mediated platelet aggregation

In order to see if the *in vitro* effects of ibrutinib on CLEC-2 function were applicable at physiological concentrations blood was taken patients with CLL

who were being treated with ibrutinib, acalabrutinib or the non-Btk inhibitor containing treatment regime FCR. PRP was isolated from blood samples taken prior to starting treatment and then at various time points during their treatment. Similar to the results from experiments examining GPVI-mediated platelet function, platelets from patients with CLL prior to starting any treatment showed absent or reduced/delayed CLEC-2 mediated platelet aggregation (Figure 4.2A, Bii-iii). This inhibition, however, was much more marked than that seen with GPVI-mediated platelet aggregation shown in Figure 3.15. Data in Figure 3.15 and previous studies show that a high WCC in patients with CLL is associated with impaired ADP mediated platelet aggregation (Lipsky et al. 2015; Glenn et al. 2009).

Figure 4.2Ai shows that as the WCC reduces, CLEC-2 mediated platelet responses are restored for patients treated with the non-Btk containing chemotherapy regimen FCR. This is consistent with the restoration of ADP mediated platelet function as seen in Figure 3.15 and previous studies showing that ADP is an essential secondary mediator in platelet activation secondary to CLEC-2 ligation (Pollitt et al. 2010).This restoration of CLEC-2 mediated platelet aggregation does not occur in patients treated with ibrutinib (Figure 4.2Aii). It is clear that a high WCC is a potential confounder, thus, once this was realised all further platelet function analysis was performed in patients with a WCC in the normal range (ie once the initial lymphocytosis, known to be associated with Btk inhibitor treatment had resolved (Rossi & Gaidano 2014)). All the subsequent results, with the exception of 4 patients taking ibrutinib, are shown on patients with a WCC in the normal range of < 11 $x10^9$/l.

Once this initial confounder had been identified, studies were extended to

include more patients on different treatment regimens and also to study the effects of Btk inhibitor treatment on aggregation in response to different concentrations of the CLEC-2 agonist rhodocytin.

Regardless of the concentration of rhodocytin, CLEC-2 mediated platelet aggregation was completely blocked in all patients receiving Btk inhibitor treatment and in none of the patients receiving the control chemotherapy (Figure 4.2B).

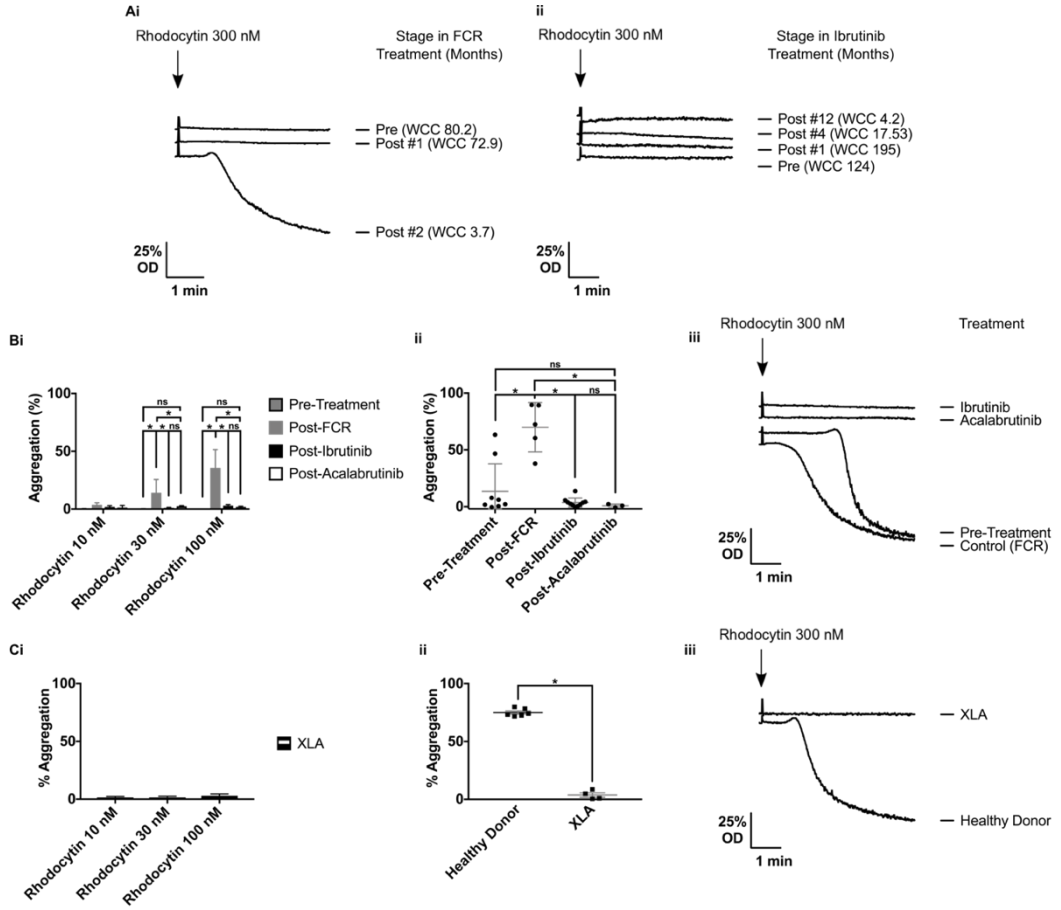

Figure 4.2: CLL patients on Btk inhibitors have complete blockade of CLEC-2 mediated platelet aggregation.
PRP was isolated from the blood of patients with CLL immediately prior to and following treatment with FCR, ibrutinib or acalabrutinib based chemotherapy regimens. (A) Representative traces of 3 similar experiments showing PRP from patients at different time points in their treatment with (i) FCR or (ii) ibrutinib following stimulation with rhodocytin 300 nM and optical density measurement over 5 minutes. WCCs ($x10^9$/l, normal range: 4-11) are shown for each trace. (B) Mean ± SEM (Pre-treatment n=9, post-FCR n=5, post-ibrutinib n=12, post-acalabrutinib n=3) of optical density 5 minutes after stimulation with (i) rhodocytin 10 - 100 nM or (ii) 300 nM. (iii) Representative trace. Statistical analysis was performed with a 2-way ANOVA with Tukey's correction for multiple comparisons. (C) Mean ± SEM (healthy donor n=6, XLA

n=4) of optical density 5 minutes after stimulation with (i) rhodocytin 10 - 100 nM or (ii) 300 nM. (iii) Representative trace. Statistical analysis was performed with a two-tailed t-test. *P<0.05, ns = non-significant.

4.2.1.7 Platelets from patients with XLA have inhibited CLEC-2 mediated platelet aggregation

To enable the study of the effect of Btk inhibition on CLEC-2 mediated platelet function without any off-target effects on Tec that might be occurring (shown by the ibrutinib treated XID mouse studies by Manne *et al*. (Manne et al. 2015) and the results from Chapter 3 looking at the additional effect of low concentration ibrutinib on GPVI-mediated platelet function in XLA patients), PRP from patients with XLA was also used. Analogous to the results from patients taking Btk inhibitors, PRP from patients with XLA also failed to aggregate in response to low, medium or high concentrations of rhodocytin (Figure 4.2C).

4.2.2 The inhibition of CLEC-2 mediated platelet function with ibrutinib is irreversible

Because of the similar IC_{50} for ibrutinib's inhibition of CLEC-2 mediated platelet activation in human washed platelets and its blockade of Btk pY223 downstream of GPVI, it may be that CLEC-2 induced platelet function may be critically dependent on Btk's kinase activity. A further piece of evidence towards this would be if, like ibrutinib's actions on Btk, its inhibition of CLEC-2 mediated platelet activation was also irreversible.

4.2.2.1 Ibrutinib induced blockade of CLEC-2 mediated platelet function is time-dependent

The first indication that an interaction is irreversible is if it is time-dependent. Thus human washed platelets were incubated with several concentrations of ibrutinib for increasing time periods from 30 seconds up to 60 minutes before being stimulated with rhodocytin. Again, this time-dependent assay was performed, under supervision, as part of a BMedSci degree by Josh Hinds. Light transmission aggregometry and granule secretion were then measured and results are shown in Figure 4.3A and B as well as Table 4.1. The IC_{50} values for the 30 second and 5 minute incubation dose response curves could not be calculated. Despite this it is clear from these results that the effect of ibrutinib is indeed time-dependent in both its inhibition of LTA and granule secretion.

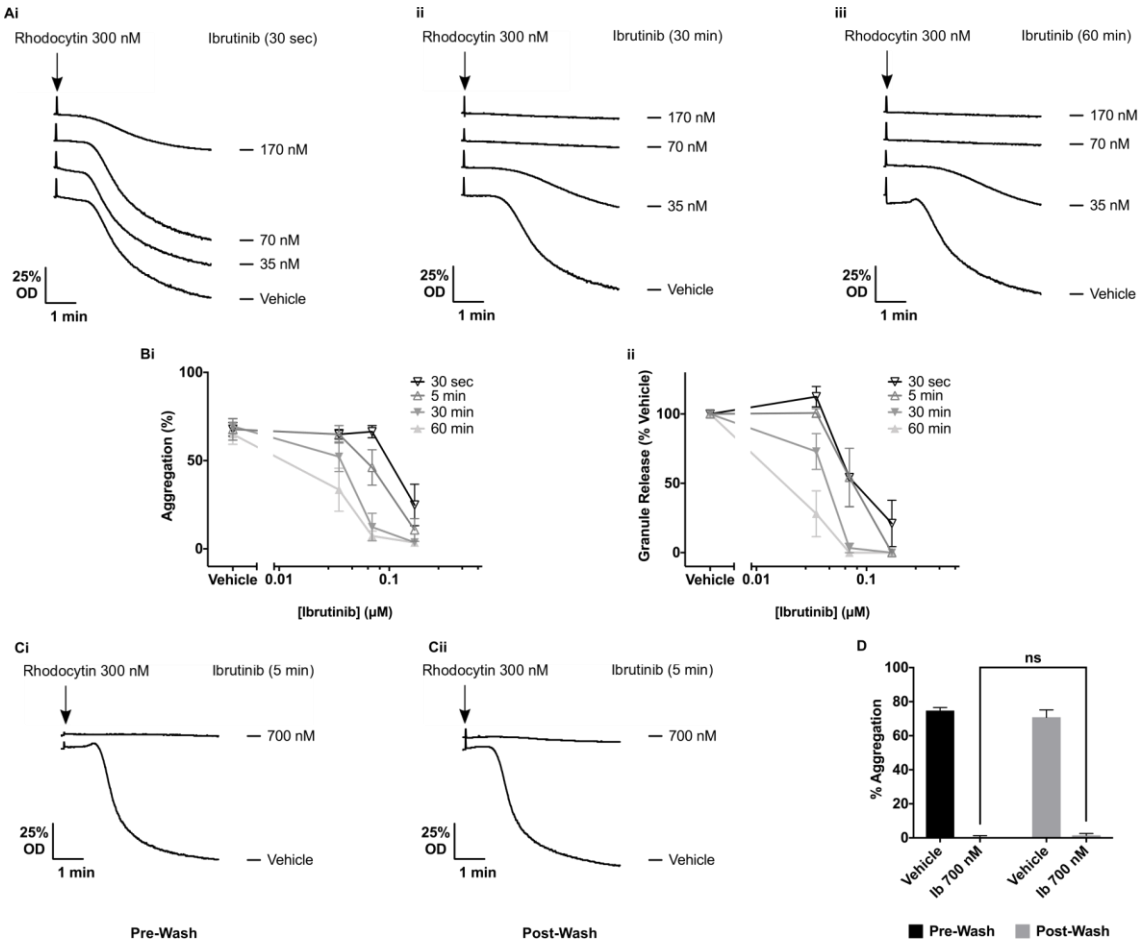

Figure 4.3: Ibrutinib's blockade of CLEC-2 mediated platelet function is both time-dependent and irreversible.
Human healthy donor washed platelets at $4x10^8$/ml were incubated with ibrutinib or vehicle for 30 seconds - 60 minutes before being stimulated with rhodocytin 300 nM for 5 minutes. (A) Representative aggregation traces from one of the five identical experiments. (B) Mean data ± SEM showing the effect of ibrutinib incubation time on CLEC-2 mediated platelet (i) aggregation and (ii) granule secretion. (C) Healthy donor human washed platelets at $4x10^8$/ml were incubated with ibrutinib or vehicle for 5 minutes before being stimulated with rhodocytin 300 nM (i). Alongside, washed platelets at 4 $x10^8$/ml, treated identically with either ibrutinib or vehicle, were washed twice in modified-Tyrode's-HEPES buffer and resuspended to $4x10^8$/ml. Platelets were then stimulated with rhodocytin 300 nM (ii). Traces are representative of three identical experiments (D) Mean data (n=3) analysed with one-way ANOVA and shown as mean ± SEM.Results shown are mean ± SEM and were analysed with one-way ANOVA. ns = non-significant.

4.2.2.2 Ibrutinib induced blockade of CLEC-2 mediated platelet function is irreversible

In an identical way to the experiments performed while investigating the effect

of ibrutinib on GPVI-mediated platelet function; after incubation with the drug or vehicle platelets were either stimulated with rhodocytin or washed twice in modified-Tyrode's HEPES buffer to see if the inhibitory effect of ibrutinib could be washed out. The results seen in Figure 4.3 clearly show that the inhibitory effect of ibrutinib on CLEC-2 mediated platelet aggregation is irreversible. This result contrasts markedly with the result from the same experiment involving GPVI-mediated platelet aggregation.

4.2.3 Ibrutinib inhibits phosphorylation events downstream of the CLEC-2 receptor

The concentration at which ibrutinib inhibits CLEC-2 mediated platelet function in human washed platelets is identical to that which inhibits Btk Y223 phosphorylation downstream of GPVI activation. This raises the possibility that, unlike GPVI-mediated platelet function, CLEC-2 might be critically dependent on Btk kinase function. To study this further experiments were carried out to look at tyrosine phosphorylation events downstream of the CLEC-2 receptor and how these were affected by ibrutinib.

4.2.3.1 Whole cell phosphorylation levels plateau and do not reduce following stimulation with rhodocytin for up to 5 minutes

There are reports showing that phosphorylation events downstream of the multiple platelet receptors are time-dependent (Kralisz & Cierniewski 1998; Mazet et al. 2015; Gibbins et al. 1996). To ensure no phosphorylation events

were missed due to lysing activated platelets too long after addition of agonist pan-tyrosine phosphorylation downstream of the CLEC-2 receptor were measured at different time points following ligation of the receptor with rhodocytin 300 nM. Time points up to 300 seconds were sampled and it was found that, in the presence of eptifibatide, phosphorylation levels reached a maximum at 90 seconds with no reduction visible up to 300 seconds (see Figure 4.4A).

4.2.3.2 Ibrutinib inhibits autophosphorylation of Btk Y223, PLCɣ2, Syk and Btk Y551 phosphorylation with the same potency as it inhibits aggregation

CLEC-2 signalling utilises the same protein kinase signalling architecture as GPVI and so the experiment performed to examine the effects of ibrutinib on tyrosine phosphorylation events downstream of CLEC-2 utilised the same methods and antibodies as seen in Chapter 3 in Figure 3.7. The only differences being that, despite robust phosphorylation seen at these sites downstream of GPVI, blots for PLCɣ2 pY753 (not shown) and pY759 (see Figure 4.4Bi) did not detect any phosphorylation and so these have not been quantified.

Despite the similar signalling architecture, the effect of ibrutinib on CLEC-2 mediated tyrosine phosphorylation was markedly different to that seen on the phosphorylation events downstream of GPVI (see Figure 4.4B). All phosphorylation events studied, except Src pY418, showed complete loss of phosphorylation at 70 nM ibrutinib with virtually identical IC_{50}s to the inhibition of CLEC-2 mediated platelet aggregation and granule secretion as well as GPVI-

mediated Btk Y223 phosphorylation (see Table 4.1). Manne *et al.* had similar findings (but notably did not study Btk pY551) and concluded that, downstream of CLEC-2, Btk must lie upstream of Syk (Manne et al. 2015). Of note, Btk pY223 was far weaker in all the rhodocytin stimulated samples than in those stimulated by CRP. Attempts to examine Tec phosphorylation by immunoprecipitation were unsuccessful.

The finding that Btk pY551 is lost downstream of CLEC-2 in platelets treated with low concentration ibrutinib suggests that the Manne *et al*. model of Btk lying upstream of Syk, but downstream of SFKs may not be correct, as, if this were the case, it would be predicted to be phosphorylated even in the presence of low concentration ibrutinib (see Figure 4.5).

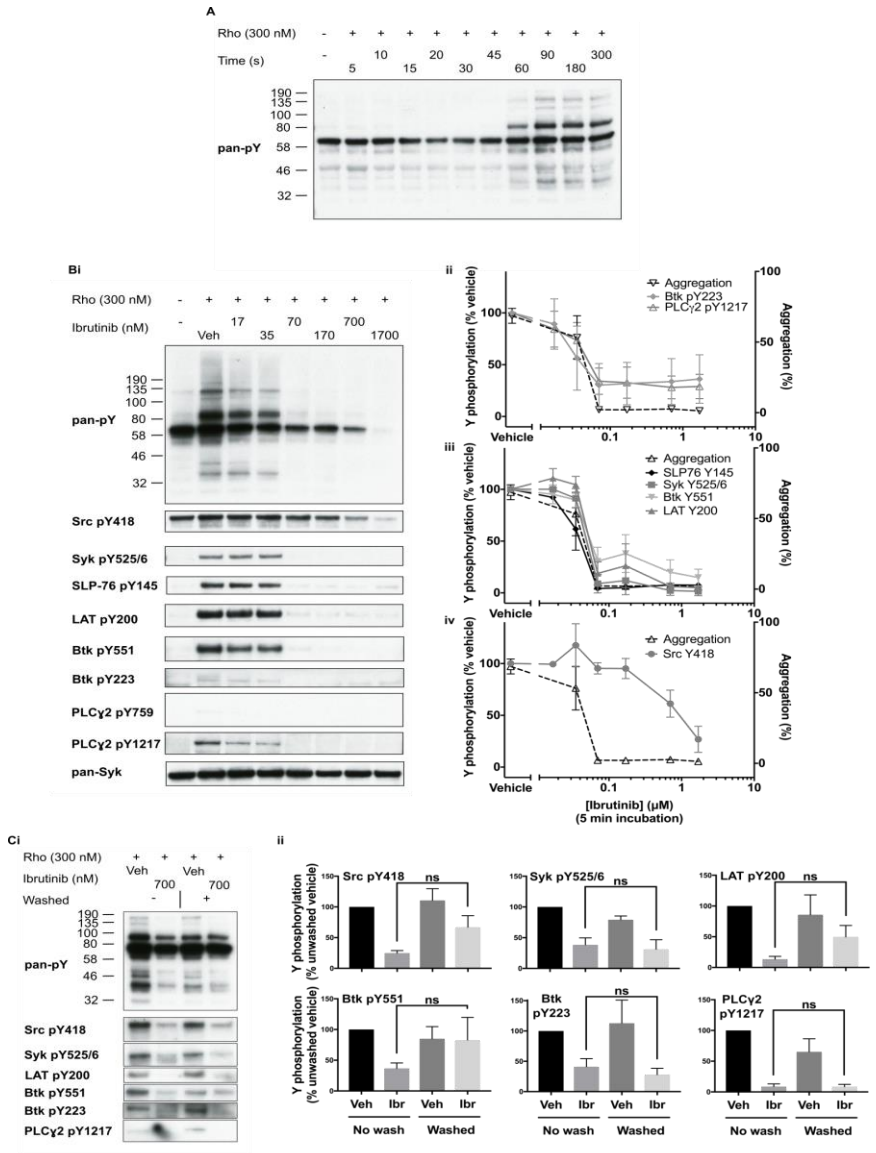

Figure 4.4: Ibrutinib irreversibly inhibits multiple tyrosine phosphorylation events downstream of the CLEC-2 receptor on human platelets.
Healthy donor washed human platelets at $4x10^8$/ml in the presence of eptifibatide 9 μM were incubated with ibrutinib or vehicle for 5 minutes prior to stimulation with rhodocytin 300 nM. Platelets were then lysed with 5X reducing sample buffer 5 minutes after addition of agonist unless otherwise stated. Whole cell lysates were then separated by SDS-PAGE and Western blots were probed for whole cell phosphorylation or kinase phosphorylation with the stated antibodies downstream of the platelet CLEC-2 receptor. (A) Blot from single experiment with addition of sample buffer at stated time points. (B) Representative blot from 4 identical experiments (i). Mean ± SEM of 4 identical experiments for phosphorylation events downstream (ii) and upstream (iii) of Btk pY223 as well as Src pY418 (iv). (C) Before lysis, platelets were either washed twice in modified-Tyrode's-HEPES buffer or not. Representative blots (i) and quantification of phosphorylation shown as Mean ± SEM of 3 identical experiments (ii) are shown. Results were analysed statistically using a paired two-tailed t-test *P<0.05, ns = non-significant.

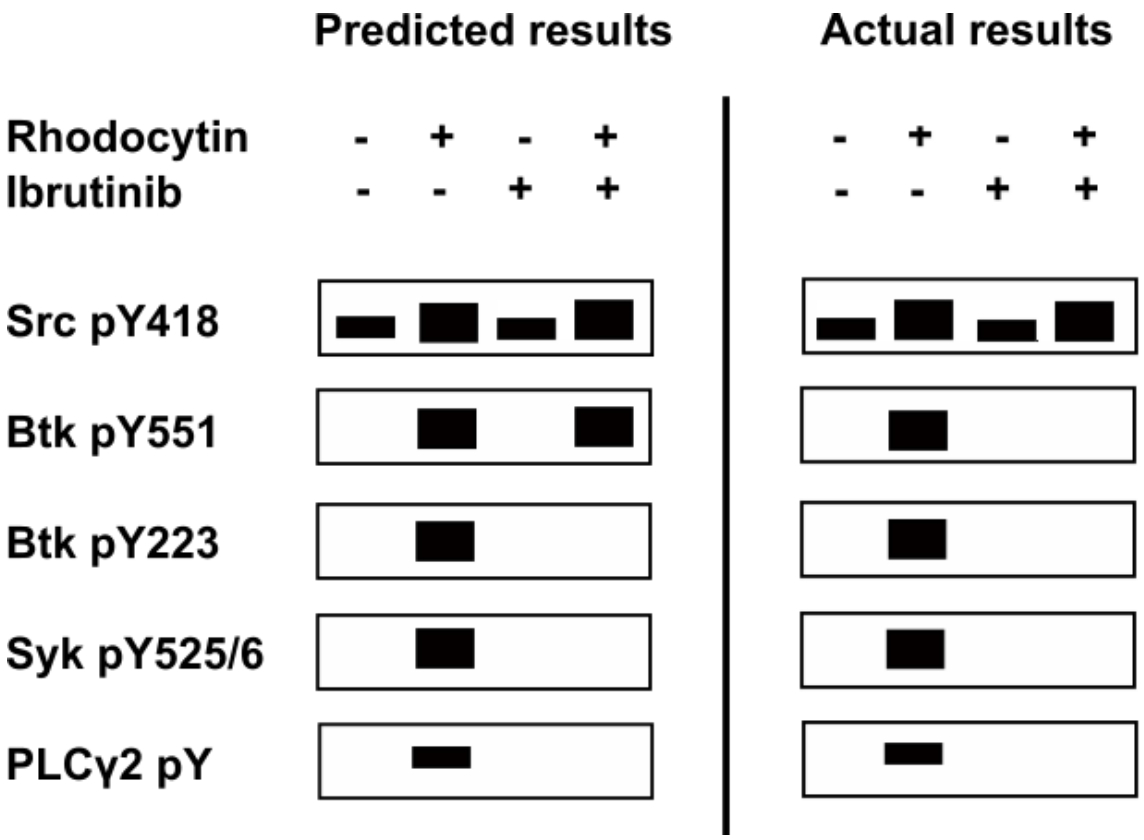

Figure 4.5: Schematic representation of predicted and actual pattern of inhibition of CLEC-2 mediated tyrosine phosphorylation in the presence of ibrutinib.
Left panel depicts predicted phosphorylation results downstream of CLEC-2 in the absence and presence of 70 nM ibrutinib based on Manne *et al*. model of Btk lying upstream of Syk but downstream of SFKs. Right panel depicts actual phosphorylation results in the same conditions.

4.2.3.3 Ibrutinib's inhibition of phosphorylation events downstream of the CLEC-2 receptor is irreversible

As ibrutinib's inhibition of CLEC-2 mediated platelet function is irreversible, it is important to study whether this irreversibility extends to its inhibition of tyrosine phosphorylation events. To this end platelets treated with ibrutinib and were either stimulated with rhodocytin or washed twice with modified-Tyrode's-HEPES buffer before being stimulated, with subsequent lysis being performed 5 minutes afterwards.

Like the findings for phosphorylation events downstream of GPVI, results shown

in Figure 4.4 indicate that ibrutinib's effects on Btk pY223 and PLCɣ2 phosphorylation downstream of CLEC-2 are also irreversible. Unlike the GPVI results however, they also show that its inhibition of global phosphorylation or that which is upstream of Btk pY223 is also not reversible. The apparent irreversibility of the upstream signalling events need some further qualification however. Phosphorylation of Syk Y525/6 was clearly irreversible in all experiments. That for Src Y418, LAT Y200 and Btk Y551 appeared irreversible in some blots, and reversible in others, hence the wide error bars seen at these phosphorylation sites in Figure 4.4Cii. It is possible that these phosphorylation events are reversible but that the western blotting technique used was not sensitive enough to detect it in all instances.

4.2.3.4 Ibrutinib's inhibition of tyrosine phosphorylation downstream of mouse CLEC-2 mimics human and mouse GPVI but not human CLEC-2. The use of human ADP-sensitive platelets corrects this difference

The use of human ADP-sensitive washed platelets rather than conventionally prepared washed platelets in the above functional assays increased the concentration of ibrutinib required to block CLEC-2 mediated platelet function by 10-fold. To investigate the effect that this method of platelet preparation has on ibrutinib's inhibition on tyrosine phosphorylation; biochemical studies were performed to examine whole cell tyrosine phosphorylation as well as that on specific tyrosine residues of kinases and proteins downstream of CLEC-2.
The results are shown in Figure 4.6 and Table 4.1. Strikingly, there is no longer

loss of whole cell phosphorylation at 70 nM ibrutinib as is seen in conventionally prepared platelets, but there is partial loss of whole cell phosphorylation at 700 nM. The loss of Btk Y223 and downstream PLCγ2 phosphorylation mirrors that of inhibition of platelet aggregation with similar IC_{50}s for all these dose response curves. Unlike in conventionally prepared platelets, however, phosphorylation events upstream of Btk pY223 were not blocked by 70 nM ibrutinib but, in fact, were unaffected by all but the highest concentrations of ibrutinib (7 μM). This pattern of phosphorylation inhibition mirrored that which was seen when examining the effects of ibrutinib on phosphorylation events downstream of the GPVI receptor.

Although the results from Figure 4.4B using conventionally prepared platelets are similar to Manne *et al.*, the findings using ADP-sensitive platelets contrast significantly with their study and confirm that Btk does not lie upstream of Syk in the CLEC-2 signalling cascade as it does downstream of GPVI.

WT mouse platelets were much less sensitive to ibrutinib's inhibition of CLEC-2 mediated platelet aggregation than human platelets. To investigate whether this was merely to do with a reduced potency of inhibition of Btk or whether there was another explanation, similar biochemistry studies were performed in mouse platelets.

The results are shown in Figure 4.6B. Similar to results using ibrutinib to inhibit GPVI-mediated phosphorylation events in human and mouse platelets and its inhibition of CLEC-2-mediated phosphorylation, Btk Y223 and downstream PLCγ2 phosphorylation were blocked by low concentrations of ibrutinib (IC_{50} 65 – 122 nM). Upstream phosphorylation events, with the exception of Src pY418, were unaffected by even very high concentrations of ibrutinib.

Both of these sets of results are consistent with the known reliance of human CLEC-2, but not mouse CLEC-2, on secondary mediator feedback for robust signalling following ligation of the receptor (Pollitt et al. 2010).

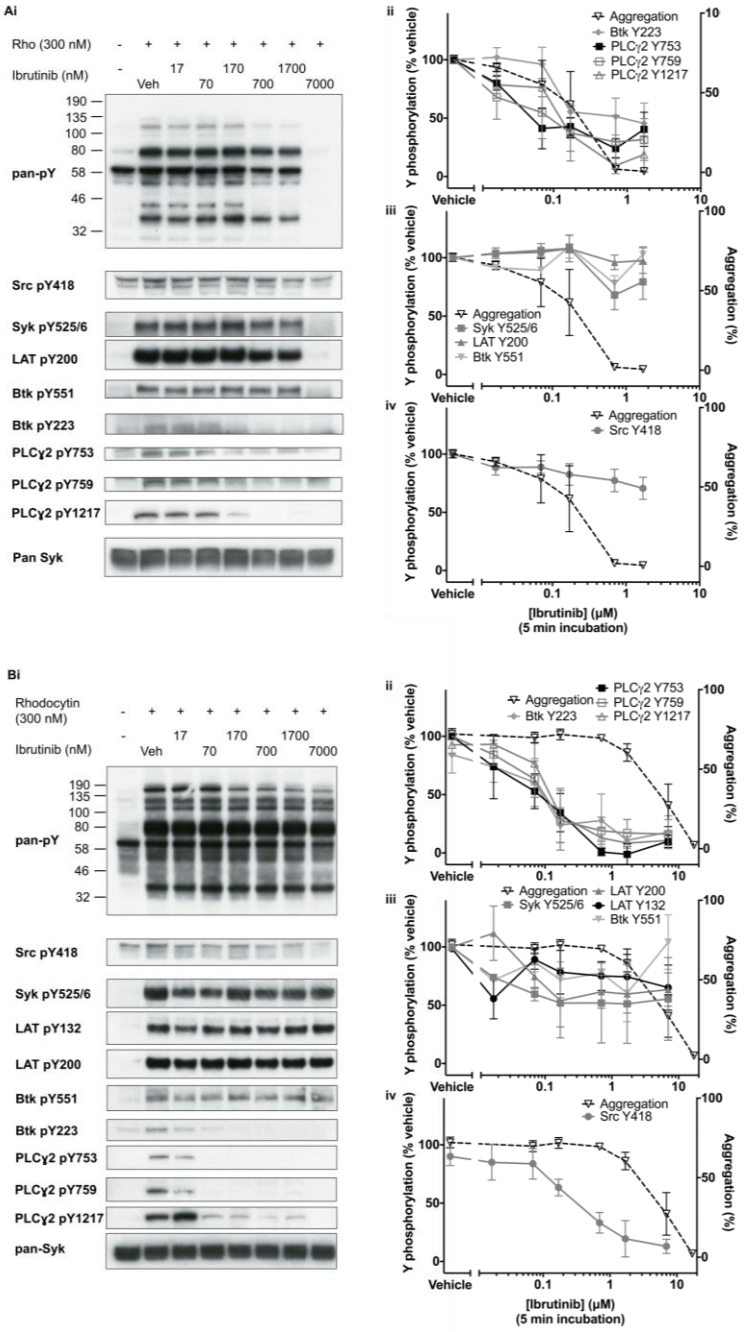

Figure 4.6: Ibrutinib dose-dependently inhibits platelet aggregation and tyrosine phosphorylation in ADP-sensitive human washed platelets and WT mouse platelets at higher concentrations than are required to inhibit conventionally prepared human washed platelets.

Eptifibatide (9 μM) treated healthy human donor washed platelets at $4x10^8$/ml that had been prepared with a method to retain their sensitivity to ADP stimulation (A) and WT mouse washed platelets at $4x10^8$/ml (B) were incubated with ibrutinib or vehicle for 5 minutes before being stimulated with rhodocytin 300 nM. Platelets were then lysed with 5X reducing sample buffer 5 minutes after addition of agonist. Whole cell lysates were then separated by SDS-PAGE and Western blots were probed for whole cell phosphorylation or kinase phosphorylation with the stated antibodies downstream of the platelet CLEC-2 receptor. (i) Representative blots and (ii-iv) mean ± SEM of three identical experiments examining the tyrosine phosphorylation levels of the proteins shown.

Figure	Name of Curve	IC_{50} (μM)	95% C.I.
4.1	HD PRP Aggregation	5.417	2.869 — 11.32
4.1	HD Aggregation	0.023	0.009 — 0.053
4.1	HD Secretion	0.072	0.043 — 0.124
4.1	HD Ca^{2+} Mobilisation	1.016	0.399 — 4.582
4.1	HD Aggregation (ADP-sensitive)	0.282	0.080 — 1.428
4.1	WT Mouse WP Aggregation	13.28	4.650 — 129.2
4.3	Aggregation. 30 seconds Ibru	-	-
4.3	Aggregation. 5 minutes Ibru	-	-
4.3	Aggregation. 30 minutes Ibru	0.086	0.027 — 0.578
4.3	Aggregation. 60 minutes Ibru	0.038	0.007 — 0.153
4.3	Secretion. 30 seconds Ibru	-	-
4.3	Secretion. 5 minutes Ibru	-	-
4.3	Secretion. 30 minutes Ibru	0.072	0.026 — 0.257
4.3	Secretion. 60 minutes Ibru	0.016	0.001 — 0.044
4.4	HD Btk pY223	0.024	0.002 — 0.133
4.4	HD PLCγ2 pY1217	0.034	0.010 — 0.119
4.4	HD Syk pY525/6	0.052	0.020 — 0.150
4.4	HD LAT pY200	0.036	0.028 — 0.189
4.4	HD SLP76 pY145	0.032	0.015 — 0.066
4.4	HD Btk pY551	0.059	0.023 — 0.179
4.4	HD Src pY418	-	-
4.6	HD Btk pY223 (ADP-sensitive)	0.142	0.029 — 1.301
4.6	HD PLCγ2 pY753 (ADP-sensitive)	0.024	0.005 — 0.093
4.6	HD PLCγ2 pY759 (ADP-sensitive)	-	-
4.6	HD PLCγ2 pY1217 (ADP-sensitive)	0.1149	0.032 — 0.421
4.6	HD Syk pY525/6 (ADP-sensitive)	-	-
4.6	HD LAT pY200 (ADP-sensitive)	-	-
4.6	HD Btk pY551 (ADP-sensitive)	-	-
4.6	HD Src pY418 (ADP-sensitive)	-	-
4.6	WT Mouse Btk pY223	0.076	0.011 — 0.559
4.6	WT Mouse PLCγ2 pY753	0.074	0.026 — 0.200
4.6	WT Mouse PLCγ2 pY759	0.065	0.017 — 0.232
4.6	WT Mouse PLCγ2 pY1217	0.122	0.044 — 0.363
4.6	WT Mouse Syk pY525/6	-	-
4.6	WT Mouse LAT pY132	-	-
4.6	WT Mouse LAT pY200	-	-
4.6	WT Mouse Btk pY551	-	-
4.6	WT Mouse Src pY418	0.35	0.126 — 1.036

Table 4.1: IC_{50} values for all dose response curves for experiments involving stimulation with rhodocytin and inhibition with ibrutinib
Dose-response curves from all figures in Chapter 4 are summarised in this table. Confidence intervals are provided to better enable comparison between curves.

4.2.3.5 Platelets taken from patients on ibrutinib have inhibited tyrosine kinase phosphorylation

In order to ascertain whether the *in vitro* observations occurred at concentrations of drug achieved *in vivo*, samples taken from patients with CLL were also examined to look at the effects of Btk inhibition on tyrosine phosphorylation downstream of CLEC-2 *ex vivo*. Consistent with the *in vitro* results where low concentrations of ibrutinib caused loss of tyrosine phosphorylation both up- and downstream of Btk pY223; patients on ibrutinib and the more Btk-specific acalabrutinib had a similar pattern of loss of phosphorylation (see Figure 4.7).

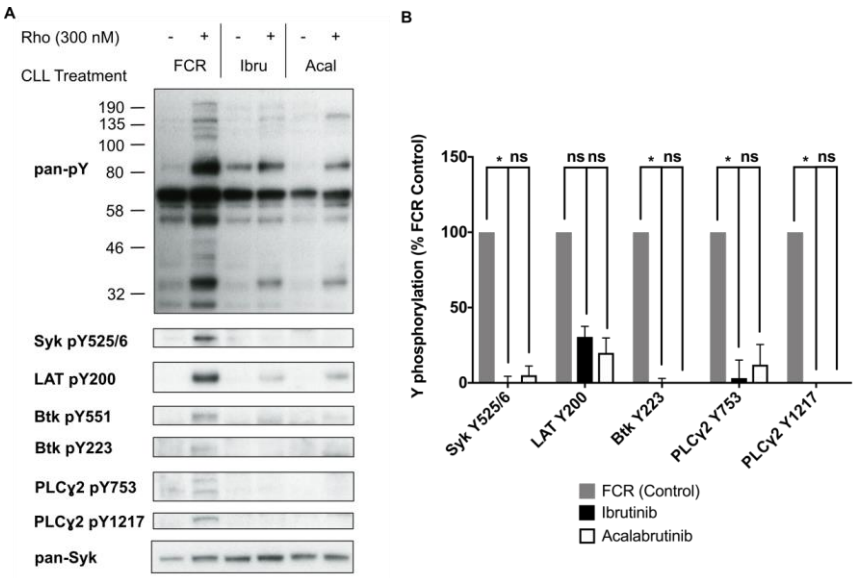

Figure 4.7: Patients treated with Btk inhibitors have globally reduced phosphorylation downstream of CLEC-2.
Eptifibatide (9 μM) treated washed platelets at 4×10^8/ml from patients with CLL treated with FCR, ibrutinib or acalabrutinib were stimulated with rhodocytin 300 nM. Samples were lysed with 5X SDS reducing sample buffer after 5 minutes. Whole cell lysates were then separated by SDS-PAGE and underwent Western blot with the stated antibodies for whole cell phosphorylation, kinases and proteins downstream of CLEC-2. (A) Blots are representative of similar blots from twelve patients; three treated with FCR, six with ibrutinib and three with acalabrutinib. (B) Percentage tyrosine phosphorylation as compared to FCR treated patient platelets was measured and is represented as the means ± SEM (ibrutinib n=6, acalabrutinib n=3). Statistical analysis was performed with a two way ANOVA with Tukey's correction for multiple comparisons.

4.2.3.6 Platelets from patients with XLA have reduced CLEC-2 mediated tyrosine phosphorylation.

In order to see which of the ibrutinib induced biochemical changes downstream of CLEC-2 were secondary to Btk inhibition, or which were due to any off-target effects, platelet lysates from patients with XLA were probed with whole cell phosphorylation and phosphospecific antibodies after stimulation with rhodocytin. As seen in Figure 4.8A; whole cell phosphorylation was globally reduced, but not to the same extent as with patients treated with ibrutinib. Notably, similar to ibrutinib treated patients, the band at ~140 kDa representing phosphorylated PLCɣ2 was absent in XLA patient platelets, but, contrary to the results from ibrutinib treated patients and platelets from healthy donors treated with 70 nM ibrutinib, the band at 80 kDa comprising a combination of Syk and SLP76 (among other proteins) was only marginally reduced. As seen in Figure 4.8A and B, Syk phosphorylation is reduced but not absent like it is in *ex vivo* and *in vitro* ibrutinib treated platelets. Src phosphorylation was unaltered, as was LAT phosphorylation, though there was a trend to reduction in LAT pY200, though this is not statistically significant.

PLCɣ2 pY1217 was absent, as is the case with *in vitro* and *ex vivo* ibrutinib treated platelets stimulated with rhodocytin. This is different to the XLA platelets simulated with CRP, however, where PLCɣ2 pY1217 is reduced but still present.

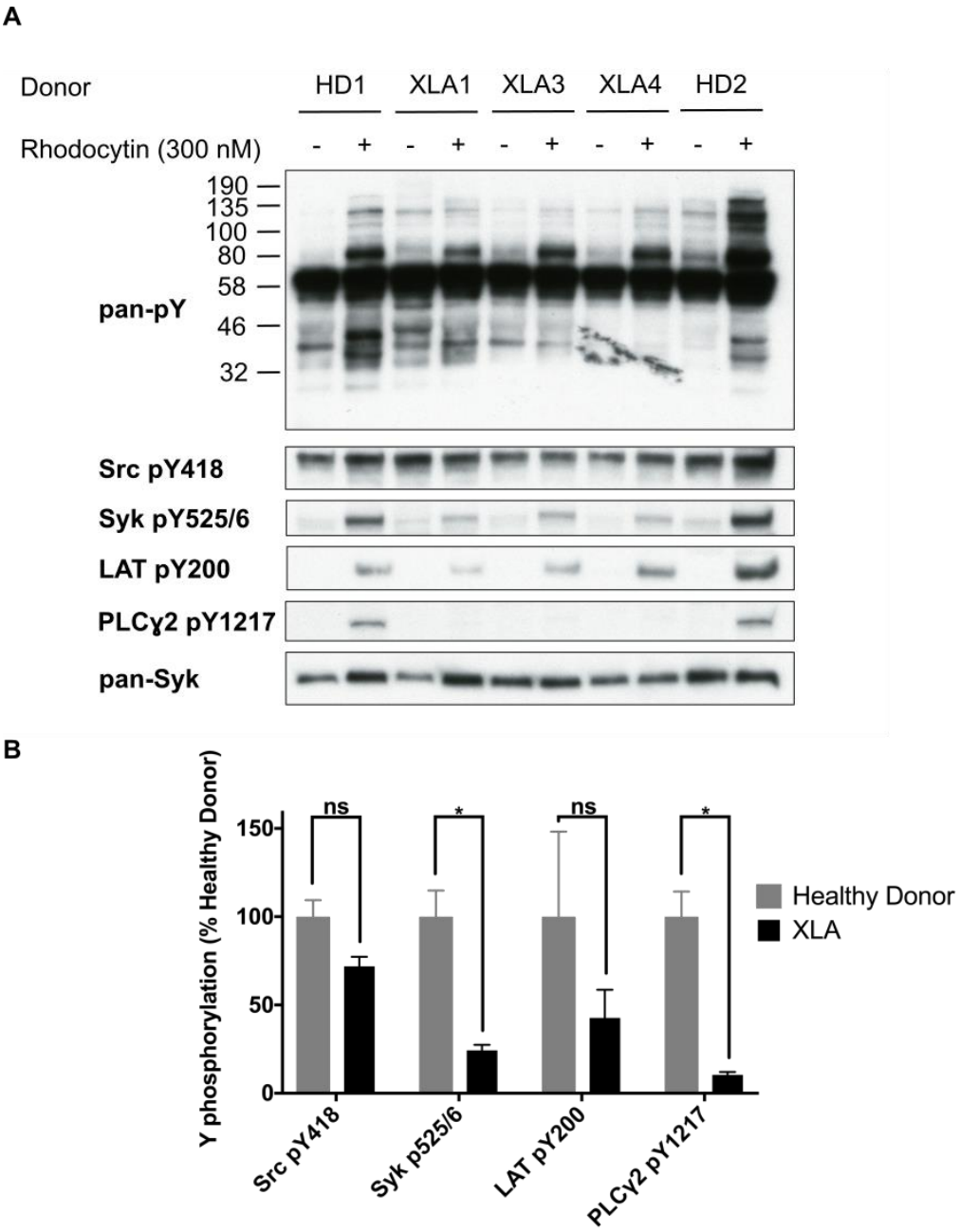

Figure 4.8: Patients with XLA have absent PLCγ2 phosphorylation downstream of the CLEC-2 receptor but Src, Syk and LAT phosphorylation are present.
Eptifibatide (9 μM) treated washed platelets at 4 x 10^8/ml from patients with XLA were lysed with 5X reducing sample buffer 5 minutes after addition of rhodocytin 300 nM or PBS as shown. Whole cell lysates were then separated by SDS-PAGE and Western blots were probed for whole cell or kinase phosphorylation with the stated antibodies. (A) Blot and (B) mean ± SEM (n=3) for phosphorylation events downstream of the CLEC-2 receptor. Results were analysed statistically using a one way ANOVA with Sidak's correction for multiple comparisons. *P<0.05, ns = non-significant.

4.2.4 Ibrutinib inhibits platelet spreading but not clustering of CLEC-2 on podoplanin

4.2.4.1 Btk-specific concentrations of ibrutinib reduce both number of platelets and the spread area of platelets when adhering to immobilised podoplanin

In order to look at the effect of ibrutinib on how CLEC-2 affects adhesion and subsequent activation of cytoskeletal machinery, the effect on platelet spreading on immobilised CLEC-2 ligands was studied. rhodocytin was used initially but attempts to get the platelets to adhere to immobilised rhodocytin were unsuccessful. Human Fc-conjugated podoplanin was used as a CLEC-2 ligand. This has been used in previous publications involving platelet spreading that has been shown to be mediated by CLEC-2 without involvement of the Fc-receptor FCγRIIa (Navarro-Núñez et al. 2015). Adhesion and spreading was assessed by isolating washed platelets from healthy donors and allowing them to spread on podoplanin coated coverslips for 45 minutes prior to fixation, antibody staining and imaging. Blockade of aggregation to rhodocytin 300 nM with ibrutinib 170 nM was confirmed prior to commencing the spreading experiment (not shown). Platelets were treated with ibrutinib 170 nM or vehicle either for 5 minutes prior to spreading or after spreading had been ongoing for 30 minutes. Results are shown in Figure 49. There was a statistically significant reduction in spread platelet area and number of adherent platelets when ibrutinib was added to the platelets before spreading took place. There was no effect on number of adherent platelets or spread area in samples where ibrutinib was added after the initiation of spreading. This shows that Btk is

important for platelet adhesion to podoplanin and also the subsequent initiation, but not the maintenance of spreading.

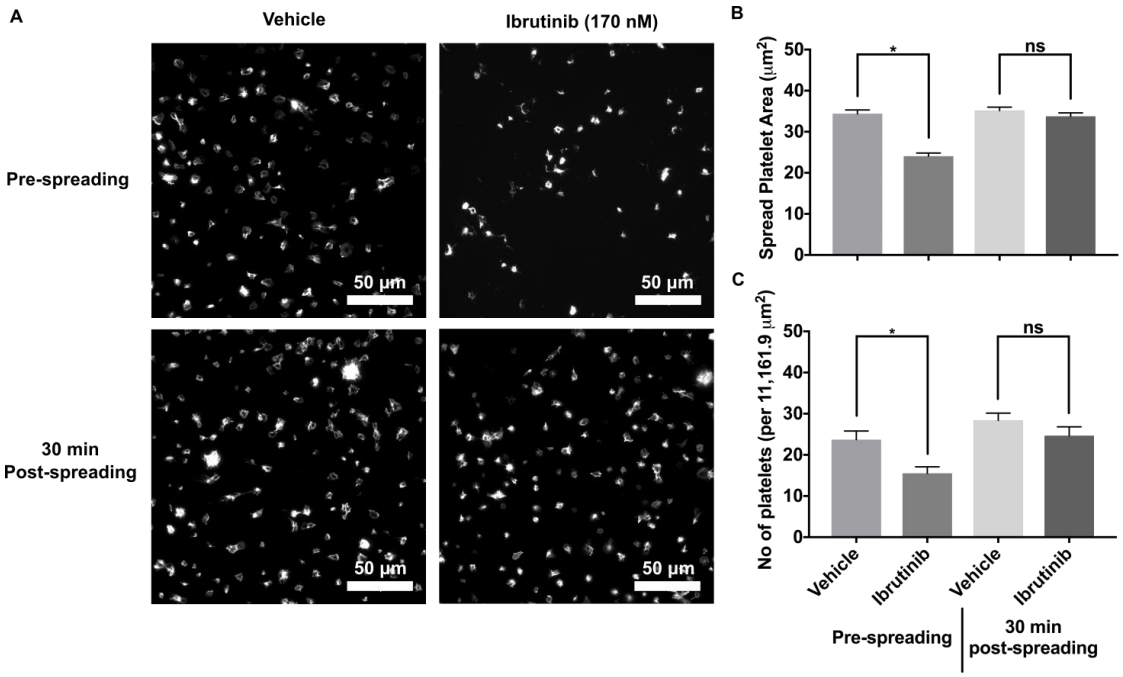

Figure 4.9: Incubation of platelets with ibrutinib prior to adhesion on podoplanin reduces both number and area of spread platelets.
Human healthy donor washed platelets at $2x10^7$/ml were incubated with ibrutinib (170 nM) or vehicle for 5 minutes before spreading on podoplanin coated coverslips at 37°C for 45 minutes. Simultaneously, untreated platelets were spread on podoplanin coated coverslips at 37°C for 30 minutes before ibrutinib (170 nM) or vehicle was added and incubated for 15 minutes at 37°C. Coverslips were then washed to remove non-adherent platelets before fixation with formalin and staining with AF 488-conjugated phalloidin. (A) Representative images of three identical experiments. Ilastik 1.1.2 machine learning software was used to automatically and reproducibly identify platelets and data on platelet number and surface area was measured using the KNIME 3.4 analytics platform. (B) Mean data ± SEM (n=3). Statistical analysis performed using two-tailed Welch's t-test. (C) Mean data ± SEM (n=3). Statistical analysis performed using a one-way ANOVA with Tukey's correction for multiple comparisons.

4.2.4.2 Platelets taken from patients on Btk inhibitors and those with XLA have normal adhesion but reduced spreading when bound to immobilised podoplanin

To ensure that the effect of ibrutinib on platelet spreading on podoplanin-Fc was a Btk-specific effect and occurred at physiologic concentrations Btk inhibitor, further experiments using platelets from patients with XLA and those taking Btk inhibitors for CLL were performed. Patients with XLA, those taking ibrutinib 420 mg once daily or acalabrutinib 100 mg twice daily were sampled and washed platelets were isolated and incubated on immobilised podoplanin for 45 minutes before fixing and staining. Patients on FCR were not used as the control for this experiment as they were unavailable at the time of performing this assay. Consistent with the *in vitro* results, the results in Figure 4.10 show that both congenital lack of Btk or its inhibition with both ibrutinib and acalabrutinib treatment resulted in a reduced spread platelet area. Platelet adhesion to podoplanin was, however, unchanged. This, then, confirms that Btk is involved in the initiation of platelet spreading after activation of CLEC-2 by podoplanin, but it fails to support the *in vitro* data which showed that Btk is important for supporting the initial adhesion of CLEC-2 to podoplanin.

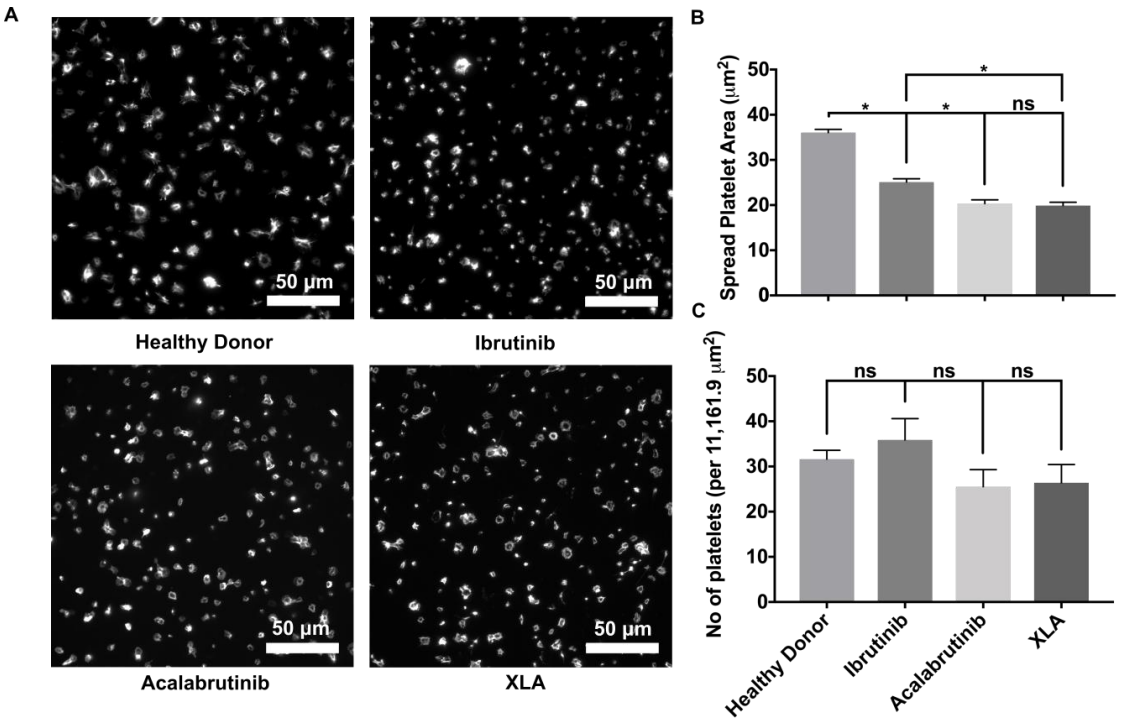

Figure 4.10: Platelets from patients on Btk inhibitors or those with XLA adhere in normal numbers but with a reduced spread area when bound to immobilised podoplanin-Fc.
Washed platelets at $2x10^7$/ml from healthy human donors, patients taking ibrutinib or acalabrutinib and those with XLA were incubated on podoplanin-Fc (10 µg/ml) coated coverslips at 37°C for 45 minutes. Coverslips were then washed to remove non-adherent platelets before fixation with formalin and staining with AF 488-conjugated phalloidin. (A) Representative images. Ilastik 1.1.2 machine learning software was used to automatically and reproducibly identify platelets and data on platelet number and surface area was measured using the KNIME 3.4 analytics platform. (B) and (C) Data shown as mean ± SEM for healthy donors (n=5), ibrutinib (n=4), acalabrutinib (n=2) and XLA patients (n=2). Statistical analysis performed using a one-way ANOVA with Tukey's correction for multiple comparisons.

4.2.4.3 Btk-specific concentrations of ibrutinib have no effect on CLEC-2 receptor clustering when binding to immobilised podoplanin

CLEC-2 clustering upon ligand binding is an important part of the activation of its downstream signalling. It has previously been shown that the clustering of CLEC-2 in response to ligation with podoplanin is dependent on the actions of the tyrosine kinases Syk and SFKs (Pollitt et al. 2014).Thus it seemed reasonable to suspect, given the potent inhibition of CLEC-2 mediated platelet

function and Btk's close interaction with both Syk and SFKs, that Btk might also affect CLEC-2 receptor clustering. Pilot experiments were carried out to establish a method that enabled visualisation of CLEC-2 clustering (or lack thereof) when platelets were spread on immobilised podoplanin-Fc and collagen respectively. They were then probed with the anti-human CLEC-2 antibody AYP1 and the distribution of CLEC-2 was then imaged using dSTORM super-resolution microscopy (see Figure 4.11).From this single pilot experiment it was clear there was a difference in CLEC-2 distribution on the surface of the platelet when platelets were spread on collagen or podoplanin-Fc.

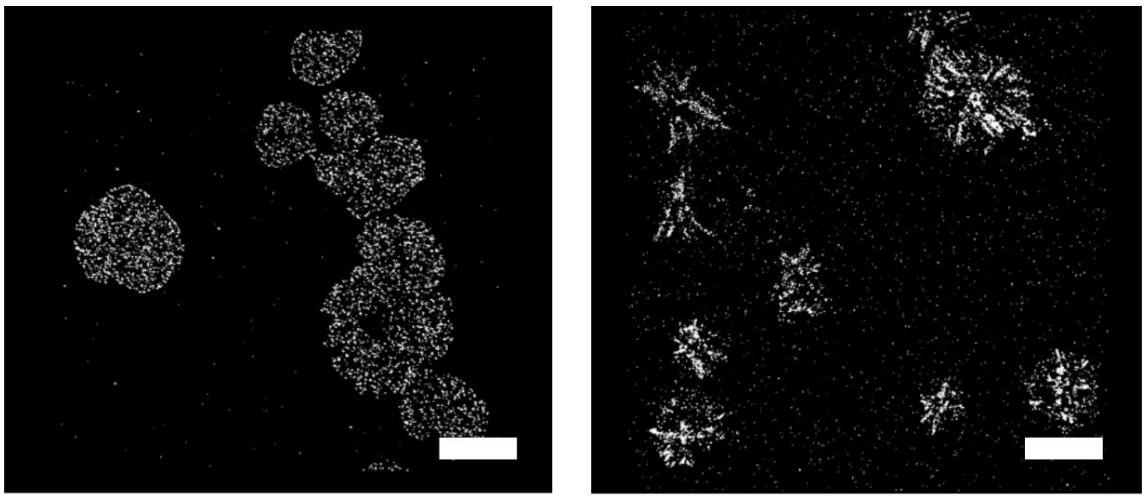

Figure 4.11: CLEC-2 clustering is seen when platelets are spread on immobilised podoplanin-Fc but not on collagen.
Washed platelets ($2x10^7$/ml) from a single healthy human donor were spread on immobilised collagen (10 µg/ml) or podoplanin-Fc (10 µg/ml) for 45 minutes before fixation and probing with the anti-human CLEC-2 antibody AYP1 and secondary staining with goat anti-mouse antibody conjugated to AF 647. Spread platelets were imaged using a Nikon Eclipse Ti-E N-STORM system in dSTORM mode. Scale bar = 5 µm.

To examine whether Btk inhibition blocked CLEC-2 clustering, platelets were treated with ibrutinib or vehicle in exactly the same manner as for the spreading experiments and were allowed to settle on immobilised podoplanin-Fc. They were imaged using dSTORM super-resolution microscopy as above. The resultant image was reconstructed with the ThunderSTORM plugin for ImageJ 1.5 and the size and density of the CLEC-2 clusters on it were measured using persistence based clustering that has been described recently (Pike et al. 2018). Surprisingly, the results, shown in Figure 4.12 show that treatment with ibrutinib, either before or after the initiation of spreading, has no effect on the mean size or density of CLEC-2 clusters.

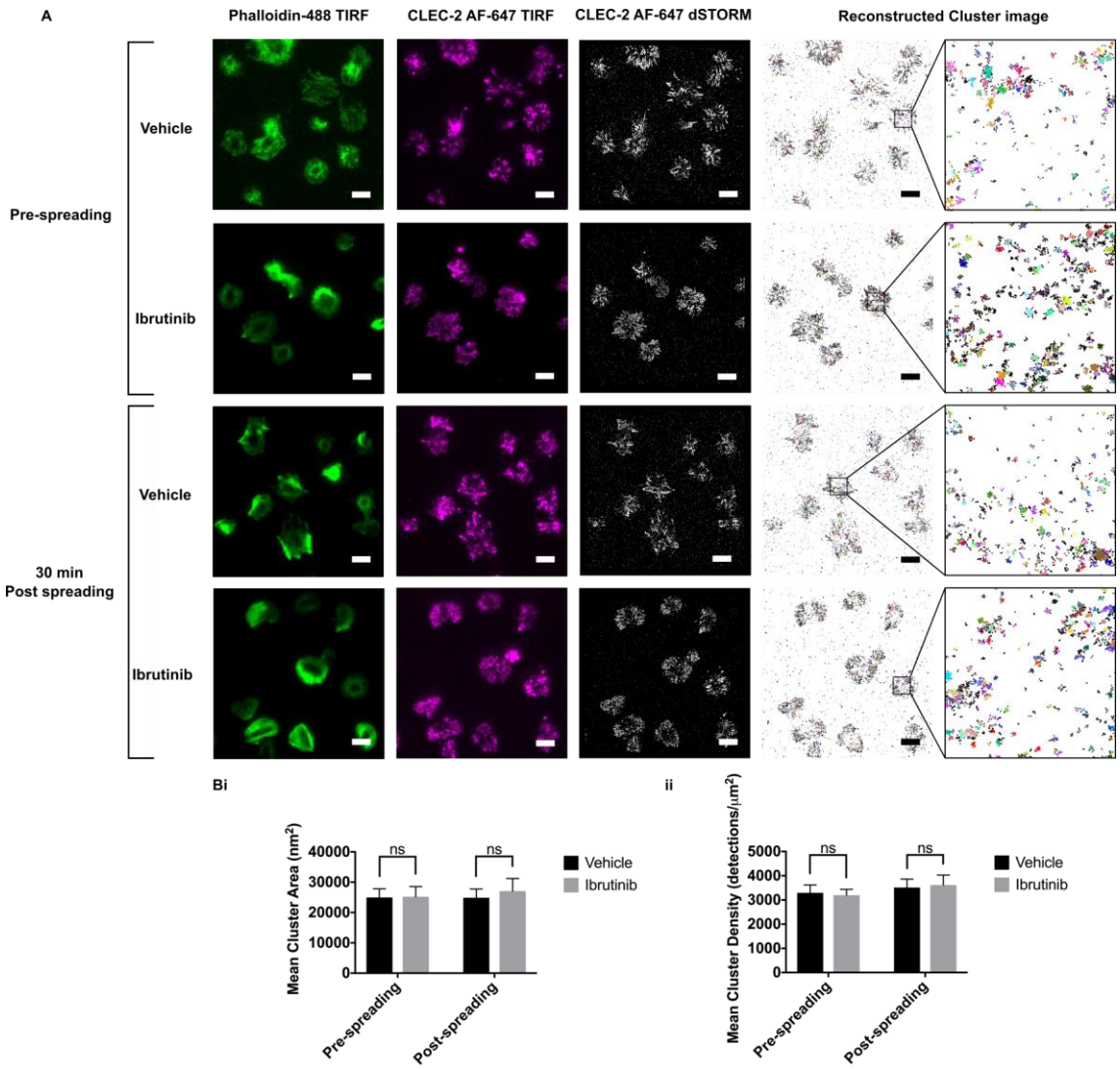

Figure 4.12: CLEC-2 clustering on immobilised podoplanin-Fc is unchanged in the presence of Btk inhibition with ibrutinib.
Human healthy donor washed platelets at 2x10^7/ml were incubated with ibrutinib (170 nM) or vehicle for 5 minutes before spreading on podoplanin-Fc (10 µg/ml) coated coverslips at 37°C for 45 minutes. Simultaneously, untreated platelets were spread on podoplanin-Fc (10µg/ml) coated coverslips at 37°C for 30 minutes before ibrutinib (170 nM) or vehicle (DMSO) was added and incubated for 15 minutes at 37°C. Platelets were then fixed and probed with the anti-human CLEC-2 antibody AYP1. Secondary antibody staining was performed with goat anti-mouse antibody conjugated to AF 647 as well as AF 488-conjugated phalloidin. Spread platelets were imaged using a Nikon Eclipse Ti-E N-STORM system in dSTORM mode. (A) representative images from five identical experiments with the microscope in Total Internal Reflection Fluorescence (TIRF) or dSTORM mode or reconstructed images with false colour added to individual clusters. (B) Cluster area (i) and density (ii) are depicted as mean ± SEM (n=5). Statistical analysis was with two-way ANOVA with Sidak's correction for multiple comparisons. ns=non-significant. Scale bar = 5 µm.

4.2.4.4 Platelets taken from patients with XLA or those on ibrutinib have normal clustering of CLEC-2 when adhering to immobilised podoplanin

Simultaneously, in order to see if any effect on clustering was Btk-specific and occurred at concentrations of ibrutinib achieved in patients, platelets from healthy donors, patients with XLA and those with CLL on ibrutinib 420 mg once daily were spread on immobilised podoplanin-Fc in order to examine CLEC-2 clustering. Patients receiving FCR chemotherapy were unavailable for use as controls at the time of performing this assay. After fixation, the platelets were probed with AYP1 and then imaged using dSTORM super-resolution microscopy. The size and density of CLEC-2 clusters were then analysed using persistence based clustering as before. As for the *in vitro* ibrutinib treated platelets, there was no difference in the size and density of CLEC-2 clusters between platelets from healthy donors and those from patients with XLA or with CLL treated with ibrutinib (see Figure 4.13).

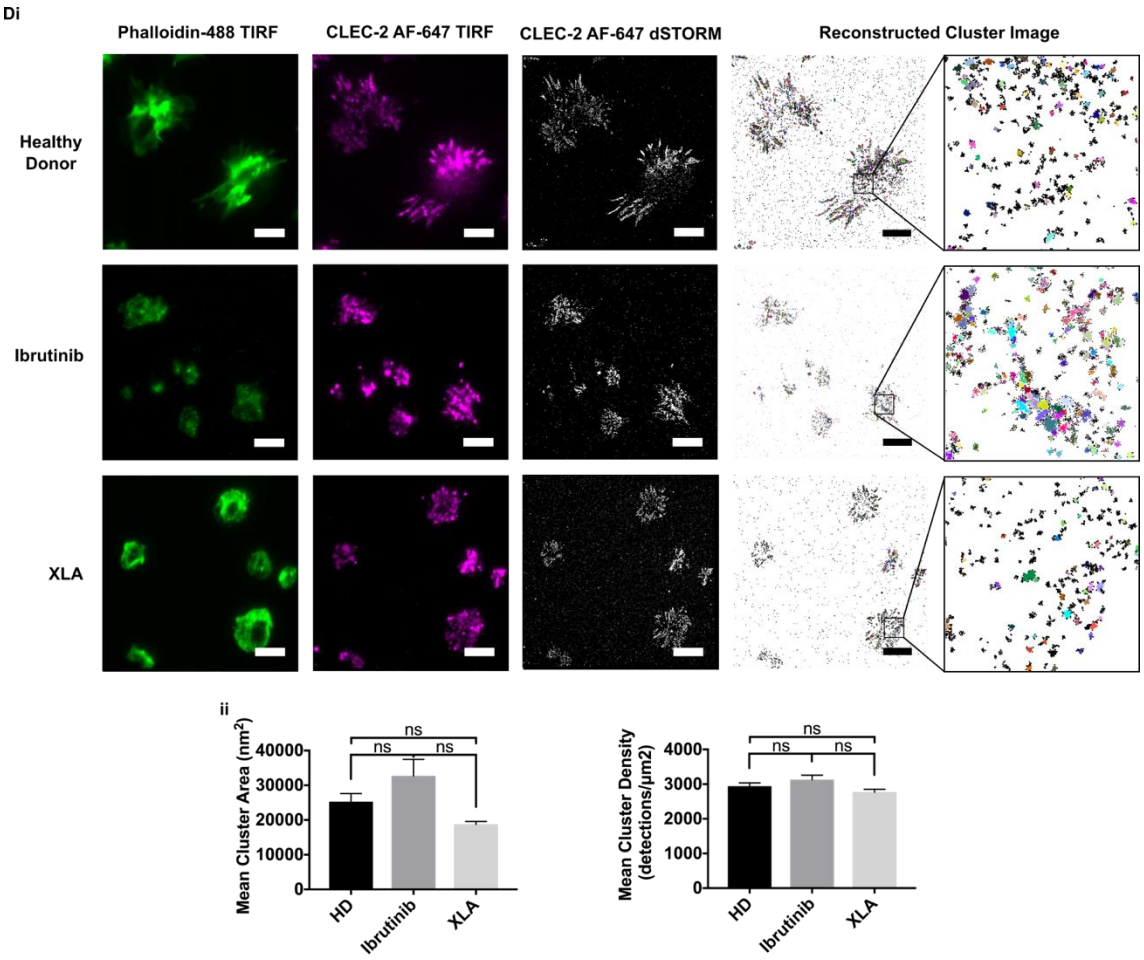

Figure 4.13: Platelets from ibrutinib treated patients have normal CLEC-2 clustering.
Washed platelets at 2x10^7/ml from healthy donors, patients with CLL taking ibrutinib or patients with XLA were spread on podoplanin-Fc (10 µg/ml) coated coverslips at 37°C for 45 minutes. Platelets were then fixed and probed with the anti-human CLEC-2 antibody AYP1. Secondary antibody staining was performed with goat anti-mouse antibody conjugated to AF 647 as well as AF 488-conjugated phalloidin. Spread platelets were imaged using a Nikon Eclipse Ti-E N-STORM system in dSTORM mode. (A) representative images from seven healthy donors, four patients taking ibrutinib and two patients with XLA with the microscope in Total Internal Reflection Fluorescence (TIRF) or dSTORM mode or reconstructed images with false colour added to individual clusters. (B) Cluster area (i) and density (ii) are depicted as mean ± SEM (HD n=7, ibrutinib n=4, XLA n=2). Statistical analysis was with one-way ANOVA with Tukey's correction for multiple comparisons. ns=non-significant. Scale bar = 5 µm.

4.2.5 The effect of Btk inhibition on platelet adhesion to podoplanin under venous flow

4.2.5.1 *In vitro* ibrutinib inhibits platelet activation after adhesion to podoplanin under flow at venous shear

Given platelets adhered in lower numbers but retained the ability to cluster CLEC-2 on podoplanin in the presence of ibrutinib, it was important to establish, in a more physiological model, whether these observations meant that platelets in which Btk had been inhibited would still be able to bind to podoplanin under flow conditions, and, if so, was the stimulation powerful enough to overcome Btk blockade and enable aggregate formation. Thus a flow adhesion assay was performed by Josh Hinds and supervised as part of this project. Healthy human donor washed platelets were isolated and treated with low concentration ibrutinib (170 nM) or vehicle before being reconstituted with autologous red cells and PPP. Prior to adding back into whole blood, the platelets were sampled and it was confirmed that the ibrutinib treated platelets were no longer able to aggregate to 300 nM rhodocytin (not shown). Because of the lack of success with getting platelets to adhere to immobilised rhodocytin, reconstituted whole blood was then flowed over podoplanin-Fc under direct microscopic vision at venous shear for 5 minutes.

As seen in Figure 4.14, treatment with ibrutinib did not prevent platelet adhesion to a statistically significant degree, although there was a clear trend towards a reduction in adhesion. It did, however, reduce the size of the platelet clusters that formed. This is consistent with platelets still being able to bind podoplanin, but not being able to activate, secrete secondary mediators, and recruit other

platelets to form aggregates.

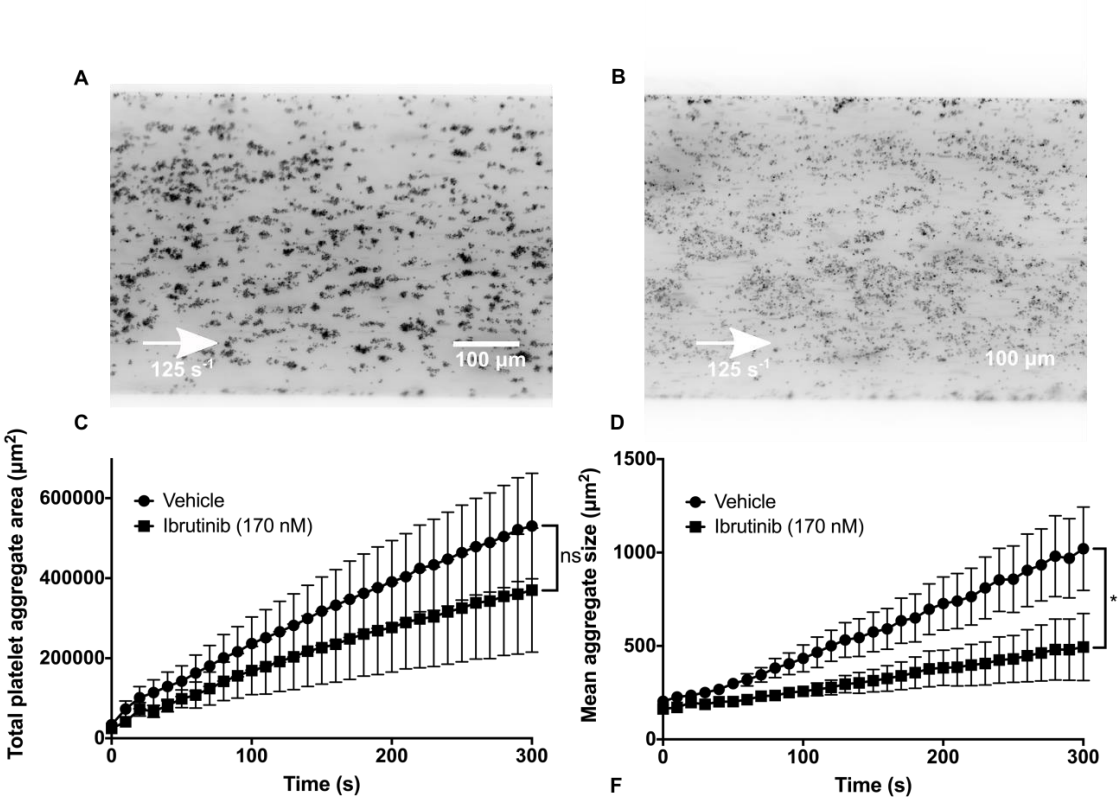

Figure 4.14: *In vitro* Btk inhibition has no effect on adhesion but does reduce aggregate size when flowed over immobilised podoplanin-Fc at venous shear. Human healthy donor washed platelets at $10x10^8$/ml were incubated with ibrutinib (170 nM) or vehicle for 5 minutes before being reconstituted with autologous red cells and PPP to a final platelet concentration of $400x10^9$/l. The resultant whole blood was then incubated with $DiOC_6$ dye for 5 minutes before being flowed over immobilised podoplanin-Fc (100 µg/ml) at 125 s^{-1} for 5 minutes. Images were taken every second using fluorescent channels on a Zeiss Axio inverted microscope at 20X magnification. (A) Representative images from (A) vehicle treated (n=5) and (B) ibrutinib treated samples (n=5) are shown. Ilastik 1.1.2 machine learning software was used to automatically and reproducibly identify platelets and data on platelet surface area coverage and cluster size was measured using the KNIME 3.4 analytics platform. Mean data ± SEM showing (C) increase in total platelet aggregate area over time and (D) increase in mean aggregate size over time. Statistical analysis was performed with two-way ANOVA. *P<0.05, ns=non significant.

4.2.5.2 Platelets taken from patients on ibrutinib and acalabrutinib and those with XLA have deficient adhesion to podoplanin under flow conditions at venous shear

It was important to look at whether this reduced platelet activation on adhesion to podoplanin under flow was achieved at physiological concentrations of Btk inhibitor and whether it was a Btk-specific effect. To achieve this, flow adhesion studies were also extended by Josh Hinds, but supervised under this project, to include blood *ex vivo* from patients treated with Btk inhibitors and from those with XLA. Like with the *in vitro* studies, blood was flowed over podoplanin-Fc at venous shear for 5 minutes. As for the spreading experiments, no patients on FCR were available as controls for this assay.

Figure 4.15A, C and D shows that platelets from patients taking ibrutinib almost completely failed to adhere to podoplanin-Fc. The effect was considerably more marked than in the *in vitro* assay. It was initially felt that this probably reflected the additional off-target effects of the high concentrations of ibrutinib that these patients take. The results shown in Figure 4.15B, E and F, however, from patients on acalabrutinib (n=2) and those with XLA (n=2) (which are Btk-specific effects) do not support this conclusion. Instead, they show that Btk appears to be critical for platelet adhesion to podoplanin under venous flow conditions. The difference in the results from the *in vitro* and *ex vivo* assays could be due to the lower (but still normal range) of platelet counts in the patients with XLA (see Figure 3.24Bi) or those on Btk inhibitors (see Figure 3.15Bi) rather than the $400x10^9$/l used in the *in vitro* assay.

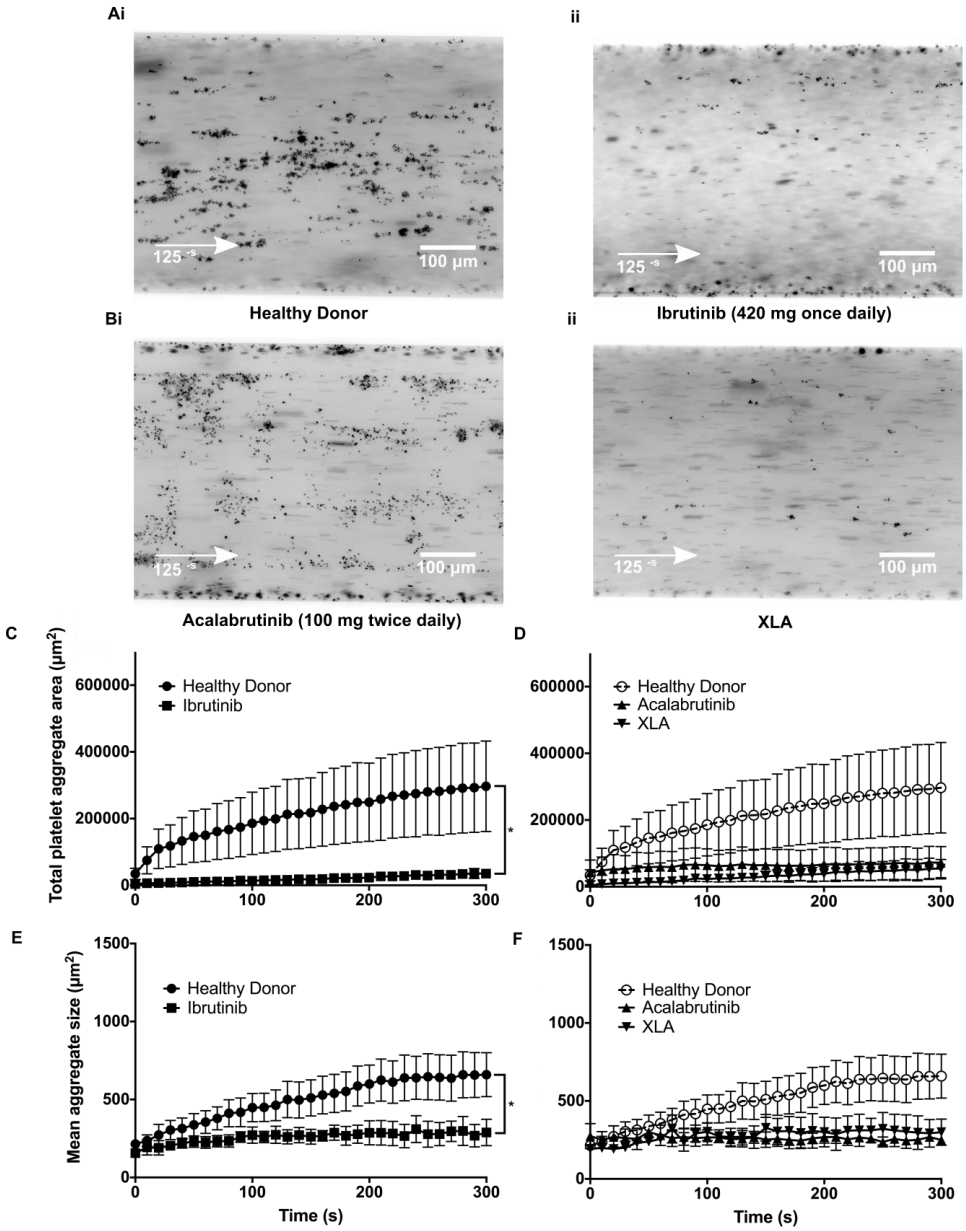

Figure 4.15: *Ex vivo* Btk inhibition reduces adhesion to podoplanin under flow. Whole blood from healthy donors, patients treated with ibrutinib or acalabrutinib or those with XLA was incubated with $DiOC_6$ dye for 5 minutes before being flowed across a capillary coated with podoplanin-Fc (100 µg/ml) at 125 $s^{-1}$for 5 minutes. Images were taken every second using fluorescent channels on a Zeiss Axio inverted microscope at 20X magnification. (A) Representative images from (i) healthy donors, patients treated with (ii) ibrutinib 420 mg once daily, (iii) acalabrutinib 100 mg twice daily or (iv) patients with XLA. Ilastik 1.1.2 machine learning software was used to automatically and reproducibly identify platelets. Data on platelet surface area coverage and cluster size was measured using the KNIME 3.4 analytics platform. Mean data ± SEM showing increase in total platelet aggregate area over time of (C) healthy donors (n=4) and ibrutinib treated patients (n=5) and (D) acalabrutinib treated patients (n=2) and those with XLA (n=2). Mean data ± SEM showing increase in mean aggregate size over time of (E) healthy donors and ibrutinib treated patients and (F) acalabrutinib treated patients and those with XLA, the curve from healthy donor platelets is included for comparison. Statistical analysis was performed with two-way ANOVA. *P<0.05, ns=non significant.

4.3 Discussion

The main findings from the above studies into the role of Btk downstream of CLEC-2 receptor ligation in platelets are:

i) Btk inhibitors are highly effective at blocking almost all aspects of CLEC-2 mediated platelet function and, in human platelets, this is likely to be a Btk-specific effect in which Tec does not play a role.

ii) The role of Btk downstream of CLEC-2 in human vs mouse platelets is different with the function in humans being critically dependent on its kinase activity whereas in mice it behaves in a similar way to that downstream of GPVI in both human and mouse platelets where it also operates as an adapter.

iii) Btk does not lie upstream of Syk in the CLEC-2 signalling cascade, as it does when activated by GPVI ligation.

4.3.1 Btk kinase activity is critical for platelet CLEC-2 function in human platelets

These results have shown that, with the exception of Ca^{2+} mobilisation, Btk inhibitors block all aspects of CLEC-2 mediated human platelet function and signalling at very low concentrations consistent with the effect being mediated through their inhibition of Btk kinase function.

This is manifest in the *in vitro* experiments with ibrutinib and the *ex vivo* experiments using platelets from patients with XLA. The time-dependent and irreversible nature of the inhibition of CLEC-2 mediated platelet function by

ibrutinib points to an effect on Tec kinases. The results of the biochemical experiments with the IC_{50} for ibrutinib's inhibition of Btk pY223 being the same as that for aggregation, regardless of the method of platelet preparation, points further towards it being a specific effect on Btk. Finally the *ex vivo* experiments performed on patients with XLA show that they have no demonstrable CLEC-2 function or PLCɣ2 phosphorylation downstream of CLEC-2. This is despite the presence of Tec in these platelets. Taken together, these results show that Btk kinase function is critical for CLEC-2 signalling in human platelets. Further experiments performed by Craig Hughes at the University of Reading using DT40 cells transfected with CLEC-2 and WT or KD Btk show that, unlike in GPVI signalling, only WT but not KD Btk can restore Ca^{2+} mobilisation downstream of CLEC-2 as measured by the NFAT reporter assay (unpublished data).

The higher concentrations of ibrutinib required to prevent Ca^{2+} mobilisation than in other platelet function assays can be explained simply. Rather than a biological effect this appears to merely be dependent on the platelet preparation method used for the assay. This is because aggregation studies done with this different platelet preparation also needed higher concentrations of ibrutinib to be blocked. This blockade was still critically dependent on Btk pY223 inhibition as shown by the biochemical studies where the IC_{50} for Btk pY223, Ca^{2+} mobilisation and aggregation were the same in platelets prepared with this ADP-sensitive method.

With most experiments it is expected that *in vitro* tests will yield more clear-cut results than *ex vivo* ones because the variables of the experiment are more controllable. Interestingly, with the flow adhesion experiments using immobilised

podoplanin, the opposite was true. *In vitro* tests showed platelet aggregate size was significantly reduced but that while overall adhesion appeared lower, this was not statistically significant. This would imply that platelet CLEC-2 does not have to be activated to adhere to podoplanin. This is contrary to what is seen in similar flow assays performed by Navarro-Núñez *et al*. where blockade of platelet activation with the Src inhibitor dasatinib caused reduced platelet adhesion to podoplanin (Navarro-Núñez et al. 2015). *Ex vivo* blood from patients treated with ibrutinib, however, showed that both overall adhesion and aggregate size was markedly reduced. This discrepancy with the *in vitro* results could be due to off-target inhibition of SFKs or other kinases by the high doses of ibrutinib used in patients with CLL. But if this were so then the results using blood from the acalabrutinib treated patients or those with XLA would match the *in vitro* results. Even allowing for the suboptimal number of acalabrutinib treated and XLA patients (two in each group) the results appear to strongly suggest that Btk inhibition alone is sufficient to reduce platelet adhesion and activation when flowed across immobilised podoplanin-Fc at venous shear rates. The *in vitro* assay, therefore, was probably not sensitive enough to pick up this reduction in adhesion. This was probably as a result of the high-normal platelet count of $400x10^9$/l in the reconstituted blood used for the assay or the experiment not being performed over a long enough time period. Ideally these experiments would be repeated using a longer time course with lower platelet counts in the reconstituted blood in the *in vitro* assay and also non-Btk inhibitor treated CLL patients used as the controls in the *ex vivo* assay.

4.3.2 Off-target effects of ibrutinib mediate blockade of CLEC-2

function in mouse platelets in a similar manner to its inhibition downstream of GPVI

The role of Btk downstream of CLEC-2 in mouse platelets is markedly different to that in humans. This is shown by two main observations:

Firstly by the >500-fold difference in IC_{50}s for aggregation upon stimulation with rhodocytin between human and mouse platelets. This difference is not accounted for by differing levels of ADP sensitivity of the different methods of washed platelet preparation because a) the mouse platelets are not sensitive to ADP (not shown) and b) even ADP-sensitive human platelets are still ~50-fold more sensitive to aggregation blockade by ibrutinib than mouse platelets.

Secondly this is manifest in the strikingly different tyrosine phosphorylation patterns seen downstream of CLEC-2 when human and mouse platelets are inhibited with low concentrations of ibrutinib. Human platelets have nothing except basal levels of SFK phosphorylation when treated with 70 nM ibrutinib whereas mouse platelets only show loss of Btk Y223 and downstream PLCɣ2 phosphorylation. Changing the method of platelet preparation such that the platelets are responsive to stimulation by ADP, however, restores the phosphorylation upstream of Btk pY223 in human platelets. This supports the observations of Pollitt *et al*. showing that CLEC-2 signalling in human but not mouse platelets is dependent on positive feedback with secondary mediators such as ADP (Pollitt et al. 2010). It is likely that this effect is being mediated via $P2Y_1$. To prove this, $P2Y_1$ inhibitors would need to be added to ADP-sensitive platelets in the presence of low concentrations of ibrutinib.

From these observations it is evident that, as with GPVI-mediated activation of both human and mouse platelets, CLEC-2 mediated mouse platelet function is

only blocked by the off-target effects of Btk inhibitors. Indeed, consistent with the results of Lee *et al*. even bigger concentrations of ibrutinib are required to block CLEC-2 mediated platelet function than those previously shown to block activation after GPVI ligation (Lee et al. 2017). These results cannot be reconciled with the observations of Manne *et al*. however where they used the same low concentration of ibrutinib to block human and mouse CLEC-2 mediated signalling and aggregation (Manne et al. 2015). One potential explanation is that they used a very low agonist concentration (10 nM rhodocytin). Manne *et al*. themselves, however, showed that ibrutinib increases platelet inhibition downstream of CLEC-2 in XID mice pointing to an off-target action of ibrutinib that is required to block murine CLEC-2 signalling (Manne et al. 2015).

Unlike ibrutinib's blockade of GPVI signalling however, there is reduction but not loss of the 140 kDa band corresponding to PLCɣ2 phosphorylation when concentrations > 70 nM are used to inhibit mouse CLEC-2 signalling (Figure 4.6B). The phosphorylation of Y1217 is also not completely blocked, though this is not borne out when this is quantified. Again, like with GPVI signalling blockade, this might point to the fact that PLCɣ2 phosphorylation is markedly reduced but not completely lost until very high concentrations of ibrutinib but that the assay used to measure this phosphorylation is not sensitive enough to reliably pick this up. Sensitive methods to measure tyrosine phosphorylation do exist, such as that marketed by ProteinSimple (Padhan et al. 2017), and these could be employed in future studies.

4.3.3 Btk does not lie upstream of Syk following CLEC-2 ligation in

human and mouse platelets

The results depicted here do not support the conclusions by Manne *et al*. that Btk lies upstream of Syk in both mouse and human platelet CLEC-2 signalling (Manne et al. 2015):

Firstly, given that Syk function is required for the formation of CLEC-2 clusters, the fact that both *in vitro* and *ex vivo* Btk inhibition failed to inhibit this in human platelets could be seen as evidence that Btk lies downstream of Syk. There are some potential confounders with this assay however that mean its results need to be interpreted with caution; the assay did not measure change in clustering over time, a dynamic effect of Btk inhibition which delayed rather than prevented CLEC-2 clustering may have been missed. The primary issue, however, was that the experiment was performed using a fixed ligand. The clustering experiments performed by Pollitt *et al*. which identified the critical role of Syk and SFKs were performed using mobile podoplanin in lipid bilayers and cell membranes. Thus CLEC-2 clustering brought mobile podoplanin molecules together. This is not possible with a fixed ligand, the CLEC-2 will bind to podoplanin, but it cannot move after this. The lack of the use of Syk or SFK inhibitors as positive controls in this experiment was a significant omission.

Secondly, despite identical methods of platelet preparation and the use of the same assays and reagents, these experiments could only replicate the results of the Manne *et al*. paper in human platelets but not in mice. The results shown in Figure 4.6B indicate clearly that Btk does not lie upstream of Syk in mouse platelet CLEC-2 signalling.

Thirdly, with regards to the position of Btk in human platelet CLEC-2 signalling; unlike Manne *et al*. the experiments reported here measured Btk pY551 as well

as Btk pY223. The results showed that, even at the lowest concentration of ibrutinib that inhibited Btk pY223, Btk pY551 was also blocked. Even if Btk lay upstream of Syk, Y551 would still need to be phosphorylated by the SFK Lyn as part of its activation as illustrated in Figure 4.5. Loss of pY551 indicates an alternative explanation for the loss of phosphorylation events upstream of Btk; it is likely that some positive feedback mechanism that reinforces all the phosphorylation events is being blocked in the presence of Btk kinase inhibition. Finally, the loss of phosphorylation events upstream of Btk in ibrutinib treated human platelets was shown to be partly due to an off-target effect of ibrutinib and partly due to an artefact secondary to the method of platelet production; upstream phosphorylation of Syk and LAT was still present in patients with XLA, revealing that the loss of phosphorylation seen in ibrutinib treated platelets is likely to be due to an off-target effect; also when platelets were prepared by the ADP-sensitive method, the upstream phosphorylation was restored.

In conclusion; the present study shows that Btk does not lie upstream of Syk in human and mouse platelets, it provides further evidence of off-target effects of ibrutinib and also shows that Btk inhibitors block CLEC-2 mediated platelet function at >10-fold lower concentrations than they block GPVI signalling. The mechanism underlying this selectivity is shown to be because Btk kinase activity is critical for human platelet CLEC-2 function, which is not the case for GPVI. This means that low dose Btk inhibitors could be used therapeutically to inhibit CLEC-2 in platelets without any off-target effects on GPVI.

CHAPTER 5: THE ROLE OF CLEC-2 IN HUMAN THROMBOSIS AND THE EFFECT OF BTK BLOCKADE ON HUMAN AND MOUSE VTE

5.1 Introduction

5.1.1 Problems with current drugs for VTE

As previously mentioned, the mainstay of treatment for VTE is with anticoagulants. Despite the introduction of DOACs, which reduce the annual rate of patients experiencing major haemorrhage from 3% to 1.5-2% (Crowther & Warkentin 2008), these have not been adopted universally for all forms of VTE for several reasons:

i) the first is because of the perceived increase in drug costs. Though the overall cost of anticoagulant treatment however is not just down to the drug costs and in fact there are savings to be made when the lack of international normalised ratio (INR) monitoring for DOACs are taken into account (Amin et al. 2015).

ii) the second is because of a lack of proven superiority over VKAs and LMWH in particular settings such as in patients with metallic heart valves or those with cancer associated VTE (Keeling et al. 2011; H. G. Watson et al. 2015).

iii) the third is the lack of reversal agents. For VKAs major bleeding events can be treated with intravenous (IV) vitamin K and an infusion of clotting factors called prothrombin complex concentrate (PCC) (Makris et al. 2012). These rapidly correct the INR but, in fact, may not actually confer a survival benefit (Sarode et al. 2013). Until recently, however, DOACs have not had reversal agents. But the monoclonal antibody idarucizumab has now been introduced into clinical practice for the immediate reversal of the direct thrombin inhibitor dabigatran (Pollack et al. 2017). The decoy Factor Xa Andexanet Alfa is likely to be licensed soon for use for acute reversal of the Xa inhibitors (Connolly et al. 2016).

iv) the fourth and final reason is the rapid off-effect of the DOACs. Because of their short half-lives, if a dose is missed then the patient will lose their therapeutic anticoagulation within a few hours. This is not the case with warfarin which has a very long half-life and so is considered more forgiving for elderly patients who intermittently forget to take their medications (Burn & Pirmohamed 2018).

There is still an unmet clinical need, therefore, for a treatment or primary/secondary prophylaxis for VTE that does not cause bleeding and does not have the rapid off-effect associated with the DOACs. An irreversible inhibitor of platelet CLEC-2 or its downstream signalling. might provide the answer to this need if it can be shown to be effective in the setting of VTE.

5.1.2 CLEC-2 as a potential therapeutic target for

5.1.2.1 Platelet CLEC-2 is critical for thromboinflammation in mice

The principal studies that show a role for CLEC-2 in reduction of thromboinflammation are those by Hitchcock *et al.* and by Payne *et al*. (Hitchcock et al. 2015; Payne et al. 2017). In the former, mice were inoculated with an attenuated strain of mouse salmonella (*S. Typhimurium*). 7 days after infection mice were shown to have thrombi in portal vein branches that were surrounded by leukocytes which suggested they were not emboli but had formed *de novo* in the liver. These thrombi were rich in fibrin and had podoplanin upregulated in the subendothelium surrounding the vessel. The mechanism for thrombus development was shown, using a mixture of drug treatment and genetic knockout mice, to be critically dependent on macrophages, podoplanin and platelet CLEC-2. The pathophysiological model they proposed was that bacteria triggered monocyte recruitment to the liver, the monocytes then matured into macrophages and expressed podoplanin. The trigger for thrombosis then was activation of CLEC-2 on platelets at sites of breach in the endothelial wall with downstream processes similar to that which occurs in classical thrombosis.

In the study by Payne *et al*. mice underwent IVC stenosis surgery whereby the IVC side branches were tied off and then a ligature was placed around the IVC and tightened around a 30-gauge spacer. Mice were then allowed to recover from surgery for 48 hours prior to being culled and having their IVC examined for the presence of thrombus. Like in the study of Hitchcock *et al*. the thrombi that developed were rich in fibrin and resembled DVTs in humans. Again, like

the results of Hitchcock *et al*. the subendothelium surrounding the thrombus was shown to contain upregulated podoplanin but also showed adjacent platelets invading into this subendothelial layer. Finally, analogous to the results of Hitchcock *et al*., the development of thrombosis was shown, through a mixture of genetic knock out mice and treatment with blocking antibody, to be critically dependent on podoplanin and platelet CLEC-2. The proposed mechanism here was also that podoplanin was up-regulated by leukocytes and it was the activation of platelet CLEC-2 by podoplanin which triggered the thrombosis.

It is perhaps surprising that IVC stenosis causes an inflammatory response such that leukocytes are recruited to the vessel wall. It was previously thought that this model caused thrombosis through disruption to blood flow in the same way an intra-abdominal mass might press on the iliac veins in a patient developing proximal DVT. Whether this process of upregulated podoplanin triggering venous thrombosis via platelet CLEC-2 occurs in humans has not been shown.

5.1.2.2 Platelet CLEC-2 plays minimal/no role in haemostasis

Consistent with presence of a single endogenous ligand which is not present in the vasculature under normal conditions, studies examining the role of CLEC-2 in maintaining haemostasis show only a minor contribution. Because CLEC-2 deficient mice die before or soon after birth and display prominent blood-filled lymphatics and oedema (Suzuki-Inoue et al. 2010) two methods have been developed in order to study the effect of CLEC-2 depletion on platelet function in adult animals; namely restoration of radiation chimeric mice from CLEC-2

deficient fetal liver cells or antibody mediated reversible down regulation of the receptor. These methods produce conflicting results. Radiation chimeric mice reconstituted with CLEC-2 deficient fetal liver cells had no impairment of haemostasis as shown by tail bleeding time in two studies (Suzuki-Inoue et al. 2010; Hughes et al. 2010) whereas those with antibody mediated depletion had a prolonged bleeding time in one study (May et al. 2009) but not in another which used the same antibody (Bender et al. 2013). Radiation chimeric mice reconstituted with fetal liver cells display either no effect or only minor impairment in flow adhesion assays over collagen, VWF and fibrinogen (Suzuki-Inoue et al. 2010; Hughes et al. 2010).

In vivo data looking at thrombus formation after vessel wall injury shows a mild reduction in thrombus formation in a laser injury model of mesenteric capillaries in the radiation chimeric mice (Suzuki-Inoue et al. 2010) and a more marked effect in a ferric chloride injury model of mesenteric arterioles in antibody depleted mice (May et al. 2009) The same, latter, assay using CLEC-2 fl/fl PF4-Cre mice only produced a very subtle reduction in thrombus formation but these mice also had a lower platelet count than their wild type counterparts (Bender et al. 2013). The reason for the different results could merely be an effect of the induced thrombocytopenia/secondary thrombocytosis which occurs in the antibody treated mice. There could be additional, unaccounted for, effects of antibody treatment such as occurred in a study of antibody-mediated depletion of GPVI where the antibody treatment unexpectedly lowered the ability for platelets to respond to thrombin mediated activation (Schulte et al. 2006). In further support of CLEC-2 not playing a significant role in haemostasis, mice treated with a Syk inhibitor have been shown not to have a prolongation of tail

bleeding time (Andre et al. 2011).

It follows then that CLEC-2 is an exciting prospect as a drug target for the treatment of VTE because it is critical for the formation of venous thrombus in mouse models of thromboinflammation but has little or no role in haemostasis. Therefore CLEC-2 blockade may be able to treat or prevent venous thrombosis triggered by inflammation without causing the bleeding that is the main side effect of all of the current treatments for VTE.

5.1.3 Btk inhibitors as means of blocking platelet activation by CLEC-2 ligation

The studies in Chapter 4 have shown that Btk inhibitors are a potent and specific means of blocking CLEC-2 mediated platelet activation *in vitro* and *ex vivo*. The attraction of using Btk inhibitors for this therapeutic indication is lessened, however, by the reports of bleeding in the early trials of ibrutinib for patients with LPDs that were not dissimilar to the rates of bleeding on anticoagulants. The results from Chapter 3, however show that blockade of GPVI-mediated platelet activation by ibrutinib (which has been correlated to bleeding events) is due to non-Tec kinase off-target effects that occur because of the high doses used. Ibrutinib, and other covalent Btk inhibitors, could be dosed at much lower levels to specifically target Btk in platelets in a way analogous to the use of aspirin.

In combination with the effects on GPVI, a contribution towards ibrutinib induced bleeding has been postulated to be due to the patients' underlying LPD as most bleeding events on ibrutinib occur in the first 6 months of treatment before the

disease is in remission (Jones et al. 2017). Therefore using Btk inhibitors in patients who do not have underlying haematological malignancy may abrogate all major bleeding events. Furthermore, using them in these patients but at doses that do not inhibit GPVI-mediated platelet activation may abolish the minor bleeding events as well.

The outstanding questions are:

i) does blockade of CLEC-2 mediated platelet activation via inhibition of its downstream signalling prevent *in vivo* venous thrombosis in mice in the same way as blocking the interaction between CLEC-2 and podoplanin?

ii) does podoplanin's activation of platelet CLEC-2 play any role in the development of human VTE?

What follows aims to answer these questions by looking at whether dosing of mice with ibrutinib prevents *in vivo* thrombosis and by looking for indirect and direct evidence that podoplanin and CLEC-2 play a role in human venous thrombosis.

5.2 Results

5.2.1 The effect of ibrutinib on mouse thromboinflammation

5.2.1.1 Ibrutinib inhibits WT mouse CLEC-2 and GPVI-mediated platelet function *ex vivo*

In order to establish if ibrutinib inhibits *in vivo* thromboinflammation in mice it was first necessary to ensure that ibrutinib blocked platelet CLEC-2 function *ex vivo.* Ibrutinib has a half-life of 4-8 hours and so it was estimated that it would take 20-40 hours (5 half-lives) for trough levels of drug to stabilise. Because it was seen in the *in vitro* experiments that high concentrations of ibrutinib were needed to block CLEC-2 mediated platelet function in mice the maximum safe dose of 35 mg/kg was used. Because of the large volume of blood required for LTA, measurement of platelet activation by flow cytometry was used in order to take blood serially before and after doses of ibrutinib. In order to look at the effect of ibrutinib on platelet function over time, mice were dosed once daily with 35 mg/kg ibrutinib by intraperitoneal (IP) injection for three days and had 30 µl heparinised blood taken pre-treatment and then at two hours following the first, second and third (final) doses as well as 24 hours after the final dose. Platelet activation in response to CRP and rhodocytin was measured by flow cytometry at these time points. Platelet activation in response to thrombin was also measured in ACD anticoagulated blood at the final time point. The results are depicted in Figure 5.1A. Similar to the *in vitro* results shown in Figure 4.1Cii and D, these show that platelet activation in response to thrombin was unaffected by

ibrutinib but that activation in response to both GPVI and CLEC-2 stimulation was blocked. There was still some breakthrough residual platelet activation in response to rhodocytin stimulation following dose 2 however. It was important to make sure that CLEC-2 blockade was as complete as possible throughout the period of time when IVC was going to be ligated and so dosing was extended to find a 48 hours window with full CLEC-2 blockade. Platelet activation was measured by flow cytometry at serial time points during the experiment with results from this extension of the experiment shown in Figure 4.16B. Combining results of these two dosing experiments showed that CLEC-2 blockade maintained from 2 hours after dose 3 until 24 hours after dose 4.

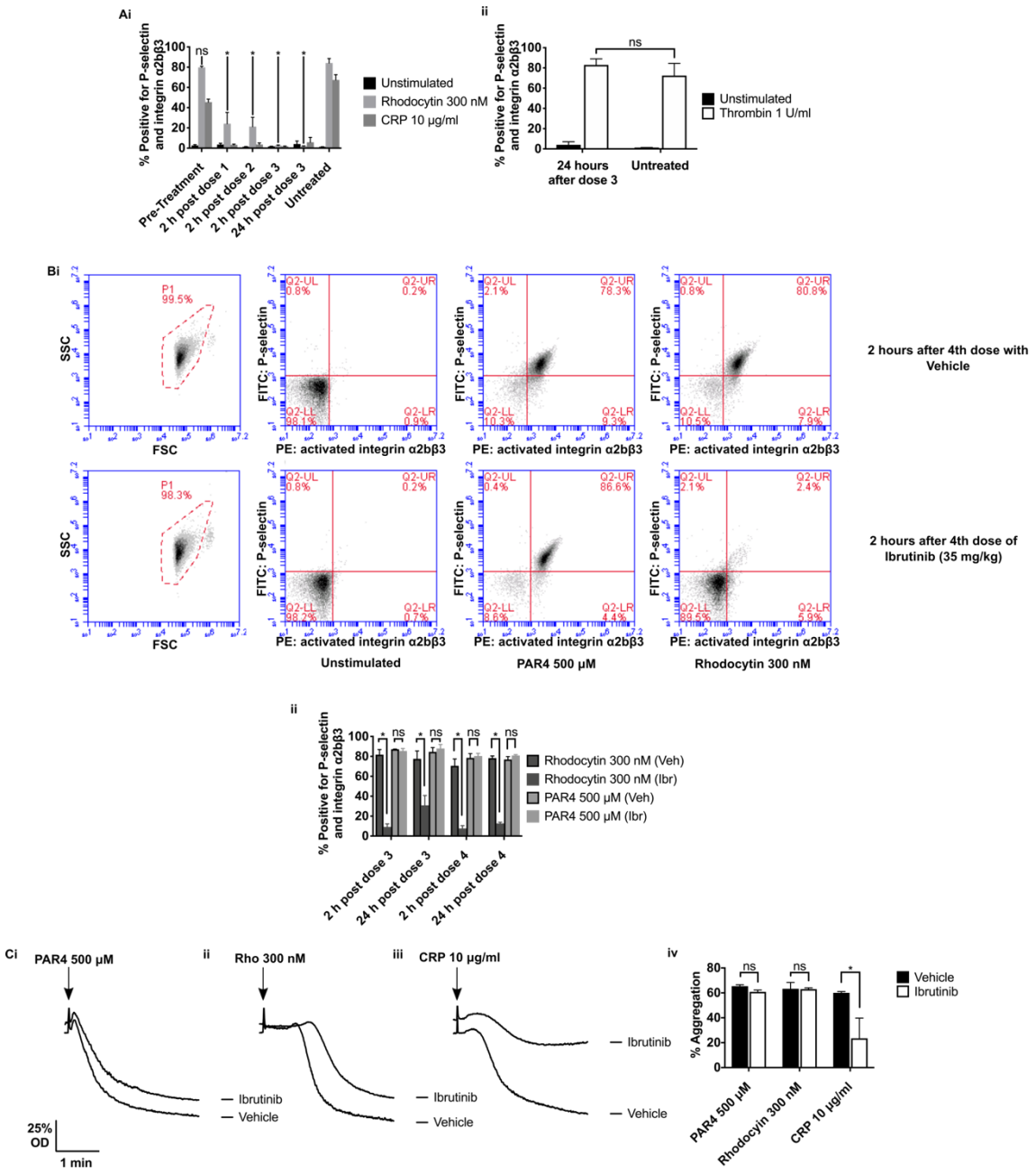

Figure 5.1: Activation of platelets by ligation of the CLEC-2 or GPVI receptors is blocked in mice dosed with ibrutinib *in vivo*.
WT Mice were dosed with ibrutinib (35 mg/kg) or vehicle and bled at the stated times. (A) Whole blood taken into ACD and incubated with the stated agonist and FITC-conjugated anti-P-selectin and PE-conjugated anti-integrin αIIbβ3 antibodies for 30 minutes before undergoing red cell lysis and fixation and analysis using flow cytometry. Mean effect on platelet activation after stimulation with (i) rhodocytin (300 nM) or CRP (10 µg/ml) and (ii) thrombin (1 U/ml) is shown. Statistical analysis was performed with (i) two-way ANOVA with a Dunnett's post test or (ii) two-way ANOVA. (B) Heparinised whole blood was incubated with the stated agonist and FITC-conjugated anti-P-selectin and PE-conjugated anti-integrin α2bβ3 antibodies for 30 minutes before undergoing red cell lysis and fixation and analysis using flow cytometry. (i) Representative plots from vehicle and ibrutinib treated mice. (ii) Mean effect on platelet activation after stimulation with rhodocytin (300 nM) or PAR4 peptide (500 µM) is shown. Statistical analysis was performed using a two-way ANOVA with Tukey's multiple comparison

test. (C) Washed platelets at $4x10^8$/ml from the same mice at the end of the experiment (i.e. 24 hours after dose 4) were stimulated with the stated agonists. (i-iii) Representative traces, (iv) mean results ± SEM is shown. Statistical analysis was performed with a two-way ANOVA with Sidak's multiple comparison test. *p<0.05, ns=non-significant.

Alongside analysis by flow cytometry in whole blood, at the very final time point LTA was performed as well in washed platelets (ie 24 hours after dose 4). These were stimulated with PAR4 peptide, rhodocytin and CRP. The results in Figure 5.1C show that, while flow cytometry indicated complete blockade of CLEC-2 and GPVI-mediated platelet activation, LTA showed delayed and partially inhibited aggregation to the same agonists at the same concentrations. This illustrates different sensitivities of LTA and the flow cytometry assay to platelet inhibition.

5.2.1.2 The effect of ibrutinib on thrombus formation in an *in vivo* model of DVT

In order to investigate if ibrutinib reduces the incidence of DVT in an *in vivo* mouse thrombosis model mice were dosed as above with ibrutinib or vehicle. Two hours following the third dose they were anaesthetised and had IVC stenosis induced with a ligature. This time point was chosen as this is when the plasma concentration of ibrutinib was expected to peak. 48 hours later they were culled and examined for the presence and size of any thrombus that had formed in the IVC. The results, shown in Figure 5.2, demonstrate that only 2 of the 7 mice formed a thrombus in the ibrutinib treated mice, whereas 4 out of the 7 vehicle treated mice formed a thrombus. This difference was not statistically significant.

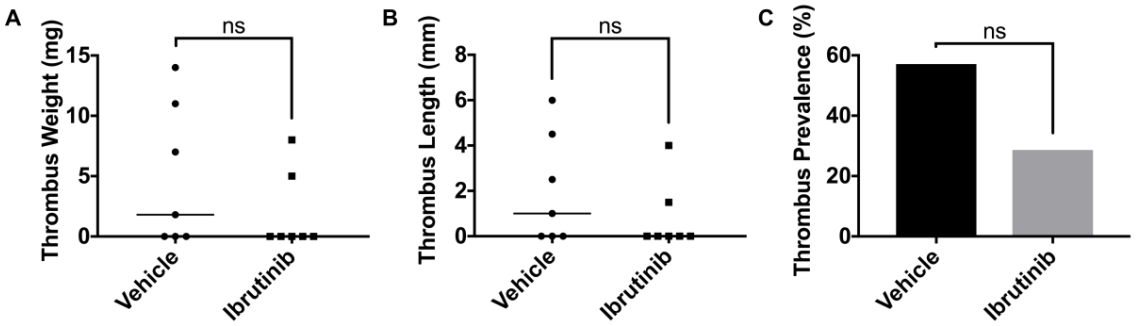

Figure 5.2: The effect of ibrutinib on the incidence of mouse DVT in mice.
8 week old WT C57/Bl6 mice were dosed with 35 mg/kg ibrutinib or vehicle via daily IP injection for 4 days. Two hours following the third dose surgical IVC stenosis was induced with a ligature. A single mouse from each group bled from the IVC intra-operatively and had to be culled. The remaining mice were allowed to recover and were then culled 46 hours later and examined for the weight and length of any IVC thrombus. (A-B) Results shown are median values (n=7 per group). Statistical analysis for these was performed with Welch's two tailed t-test. (C) Thrombus prevalence shown (n=7 per group). Statistical analysis on thrombus prevalence was done with Fisher's exact test. ns=non-significant.

5.2.2 Patients with CLL / MCL who take Btk inhibitors have lower VTE rates than patients taking control chemotherapy

One method of addressing the issue of there being no data on the role of platelet CLEC-2 in humans was to look at the existing data from clinical trials that tested drugs known to inhibit CLEC-2 (such as Btk inhibitors). These trials were performed to assess the efficacy of Btk inhibitors at treating LPDs and so were not powered to detect differences in venous thrombosis rates but, nonetheless, this information was collected and has been published as Adverse Event (AE) and Severe Adverse Event (SAE) rates. It is a requirement of American Law that clinical trials register at initiation and post results upon completion with the public registry www.clinicaltrials.gov and so this website can be used as a resource to look at venous thrombosis rates in these trials.

On the 20/9/2018 www.clinicaltrials.gov was searched using the term “ibrutinib OR PCI-32675 OR imbruvica” and results were then filtered to only include trials with results. This yielded 16 studies of which 14 involved patients with lymphoproliferative disorders. Two of these 14 were not trials for patients with low-grade LPDs but were in patients with acute lymphoblastic leukaemia and diffuse large B-cell lymphoma respectively. These were excluded in order to keep the patient population, and thus the underlying VTE rate, as uniform as possible (i.e. low grade disease only). There were 12 remaining studies for analysis. The registry records for each study were screened for all terms listed in the Common Terminology Criteria for Adverse Events (CTCAE) that related to VTE. (such as thromboembolic event, venous thrombosis, pulmonary embolism) (National Cancer Institute 2010). The number of ibrutinib treated patients and the number of reported VTE events for these trials are shown in Table 5.1.

Trial Number	Disease	RCT with comparison to a non-ibrutinib containing treatment?	Number of ibrutinib treated patients	Number of VTEs in patients treated with ibrutinib
NCT01217749	CLL	No	71	1
NCT01236391	MCL	No	111	1
NCT01292135	CLL	No	33	-
NCT01105247	CLL	No	132	-
NCT01578707	CLL	Yes	195	-
NCT01744691	CLL/SLL	No	144	1
NCT01722487	CLL/SLL	Yes	136	-
NCT01646021	MCL	Yes	139	1
NCT01973387	CLL/SLL	Yes	106	-
NCT01849263	FL	No	40	1
NCT01980628	MZL	No	63	1
NCT01500733	CLL	No	86	1
Total			**1256**	**7**

Table 5.1: VTE rates experienced in trials of ibrutinib with results posted on www.clinicaltrials.gov.
Chronic Lymphocytic Leukaemia (CLL), Mantle Cell Lymphoma (MCL), Small Lymphocytic Lymphoma (SLL), Follicular Lymphoma (FL), Marginal Zone Lymphoma (MZL).

The VTE rate for the ibrutinib treated patients was very low (7/1256) which is lower than the 5.1% per year that has been reported in historic controls with CLL (Kroll et al. 2013). But the data in the above table does not give information on how long patients were studied for and the study by Kroll *et al*. only included hospitalised patients and so is likely to have a higher event rate than applies to most patients with CLL. To account for these limitations the four studies which were RCTs where treatment was compared to a non-ibrutinib containing control chemotherapy were examined further. Details on median duration for each treatment arm was looked for but was not reliably reported in the registry and so the publications relating to each of these studies were found and scrutinised to

gain this information (see Table 5.2).

Because the time that patients were taking ibrutinib on these studies was longer than the time patients took the control treatments it was necessary to express the total number of patients treated with each drug as total exposure to drug in person years. This is a standard method for comparing event rates when exposure times to treatment and control drugs differ. These data are shown in Table 5.3. Of the two studies which had VTE events (NCT01578707 and NCT0172487), the lower rate of VTE in ibrutinib treated patients when compared to those treated with conventional chemotherapy was statistically significant for NCT01578707 but not for NCT0172487. When results from these trials were combined together with the results of individual studies weighted according to the drug exposure time for each arm of the trial using a stratified cohort Cox's regression model as previously described (Giganti et al. 2015) the rate of VTE in patients treated with ibrutinib was lower than patients treated with a control chemotherapy. This result was statistically significant.

Trial Number	Reference	Disease	Control arm	No. of ibrutinib treated patients	Median treatment duration (months)	No. of VTEs	No. of control patients	Median treatment duration (months)	No. of VTEs
NCT01578707	Montillo *et al*.	CLL	Ofatumumab	195	44	0	196	8.1	2
NCT01722487	Barr *et al*.	CLL/SLL	Chlorambucil	136	28.5	0	133	18.9	0
NCT01646021	Dreyling *et al*.	MCL	Temsirolimus	139	15.6	1	141	6.2	2
NCT01973387	Huang *et al*.	CLL/SLL	Rituximab	106	16.4	0	54	8.4	0

Table 5.2: Ibrutinib containing RCTs with reported VTE SAEs and AEs.

Trial Number	Ibrutinib Exposure (person years)	VTEs in ibrutinib group	Control chemotherapy exposure (person years)	VTEs in control group	Relative VTE rate reduction (95% CI)	P-value
NCT01578707	715	0	132.3	2	0	0.024[a]
NCT01722487	323	0	209.5	0		
NCT01646021	139	1	72.9	2	0.263	0.22[a]
NCT01973387	144.9	0	37.8	0		
Total	1363.6	1	452.5	4	0.071 (0.003-0.584)	0.012[b]

Table 5.3: Ibrutinib RCTs with VTEs expressed as drug exposure in person years.
[a]Statistical analysis performed using a Mid-P exact test. [b]Statistical analysis performed using a Cox's regression analysis with a stratified

cohort approach.

The same search was performed using the search term “acalabrutinib OR ACP-196 OR calquence”. This yielded 34 studies but none of these had any results reported. As well as Btk inhibitors, Src inhibitors have also been shown to inhibit platelet CLEC-2 signalling and adhesion under flow (Navarro-Núñez et al. 2015). A search was also performed using the search term “dasatinib OR BMS-254825 OR sprycel” to look for trials that included patients treated with the Src inhibitor dasatinib (trade name sprycel). This drug has been in clinical use (for treatment of CML and other haematological and solid organ cancers) for much longer than Btk inhibitors and so a search yielded 98 interventional studies with published results. Only two of these, however, were RCTs where there was a non-dasatinib treatment arm. One was a trial of dasatinib vs imatinib in patients with CML (NCT0048124, the DASISION trial) (Cortes et al. 2016) and the other was a trial of docetaxel and prednisolone plus dasatinib or placebo for patients with prostate cancer (NCT0074449, the READY trial) (Araujo et al. 2017). The number of VTE events and the lengths of treatment for each study are shown in Table 5.4. The number of person years of drug exposure in each trial along with number of VTEs and statistical analysis is shown in Table 5.5. Like the results with ibrutinib containing RCTs, one trial showed statistically significant reduction in the VTE rate in patients treated with dasatinib whereas the other trial showed no significant difference. When the results were combined there was a statistically significant reduction in VTE events in patients treated with dasatinib when compared to those patients treated with a control chemotherapy.

Trial Number	Reference	Disease	Control arm	No. of dasatinib treated patients	Median treatment duration (months)	No. of VTEs	No. of control patients	Median treatment duration (months)	No. of VTEs
NCT0048124	Cortes *et al*.	CML	Imatinib	259	60	2	260	60	1
NCT0074449	Araujo *et al*.	Prostate Cancer	Placebo	762	11.8	8	760	11.7	28

Table 5.4: Dasatinib containing RCTs with reported VTE SAEs and AEs.

Trial Number	Dasatinib Exposure (person years)	VTEs in dasatinib group	Control treatment exposure (person years)	VTEs in control group	Relative VTE rate reduction (95% CI)	P-value
NCT0048124	1295	2	1300	1	1.005	0.623[a]
NCT0074449	850.9	8	703	28	0.346	0<0.001[a]
Total	2145.9	10	2003	29	0.289 (0.134-0.582)	<0.001[b]

Table 5.5: Dasatinib RCTs with VTEs expressed as drug exposure in person years.
[a]Statistical analysis performed using a Mid-P exact test. [b]Statistical analysis performed using a Cox's regression analysis with a stratified cohort approach.

5.2.3 Podoplanin is not upregulated in human renal vein thrombosis following kidney transplant

Studies were undertaken to see if podoplanin is upregulated in the subendothelial layer in human venous thrombosis, like it is in mice. Ethical permission was granted through the Birmingham Human Biomaterials Resource Centre (HBRC) to harvest venous thrombosis along with surrounding venous wall from patients at post-mortem (PM) and surgery as well as already existing tissue in tissue banks. Between March 2016 and July 2018 no material was able to be sourced from PM examinations and tissue banks across the United Kingdom were searched for samples that contained appropriate material. This latter search yielded five paraffin embedded tissue blocks from renal transplants which had been excised within only a few days of transplantation because of acute renal vein thrombosis.

The renal vein thrombosis tissue was stained with an antipodoplanin antibody and an IgG isotype control and counterstained with haematoxylin. Representative slides are shown in Figure 5.3. Podoplanin was seen surrounding lymphatic vessels but there was no up-regulation of it seen in the vein wall. This implies that podoplanin and CLEC-2 do not play a role in this particular type of venous thrombosis.

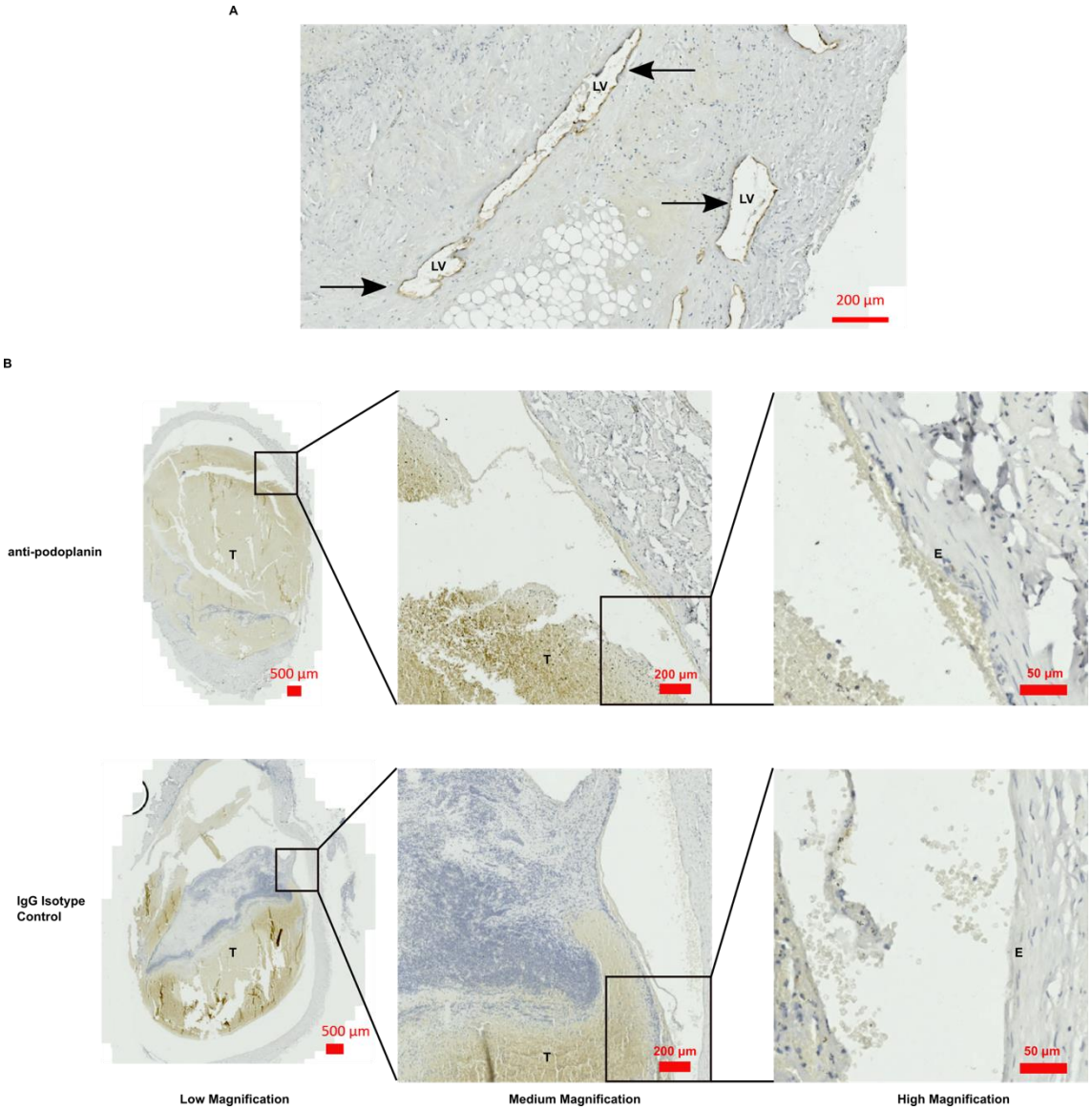

Figure 5.3: Podoplanin is not upregulated in the venous wall surrounding acute renal vein thrombosis.
Tissue blocks from five patients with acute renal transplant vein thrombosis were mounted onto slides and stained with anti-podoplanin antibody or isotype control before counterstaining with haematoxylin. (A) Kidney parenchyma showing podoplanin staining (arrows) on lymphatic endothelial cells surrounding lymphatic vessels (LV). (B) Representative slides showing equal with on podoplanin antibody and isotype control. Thrombus (T), Endothelium (E).

5.3 Discussion

The results from this chapter can be summarised thus:

i) Ibrutinib inhibits CLEC-2 signalling *ex vivo* in mice and shows a trend towards inhibition of *in vivo* thrombosis but without statistical significance

ii) Patients taking ibrutinib and dasatinib have reduced rates of VTE.

iii) Patients with acute renal vein thrombosis following renal transplant do not have upregulated podoplanin in the vessel wall surrounding the clot

5.3.1 Ibrutinib inhibits *ex vivo* CLEC-2 mediated platelet activation but not *in vivo* thrombosis in mice

As would be expected from the *in vitro* and the *ex vivo* human experiments, ibrutinib dosed to mice also caused inhibition of CLEC-2 mediated platelet function *ex vivo*. Similar to the *in vitro* results from mouse platelets, the dose required to block signalling downstream of CLEC-2 was slightly higher than for GPVI. Indeed, Figure 5.1Ai shows that GPVI was completely blocked after a single dose of ibrutinib, whereas it took three daily doses to inhibit CLEC-2. This blockade of CLEC-2 mediated platelet function did not translate into a statistically significant reduction in thrombus formation in the IVC stenosis model although there was a clear trend. The study, however, was underpowered as two animals had to be culled and the incidence of thrombosis in the controls was lower than anticipated. The experiment was powered to take into account the normal rate of thrombosis in uninhibited mice of 60% and an expected thrombosis rate of 18% in the ibrutinib treated mice. The results,

however, were a 57% and 28% thrombosis rate in the vehicle and ibrutinib treated mice respectively. The same results, but with 22 mice in each group rather than 7, would have yielded a statistically significant result. It is possible, therefore, that the experiment was underpowered because the thrombosis rate in the ibrutinib treated mice was 10% higher than expected.

It could also be because the degree of CLEC-2 inhibition was not adequate to inhibit the signalling cascade that results from podoplanin ligation. This assay used expression of activated integrin αIIbβ3 and P-selectin as measured by flow cytometry as a means of assessing platelet activation. The flow cytometry assay showed complete blockade of CLEC-2 and GPVI-mediated platelet activation for the duration of the IVC stenosis unlike LTA, which showed delay and incomplete blockade of aggregation upon activation of GPVI and delay but no reduction in overall aggregation following CLEC-2 ligation.

Another reason for there being no statistically significant reduction in thrombosis rates could be that podoplanin can still recruit platelets to the site of vessel wall inflammation even if signalling downstream of CLEC-2 is blocked. It is possible that podoplanin-recruited platelets could be activated by other means such as ADP present on damaged endothelial cells. The previous *in vivo* studies looking at thrombosis reduction by inhibiting the CLEC-2 axis have only utilised genetic CLEC-2 depletion, pharmacological depletion of podoplanin, or antibody mediated blockade of the CLEC-2:podoplanin interaction, not inhibition of signalling downstream of CLEC-2. What goes against this latter explanation however is the results of the flow adhesion assays performed on platelets from patients treated with ibrutinib or acalabrutinib, or those with XLA (Figure 4.15).

Similar to the results from Pollitt *et al*. using Syk and Src inhibitors, here platelets fail to adhere to podoplanin indicating that activation downstream of CLEC-2 is required for this interaction to result in stable adhesion of platelets (Pollitt et al. 2014).

5.3.2 Patients taking ibrutinib have reduced rates of VTE

The fact that patients treated with ibrutinib have lower VTE rates than control patients from the same clinical trials is a potential signal that CLEC-2 plays a role in at least some forms of human VTE. Given the high doses of ibrutinib used in these trials (420-560 mg once daily) the reduction in VTE rates could be due to off-target effects of ibrutinib inhibiting signalling downstream of other receptors in platelets and immune cells such as GPVI.

The same reduction in VTE rates was also seen in RCTs comparing dasatinib to control treatments. It might be considered surprising that a drug so well established as dasatinib only has two RCTs where it is compared to a control treatment but, for trials of treatment for cancer, where often patients have relapsed and are left with no remaining treatment options, even a single arm trial where a small degree of disease response is seen is useful as an indicator that the drug can be used. If this is all that is required for a drug to be licensed in cancer therapy, it would in fact make very little economic sense for pharmaceutical companies to compare their drugs directly with existing treatments where their drug might be shown to be inferior.

This reduction in VTE rates was statistically significant whether a Cox's regression analysis with a stratified cohort approach or a meta-analysis

approach was used (not shown). In a stratified analysis it is assumed that the coefficient of treatment/control is the same for each study and this is estimated from all the data. In a meta-analysis different coefficients are estimated for each study and these are then combined to produce a single estimate.

A potential confounder for both sets of results with ibrutinib and dasatinib is that risk of VTE in haematological or solid organ malignancy correlates with the burden of disease. Thus patients who are treated with a drug that produces deeper and longer remissions are likely to have lower VTE rates. In all of these trials, the overall survival (OS) and progression free survival (PFS) of patients treated with ibrutinib and dasatinib was longer than control patients (not shown). This means that in order to truly know whether patients on these tyrosine kinase inhibitors (TKIs) have lower VTE rates an appropriately powered study in patients without underlying malignancy is necessary.

Another potential problem with comparing results across different trials as has been done here is that the control groups in each trial are different but for the purposes of the analysis they are being treated as if they are the same. But when the VTE rates in the treatment and control arms of individual trials are compared half of them showed a statistically significant reduction in VTEs in patients treated with ibrutinib an dasatinib. The trials that showed a statistically significant difference were the ones that were better powered to do so, either by having the longest drug exposure times (Montillo et al. 2017), or by studying a condition (prostate cancer) with a high rate of VTE (Araujo:2017cb}. The trials that did not show a statistically significant difference were probably under powered.

5.3.3 Patients with acute renal vein thrombosis following renal transplant do not have upregulated podoplanin in the vessel wall surrounding the clot

Unlike the observations in mice, the fact that podoplanin was not seen to be upregulated in human venous thrombosis tissue was surprising, particularly given the reduction in VTE seen in patients taking ibrutinib. The likely explanation for this finding was that the pathophysiology of acute renal vein thrombosis in a transplanted kidney is mediated through reduced blood flow and not through inflammation. Renal vein thrombosis in this setting occurs either because of hypovolaemia secondary to inadequate peri-operative fluid resuscitation or because of technical problems occurring during surgery such as a kinked renal vein, or a stenosis at the point the transplanted renal vein anastomoses to the native vasculature (Hogan et al. 2015).

Ideally a variety of different types of venous thrombosis tissue would have been collected and tested for the presence of podoplanin. The aim was to collect samples from those that had already been collected for other reasons and stored in hospital pathology departments or tissue banks or collect new samples from hospital PMs where patients were found to have died from or with VTE. There are a number of reasons why these samples proved to be very difficult to obtain. First was the paucity of hospital PMs and second was the lack of any surgical procedure that is currently performed for treatment of VTE which removes both clot and surrounding vessel wall.

The frequency of hospital PMs is diminishing and thus the incidence of

discovering a VTE at PM is very low. As a result, despite efforts to the contrary, the pathologists had a lack of familiarity with this particular research project and, even if they did identify VTE during a PM, this information was not passed onto the HBRC. Because of this an additional strategy employed in this project was to ask for hospital bereavement office staff to screen death certificates and report if a patient was found to have a term relating to VTE written as having contributed to or caused death. Patients' relatives would then be approached and consented to carry out a limited PM. Unfortunately, due to staff turnover and the pressured workload in the bereavement office, no patients were identified through this route.

There are surgical procedures such as thrombectomy which are performed rarely in acute life- or limb threatening venous thrombosis or thrombosis in the arteriovenous (AV) fistulae used for intravenous haemodialysis access. The latter was not pursued because it was felt that the high shear rates in AV fistulae were not representative of VTE. The former was not suitable because the retrieved thrombus does not have vein wall along with it.

It was, therefore, necessary to rely on venous thrombus that had been detected incidentally in histological samples. This is how the renal transplant samples were sourced. There is, however, a collaborating group at the University of Pennsylvania in Philadelphia led by Mark Kahn that has managed to obtain DVT and PE with surrounding vein from PMs of two patients. Their preliminary results are very exciting as they appear to show podoplanin expressing cells infiltrating the venous valve leaflets in the area where there is a DVT, but not on the valves where there is no DVT (see Appendix 1, Supplementary Figure.1).

In conclusion: there is only indirect or preliminary evidence that CLEC-2 and podoplanin play a role in human VTE, with direct evidence only very preliminary at the time of writing this thesis. The results from the mouse *in vivo* thrombosis assay do not conclusively show that ibrutinib is effective for targeting CLEC-2 in venous thrombosis but there is enough uncertainty about whether this particular experiment was underpowered to warrant further work in this area.

CHAPTER 6: GENERAL DISCUSSION

6.1 Summary of Results

This study has investigated the effect of Btk inhibitors on platelet function and signalling downstream of GPVI, which is correlated with the bleeding side effect seen with ibrutinib, and the effect downstream of CLEC-2, which has an uncertain role in haemostasis in mouse and no known role in man. It has also examined the role that the CLEC-2/podoplanin axis plays in human VTE and whether Btk inhibitors may provide a means of targeting CLEC-2 clinically in VTE while preserving activation by GPVI and other platelet receptors.

The headline results of this study are:

i) Btk inhibitors block GPVI-mediated platelet function reversibly at concentrations that are greater than those required to block Tec kinases demonstrating that this is an off-target action.

ii) The kinase function of Btk is not critical for PLCɣ2 activation downstream of GPVI in platelets (as judged by abrogation of Btk autophosphorylation and complete loss of phosphorylation of PLCɣ2) but it also plays a role which is unveiled when the results of ibrutinib-inhibited healthy donor platelets are compared with those from ibrutinib-inhibited platelets from patients with XLA.

iii) In direct contrast to the studies downstream of GPVI, the kinase function

of Btk (but not Tec) is critical for platelet signalling downstream of CLEC-2 and this manifests in Btk inhibitors blocking CLEC-2-mediated platelet function at 50-fold lower concentrations than those required to block GPVI-mediated platelet function at maximal agonist concentrations. This difference is due to the feedback role of secondary mediators and actin in supporting platelet activation by CLEC-2.

iv) Btk does not lie upstream of Syk in human and mouse CLEC-2 induced signalling, and not upstream as proposed by Manne *et al*. If this was the case, phosphorylation of Btk on the SFK activation site would not be altered.

v) Ibrutinib has off-target effects on an unknown kinase at very low concentrations which were unmasked when it was added to platelets from patients with XLA. This occurs downstream of both GPVI and CLEC-2 but downstream of the former it manifests as loss of the residual PLCɣ2 phosphorylation whereas downstream of the latter it manifests as loss of Syk and LAT phosphorylation.

vi) Ibrutinib reduces the incidence of VTE in a meta-analysis of studies where it was compared to conventional therapies for the treatment of LPDs.

6.1.1 Patients on Btk inhibitors have platelet dysfunction, mediated by an off-target drug effect, which only manifests as bleeding when it is combined with the patients' underlying haematological malignancy

As previously discussed, in the first trials for ibrutinib as a treatment of LPDs, patients experienced a major haemorrhage rate of up to 5%. This rate is higher than occurs even with patients treated with anticoagulants and resulted in safety concerns about the combination of ibrutinib with anticoagulants/antiplatelets and the subsequent decision not to co-administer ibrutinib with VKAs. Whether due to regression to the mean or due to the contraindication of ibrutinib for patients on VKAs, the rate of major haemorrhage for patients on ibrutinib decreased to 2-4% in the subsequent trials (Wang et al. 2015; Pavlik A et al. 2016; Jones et al. 2017). The rate of minor haemorrhage was also high at 28% (Wang et al. 2015). A systematic review was performed on the four RCTs that compared ibrutinib to a control treatment. This concluded that ibrutinib treatment was associated with an increased rate of bleeding of any grade, but that the increase in major haemorrhage was not statistically significant (albeit there was a clear trend). It was acknowledged as part of the review, however, that the number of patients was not sufficient to adequately power the study for major haemorrhage (Caron et al. 2017).

The bleeding seen with ibrutinib treatment has been correlated with impaired LTA in response to collagen and reduced adhesion to VWF under flow (Levade et al. 2014). This, however, is out of keeping with reports of mild bleeding in patients who are homozygous for a truncation in GPVI that prevents expression

(Matus et al. 2013) and the absence of bleeding in patients who lack Btk and it seems likely that the major bleeding seen in patients taking ibrutinib is due to a combination of functional impairment of GPVI and GPIb signalling (and other receptors e.g. integrin αIIbβ3) and their underlying haematological malignancy. This theory is supported by reports that the bleeding seen with ibrutinib occurs in the first six months of treatment and then tails off as the disease is brought into remission (Jones et al. 2017), that baboons treated with ibrutinib analogues do not have an increased bleeding time (Rigg et al. 2016) and mice treated with ibrutinib only develop haemostatic defects if they also have deficiency of $P2Y_{12}$ (Lee et al. 2017).

What this study adds to this is to show that it is non-Tec family kinase off-target effects of ibrutinib that result in loss of platelet activation by GPVI (and probably also by GPIb and integrin αIIbβ3) and that this inhibition is reversible. It also shows that the on-target action of ibrutinib to inhibit Btk kinase function, and even its additional off-target inhibition of Tec kinase, is not sufficient to block GPVI-mediated platelet signalling most likely because Tec kinases can act as adapter proteins and support PLCγ2 activation in the absence of phosphorylation.

From this information I conclude that bleeding in patients taking ibrutinib occurs because:

i) The clinical dose is supra-maximal for blockade of Btk and causes GPVI inhibition due to off-target effects.

ii) The fact that patients have an underlying haematological malignancy

contributes to the bleeding.

6.1.2 Btk inhibitors block CLEC-2 mediated platelet function at much lower concentrations than those that block platelet activation by GPVI

Unlike the effects of Btk inhibitors on GPVI-mediated platelet function, which occur at supra-maximal concentrations and are due to reversible, off-target effects, they irreversibly abrogate CLEC-2 mediated platelet function at concentrations which are 50-fold lower and are due to on-target, specific inhibition of Btk kinase activity. Even though it has been shown as part of this study that low concentration ibrutinib has an off-target effect on one or more other tyrosine kinases, the dependence of CLEC-2 on Btk inhibition is clear from the results in XLA patients despite the presence of Tec. Unlike its role downstream of GPVI, the adapter function of Btk is not able to activate PLCɣ2 downstream of CLEC-2 and nor is Tec kinase in platelets able to substitute possibly because it is expressed at a lower level or because it cannot function as an adapter. One difference between Btk and Tec is that Tec's autophosphorylation site does not lie in a YxxM motif, which binds selectively to the SH2 domains of PI3K. It would be interesting to study whether this difference prevents it serving as an adapter with PLCɣ2 downstream of CLEC-2. These studies have shown that Btk inhibitors can block CLEC-2 function in *in vitro* and *ex vivo* models of platelet activation. They are not as convincing when considering blockade of the podoplanin-CLEC-2 axis *in vivo* however. Despite

adequate blockade of CLEC-2 mediated platelet activation as measured by flow cytometry, ibrutinib did not prevent mouse venous thrombosis *in vivo* to a statistically significant degree. It is possible that this is because CLEC-2 ligation by podoplanin is sufficient to recruit platelets and lead to thrombosis in the absence of platelet activation downstream of CLEC-2, but this is unlikely as the results from the *ex vivo* flow adhesion assay show that the platelets from patients taking Btk inhibitors and those with XLA do not adhere to podoplanin in venous flow conditions. It is more likely, instead, that this the negative result of this experiment was due to it being under powered, or due to inadequate CLEC-2 blockade and further experiments are required fully answer this question. The results from the RCTs of ibrutinib in LPD are encouraging in this regard however, as there is a statistically significant reduction in VTE in the patients treated with ibrutinib when compared to controls.

6.1.3 Podoplanin induced platelet CLEC-2 activation is involved in human VTE

The methods that I have employed to look for evidence that platelet CLEC-2 plays a role in human VTE/thromboinflammation were two-fold; firstly I looked for indirect evidence using VTE rates from clinical trials using drugs that have been shown to block CLEC-2; the second looked directly for podoplanin expression in the subendothelium of veins surrounding a thrombus.

The rates of VTE in trials of ibrutinib and dasatinib treated patients were reduced compared to controls. This gives some indirect evidence that CLEC-2 is involved in human VTE but, of course, this reduction could be due to

inhibition of other platelet receptor signalling pathways.

Direct evidence of podoplanin expression in human VTE was not found as part of this study. This was because of the difficulty in obtaining such tissue and also because the only tissue that was obtained (i.e. Transplanted kidney) has a fairly unique pathophysiology which is not representative of VTE. During the write up phase of this project, however, a histological sample of “classic” DVT has been obtained by collaborators and this does show evidence of podoplanin expression in the diseased but not control valve of the patient (see Supplementary Figure.1 in Appendix 1). This is particularly exciting as this also indirectly supports the validity of the mouse stenosis model of DVT.

Overall, therefore, I have obtained promising indirect and direct evidence that podoplanin and CLEC-2 play a role in human VTE similar to the more established role in mouse thromboinflammation.

6.2 Final conclusions

Given that CLEC-2 is critical in mouse thromboinflammation but not haemostasis, that it may have a similar role in human VTE but also not haemostasis, and that Btk inhibitors block all aspects of human platelet CLEC-2 function at a > 10 fold lower concentration than is currently achieved in their treatment of LPD, it would seem that Btk inhibitors are an attractive way of targeting platelet CLEC-2 *in vivo*. The bleeding side effect that occurs in patients treated with Btk inhibitors could be perceived as a barrier to this, but,

for reasons detailed above, bleeding is unlikely if patients without underlying haematological malignancy are treated with low doses of Btk inhibitor that lack off-target effects. Significantly, I have shown that XLA patients, who have no known bleeding phenotype, lack any demonstrable platelet CLEC-2 function. Further evidence that supports the view that Btk inhibitors can be used outside of the haematological malignancy disease setting without a bleeding side effect comes from the fact that the inhibitor PRN-1008 is undergoing phase II trials for ITP (Principia Biopharma 2018). Moreover, the Syk inhibitor fostamatinib, which has also been shown to block CLEC-2 mediated platelet activation (Spalton et al. 2009), has just been licensed as a treatment for ITP (Bussel et al. 2018). If there was any hint of extra bleeding due to platelet dysfunction in these, already thrombocytopenic, patients then they would be readily apparent.

In order to translate these findings into the clinical use of Btk inhibitors as a treatment for or prophylaxis against VTE there are several further studies and considerations that are needed. Firstly the mouse IVC stenosis experiment needs to be extended with adequate numbers of mice to ensure it is properly powered; secondly the finding that podoplanin is in the vessel wall in a single patient with VTE needs to be repeated on more patients; thirdly it is important to investigate further whether patients with XLA do not have a bleeding phenotype, for example by undertaking a bleeding assessment tool (BAT) as published by the International Society for Thrombosis and Haemostasis (ISTH) to assess their bleeding symptoms (Rodeghiero et al. 2010); fourthly it would be interesting to see if there is any evidence of blood lymphatic mixing in patients

with XLA as occurs in CLEC-2 deficient mice and can be detected in patients using ultrasound based clinical imaging techniques (Seeger et al. 2009) (albeit these are due to defects during but not post-development); fifthly *ex vivo* platelet function analysis needs to be studied in healthy volunteers taking very low doses of ibrutinib in order to look for effects on platelet CLEC-2, and indeed this line of enquiry was considered as part of the above study, but the time-frame and costs involved in order to perform these experiments as part of a clinical research training fellowship were prohibitive. Indeed, in a study that is unlikely to have received ethical approval in the UK due to concerns over self-experimentation, Busygina *et al*. showed that inhibitory effects on GPIb signalling were still detectable in two of the investigators who took daily or alternate day doses of 120 mg ibrutinib (i.e. 1/6 of the current daily dose used for treating CLL); and sixthly a phase II trial using low dose Btk inhibitors in addition to/instead of conventional VTE prophylaxis for patients undergoing surgery for high risk of VTE (e.g. for total knee replacement surgery) could provide direct evidence of the hypothesis and pave the way for a future phase III trial.

APPENDIX

Podoplanin is upregulated on the valve leaflets surrounding venous thrombosis in human veins *in vivo*

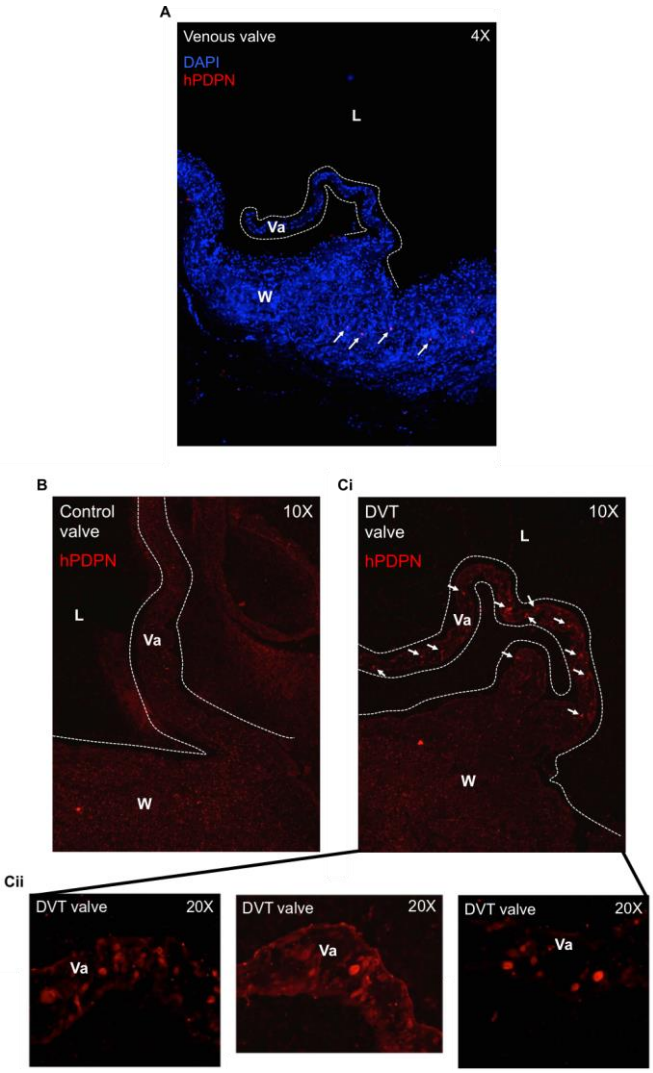

Supplementary Figure.1. Podoplanin is upregulated on venous valve surrounding thrombus in human veins *in vivo.*
Femoral vein from a patient with deep vein thrombosis (DVT) identified at post mortem was sectioned, fixed and stained with the anti-human podoplanin (hPDPN) antibody NZ-1. (A) Venous valve with no surrounding DVT stained with hPDPN (red) and 4,6-diamidino-2-phenylindole (DAPI, blue). Arrows show locations of lymphatic vessels in the vein wall. (B). Venous valve with no surrounding DVT stained with hPDPN. (C) Venous valve with surrounding DVT stained with hPDPN. Arrows show infiltrating cells staining positive for human podoplanin. Vein Lumen (L), Vein Wall (W), Venous Valve (Va). Images courtesy of John Welsh (University of Pennsylvania, Philadelphia, PA)

REFERENCES

Advani, R.H. et al., 2012. Bruton Tyrosine Kinase Inhibitor Ibrutinib (PCI-32765) Has Significant Activity in Patients With Relapsed/Refractory B-Cell Malignancies. *Journal of Clinical Oncology*, 31(1), pp.88–94.

Akinleye, A. et al., 2013. Ibrutinib and novel BTK inhibitors in clinical development. *Journal of Hematology & Oncology*, 6(1), pp.1–9.

Alshehri, O.M. et al., 2015. Fibrin activates GPVI in human and mouse platelets. *Blood*, 126(13), pp.1601–1608.

Amin, A. et al., 2015. Comparison of differences in medical costs when new oral anticoagulants are used for the treatment of patients with non-valvular atrial fibrillation and venous thromboembolism vs warfarin or placebo in the US. *Journal of Medical Economics*, 18(6), pp.399–409.

Andre, P. et al., 2011. Critical role for Syk in responses to vascular injury. *Blood*, 118(18), pp.5000–5010.

Andrews, R.K. & Berndt, M.C., 2013. The GPIb-IX-V Complex. In A. D. Michelson, ed. *Platelets*. pp. 195–213.

Arai, M. et al., 1994. Substantial expression of glycoproteins IX and V on the platelet surface from a patient with Bernard-Soulier syndrome. *British Journal of Haematology*, 87, pp.185–188.

Araujo, J.C. et al., 2017. Docetaxel and dasatinib or placebo in men with metastatic castration-resistant prostate cancer (READY): a randomised, double-blind phase 3 trial. *Lancet Oncology*, 14(3), pp.1307–1316.

Arman, M. et al., 2014. Amplification of bacteria-induced platelet activation is triggered by FcgRIIA, integrin aIIbb3, and platelet factor 4. *Blood*, 123(20), pp.3166–3174.

Arthur, J.F., Dunkley, S. & Andrews, R.K., 2007. Platelet glycoprotein VI-related clinical defects. *British Journal of Haematology*, 139(3), pp.363–372.

Astarita, J.L., Acton, S.E. & Turley, S.J., 2012. Podoplanin: emerging functions in development, the immune system, and cancer. *Frontiers in immunology*, 3, p.283.

Atkinson, B.T., Ellmeier, W. & Watson, S.P., 2003. Tec regulates platelet activation by GPVI in the absence of Btk. *Blood*, 102(10), pp.3592–3599.

Banerjee, R. et al., 2016. Comparable outcomes in Chronic Lymphocytic Leukemia patients treated with reduced dose ibrutinib: Results from a multi-center study. In EHA. p. Abstract P219.

Barf, T. et al., 2017. Acalabrutinib (ACP-196): A Covalent Bruton Tyrosine Kinase Inhibitor with a Differentiated Selectivity and In Vivo Potency Profile. *Journal of Pharmacology and Experimental Therapeutics*, 363(2), pp.240–252.

Becattini, C. et al., 2012. Aspirin for Preventing the Recurrence of Venous Thromboembolism. *New England Journal of Medicine*, 366(21), pp.1959–1967.

Bellucci, S. et al., 2004. Defective collagen-induced platelet activation in two patients with malignant haemopathies is related to a defect in the GPVI-coupled signalling pathway. *Thrombosis and Haemostasis*, 93, pp.130-138.

Belohlavek, J., Dytrych, V. & Linhart, A., 2013. Pulmonary embolism, part I: Epidemiology, risk factors and risk stratification, pathophysiology, clinical presentation, diagnosis and nonthrombotic pulmonary embolism. *Experimental and Clinical Cardiology,* 18(2), pp.129-138.

Bender, M. et al., 2013. Combined In Vivo Depletion of Glycoprotein VI and C-Type Lectin-Like Receptor 2 Severely Compromises Hemostasis and Abrogates Arterial Thrombosis in Mice. *Arteriosclerosis, thrombosis, and vascular biology*, 33, pp.926–934.

Bender, M., Stegner, D. & Nieswandt, B., 2017. Model systems for platelet receptor shedding. *Platelets*, 28(4), pp.325–332.

Bose, P. et al., 2016. Pharmacokinetic and pharmacodynamic evaluation of ibrutinib for the treatment of chronic lymphocytic leukemia: rationale for lower doses. *Expert Opinion on Drug Metabolism & Toxicology*, 0(0), pp.1–42.

Boulaftali, Y. et al., 2018. Glycoprotein VI in securing vascular integrity in inflamed vessels. *Research and Practice in Thrombosis and Haemostasis*, 2(2), pp.228–239.

Boulaftali, Y. et al., 2014. Platelet Immunoreceptor Tyrosine-Based Activation Motif (ITAM) Signaling and Vascular Integrity. *Circulation Research*, 114(7), pp.1174–1184.

Boylan, B. et al., 2004. Anti-GPVI-associated ITP: an acquired platelet disorder caused by autoantibody-mediated clearance of the GPVI/FcR -chain complex from the human platelet surface. *Blood*, 104(5), pp.1350–1355.

Bradley, L.A. et al., 1994. Mutation detection in the X-linked agammaglobulinemia gene. *Human Molecular Genetics*, 3(1), pp.79–83.

Brighton, T.A. et al., 2012. Low-Dose Aspirin for Preventing Recurrent Venous Thromboembolism. *New England Journal of Medicine*, 367(21), pp.1979–1987.

Brown, K. et al., 2004. Crystal Structures of Interleukin-2 Tyrosine Kinase and Their Implications for the Design of Selective Inhibitors. *Journal of Biological Chemistry*, 279(18), pp.18727–18732.

Brühl, von, M.-L. et al., 2012. Monocytes, neutrophils, and platelets cooperate to initiate and propagate venous thrombosis in mice in vivo. *The Journal of Experimental Medicine*, 209(4), pp.819–835.

Buggy, J.J. & Elias, L., 2012. Bruton Tyrosine Kinase (BTK) and Its Role in B-cell Malignancy. *International Reviews of Immunology*, 31(2), pp.119–132.

Burger, J.A. et al., 2016. Safety and activity of ibrutinib plus rituximab for patients with high-risk chronic lymphocytic leukaemia: a single-arm, phase 2 study. *Lancet Oncology*, 15(10), pp.1090–1099.

Burkhart, J.M. et al., 2012. The first comprehensive and quantitative analysis of human platelet protein composition allows the comparative analysis of structural and functional pathways. *Blood*, 120(15), pp.e73–82.

Burn, J. & Pirmohamed, M., 2018. Direct oral anticoagulants versus warfarin: is new always better than the old? *Open Heart*. 10.1136/openhrt-2017-000712

Bussel, J. et al., 2018. Fostamatinib for the treatment of adult persistent and chronic immune thrombocytopenia: Results of two phase 3, randomized, placebo‐controlled trials. *American Journal of Hematology*, 93, pp.921–930.

Busygina, K. et al., 2018. Oral Bruton tyrosine kinase inhibitors selectively block atherosclerotic plaque–triggered thrombus formation in humans. *Blood*, 131(24), pp.2605–2616.

Bye, A.P. et al., 2015. Ibrutinib Inhibits Platelet Integrin αIIbβ3 Outside-In Signaling and Thrombus Stability But Not Adhesion to Collagen. *Arteriosclerosis, thrombosis, and vascular biology*, p.ATVBAHA.115.306130.

Bye, A.P. et al., 2017. Severe platelet dysfunction in NHL patients receiving ibrutinib is absent in patients receiving acalabrutinib. *Blood Advances*, 1(26), pp.2610–2623.

Byrd, J.C. et al., 2016. Acalabrutinib (ACP-196) in Relapsed Chronic Lymphocytic Leukemia. *New England Journal of Medicine*, 374(4), pp.323–332.

Byrd, J.C. et al., 2014. Ibrutinib versus Ofatumumab in Previously Treated Chronic Lymphoid Leukemia. *New England Journal of Medicine*, 371(3), pp.213–223.

Byrd, J.C. et al., 2013. Targeting BTK with Ibrutinib in Relapsed Chronic Lymphocytic Leukemia. *New England Journal of Medicine*, 369(1), pp.32–42.

Caron, F. et al., 2017. Current understanding of bleeding with ibrutinib use: a systematic review and meta-analysis. *Blood Advances*, 1(12), pp.772–778.

Castellucci, L.A. et al., 2013. Efficacy and safety outcomes of oral anticoagulants and antiplatelet drugs in the secondary prevention of venous thromboembolism: systematic review and network meta-analysis. *BMJ*, 347(aug30 1), pp.f5133–f5133.

Chai-Adisaksopha, C. et al., 2015. Mortality outcomes in patients receiving direct oral anticoagulants: a systematic review and meta-analysis of randomized controlled trials. *Journal of thrombosis and haemostasis : JTH*, 13(11), pp.2012–2020.

Chan, K.-W. et al., 2006. Identification of Bruton tyrosine kinase mutations in 12 Chinese patients with X-linked agammaglobulinaemia by long PCR-direct sequencing. *International Journal of Immunogenetics*, 33(3), pp.205–209.

Chan, M. et al., 2018. Not all light transmission aggregation assays are created equal: qualitative differences between light transmission and 96-well plate aggregometry. *Platelets*. 29(7), pp.686-689.

Chanan-Khan, A. et al., 2016. Ibrutinib combined with bendamustine and rituximab compared with placebo, bendamustine, and rituximab for previously treated chronic lymphocytic leukaemia or small lymphocytic lymphoma (HELIOS): a randomised, double-blind, phase 3 study. *Lancet Oncology*, 17(2), pp.200–211.

Chang, Y.-W., Hsieh, P.-W. & Tseng, C.-P., 2015. Identification of a novel platelet antagonist that binds to CLEC-2 and suppresses podoplanin-induced platelet aggregation and cancer metastasis. Oncotarget. 6(40), pp. 42733-42748

Chen, L.S. et al., 2018. A pilot study of lower doses of ibrutinib in patients with chronic lymphocytic leukemia. *Blood*. 10.1182/blood-2018-06-860593

Clemetson, K.J. & Clemetson, J.M., 2013. Platelet Receptors. In A. D. Michelson, ed. *Platelets*. pp. 169–194.

Connolly, S.J. et al., 2016. Andexanet Alfa for Acute Major Bleeding Associated with Factor Xa Inhibitors. *New England Journal of Medicine*, 375(12), pp.1131–1141.

Cortes, J.E. et al., 2016. Final 5-Year Study Results of DASISION: The Dasatinib Versus Imatinib Study in Treatment-Naïve Chronic Myeloid Leukemia Patients Trial. *Journal of Clinical Oncology*, 34(20), pp.2333–2340.

Crowther, M.A. & Warkentin, T.E., 2008. Bleeding risk and the management of bleeding complications in patients undergoing anticoagulant therapy: focus on new anticoagulant agents. *Blood*, 111(10), pp.4871–4879.

Dorsam, R.T. & Kunapuli, S.P., 2004. Central role of the P2Y12 receptor in platelet activation. *The Journal of clinical investigation*, 113(3), pp.340–345.

Dumont, B. et al., 2009. Absence of collagen-induced platelet activation caused by compound heterozygous GPVI mutations. *Blood*, 114(9), pp.1900–1903.

Dunkley, S. et al., 2007. A familial platelet function disorder associated with abnormal signalling through the glycoprotein VI pathway. *British Journal of Haematology*, 137(6), pp.569–577.

Ellmeier, W. et al., 2000. Severe B Cell Deficiency in Mice Lacking the Tec Kinase Family Members Tec and Btk. *The Journal of Experimental Medicine*, 192(11), pp.1611–1624.

Endo, L.M. et al., 2011. Membranous Glomerulopathy in an Adult Patient with X-Linked Agammaglobulinemia Receiving Intravenous Gammaglobulin. *Journal of Investigational Allergology and Clinical Immunology*, 21(5), pp.405–409.

Engelmann, B. & Massberg, S., 2012. Thrombosis as an intravascular effector of innate immunity. *Nature Reviews Immunology*, 13(1), pp.34–45.

Estcourt, L.J. et al., 2016. Guidelines for the use of platelet transfusions. *British Journal of Haematology*, 176(3), pp.365–394.

Flumignan, C.D., Flumignan, R.L. & Baptista-Silva, J.C., 2016. Antiplatelet agents for the treatment of deep venous thrombosis Cochrane Vascular Group, ed. *Cochrane Database of Systematic Reviews*, 151(5), pp.933–14.

Fumagalli, S. et al., 2014. Psychological effects of treatment with new oral anticoagulants in elderly patients with atrial fibrillation: a preliminary report. *Aging Clinical and Experimental Research*, 27(1), pp.99–102.

Gaspar, H.B. et al., 1998. Bruton's tyrosine kinase expression and activity in X-linked agammaglobulinaemia (XLA): the use of protein analysis as a diagnostic indicator of XLA. *Clinical and Experimental Immunology*, 111, pp.334–338.

Gibbins, J.M. et al., 1996. Tyrosine Phosphorylation of the Fc Receptor γ-Chain in Collagen-stimulated Platelets. *Journal of Biological Chemistry*, 271(30), pp.18095–18099.

Giganti, M.J. et al., 2015. A Comparison of Seven Cox Regression-Based Models to Account for Heterogeneity Across Multiple HIV Treatment Cohorts in Latin America and the Caribbean. *AIDS Research and Human Retroviruses*, 31(5), pp.496–503.

Gitz, E. et al., 2014. CLEC-2 expression is maintained on activated platelets and on platelet microparticles. *Blood*, 124(14), pp.2262–2270.

Glenn, J.R. et al., 2009. Leukocyte count and leukocyte ecto-nucleotidase are major determinants of the effects of adenosine triphosphate and adenosine

diphosphate on platelet aggregation in human blood. *Platelets*, 16(3-4), pp.159–170.

Grynkiewicz, G., Poenle, M. & Tsien, R.Y., 2001. New Generation of Ca^{2+} Indicators with Greatly Improved Fluorescence Properties. *Journal of Biological Chemistry*, 260(6), pp.3440–3450.

Hamilton, J.R., Cornelissen, I. & Coughlin, S.R., 2004. Impaired hemostasis and protection against thrombosis in protease-activated receptor 4-deficient mice is due to lack of thrombin signaling in platelets. *Journal of Thrombosis and Haemostasis*, 2, pp.1429–1435.

Harker, L.A. et al., 2000. Effects of megakaryocyte growth and development factor on platelet production, platelet life span, and platelet function in healthy human volunteers. *Blood*, 95(8), pp.2514–2522.

Hartwig, J.H., 2013. The Platelet Cytoskeleton. In A. D. Michelson, ed. *Platelets*. pp. 145–168.

Hermans, C. et al., 2009. A compound heterozygous mutation in glycoprotein VI in a patient with a bleeding disorder. *Journal of Thrombosis and Haemostasis*, 7(8), pp.1356–1363.

Hitchcock, J.R. et al., 2015. Inflammation drives thrombosis after Salmonella infection via CLEC-2 on platelets. *The Journal of clinical investigation*, 125(12), pp.4429–4446.

Hogan, J.L. et al., 2015. Late-onset renal vein thrombosis: A case report and review of the literature. *International Journal of Surgery Case Reports*, 6, pp.73-76.

Holinski-Feder, E. et al., 1998. Mutation Screening of the BTK Gene in 56 Families With X-Linked Agammaglobulinemia (XLA): 47 Unique Mutations Without Correlation to Clinical Course. *Pediatrics*, 101(2), pp.276–284.

Honigberg, L. et al., 2010. The Bruton tyrosine kinase inhibitor PCI-32765 blocks B-cell activation and is efficacious in models ofautoimmune disease and B-cell malignancy. *Proceedings of the National Academy of Sciences*, 107(29), pp.13075–13080.

Hughes, C.E. et al., 2010. CLEC-2 is not required for platelet aggregation at arteriolar shear. *Journal of Thrombosis and Haemostasis*, 8(10), pp.2328–2332.

Hutter, B.O. & Kreitschmann-Andermahr, I., 2014. Subarachnoid hemorrhage as a psychological trauma. *Journal of Neurosurgery*, 120, pp.923–930.

Jandrot-Perrus, M. et al., 2000. Cloning, characterization, and functional studies of human and mouse glycoprotein VI: a platelet-specific collagen receptor from the immunoglobulin superfamily. *Blood*, 96(1), pp.1798–1807.

Janssen Inc., 2015. Imbruvica Prescribing Information. *Highlights of Prescribing Information*, pp.1–37. Accessed January 23– 2017.

Jo, E.K. et al., 2001. Characterization of mutations, including a novel regulatory defect in the first intron, in Bruton's tyrosine kinase gene from seven Korean X-linked agammaglobulinemia families. *The Journal of Immunology*, 167(7), pp.4038–4045.

Jones, J.A. et al., 2014. Pattern of Use of Anticoagulation and/or Antiplatelet Agents in Patients with Chronic Lymphocytic Leukemia (CLL) Treated with Single-Agent Ibrutinib Therapy. *Blood*, 124(21), p.1990.

Jones, J.A. et al., 2017. Use of anticoagulants and antiplatelet in patients with chronic lymphocytic leukaemia treated with single-agent ibrutinib. *British Journal of Haematology*, 178(2), pp.286–291.

Josefsson, E.C. et al., 2013. The Regulation of Platelet Life Span. In A. D. Michelson, ed. *Platelets*. pp. 51–65.

Judd, B.A. et al., 2002. Differential Requirement for LAT and SLP-76 in GPVI versus T Cell Receptor Signaling. *The Journal of Experimental Medicine*, 195(6), pp.705–717.

Kamel, S. et al., 2015. Ibrutinib inhibits collagen-mediated but not ADP-mediated platelet aggregation. *Leukemia*, 29(4), pp.783–787.

Kang, S.W. et al., 2001. PKCβ modulates antigen receptor signaling via regulation of Btk membrane localization. *The EMBO Journal*, 20(20), pp.5692–5702.

Kaushansky, K., 2005. The molecular mechanisms that control thrombopoiesis. *Journal of Clinical Investigation*, 115(12), pp.3339–3347.

Kawakami, Y. et al., 1999. Functions of Bruton’s tyrosine kinase in mast and B cells. *Journal of Leukocyte Biology*, 65, pp.286–290.

Keeling, D. et al., 2011. Guidelines on oral anticoagulation with warfarin - fourth edition. *British Journal of Haematology*, 154(3), pp.311–324.

Keeling, D. et al., 2016. Peri-operative management of anticoagulation and antiplatelet therapy. *British Journal of Haematology*, 175(4), pp.602–613.

Kerner, J.D. et al., 1995. Impaired Expansion of Mouse B Cell Progenitors Lacking Btk. *Immunity*, 3, pp.301–312.

Khan, A.O. et al., 2017. CRISPR-Cas9 Mediated Labelling Allows for Single Molecule Imaging and Resolution. Nature *Scientific Reports*, 7(8450), pp.1–9.

Khan, W.N. et al., 1995. Defective B Cell Development and Function in Bfk-Deficient Mice. *Immunity*, 3, pp.283–299.

Kil, L.P. et al., 2013. Bruton's tyrosine kinase mediated signaling enhances leukemogenesis in a mouse model for chronic lymphocytic leukemia. *American Journal of Blood Research*, 3(1), pp.71–83.

Koessler, J. et al., 2016. Role of Purinergic Receptor Expression and Function for Reduced Responsiveness to Adenosine Diphosphate in Washed Human Platelets. *PLoS ONE*, pp.1–13.

Kojima, H. et al., 2006. Characterization of a patient with glycoprotein (GP) VI deficiency possessing neither anti-GPVI autoantibody nor genetic aberration. *Journal of Thrombosis and Haemostasis*, 4, pp.2433–2442.

Kralisz, U. & Cierniewski, C.S., 1998. Tyrosine phosphorylation events during di¡erent stages of collagen-platelet activation. *Biochimica et Biophysica Acta (BBA) - Proteins and Proteomics*, 1405, pp.128–138.

Kroll, M.H. et al., 2013. Incidence Rate Of Venous Thromboembolism (VTE) and Utilization Of a VTE Prophylaxis Order Set Module In Hospitalized Patients With Leukemia. 122(21), p.2946.

Kuppers, R., 2005. Mechanisms of B-Cell Lymphoma Pathogenesis. *Nature Reviews Cancer*, 5, pp.251–262.

Kuter, D.J., 2013. The biology of thrombopoietin and thrombopoietin receptor agonists. *International Journal of Hematology*, 98(1), pp.10–23.

Langrish, C.L. et al., 2017. PRN1008, a Reversible Covalent BTK Inhibitor in Clinical Development for Immune Thrombocytopenic Purpura | Blood Journal. *ASH Abstracts*, 130(Suppl 1), p.1052.

Leblanc, R. & Peyruchaud, O., 2016. Metastasis: new functional implications of platelets and megakaryocytes. *Blood*, 128(1), pp.24–31.

Lee, R.H. et al., 2017. Effects of ibrutinib treatment on murine platelet function during inflammation and in primary hemostasis. *Haematologica,* 102, pp.e89-e92.

Levade, M. et al., 2014. Ibrutinib treatment affects collagen and von Willebrand factor-dependent platelet functions. *Blood*. 124(26), pp.3991-3995.

Levin, J., 2013. The Evolution of Mammalian Platelets. In M. D. Michelson, ed. *Platelets*. pp. 3–25.

Li, R. & Emsley, J., 2013. The organizing principle of the platelet glycoprotein Ib-IX-V complex. *Journal of thrombosis and haemostasis : JTH*, 11(4), pp.605–614.

Li, Z. et al., 2010. Signaling During Platelet Adhesion and Activation. *Arteriosclerosis, thrombosis, and vascular biology*, 30(12), pp.2341–2349.

Liang, C. et al., 2018. The development of Bruton's tyrosine kinase (BTK) inhibitors from 2012 to 2017: A mini-review. *European Journal of Medicinal Chemistry*, 151, pp.315–326.

Lipsky, A.H. et al., 2015. Incidence and risk factors of bleeding-related adverse events in patients with chronic lymphocytic leukemia treated with ibrutinib. *Haematologica*, 100(12), pp.1571–1578.

Lordkipanidzé, M. et al., 2014. Characterization of multiple platelet activation pathways in patients with bleeding as a high-throughput screening option: use of 96-well Optimul assay. *e-Blood*, 123(8), pp.e11–e22.

Makris, M. et al., 2012. Guideline on the management of bleeding in patients on antithrombotic agents. *British Journal of Haematology*, 160(1), pp.35–46.

Mammadova-Bach, E. et al., 2015. Platelet glycoprotein VI binds to polymerized fibrin and promotes thrombin generation. *Blood*, 126(5), pp.683–691.

Mangin, P.H. et al., 2018. Immobilized fibrinogen activates human platelets through glycoprotein VI. *Haematologica*, 103(5), pp.898–907.

Manne, B.K. et al., 2015. Distinct Pathways Regulate Syk Protein Activation Downstream of Immune Tyrosine Activation Motif (ITAM) and hemITAM Receptors in Platelets. *Journal of Biological Chemistry*, 290(18), pp.11557–11568.

Martin, G.G. et al., 2007. Structure and function of haemocytes in two marine gastropods, Megathura crenulata and Aplysia californica. *Journal of Molluscan Studies*, 73(4), pp.355–365.

Matus, V. et al., 2013. An adenine insertion in exon 6 of human GP6generates a truncated protein associated with a bleeding disorder in four Chilean families. *Journal of thrombosis and haemostasis : JTH*, 11(9), pp.1751–1759.

May, F. et al., 2009. CLEC-2 is an essential platelet-activating receptor in hemostasis and thrombosis. *Blood*, 114(16), pp.3464–3472.

Mazet, F. et al., 2015. A high-density immunoblotting methodology for quantification of total protein levels and phosphorylation modifications. *Nature Scientific Reports*, 5(16995), pp.1–8.

McMullen, J.R. et al., 2014. Ibrutinib increases the risk of atrial fibrillation, potentially through inhibition of cardiac PI3K-Akt signaling. *Blood*, 124(25), pp.3829–3830.

McNeil, K. & Dunning, J., 2007. Chronic thromboembolic pulmonary hypertension (CTEPH). *Heart*, 93(9), pp.1152–1158.

Mohamed, A.J. et al., 1999. Signalling of Bruton's Tyrosine Kinase, Btk. *Scandinavian Journal of Immunology*, 49, pp.113-118.

Montillo, M. et al., 2017. Long-term efficacy and safety in the RESONATE study: Ibrutinib in patients with previously treated chronic lymphocytic Leukemia (CLL) with up to four years follow-up. *Hematological Oncology*, 35, pp.235–236.

Moroi, M. et al., 1989. A Patient with Platelets Deficient in Glycoprotein VI That Lack Both Collagen-induced Aggregation and Adhesion. *Journal of Clinical Investigation*, 84, pp.1440–1445.

National Cancer Institute, 2010. Common Terminology Criteria for Adverse Events (CTCAE). pp.1–196.

National Institute for Health and Care Excellence, 2017. Cancer Drugs Fund Managed Access Agreement. *nice.org.uk*, pp.1–11. Available at: https://www.nice.org.uk/guidance/ta491/documents/final-appraisal-determination-document-2 [Accessed August 23, 2018].

National Institute for Health and Care Excellence, 2018a. Ibrutinib for previously treated chronic lymphocytic leukaemia and untreated chronic lymphocytic leukaemia with 17p deletion or TP53 mutation. *nice.org.uk*, pp.1–32. Available at: nice.org.uk/guidance/ta429 [Accessed August 2, 2018a].

National Institute for Health and Care Excellence, 2018b. Ibrutinib for treating relapsed or refractory mantle cell lymphoma. *nice.org.uk*, pp.1–22. Available at: nice.org.uk/guidance/ta502 [Accessed August 2, 2018b].

National Institute for Health and Care Excellence, 2018c. Venous thromboembolism in over 16s: reducing the risk of hospital-acquired deep vein thrombosis or pulmonary embolism. *nice.org.uk*, pp.1–41. Available at: nice.org.uk/guidance/ng89 [Accessed August 2, 2018c].

Navarro-Núñez, L. et al., 2015. Platelet adhesion to podoplanin under flow is mediated by the receptor CLEC-2 and stabilised by Src/Syk-dependent platelet signalling. *Thrombosis and Haemostasis*, 113(5), pp.1109–1120.

Nicolson, P.L.R. et al., 2018. Inhibition of Btk by Btk-specific concentrations of ibrutinib and acalabrutinib delays but does not block platelet aggregation to GPVI. *Haematologica*, 103, pp.haematol.2018.193391–36.

Nurden, P. et al., 2004. Severe deficiency of glycoprotein VI in a patient with gray platelet syndrome. *Blood*, 104(1), pp.107–114.

Oda, A. et al., 2000. Rapid tyrosine phosphorylation and activation of Bruton's tyrosine/Tec kinases in platelets induced by collagen binding or CD32 cross-linking. *Blood*, 95(5), pp.1663–1670.

Onselaer, M.-B. et al., 2017. Fibrin and D-dimer bind to monomeric GPVI. *Blood Advances*, 1(19), pp.1495–1504.

Oppermann, F.S. et al., 2009. Large-scale Proteomics Analysis of the Human Kinome. *Molecular & Cellular Proteomics*, 8, pp.1751–1764.

Padhan, N. et al., 2017. Highly sensitive and specific protein detection via combined capillary isoelectric focusing and proximity ligation. *Nature Scientific Reports,* 7(1490), pp.1–9.

Papa, A. et al., 2014. Venous thromboembolism in patients with inflammatory bowel disease: Focus on prevention and treatment. *World Journal of Gastroenterology*, 20(12), pp.3173–8.

Parguina, A.F. et al., 2012. A detailed proteomic analysis of rhodocytin-activated platelets reveals novel clues on the CLEC-2 signalosome: implications for CLEC-2 signaling regulation. *Blood*, 120(26), pp.e117–e126.

Park, H. et al., 1996. Regulation of Btk Function by a Major Autophosphorylation Site Within the SH3 Domain. *Immunity*, 4, pp.515–525.

Pavlik A et al., 2016. Major bleeding complications among patients treated with ibrutinib and concomitant antiplatelet,anticoagulant or supplemental therapy. *ASH Abstracts*, pp.1–1.

Payne, H. et al., 2017. Mice with a deficiency in CLEC-2 are protected against deep vein thrombosis. *Blood*, pp.blood–2016–09–742999–32.

Pike, J.A. et al., 2018. Topological data analysis quantifies biological nano-structure from single molecule localization microscopy. *bioRxiv*, pp.1–16.

Pollack, C.V., Jr. et al., 2017. Idarucizumab for Dabigatran Reversal — Full Cohort Analysis. *New England Journal of Medicine*, 377(5), pp.431–441.

Pollitt, A.Y. et al., 2010. Phosphorylation of CLEC-2 is dependent on lipid rafts, actin polymerization, secondary mediators, and Rac. *Blood*, 115(14) pp.2938-2946.

Pollitt, A.Y. et al., 2014. Syk and Src family kinases regulate C-type lectin receptor 2 (CLEC-2)-mediated clustering of podoplanin and platelet adhesion to lymphatic endothelial cells. *The Journal of Biological Chemistry*, 289(52), pp.35695–35710.

Poulter, N.S. et al., 2017. Clustering of glycoprotein VI (GPVI) dimers upon adhesion to collagen as a mechanism to regulate GPVI signaling in platelets. *Journal of Thrombosis and Haemostasis*, 15, pp.549–564.

Principia Biopharma, 2018. A Study of PRN1008 in Adult Patients With Immune Thrombocytopenic Purpura (ITP). *ClinicalTrials.gov*, pp.1–6. Available at: https://clinicaltrials.gov/ct2/show/NCT03395210 [Accessed August 28, 2018].

Principia Biopharma, 2017. Principia Biopharma Announces PRN1008 Receives Orphan Drug Designation From FDA for Treatment of Pemphigus Vulgaris. pp.1–1. Available at: https://ir.principiabio.com/news-releases/news-release-details/principia-biopharma-announces-prn1008-receives-orphan-drug [Accessed August 23, 2018].

Quek, L.S., Bolen, J. & Watson, S.P., 1998. A role for Bruton's tyrosine kinase (Btk) in platelet activation by collagen. *Current Biology*, 8(20) pp.1137-1140.

Raskob, G.E. et al., 2014. Thrombosis: A major contributor to global disease burden. *Thrombosis research*, 134(5), pp.931–938.

Rawlings, D.J. et al., 1993. Mutation of Unique Region of Bruton's Tyrosine Kinase in Immunodeficient XID Mice. *Science*, 261, pp.358–361.

Rigg, R.A. et al., 2016. Oral administration of Bruton's tyrosine kinase inhibitors impairs GPVI-mediated platelet function. *American Journal of Physiology - Cell Physiology*, 310(5), pp.C373–80.

Rodeghiero, F. et al., 2010. ISTH/SSC bleeding assessment tool: a standardized questionnaire and a proposal for a new bleeding score for inherited bleeding disorders. *Journal of Thrombosis and Haemostasis*, 8(9), pp.2063–2065.

Rodriguez, R. et al., 2001. Tyrosine Residues in Phospholipase Cγ2 Essential for the Enzyme Function in B-cell Signaling. *Journal of Biological Chemistry*, 276(51), pp.47982–47992.

Rossi, D. & Gaidano, G., 2014. Lymphocytosis and ibrutinib treatment of CLL. *Blood*, 123(12), pp.1772–1774.

Rushworth, S.A., MacEwan, D.J. & Bowles, K.M., 2013. Ibrutinib in Relapsed Chronic Lymphocytic Leukemia. *New England Journal of Medicine*, 369(13), pp.1277–1279.

Ryo, R. et al., 1991. Deficiency of P62, a putative collagen receptor, in platelets from a patient with defective collagen-induced platelet aggregation. *American Journal of Hematology*, 39, pp.25–31.

Salto, K. et al., 2003. Btk Regulates PtdIns-4,5-P_2 Synthesis: Importance for Calcium Signaling and PI3K Activity. *Immunity*, 19, pp.669–678.

Sarode, R. et al., 2013. Efficacy and Safety of a Four-Factor Prothrombin Complex Concentrate (4F-PCC) in Patients on Vitamin K Antagonists

Presenting with Major Bleeding: A Randomized, Plasma-Controlled, Phase IIIb Study. *Circulation*, 128, pp.1234–1243.

Schulman, S., Ageno, W. & Konstantinides, S.V., 2017. Venous thromboembolism: Past, present and future. *Thrombosis and Haemostasis*, 117(7), pp.1219–1229.

Schulte, V. et al., 2006. Two-Phase Antithrombotic Protection After Anti-Glycoprotein VI Treatment in Mice. *Arteriosclerosis, thrombosis, and vascular biology*, 26(7), pp.1640–1647.

Seeger, M. et al., 2009. Terminal Part of Thoracic Duct: High-Resolution US Imaging. *Radiology*, 252(3), pp.897–904.

Sekiya, F., Bae, Y.S. & Rhee, S.G., 1999. Regulation of phospholipase C isozymes: activation of phospholipase C-ɣ in the absence of tyrosine-phosphorylation. *Chemistry and Physics of Lipids*, 98, pp.3–11.

Shatzel, J.J. et al., 2015. Ibrutinib-associated bleeding: pathogenesis, management, and risk reduction strategies. *Journal of Thrombosis and Haemostasis : JTH*, 38(1), pp.42–49.

Smyth, E.M., 2010. Thromboxane and the thromboxane receptor in cardiovascular disease. *Clinical Lipidology*, 5(2), pp.209–219.

Spalton, J.C. et al., 2009. The novel Syk inhibitor R406 reveals mechanistic differences in the initiation of GPVI and CLEC-2 signaling in platelets. *Journal of Thrombosis and Haemostasis*, 7(7), pp.1192–1199.

Sugiyama, T. et al., 1987. A Novel Platelet Aggregating Factor Found in a Patient wiht Defective Collagen-Induced Platelet Aggregation and Autoimmune Thrombocytopenia. *Blood*, 69(6), pp.1712–1720.

Suzuki-Inoue, K. et al., 2010. Essential in vivo roles of the C-type lectin receptor CLEC-2: embryonic/neonatal lethality of CLEC-2-deficient mice by blood/lymphatic misconnections and impaired thrombus formation of CLEC-2-deficient platelets. *The Journal of biological chemistry*, 285(32), pp.24494–24507.

Suzuki-Inoue, K. et al., 2004. Glycoproteins VI and Ib-IX-V stimulate tyrosine phosphorylation of tyrosine kinase Syk and phospholipase Cgamma2 at distinct sites. *Biochemical Journal*, 378(3), pp.1023–1029.

Takahashi, H. & Moroi, M., 2001. Antibody against platelet membrane glycoprotein VI in a patient with systemic lupus erythematosus. *American Journal of Hematology*, 67, pp.262–267.

Tani, S.M. et al., 2002. Identification of mutations of Bruton's tyrosine kinase gene (BTK) in Brazilian patients with X-linked agammaglobulinemia. *Human Mutation*, 20(3), pp.235–236.

Temgoua, M.N. et al., 2017. Global incidence and case fatality rate of pulmonary embolism following major surgery: a protocol for a systematic review and meta-analysis of cohort studies. pp.1–6.

Tomlinson, M.G. et al., 2001. A conditional form of Bruton's tyrosine kinase is sufficient to activate multiple downstream signaling pathways via PLC Gamma 2 in B cells. *BMC Immunology*, 2(4), pp.1–12.

Tomlinson, M.G. et al., 1999. Reconstitution of Btk Signaling by the Atypical Tec Family Tyrosine Kinases Bmx and Txk*. *Journal of Biological Chemistry*, 274(19), pp.13577–13585.

Treon, S.P. et al., 2015. Ibrutinib in Previously Treated Waldenström's Macroglobulinemia. *New England Journal of Medicine*, 372(15), pp.1430–1440.

Tricoci, P. et al., 2012. Thrombin-Receptor Antagonist Vorapaxar in Acute Coronary Syndromes. *New England Journal of Medicine*, 366(1), pp.20–33.

Tsuji, M. et al., 1997. A Novel Association of Fc Receptor□ ɣ-Chain with Glycoprotein VI and Their Co-expression as a Collagen Receptor in Human Platelets. *Journal of Biological Chemistry*, 272(38), pp.23528–23531.

Tsukada, S. et al., 1993. Deficient Expression of a B Cell Cytoplasmic Tyrosine Kinases in Human X-Linked Agammaglobulinemia. *Cell*, 72, pp.279–290.

Varnai, P., Rother, K.I. & Balla, T., 1999. Phosphatidylinositol 3-Kinase-dependent Membrane Association of the Bruton's Tyrosine Kinase Pleckstrin Homology Domain Visualized in Single Living Cells. *Journal of Biological Chemistry*, 274(16), pp.10983–10989.

Vassilev, A. et al., 1998. Bruton's Tyrosine Kinase as an Inhibitor of the Fas/CD95 Death-inducing Signaling Complex. *Journal of Biological Chemistry*, 274(3), pp.1646–1656.

Vetrie, D. et al., 1993. The gene involved in X-linked agammaglobulinaemia is a member of the Src family of protein-tyrosine kinases. *Nature*, 361, pp.226–233.

Vihinen, M., 1995. BTKbase:a database of XLA-causing mutations. *Immunology Today*, 16(10), pp.460–465.

Vihinen, M. et al., 1997. BTKbase, mutation database for X-linked agammaglobulinemia (XLA). *Nucleic Acids Research*, 26(1), pp.242–247.

Vihinen, M. et al., 1995. Structural Basis for Pleckstrin Homology Domain Mutations in X-Linked Agammaglobulinemia. *Biochemistry*, 1995(34), pp.1475–1481.

Vihinen, M., Nilsson, L. & Smith, C.I.E., 1994. Tec homology (TH) adjacent to the PH domain. *FEBS*, 350, pp.263–265.

Wahl, M.I. et al., 1997. Phosphorylation of two regulatory tyrosine residues in the activation of Bruton's tyrosine kinase via alternative receptors. *PNAS*, 94, pp.11526–11533.

Wakefield, T.W., Myers, D.D. & Henke, P.K., 2008. Mechanisms of Venous Thrombosis and Resolution. *Arteriosclerosis, thrombosis, and vascular biology*, 28(3), pp.387–391.

Wang, M.L. et al., 2015. Long-term follow-up of MCL patients treated with single-agent ibrutinib: updated safety and efficacy results. *Blood*, 126(6), pp.739–745.

Watanabe, D. et al., 2001. Four tyrosine residues in phospholipase C-gamma 2, identified as Btk-dependent phosphorylation sites, are required for B cell antigen receptor-coupled calcium signaling. *Journal of Biological Chemistry*, 276(42), pp.38595–38601.

Watson, H.G. et al., 2015. Guideline on aspects of cancer-related venous thrombosis. *British Journal of Haematology*, 170(5), pp.640–648.

Watson, S.P., Herbert, J.M.J. & Pollitt, A.Y., 2010. GPVI and CLEC-2 in hemostasis and vascular integrity. *Journal of Thrombosis and Haemostasis*, 8(7), pp.1456–1467.

Weers, M. de et al., 1993. The Bruton's tyrosine kinase gene is expressed throughout B cell differentiation, from early precursor B cell stages preceding immunoglobulin gene rearrangement up to mature B cell stages. *European Journal of Immunology*, 23, pp.3109–3114.

Wiczer, T.E. et al., 2017. Cumulative incidence, risk factors, and management of atrial fibrillation in patients receiving ibrutinib. *Blood Advances*, 1(20), pp.1739–1748.

Wu, J., Zhang, M. & Liu, D., 2016. Acalabrutinib (ACP-196): a selective second-generation BTK inhibitor. *Journal of Hematology & Oncology*, 9(1), pp.1–4.

Yang, W. & Desiderio, S., 1997. BAP-135, a target for Bruton's tyrosine kinase in response to B cell receptor engagement. *PNAS*, 94, pp.604–609.

Yoshimura, N. et al., 2012. Where is the most common site of DVT? Evaluation by CT venography. *Japanese Journal of Radiology*, 30(5), pp.393–397.

Yun, S. et al., 2017. Risk of Atrial Fibrillation and Bleeding Diathesis Associated With Ibrutinib Treatment: A Systematic Review and Pooled Analysis of Four Randomized Controlled Trials. *Clinical Lymphoma, Myeloma and Leukemia*, 17(1), pp.31–37.

Zeiler, M., Moser, M. & Mann, M., 2014. Copy Number Analysis of the Murine Platelet Proteome Spanning the Complete Abundance Range. *Molecular & Cellular Proteomics*, 13(12), pp.3435–3445.

Zhou, Z. et al., 2013. Signal Transducer and Activator of Transcription 3 (STAT3) Regulates Collagen-Induced Platelet Aggregation Independently of Its Transcription Factor Activity. *Circulation*, 127(4), pp.476–485.